

**Deciphering the genetic basis of quantitative  
traits in *Brachypodium distachyon***

**Jan Bettgenhaeuser**

**Thesis submitted to the University of East Anglia  
for the degree of Doctor of Philosophy**

**September 2016**

© This copy of this thesis has been supplied on condition that anyone who consults it is understood to recognise that its copyright rests with the author and that use of any information derived there-from must be in accordance with current UK Copyright Law. In addition, any quotation or extract must include full attribution.

## Abstract

The domestication of plants and animals has been a powerful force in the development of human societies over the past millennia. Domestication of plants is underscored by the selection of agriculturally favourable traits, such as flowering time and disease resistance, which are often inherited in a quantitative manner. Advances in techniques relating to the study of quantitative traits over the past decades enable the dissection of the genetic architecture and molecular basis of these traits. In this thesis, I discuss the natural diversity governing flowering time and intermediate nonhost resistance in the non-domesticated grass *Brachypodium distachyon*. Three major loci were found to govern flowering time, two of which colocalise with the *B. distachyon* homologs of major flowering pathway genes identified in crop species. However, the identification of additional loci suggests that greater complexity underlies flowering time in this non-domesticated system. In contrast, a natural stack of three resistance genes protects *B. distachyon* against colonisation by *Puccinia striiformis* and highlights a relatively simple genetic architecture for intermediate nonhost resistance. One broad spectrum major effect locus was narrowed down to genes that are commonly associated with isolate-specific host resistance. While it has been proposed that nonhost and host resistance are inherently different, the genetic architecture and molecular basis of resistance in this intermediate nonhost system is reminiscent of a host system, which suggests that the genetic architectures of host and nonhost systems are structurally coupled and share conserved components. Studying the genetic basis of these quantitative traits in *B. distachyon* elucidates the way humans have utilised the natural variation present in grasses to create modern temperate cereals. Additionally, exploring the interaction between *B. distachyon* and *P. striiformis* has provided an ideal system to investigate the transfer of resistance genes from wild relatives to agronomically important crops.

## Acknowledgments

First and foremost, I would like to thank Matthew Moscou for all the learning opportunities, mentoring, and support over the past four years. It has truly been quite a journey for both of us, from him being my post-doc mentor at the start of the PhD to him being my group leader now that I am finishing. But no matter how stressful times were, making sure that the research is moving forward was always a priority for him. Thank you!

I would also like to thank Paul Nicholson and Brande Wulff, who as part of my supervisory team provided valuable input and constructive feedback throughout my PhD.

A very special thanks goes to all members of the old 2Blades group and the Moscou group, both past and present. You have made the PhD a fun experience! In particular, Inma Hernández-Pinzón has been a fountain of knowledge and experience, Phon Green has been an amazing help for everything greenhouse related, Matt Gardiner often lent an extra pair of hands, and Andrew Dawson was a great co-PhD student and at times also a bearable flatmate.

I also had the chance to work with two amazing undergraduate and MSc students, which was a great experience. Thanks for all your hard work, Maëlys Ordoqui and Rebecca Spanner!

My time in Norwich has been made very enjoyable by all the friends I made over the years. I will definitely miss weekend brunches with Leonie Lugimbühl, Tom Vincent, and Amitesh Pratap, pizza, beer, and Settlers of Catan evenings with Andrew Dawson, Oliver Furzer, and Will Heard, and Friday evening drinks with Sara Ben Khaled, Sebastian Pfeilmeier, and Daniel Couto.

Last, but by no means least, I would like to thank my family, who have always been there for me. Especially my parents always encouraged me in my endeavours and continue to support me in every way they possibly can. Danke, Mama und Papa!

## Contributions to research

Jan Bettgenhaeuser (JB), Fiona Corke (FC), Magdalena Opanowicz (MO), Phon Green (PG), Inmaculada Hernández-Pinzón (IHP), John Doonan (JD), Matthew Moscou (MM), Rebecca Spanner (RS), Matthew Gardiner (MG), Michael Ayliffe (MA), Amelia Hubbard (AH), Brande Wulff (BW), Eric Ward (EW)

### Chapter 2:

The genetic architecture of flowering regulation in *Brachypodium distachyon*

Conception and design of experiments: JB, FC, MO, JD, MM

Experimentation: JB, FC, MO, PG, IHP

Data analysis: JB, MM

### Chapter 3:

The genetic architecture of intermediate nonhost resistance to stripe rust (*Puccinia striiformis*) in *Brachypodium distachyon*

Conception and design of experiments: JB, MM, MA, BW, EW

Experimentation: JB, MG, PG, IHP, AH, MM

Data analysis: JB, MM

### Chapter 4:

Isolation, fine-mapping, and characterisation of *Yrr3*, an intermediate nonhost resistance locus to stripe rust in *Brachypodium distachyon*

Conception and design of experiments: JB, MM

Experimentation: JB, RS, PG, IHP, AH

Data analysis: JB, MM, RS

## Table of Contents

<b>1. General Introduction .....</b>	<b>1</b>
<i>Pre-Mendelian views on inheritance .....</i>	<i>1</i>
<i>Mendelian inheritance .....</i>	<i>2</i>
<i>Discrete versus quantitative phenotypes .....</i>	<i>3</i>
<i>The beginning of quantitative genetics .....</i>	<i>4</i>
<i>Advancements in analysing the genetic architecture of quantitative traits .....</i>	<i>5</i>
<i>Using QTLs and identifying the underlying genes .....</i>	<i>8</i>
<i>Dissertation organisation .....</i>	<i>10</i>
<i>Chapter 2. The genetic architecture of flowering regulation in <i>B. distachyon</i> .....</i>	<i>11</i>
<i>Chapter 3. The genetic architecture of intermediate nonhost resistance to stripe rust (<i>P. striiformis</i>) in <i>B. distachyon</i> .....</i>	<i>12</i>
<i>Chapter 4. Isolation, fine-mapping, and characterisation of Yrr3, an intermediate nonhost resistance locus to stripe rust in <i>B. distachyon</i> .....</i>	<i>12</i>
<b>2. The genetic architecture of flowering regulation in <i>B. distachyon</i> .....</b>	<b>13</b>
Introduction .....	13
Results .....	17
<i>Development of a <i>B. distachyon</i> mapping population between geographically and phenotypically distinct accessions .....</i>	<i>17</i>
<i>Multiple QTLs control flowering in the ABR6 x Bd21 mapping population .....</i>	<i>19</i>
<i>Natural variation in FT and VRN2 .....</i>	<i>24</i>
<i>Expression of VRN1, VRN2, and FT in response to vernalisation .....</i>	<i>26</i>
Discussion .....	27
<i>Segregation distortion in the ABR6 x Bd21 population .....</i>	<i>27</i>
<i>The genetic architecture of flowering time in <i>B. distachyon</i> .....</i>	<i>28</i>
<i>Conclusions .....</i>	<i>31</i>
Materials and methods .....	33
<i>Plant growth for assessing ABR6 and Bd21 vernalisation response .....</i>	<i>33</i>
<i>Resequencing of ABR6 .....</i>	<i>33</i>
<i>Development of the ABR6 x Bd21 F<sub>4</sub> population and genetic map .....</i>	<i>34</i>
<i>Plant growth and phenotyping of flowering time in the ABR6 x Bd21 F<sub>4:5</sub> families .....</i>	<i>35</i>
<i>Quantitative trait locus analysis for flowering time .....</i>	<i>35</i>
<i>RNAseq of ABR6 and Bd21 .....</i>	<i>36</i>
<i>RT-qPCR analyses .....</i>	<i>37</i>
<i>Accession numbers for data in public repositories .....</i>	<i>38</i>

<b>3. The genetic architecture of intermediate nonhost resistance to stripe rust (<i>Puccinia striiformis</i>) in <i>B. distachyon</i> .....</b>	<b>39</b>
Introduction .....	39
Results .....	43
<i>Leaf browning and hyphal colonisation are strongly correlated in segregating B. distachyon mapping populations.....</i>	<i>43</i>
<i>A simple genetic architecture underlies resistance to Pst isolate 08/21 in three B. distachyon mapping populations.....</i>	<i>46</i>
<i>Yrr1 and Yrr3 confer resistance to diverse Pst isolates in the ABR6 x Bd21 mapping population .....</i>	<i>51</i>
<i>Yrr3 confers intermediate nonhost resistance to both <i>P. striiformis</i> f. sp. <i>tritici</i> and <i>P. striiformis</i> f. sp. <i>hordei</i> .....</i>	<i>52</i>
<i>Canonical resistance genes are associated with intermediate nonhost resistance to stripe rust in <i>B. distachyon</i> .....</i>	<i>53</i>
Discussion.....	55
<i>No life cycle completion of stripe rust in <i>B. distachyon</i> .....</i>	<i>55</i>
<i>A simple genetic architecture underlies resistance to stripe rust in <i>B. distachyon</i>.....</i>	<i>56</i>
<i>The molecular basis of resistance on the continuum from host to nonhost systems .....</i>	<i>57</i>
<i>Intermediate nonhost resistance as a source for durable, broad spectrum resistance.</i>	<i>59</i>
<i>A shared basis for host and nonhost resistance .....</i>	<i>59</i>
Materials and methods.....	61
<i>Plant and fungal material .....</i>	<i>61</i>
<i>Development of the <i>Luc1</i> x <i>Jer1</i> and <i>Foz1</i> x <i>Luc1</i> genetic maps .....</i>	<i>61</i>
<i>Plant growth, inoculation and phenotyping.....</i>	<i>62</i>
<i>Quantitative trait locus analyses.....</i>	<i>63</i>
<i>Candidate gene analysis at Yrr1 and Yrr3 .....</i>	<i>63</i>
<b>4. Isolation, fine-mapping, and characterisation of <i>Yrr3</i>, an intermediate nonhost resistance locus to stripe rust in <i>B. distachyon</i>.....</b>	<b>65</b>
Introduction .....	65
Results .....	69
<i>Parallel fine-mapping delineates Yrr3 to a 72 kb gain of function interval.....</i>	<i>69</i>
<i>Yrr3 recombination screen demarcates two SNPs separating an 11.3 kb interval .....</i>	<i>72</i>
<i><i>Luc1</i> and <i>Jer1</i> are near identical across the CC-NB/NB-LRR cluster .....</i>	<i>73</i>
<i><i>ABR6</i> and <i>Bd21</i> possess greater structural variation across the CC-NB/NB-LRR cluster .....</i>	<i>75</i>
<i>The delineated CC-NB/NB-LRR cluster is highly conserved across monocot species .</i>	<i>76</i>

<i>All three candidate genes in the cluster are expressed in resistant and susceptible accessions.....</i>	76
<i>Two non-synonymous mutations in conserved NB motifs differentiate <i>Luc1</i> from the resistant accessions.....</i>	77
<i>Complementation of candidate genes .....</i>	79
<b>Discussion.....</b>	<b>79</b>
<i>Non-synonymous mutations are associated with NB motifs that regulate nucleotide binding.....</i>	79
<i>The NB-LRR and CC-NB pose different modes of stripe rust recognition at <i>Yrr3</i>.....</i>	83
<i>How could NB-LRR mediated resistance be broad spectrum and durable? .....</i>	86
<b>Materials and methods.....</b>	<b>89</b>
<i>Plant growth and inoculation.....</i>	89
<i><i>Luc1</i> x <i>Jer1</i> recombination screen.....</i>	89
<i>Marker development.....</i>	89
<i>Marker regression analysis.....</i>	89
<i>BAC library screening and BAC sequencing.....</i>	90
<i>RNAseq of <i>Luc1</i>, <i>Jer1</i>, and <i>Foz1</i> and RNA analyses .....</i>	90
<i>Characterisation of <i>Yrr3</i> candidate genes.....</i>	91
<i>Construct development for complementation.....</i>	92
<b>5. General Discussion.....</b>	<b>94</b>
<i>What prevents life cycle completion of <i>P. striiformis</i> on <i>B. distachyon</i>?.....</i>	96
<i>What role does the effector repertoire play in the interaction between <i>P. striiformis</i> and infected plants? .....</i>	98
<i>Can the resistance identified be transferred to crop species? .....</i>	100
<b>6. Appendices.....</b>	<b>102</b>
<i>Supplemental figures .....</i>	102
<i>Supplemental tables.....</i>	110
<i>Unpublished primer sequences from Chapter 3 and Chapter 4 .....</i>	119
<i>Published version of Chapter 2.....</i>	127
<b>7. Abbreviations .....</b>	<b>140</b>
<b>8. References .....</b>	<b>141</b>

## List of Tables

<b>Table 1.</b> Significant flowering time QTLs ( <i>qFLT</i> ) in the different environments identified using several binary, non-parametric, and parametric approaches....	21
<b>Table 2.</b> Significant QTLs from composite interval mapping of transformed flowering time phenotypes (T3) in the ABR6 x Bd21 F <sub>4:5</sub> families. ....	21
<b>Table 3.</b> Previously identified <i>B. distachyon</i> homologs of flowering regulators in <i>Arabidopsis</i> ( <i>At</i> ), hexaploid and diploid wheat ( <i>Ta</i> and <i>Tm</i> ), barley ( <i>Hv</i> ), and rice ( <i>Os</i> ) within the one-LOD support intervals of the statistically significant QTLs under transformation T3. ....	23
<b>Table 4.</b> Significant QTLs from composite interval mapping of averaged leaf browning and percent colonisation phenotypes for <i>P. striiformis</i> isolates in the ABR6 x Bd21 F <sub>4:5</sub> families. ....	47
<b>Table 5.</b> Significant QTLs from composite interval mapping of leaf browning and percent colonisation phenotypes for <i>P. striiformis</i> f. sp. <i>tritici</i> isolate 08/21 in the Foz1 x Luc1 and Luc1 x Jer1 F <sub>2</sub> populations. ....	51
<b>Table 6.</b> Average phenotypic scores from progeny testing of selected ABR6 x Bd21 F <sub>2</sub> and F <sub>3</sub> lines based on genotype at the <i>Yrr3</i> peak marker. ....	70
<b>Table 7.</b> Nucleic acid and amino acid differences between the three <i>Yrr3</i> candidates among the five accessions.....	78

## List of Figures

<b>Figure 1.</b> Vernalisation and flowering control in the model plant <i>Arabidopsis thaliana</i> and the core Pooideae (e.g. wheat and barley).....	14
<b>Figure 2.</b> Flowering behaviour within the ABR6 x Bd21 mapping population.....	17
<b>Figure 3.</b> Effect of vernalisation on flowering time in ABR6 and Bd21.....	18
<b>Figure 4.</b> Segregation distortion in the ABR6 x Bd21 F <sub>4</sub> population. ....	19
<b>Figure 5.</b> Frequency distribution of flowering time in the ABR6 x Bd21 population. ....	20
<b>Figure 6.</b> Linkage mapping of flowering time in the ABR6 x Bd21 population. ....	22
<b>Figure 7.</b> Phenotype by genotype plot for the two major loci controlling flowering time in the ABR6 x Bd21 mapping population. ....	23
<b>Figure 8.</b> Comparison of the flowering regulators <i>FT</i> and <i>VRN2</i> between the <i>B. distachyon</i> accessions Bd21 and ABR6.....	25
<b>Figure 9.</b> <i>VRN1</i> , <i>VRN2</i> , and <i>FT</i> expression in fourth leaf of ABR6 and Bd21 after varying periods of cold treatment. ....	26
<b>Figure 10.</b> <i>Puccinia striiformis</i> f. sp. <i>tritici</i> (wheat stripe rust) infection symptoms on several <i>Brachypodium distachyon</i> accessions. ....	43
<b>Figure 11.</b> Frequency distribution and correlation of leaf browning and pCOL phenotypes in the ABR6 x Bd21 population inoculated with several isolates of <i>P. striiformis</i> f. sp. <i>tritici</i> . ....	45
<b>Figure 12.</b> Frequency distribution and correlation of leaf browning and pCOL phenotypes in the Foz1 x Luc1 and Luc1 x Jer1 F <sub>2</sub> populations inoculated with <i>P. striiformis</i> f. sp. <i>tritici</i> isolate 08/21. ....	46
<b>Figure 13.</b> Two major effect loci govern <i>P. striiformis</i> resistance in the ABR6 x Bd21 population. ....	48

<b>Figure 14.</b> Restriction of <i>P. striiformis</i> f. sp. <i>tritici</i> and <i>P. striiformis</i> f. sp. <i>hordei</i> colonisation in the ABR6 x Bd21 population by <i>Yrr1</i> and <i>Yrr3</i> .....	49
<b>Figure 15.</b> Restriction of <i>P. striiformis</i> f. sp. <i>tritici</i> colonisation in Foz1 x Luc1 and Luc1 x Jer1 F <sub>2</sub> populations by <i>Yrr1</i> and <i>Yrr3</i> .....	50
<b>Figure 16.</b> Canonical resistance genes associated with <i>Yrr1</i> and <i>Yrr3</i> loci.....	54
<b>Figure 17.</b> Isolation and fine-mapping of <i>Yrr3</i> in two independent populations.....	69
<b>Figure 18.</b> <i>Yrr3</i> cosegregates with resistance in ABR6 x Bd21 F <sub>5</sub> progeny from line F <sub>3-147</sub> F <sub>4-4</sub> .....	70
<b>Figure 19.</b> <i>Yrr3</i> is almost mendelised in the Luc1 x Jer1 population.....	71
<b>Figure 20.</b> Fine-mapping of a 72 kb consensus gain of function interval in two independent populations.....	72
<b>Figure 21.</b> Fine-mapping of <i>Yrr3</i> within the Luc1 x Jer1 population.....	74
<b>Figure 22.</b> Nucleotide identity between ABR6 and Bd21 drops within the CC-NB/NB-LRR cluster.....	75
<b>Figure 23.</b> All three candidate genes are expressed in both resistant and susceptible accessions.....	76
<b>Figure 24.</b> Structure of nucleotide-binding (NB) domain containing proteins.....	81

## 1. General Introduction

*“And Jacob took him rods of green poplar, and of the hazel and chestnut tree; and pilled white strakes in them, and made the white appear which was in the rods. And he set the rods which he had pilled before the flocks in the gutters in the watering troughs when the flocks came to drink, that they should conceive when they came to drink. And the flocks conceived before the rods, and brought forth cattle ringstraked, speckled, and spotted.”*

Genesis 30: 37 – 39 (King James Bible)

In parallel with the domestication of plants and animals, humans for the first time observed the inheritance of both desirable and undesirable traits from one generation to the next (Klug and Cummings 1991). Although for most of human history the selection of these traits was probably not guided by specific breeding targets, this soon lead to the formation of ideas as to how this inheritance takes place and what specifically is passed on from one generation to the next (Klug and Cummings 1991). Some of these ideas and theories we now know to be wrong, such as the maternal impression described in the example above, but others have been developed over time and form the basis of our current understanding of genetics.

### *Pre-Mendelian views on inheritance*

The earliest formalised ideas on inheritance were proposed by the Greek philosophers Hippocrates and Aristotle (Klug and Cummings 1991). Hippocrates suggested that heritable material was contributed by all body parts and passed to the offspring during conception, explaining the resemblance between parent and offspring (Reeve 2001). This theory was later termed pangenesis by Charles Darwin (Darwin 1868). In contrast, Aristotle advocated an idea where purified blood in the form of semen and menstrual blood come together and interact. He proposed that the embryo continuously develops, a theory later described as epigenesis by the anatomist William Harvey (Harvey 1651; Klug and Cummings 1991). Klug and Cummings (1991) point out that although these early views sound alien to our current understanding of

inheritance and genetics, they did provide useful stepping stones. Notably, inheritance in both of these theories is biparental and mediated by defined heritable units (Klug and Cummings 1991).

Two millennia later, the publication of the *Systema Naturae* by Carl Linnaeus in 1735 for the first time provided a system to categorise organisms based on their inherited characteristics and their ability to reproduce (Linnaeus 1735; Reeve 2001). However, Linnaeus also observed variants that did not fit into this system. For example, he described a mutant form of *Linaria vulgaris*, which produced abnormal flowers, and called this phenomenon pelorism (Linnaeus and Rudberg 1744; Reeve 2001). In this context, Klug and Cummings (1991) reinforce that Linnaeus and other naturalists of the 18<sup>th</sup> and 19<sup>th</sup> centuries were held back by their conviction that species are fixed and cannot change over time. They give the example of the plant breeder Joseph Gottlieb Kölreuter, who developed new tobacco hybrids by crossing different *Nicotiana* spp. and recreated the phenotypes of the parental species by repeated backcrossing (Kölreuter 1761). They argue that the conviction that the whole species is fixed and not made up of individual traits prevented him from understanding how much his observations revealed about the inheritance of traits (Klug and Cummings 1991). “Blending inheritance”, a popular pre-Mendelian theory which was also advocated by Darwin, describes the idea that the parental phenotypes fuse in the progeny and manifest themselves as an intermediate phenotype (Darwin 1868; Klug and Cummings 1991). Although Darwin noticed how peloric and other morphological traits often only appeared as one of the parental phenotype in a hybrid derived from differential parental lines and the second parental phenotype reappeared in the next generation, he failed to understand the significance of this segregation pattern (Darwin 1868; Reeve 2001).

### *Mendelian inheritance*

During the 18<sup>th</sup> and 19<sup>th</sup> century several researchers performed studies similar to the ones later described by Mendel (Zirkle 1951). Notably, studies on maize, pea, and muskmelon suggested that a phenotype can be dominant or recessive, that recessive phenotypes can resurface in subsequent generations, or that different traits are inherited independently of each other (reviewed by Zirkle (1951)). However, although

other researchers had studied the inheritance of traits in a variety of different species, Mendel was the first to do so in a methodical way by recording the numbers associated with the segregation of carefully chosen phenotypes in a specific system (Mendel 1866). By identifying the ratios associated with the inheritance of these traits over several generations, he was able to propose four postulates regarding heritable unit factors, which form the basis of our modern understanding of genetics. The postulates can be reduced to these core statements (Klug and Cummings 1991):

- 1) Unit factors occur in pairs.
- 2) Unit factors can be dominant or recessive.
- 3) Unit factors segregate during inheritance.
- 4) Pairs of unit factors segregate independently of each other.

This means that a hybrid can possess two different alleles of a gene (e.g. encoding wrinkled and round seed shape), but only one will be observable as a phenotype. In the subsequent generation both phenotypes will reappear in a 3:1 ratio. Individuals with the recessive phenotype will only produce offspring with the recessive phenotype (i.e. they are homozygous for this trait), whereas individuals with the dominant phenotype may produce offspring that either all show the dominant phenotype or segregate (i.e. they are either homozygous for the dominant trait or heterozygous). When two or more traits are studied (e.g. seed shape and flower colour), these are inherited independently of each other, but still according to the postulates set out above. Mendel's postulates were in contrast to the theory of blending inheritance, as they suggested that a trait is governed by discrete and defined units, which manifest themselves as discontinuous phenotypes (Klug and Cummings 1991).

### *Discrete versus quantitative phenotypes*

The traits studied by Mendel were unique in that they largely consisted of discrete phenotypes (Lynch and Walsh 1998). Progeny clearly expressed one of the parental phenotypes and could be assigned to one of the parental categories. After the rediscovery of Mendel's work and the acceptance of Mendelian inheritance, a major focus was therefore on clearly segregating phenotypes (Wright 1968). However, most phenotypes of interest for plant and animal breeding and other applications are of a quantitative nature. For example, crop yield cannot be classified into two discrete

categories, but manifests itself in a continuous distribution from low to high yield. Darwin's cousin Francis Galton was influenced by Darwin's detailed discussion on the domestication of plants and animals, but disagreed with Darwin's description of blended inheritance (Lynch and Walsh 1998). By investigating the basis of genius or human ability, Galton was the first to study the inheritance of a quantitative trait (Galton 1869). However, after the rediscovery of Mendel's work the field split into two branches over the subsequent decades, with biometrists led by Karl Pearson studying the inheritance of quantitative characteristics, while Mendelians led by William Bateson studied the inheritance of discrete characteristics (Wright 1968). Debates in the early 20<sup>th</sup> century centred around the question, whether inheritance and evolution of quantitative and discrete phenotypes are governed by the same or differing principles (Lynch and Walsh 1998).

### *The beginning of quantitative genetics*

Wright (1968) and Lynch and Walsh (1998) point out that Mendel already suggested how a continuous or quantitative character could be inherited by multiple independently segregating genes. With regard to the colour of flowers and seeds of *Pisum multiflorus*, Mendel suggested that these might be a combination of different colours conferred by independently segregating factors and explains the adjusted ratios with which the parental phenotypes should reappear in the progeny if two or three genes were to control these colours (Mendel 1866). Yule (1902) provided the mathematical proof for this idea, but as Lynch and Walsh (1998) remark: "Unfortunately for Yule, the only thing that the biometrists and the Mendelians could publicly agree on was the incompatibility of Mendelian genetics and the inheritance of continuous characters."

The idea that independent factors each adhering to Mendelian inheritance underlie a quantitative trait gained momentum with the development of the multiple-factor hypothesis in the early 20<sup>th</sup> century (Lynch and Walsh 1998). The first observation in this direction was that inbred maize lines did not possess the variation in quantitative traits that was present within the original outbred lines from which they were derived, which suggested that Mendelian inheritance must underlie these traits (Shull 1908; Lynch and Walsh 1998). As Mendel had observed, during self-fertilisation half of the

heterozygosity is removed each generation (Mendel 1866; Wright 1968). The first direct demonstration of Mendelian inheritance for a quantitative trait was provided by Nilsson-Ehle (Nilsson-Ehle 1909; Wright 1968). Nilsson-Ehle was able to show that three genes conferred red seed colour in wheat and that each of them segregated independently in a 3:1 manner in F<sub>2</sub> populations (Nilsson-Ehle 1909; Mather and Jinks 1971). In this case red seed colour is the dominant phenotype and progeny with white seed colour could only occur in triple homozygotes for the recessive phenotype (Nilsson-Ehle 1909; Wright 1968). Moreover, different degrees of redness in the progeny were not associated with which of the three genes conferring red seed colour was present, but rather how many of these genes were present in the progeny (Nilsson-Ehle 1909; Mather and Jinks 1971). The three genes identified by Nilsson-Ehle individually possessed a great enough effect to be detected in segregating families (Mather and Jinks 1971); however, Nilsson-Ehle noted that Mendelian inheritance of genes with a smaller phenotypic effect could explain the quantitative nature observed for other phenotypes (Nilsson-Ehle 1909; Mather and Jinks 1971). In summary, the work by Nilsson-Ehle showed that sexual reproduction can give rise to a great diversity of phenotypes and allows the occurrence of rare segregants, which is incompatible with the theory of blending inheritance (Lynch and Walsh 1998).

#### *Advancements in analysing the genetic architecture of quantitative traits*

The early work on quantitative traits and their inheritance focused on the development of statistical techniques to describe these traits and their variation (Tanksley 1993; Kearsey and Farquhar 1998). These techniques allowed the approximation of the number of loci that control the trait, an estimation of their action, and to what degree they interact with each other or the environment (Tanksley 1993). The genes underlying quantitative traits were termed “polygenes” (Mather and Jinks 1971), but their number was only approximated and their location within the genome was largely unknown (Kearsey and Farquhar 1998). However, several observations highlighted that polygenes could be linked to major effect genes, facilitating their analysis (Mather and Jinks 1971). For example, seed colour in one *Phaseolus vulgaris* population was found to be conferred by a single major gene, but was also linked to polygenes controlling seed weight (Sax 1923). Rasmusson (1935) found a similar association between flower colour and flowering time in a *Pisum sativum* population. Other

studies attempted to examine the location of polygenes, such as those regulating abdominal and sternopleural chaetae number in *Drosophila melanogaster*, which were dissected by creating recombinant chromosomes (Breese and Mather 1957). The authors showed that at least six genes on chromosome 3 must be involved in the phenotype (Breese and Mather 1957).

Tanksley (1993) highlights that although some knowledge existed regarding the combined action of polygenes and their interaction, it was impossible to scrutinise the action and interaction between specific loci without a suitable marker system. Early markers consisted of discrete phenotypes, for which the underlying genes and their genomic position were known and which could be used to study a linked polygene (Thoday 1961). If such a morphological marker was linked with a quantitative trait, one could infer the genomic location of the polygene underlying the quantitative trait (Thoday 1961; Tanksley 1993). However, the major drawback of this technique was the limited number of suitable morphological traits, as only few monogenic phenotypes were known for most organisms (Thoday 1961; Tanksley 1993; Hackett 2002). Additionally, the epistatic effect of the morphological marker (e.g. dwarfism) on the quantitative phenotype of interest often prevented mapping of many quantitative phenotypes (Tanksley 1993).

Kearsey and Farquhar (1998) assert that two developments of the 1980s alleviated these problems associated with mapping and analysing the genetic basis of quantitative traits. The discovery of a great extent of molecular variation between parents of a mapping population facilitated the development of phenotypically neutral, but abundant, markers (Tanksley 1993; Kearsey and Farquhar 1998). The second development was the introduction of the “catchy” acronym QTL (quantitative trait locus) (Geldermann 1975), which according to Kearsey and Farquhar (1998) liberated quantitative genetics from its longstanding associations with heavy statistical analyses. Molecular markers were first introduced by studying different isozymes present between parental lines and segregating among the progeny, but with the discovery of an even greater number of polymorphisms at the DNA level and the relative ease of working with DNA rather than proteins, DNA-based markers superseded protein-based markers (Tanksley 1993).

Molecular markers possess five major advantages over morphological markers, summarised by Tanksley as follows (Tanksley 1993):

- 1) Molecular markers, especially DNA markers, are usually phenotypically neutral, as they largely map to non-coding regions of the genome. They are therefore unbiased and do not impact the quantitative phenotype of interest.
- 2) As molecular markers are usually phenotypically neutral, they are associated with a reduced selection pressure and higher mutation rates, giving rise to a greater number of polymorphisms among molecular markers than morphological markers.
- 3) Molecular markers are abundant throughout the organism's genome, allowing the construction of whole genome genetic maps. This possibility also enabled the development of new statistical approaches, such as interval analyses (see below).
- 4) Codominant molecular markers allow the identification of all three possible states (homozygous parent A, heterozygous, and homozygous parent B), whereas dominant morphological markers only allowed the unambiguous identification of the homozygous recessive state (see Mendelian inheritance above).
- 5) Epistatic interactions associated with morphological markers, e.g. the influence of dwarfism on other quantitative traits, are rarely observed for molecular markers and therefore do not significantly reduce the number of molecular markers that can be used.

The physical linkage of molecular markers and the gene or genes controlling the phenotype give rise to a non-random association between markers and phenotype, also called linkage disequilibrium (Tanksley 1993; Lynch and Walsh 1998). The existence of linkage disequilibrium forms the basis of any marker-based approach to dissect the genetic architecture controlling a quantitative phenotype (Tanksley 1993). In its simplest form, one can think of a QTL analysis as looking at each marker in turn, separating the phenotypes based on the marker genotype, and identifying markers that are associated with statistically significant differences between the two pools of phenotypes (i.e. performing an analysis of variance (ANOVA) or marker regression) (Lynch and Walsh 1998; Hackett 2002). The major limitation of this approach is the need for a high marker coverage, as QTLs will be missed if the gaps between markers

are too large and no marker is linked with the causal gene (Lynch and Walsh 1998; Hackett 2002). Interval mapping was developed to address this and other problems by calculating the logarithm of the odds (LOD) score and estimating the likelihood that a QTL is located between two markers (Lander and Botstein 1989). However, marker regression and interval mapping both work under the assumption of a single major effect QTL, which is rarely the case when studying quantitative traits (Jansen 1993; Zeng 1993). Composite interval mapping combines interval mapping with regression analyses on several background markers that serve as substitutes for other QTLs influencing the phenotype (Jansen 1993; Zeng 1993; Zeng 1994). This feature increases the precision obtained with composite interval mapping compared to standard interval mapping (Jansen and Stam 1994; Zeng 1994).

#### *Using QTLs and identifying the underlying genes*

The use of molecular markers on the one hand allowed the evaluation of the location, action, and interaction of QTLs, and on the other hand facilitated the use of QTLs, for example in marker assisted breeding programmes or the diagnosis of diseases (Kearsey and Farquhar 1998). Additionally, the continuous development of new techniques allows the incorporation of ever more QTLs in breeding programmes and other applied approaches (Morgante and Salamini 2003). As QTLs with only a small effect are difficult to detect and a small population size in many studies hinders the separation of physically close QTLs, one will probably never be able to detect, map and characterise all QTLs affecting a phenotype (Tanksley 1993). However, in practice only QTLs with a relatively large phenotypic effect will be of interest for breeding programmes and other applications (Tanksley 1993).

Due to the quantitative nature of the studied traits and possible small effect of QTLs, the molecular basis and function of many QTLs is never uncovered. As an example, the underlying genes were only identified for less than 1% of over 2,000 QTLs mapped in rodents over a 15-year period (Flint *et al.* 2005). After a QTL has been mapped, several steps need to be taken in order to locate the underlying causal gene or genes. Namely, these consist of isolating the QTL of interest from other QTLs segregating in the population, fine-mapping the genetic interval responsible for the phenotype of interest, identifying the physical sequence associated with the fine-mapped genetic

interval, annotating and prioritising the candidate genes present in this interval, and lastly confirming the causal gene or genes by complementation or mutagenesis studies (Salvi and Tuberosa 2005). However, it should be noted that these steps do not necessarily form a linear path to be taken, but can be seen as stepping stones one might take. For example, with the availability of sequenced genomes for many species, as well as a wealth of other resources, a physical interval might be directly determined and fine-mapped for a QTL in these species. The identification of genes underlying QTLs in the past decades has demonstrated that the nature of polymorphisms underlying quantitative traits does not differ from discrete traits (Paran and Zamir 2003). In addition, successful map-based cloning projects have shown that single genes are often responsible for the variation controlled by the QTL (Remington *et al.* 2001).

The first step in the direction of cloning the causal gene involves the separation of the QTL of interest from other QTLs segregating in the population, a process also referred to as the “Mendelisation” of a QTL (Salvi and Tuberosa 2005). If no segregating lines can be identified that are fixed for these other QTLs, those lines can be developed with the aid of phenotypic and genotypic selection during successive rounds of self-fertilisation or backcrossing (Salvi and Tuberosa 2005; Drinkwater and Gould 2012). The aim is to identify lines that are homozygous (i.e. fixed) at the other QTLs, while being heterozygous (i.e. segregating) at the QTL of interest. Fine-mapping is used to reduce the genetic (for organisms without a sequenced genome) or physical (for organisms with a sequenced genome) intervals that harbour the QTL (Salvi and Tuberosa 2005) and involves additional marker saturation and the identification of lines with recombination events in the region of interest (Drinkwater and Gould 2012).

Once a sufficiently small interval has been delineated, the physical candidate region needs to be annotated. However, this will often differ from system to system, as a range of resources may be available already. For species with a sequenced and annotated genome, one may be able to directly look for promising candidate genes within the interval (Pflieger *et al.* 2001). Especially for major effect QTLs, the initial mapping can be very accurate and many cloned genes were often found to be physically close to the original LOD peak (Price 2006). Jumping from the initial mapping directly to analysing candidate genes without any additional fine-mapping

can be particularly useful, if the trait of interest has already been studied extensively in other systems and one has an idea of the kind of genes that might contribute to the phenotype of interest (Morgante and Salamini 2003; Price 2006). To give an example, the regulation of flowering time has been studied extensively in the model plant *Arabidopsis thaliana*, which has accelerated the identification of orthologous genes in different crop species (Blümel *et al.* 2015).

On the other hand, if no sequenced genome is available the general way forward is to characterise a segment of physical sequence that was isolated with a marker linked to the genetically fine-mapped region, e.g. a bacterial artificial chromosome (BAC) obtained from screening a BAC library (Salvi and Tuberosa 2005). Such a newly obtained sequence can be further annotated by identifying open reading frames and confirming these by analysing gene expression (Salvi and Tuberosa 2005; Drinkwater and Gould 2012). Structural or sequence variation between differential parental lines might aid in the prioritisation of candidate genes, as well as the identification of mutant lines (Salvi and Tuberosa 2005; Drinkwater and Gould 2012). In most cases, including the ones described in this thesis, the identification and prioritisation of candidate genes will involve a combination of different approaches. However, the confirmation of a candidate gene as the causal gene underlying a QTL ultimately rests on complementing the phenotype in a line that does not express it (Pflieger *et al.* 2001).

### *Dissertation organisation*

My dissertation is structured into three research chapters, which explore the genetic architecture and underlying molecular basis of two quantitative traits in the monocot *Brachypodium distachyon*. In the second chapter I describe the genetic architecture of flowering regulation, a trait for which considerable previous knowledge has been established by both forward and reverse genetic studies in many model and crop species. In contrast, only limited knowledge exists regarding the genetic architecture and molecular basis of nonhost resistance (i.e. the resistance to nonadapted pathogens), which I describe in the following two chapters. In the third chapter I establish the genetic architecture of resistance to stripe rust (*Puccinia striiformis*), for which *B. distachyon* is an intermediate nonhost. Subsequently, in the fourth chapter I transition into the isolation, fine-mapping, and characterisation of *Yrr3*, one of the

major effect loci conferring stripe rust resistance identified in the third chapter. Owing to the diverse topics covered, each chapter has its own introduction, results, discussion, and materials and methods sections. A more general discussion at the end connects the two research chapters on stripe rust resistance and highlights open questions for future research regarding this aspect of the thesis.

### *Chapter 2. The genetic architecture of flowering regulation in *B. distachyon**

The domestication of plants is underscored by the selection of agriculturally favourable developmental traits, including flowering time, which resulted in the creation of varieties with altered growth habits. Research into the pathways underlying these growth habits in cereals has highlighted the role of three main flowering regulators: *VRN1*, *VRN2*, and *FT*. To investigate the natural diversity governing flowering time pathways in a non-domesticated grass, the reference *B. distachyon* accession Bd21 was crossed with the vernalisation-dependent accession ABR6. Three major loci were found to govern flowering time. Interestingly, two of these loci colocalise with the *B. distachyon* homologs of the major flowering pathway genes *VRN2* and *FT*, whereas no linkage was observed at *VRN1*. Characterisation of these candidates identified sequence and expression variation between the two parental genotypes, which may explain the contrasting growth habits. However, the identification of additional QTLs suggests that greater complexity underlies flowering time in this non-domesticated system. Studying the interaction of these regulators in *B. distachyon* provides insights into the evolutionary context of flowering time regulation in the Poaceae, as well as elucidates the way humans have utilised the natural variation present in grasses to create modern temperate cereals.

*The research presented in the second chapter has been published in the journal Plant Physiology (<http://www.plantphysiol.org/>) and copyright rests with the American Society of Plant Biologists. The full publication details are:*

*Bettgenhaeuser J., Corke F.M.K., Opanowicz M., Green P., Hernández-Pinzón I., Doonan, J.H., Moscou M.J. (2017). Natural variation in Brachypodium links vernalization and flowering time loci as major flowering determinants. Plant Physiology. doi:10.1104/pp.16.00813*

*Chapter 3. The genetic architecture of intermediate nonhost resistance to stripe rust (*P. striiformis*) in *B. distachyon**

Previously, we have shown that the majority of *B. distachyon* accessions are completely resistant to two diverse UK wheat stripe rust (*P. striiformis* f. sp. *tritici*, *Pst*) isolates, whereas relatively few accessions showed a range of infection symptoms in the form of leaf browning (Dawson *et al.* 2015). The pathogen was not able to complete its life cycle on *B. distachyon* and we developed a microscopy-based assay to measure hyphal growth within the leaf tissue (Dawson *et al.* 2015). To dissect the genetic architecture of resistance to stripe rust in *B. distachyon*, we mapped the underlying resistance loci for three *Pst* isolates and one barley stripe rust (*P. striiformis* f. sp. *hordei*, *Psh*) isolate in three diverse *B. distachyon* populations. These analyses highlighted that only three major resistance genes to *P. striiformis* seem to exist in *B. distachyon*, which we have named *Yrr1*, *Yrr2*, and *Yrr3* (*Yrr* = *Yellow rust resistance*). This was striking, as we tested geographically diverse *B. distachyon* lines from around the Mediterranean and phylogenetically diverse *P. striiformis* isolates. The results suggest that a natural stack of three resistance genes protects *B. distachyon* against colonisation by *P. striiformis* and highlights a relatively simple genetic architecture for intermediate nonhost resistance.

*Chapter 4. Isolation, fine-mapping, and characterisation of Yrr3, an intermediate nonhost resistance locus to stripe rust in *B. distachyon**

*Yrr3*, one of the major effect loci identified in the previous chapter, was isolated and fine-mapped in two independent *B. distachyon* populations. A recombination screen narrowed *Yrr3* down to two SNPs, which cause non-synonymous mutations in conserved motifs within nucleotide-binding domains of genes that are commonly associated with isolate-specific host resistance (i.e. the resistance to single isolates of adapted pathogens). The candidate genes are characterised based on resequencing data and RNAseq data for the different parental lines, as well as homology in other species. While it has been proposed that nonhost and host resistance are inherently different, the genetic architecture and molecular basis of resistance in this intermediate nonhost system is reminiscent of a host system, which suggests that the genetic architectures of host and nonhost systems are structurally coupled and share conserved components.

## 2. The genetic architecture of flowering regulation in *B. distachyon*

*The research presented in this chapter has been published in the journal Plant Physiology (<http://www.plantphysiol.org/>) and copyright rests with the American Society of Plant Biologists. The full publication details are:*

*Bettgenhaeuser J., Corke F.M.K., Opanowicz M., Green P., Hernández-Pinzón I., Doonan, J.H., Moscou M.J. (2017). Natural variation in *Brachypodium* links vernalization and flowering time loci as major flowering determinants. Plant Physiology. doi:10.1104/pp.16.00813*

One sentence summary: Natural variation in *Brachypodium distachyon* links *VRN2* and *FT* loci as major flowering determinants.

### Introduction

Coordination of flowering time with geographic location and seasonal weather patterns has a profound effect on flowering and reproductive success (Amasino 2010). The mechanisms underpinning this coordination are of great interest for understanding plant behaviour and distribution within natural ecosystems (Wilczek *et al.* 2010). Plants that fail to flower at the appropriate time are unlikely to be maximally fertile and therefore will be less competitive in the longer term. Likewise, optimal flowering time in crops is important for yield and quality: seed and fruit crops need to flower early enough to allow ripening or to utilise seasonal rains, while delayed flowering may be advantageous for leaf and forage crops (Distelfeld *et al.* 2009; Jung and Müller 2009).

Although developmental progression towards flowering can be modulated in several ways, many plants have evolved means to detect seasonal episodes of cold weather and adjust their flowering time accordingly, a process known as vernalisation (Ream *et al.* 2012). Despite the importance of flowering time, the molecular and genetic mechanisms underlying this dependency have been studied in only a few systems, notably the Brassicaceae, Poaceae, and Amaranthaceae (Andrés and Coupland 2012; Ream *et al.* 2012).

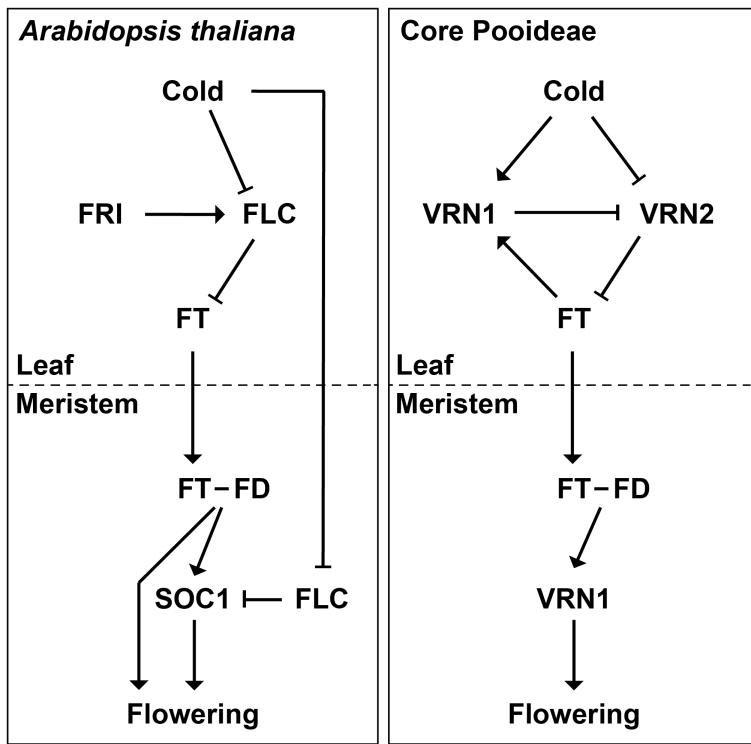


**Figure 1.** Vernalisation and flowering control in the model plant *Arabidopsis thaliana* and the core Pooideae (e.g. wheat and barley). Positive (FRIGIDA (FRI), VERNALISATION1 (VRN1), and FLOWERING LOCUS T (FT)) and negative (FLOWERING LOCUS C (FLC) and VERNALISATION2 (VRN2)) regulators of flowering in leaves are directly or indirectly influenced by cold exposure. Vernalisation results in *FT* expression in leaves, which then moves to the shoot apical meristem. *FT* interacts with FLOWERING LOCUS D (FD) in the shoot apical meristem and initiates flowering via the positive regulators SUPPRESSOR OF OVEREXPRESSIN OF CO1 (SOC1) and VRN1. Adapted from Bouché *et al.* (2017).

Research on the model plant *Arabidopsis thaliana* in particular has identified a pathway consisting of positive and negative regulators that control the vernalisation response and flowering (Figure 1) (Andrés and Coupland 2012; Bouché *et al.* 2017). Key to this vernalisation response is the perception of ambient temperature. Although the molecular basis of this perception remained largely unclear, early research already suggested that the light receptor phytochrome B may also be implicated in temperature perception (Penfield 2008; Legris *et al.* 2016b). Recent findings have confirmed that phytochrome B directly interacts with target genes and that altered reversion rates between active and inactive phytochrome B states account for the temperature dependency of these interactions (Jung *et al.* 2016; Legris *et al.* 2016a).

In the temperate grasses, three major *VERNALISATION* (*VRN*) genes appear to act in a regulatory loop (Figure 1). The wheat *VRN1* gene is a MADS-box transcription factor, which is induced in the cold (Yan *et al.* 2003; Andrés and Coupland 2012). This gene is related to the *A. thaliana* genes *APETALA1* and *FRUITFUL* (Yan *et al.*

2003; Andrés and Coupland 2012). *VRN2* encodes a small CCT-domain protein (Yan *et al.* 2004) that is repressed by *VRN1* and in turn represses *FLOWERING LOCUS T* (*FT*), a strong universal promoter of flowering (Kardailsky *et al.* 1999; Yan *et al.* 2006; Andrés and Coupland 2012; Ream *et al.* 2012). In cereals, active *VRN2* alleles are necessary for a vernalisation requirement. Spring barley and spring wheat varieties, which do not require vernalisation to flower, either lack *VRN2* (Dubcovsky *et al.* 2005; Karsai *et al.* 2005; von Zitzewitz *et al.* 2005), have point mutations in the conserved CCT domain (Yan *et al.* 2004), or possess dominant constitutively active alleles of *VRN1* (repressor of *VRN2*) (Yan *et al.* 2003; Fu *et al.* 2005) or *FT* (repressed by *VRN2*) (Yan *et al.* 2006).

Investigations on the regulation of flowering in the Poaceae have focused on rice (*Oryza sativa*), wheat (*Triticum aestivum*), and barley (*Hordeum vulgare*), all domesticated species that have been heavily subjected to human selection over the past 10,000 years. Little information is available on wild species within this family that have not been subjected to human selection. Such a study could provide additional insights into the standing variation present within wild systems and its likely pre-domestication adaptive significance in the Poaceae (Schwartz *et al.* 2010). A favourable species for such a study is *Brachypodium distachyon*, a small, wild grass, with a sequenced and annotated genome. *B. distachyon* was originally developed as a model system for the agronomically important temperate cereals (Draper *et al.* 2001; Opanowicz *et al.* 2008; The International Brachypodium Initiative 2010; Catalán *et al.* 2014). With the recent availability of geographically dispersed diversity collections, we can ask how wild grasses have adapted to different climatic zones.

Previous studies have begun to explore the molecular basis of vernalisation in this system. Higgins *et al.* (2010) identified homologs of the various flowering pathway genes in *B. distachyon*, and several mainly reverse genetic studies have focused on characterising these genes further (Schwartz *et al.* 2010; Lv *et al.* 2014; Ream *et al.* 2014; Woods *et al.* 2014; Woods *et al.* 2016). Schwartz *et al.* (2010) did not find complete correlation between expression of *VRN1* and flowering and hypothesised that *VRN1* could therefore have different activity or roles that are dependent on the genetic background. Yet, Ream *et al.* (2014) found low *VRN1* and *FT* levels in *B. distachyon* accessions with delayed flowering, suggesting a conserved role of these

homologs. Further support for a conserved role of *VRN1* and *FT* comes from the observation that overexpression of these genes leads to extremely early flowering (Lv *et al.* 2014; Ream *et al.* 2014) and RNAi-based silencing of *FT* and amiRNA-based silencing of *VRN1* prevent flowering (Lv *et al.* 2014; Woods *et al.* 2016). The role of *VRN2* in *B. distachyon* is less clear. Higgins *et al.* (2010) failed to identify a homolog of *VRN2* in *B. distachyon*; however, other studies identified Bradi3g10010 as the best candidate for the *B. distachyon* *VRN2* homolog (Schwartz *et al.* 2010; Ream *et al.* 2012). Recent research supports the functional conservation of *VRN2* in the role as a flowering repressor, but suggests that the regulatory interaction between *VRN1* and *VRN2* evolved after the diversification of the Brachypodieae and the core Pooideae (e.g. wheat and barley) (Woods *et al.* 2016).

To date most studies on the regulation of flowering time of *B. distachyon* have used reverse genetic approaches to implicate the role of previously characterised genes from other species (Higgins *et al.* 2010; Lv *et al.* 2014; Ream *et al.* 2014; Woods *et al.* 2016), while only few studies have used the natural variation present among *B. distachyon* accessions to identify flowering loci (Tyler *et al.* 2016; Wilson *et al.* 2016). Currently lacking is the characterisation of loci that control variation in flowering time in a biparental *B. distachyon* mapping population. The Iraqi reference accession Bd21 does not require vernalisation (Vogel *et al.* 2006; Garvin *et al.* 2008) and in addition, vernalisation does not greatly reduce time to flowering in a 16 h or 20 h photoperiod (Schwartz *et al.* 2010; Ream *et al.* 2014). In contrast, the Spanish accession ABR6 can be induced to flower following a six-week vernalisation period (Draper *et al.* 2001; Routledge *et al.* 2004).

In this chapter, I report on the genetic architecture underlying flowering time in a mapping population developed from ABR6 and Bd21. We observed the segregation of vernalisation dependency during population advancement (Figure 2) and characterised the genetic basis of this dependency in detail at the F<sub>4:5</sub> stage in multiple environments (i.e. by phenotyping F<sub>5</sub> progeny derived from genotyped F<sub>4</sub> lines). The ability to flower without vernalisation was linked to three major loci, two of which colocalise with the *B. distachyon* homologs of *VRN2* and *FT*. Notably, our results further support the role of the *VRN2* locus as a conserved flowering time regulator in *B. distachyon*.

## Results

### *Development of a B. distachyon mapping population between geographically and phenotypically distinct accessions*

Initial investigations into the flowering time of ABR6 and Bd21 in response to different vernalisation periods showed contrasting effects on the two accessions (Figure 2; Figure 3). ABR6 responded strongly to increasing vernalisation times with a reduction in flowering by 93 days, ranging from 117 days for a two-week vernalisation period to 24 days for an eight-week vernalisation period. This reduction in flowering time for ABR6 was not linear and the greatest drop of 43 days occurred between four and five weeks of vernalisation (Figure 3). In contrast, no statistically significant difference was found with respect to the vernalisation response of Bd21, although a consistent trend towards a reduced flowering time was observed. A cross was generated from these phenotypically diverse accessions for the creation of a recombinant inbred line population.



**Figure 2.** Flowering behaviour within the ABR6 x Bd21 mapping population. Three months after a six-week vernalisation period, ABR6 (left) is not flowering, whereas Bd21 (centre) is flowering and an individual in the ABR6 x Bd21 mapping population displays an intermediate flowering phenotype (right).

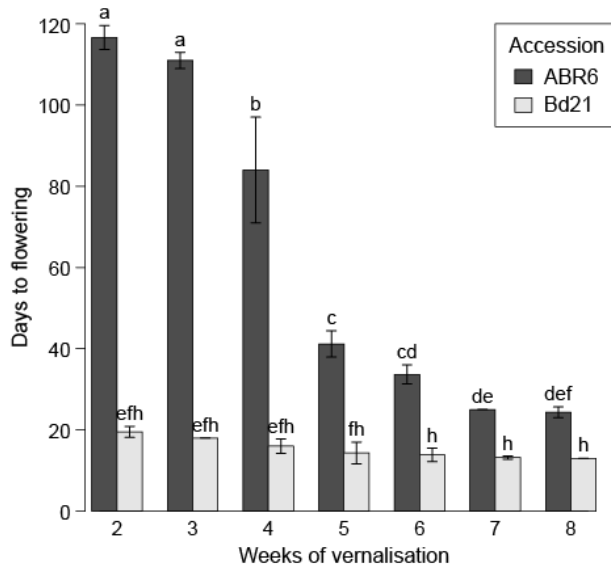


**Figure 3.** Effect of vernalisation on flowering time in ABR6 and Bd21. Days to flowering was measured from the end of vernalisation for seven different vernalisation periods. After vernalisation plants were grown in a growth chamber (16 h photoperiod) for 35 days and then transferred to a greenhouse without light and temperature control (late April to mid July 2013; Norwich, UK). Mean days to flowering and standard error are based on six biological replicates. Different letters represent statistically significant differences based on pairwise comparisons using *t*-tests with pooled standard deviations and Bonferroni correction for multiple comparisons.

To develop a SNP-based genetic map, ABR6 was resequenced and reads were aligned to the reference genome. A total of 1.36 million putative SNPs were identified between ABR6 and Bd21, of which 711,052 constituted non-ambiguous polymorphisms based on a minimum coverage of 15x and a strict threshold for SNP calling (i.e. 100% of reads with an ABR6 allele, 0% of reads with a Bd21 allele). Following iterative cycles of marker selection, the final genetic map consists of 252 non-redundant markers and has a cumulative size of 1,753 cM (Figure S1). This size is comparable to the previously characterised Bd3-1 x Bd21 mapping population (Huo *et al.* 2011) and confirms that *B. distachyon* has a high rate of recombination compared to other grass species. The quality of the genetic map was verified by assessing the two-way recombination fractions for all 252 markers (Figure S2). All five chromosomes were scanned for segregation distortion by comparing observed and expected genotype frequencies for each marker. The expected heterozygosity at the F<sub>4</sub> stage is 12.50% and the expected parental allele frequencies are 43.75% for ABR6 and Bd21 alleles, respectively. Although all five chromosomes contained regions of potential segregation distortion (Figure 4), only two loci on chromosomes Bd1 (peak at 474.1 cM) and Bd4 (peak at 77.0 cM) deviated significantly from these expected frequencies.

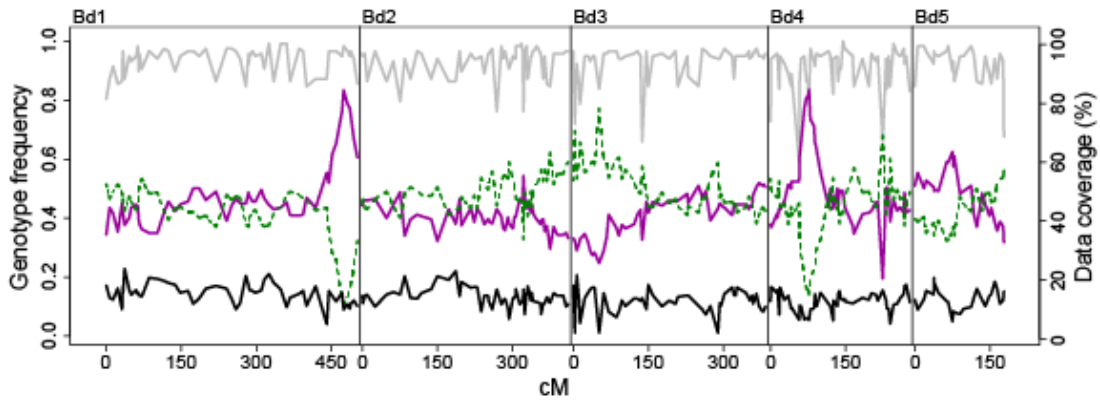


**Figure 4.** Segregation distortion in the ABR6 x Bd21 F<sub>4</sub> population. For each marker of the genetic map the frequencies of F<sub>4</sub> individuals with homozygous ABR6 genotype (solid magenta), homozygous Bd21 genotype (dashed green), or heterozygous genotype (solid black) were calculated (scale on left). Data coverage (percent of F<sub>4</sub> individuals with genotype calls per marker) is represented by the grey line (scale on right).

#### *Multiple QTLs control flowering in the ABR6 x Bd21 mapping population*

We evaluated the ABR6 x Bd21 F<sub>4:5</sub> population in a number of environments to identify the genetic architecture underlying flowering time (Table S1). Four sets of the population were grown without vernalisation, whereas in one additional set flowering was scored in response to six weeks of vernalisation. In all experiments, the population was exposed to natural light, although in three experiments supplemental light was used to ensure a minimum 16 h or 20 h growth period. In addition, two experiments did not have any temperature control (i.e. plants were exposed to the natural temperature in the greenhouse), two experiments had the temperature controlled at 22°C/20°C during light/dark cycles, and one experiment had the temperature maintained at a minimum of 18°C/11.5°C during light/dark cycles.

Analysis of the non-vernalised environments revealed a bimodal distribution between families that flowered and families that did not flower (Figure 5). However, considerable residual variation in flowering time existed among the flowering families. For example, in Environment 5 flowering occurred over a 42-day period from 63 days to 105 days after germination (Figure 5E). Flowering in the other non-vernalised environments occurred over a similar time period (Figure 5). Interestingly, transgressive segregation for early and late flowering phenotypes was observed in Environment 4 (Figure 5D).

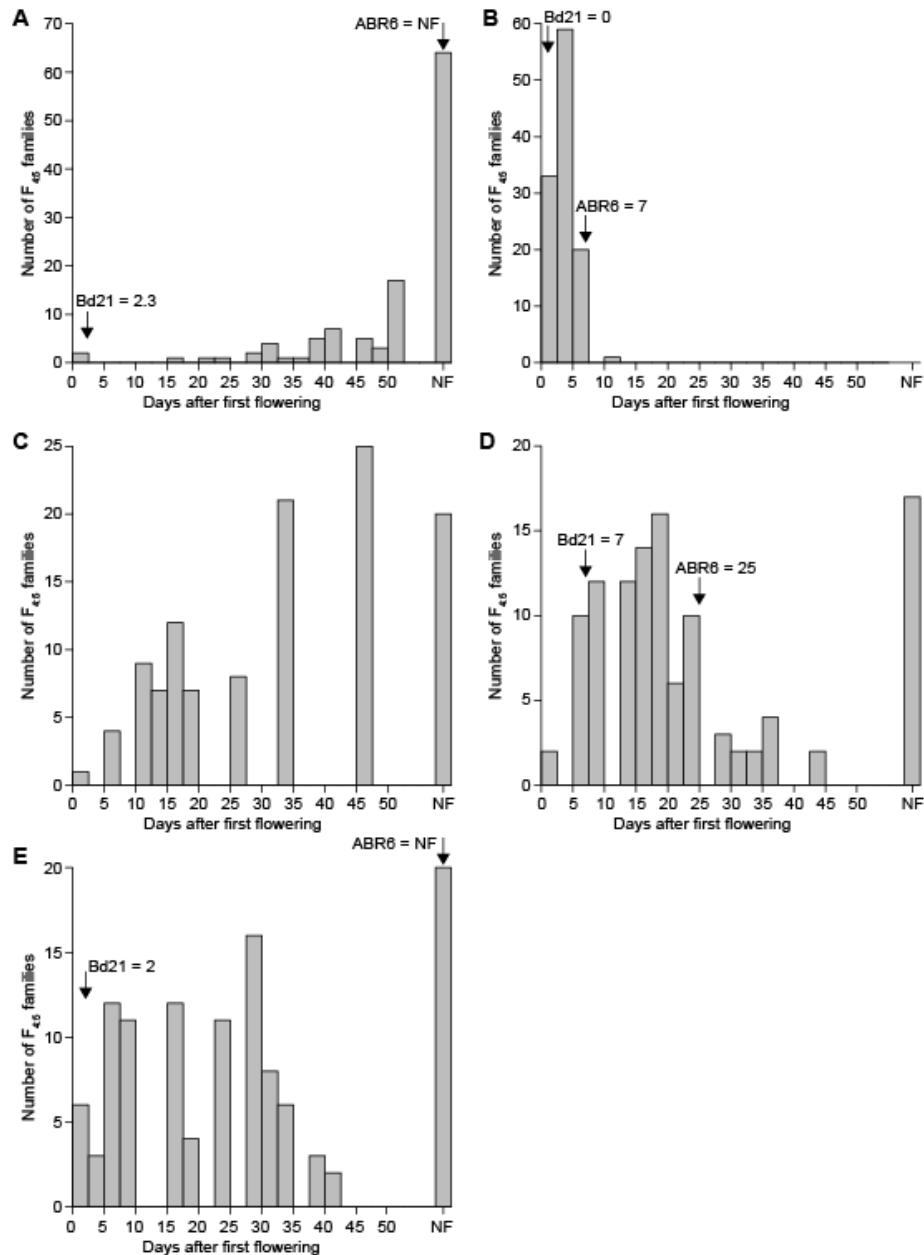


**Figure 5.** Frequency distribution of flowering time in the ABR6 x Bd21 population. Flowering time was measured from the first day that flowering was observed in the entire population. (A) Environment 1 (April to July, natural light supplemented for 20h, 22°C/20°C, no vernalisation), (B) Environment 2 (April to July, natural light supplemented for 20h, 22°C/20°C, six weeks vernalisation), (C) Environment 3 (May to July, natural light and temperatures, no vernalisation), (D) Environment 4 (September to November, natural light supplemented for 16h, minimum 18°C/11.5°C, no vernalisation), (E) Environment 5 (March to May, natural light and temperatures, no vernalisation). Flowering times for the parental lines are indicated by arrows (no data for Environment 3). NF = not flowering.

Phenotypes in the vernalised environment were heavily skewed towards early flowering (Figure 5B). Only limited residual variation existed among the vernalised F<sub>4.5</sub> families and all plants flowered within 11 days from the first observation of flowering in the population. The variation in flowering time for all five environments was found to be not normally distributed.

**Table 1.** Significant flowering time QTLs (*qFLT*) in the different environments identified using several binary, non-parametric, and parametric approaches.

Locus	Chr <sup>a</sup>	cM	Allele <sup>b</sup>	E1 <sup>c</sup>	E2	E3	E4	E5
<i>qFLT1</i>	Bd1	297.6	Bd21	B, T2, T3, NP <sup>d</sup>	T1, T3, NP	T2, T3, NP	T2, T3	T1, T2, T3, NP
<i>qFLT2</i>	Bd1	465.2	Bd21	T2	-	-	-	-
<i>qFLT3</i>	Bd2	338.3	ABR6	-	-	-	NP	T2, T3
<i>qFLT4</i>	Bd2	409.0	Bd21	-	T1, T3	-	-	-
<i>qFLT5</i>	Bd3	60.8	Bd21	-	-	-	T1	-
<i>qFLT6</i>	Bd3	91.2	Bd21	T2, T3	T1, T3	T2, T3	-	-
<i>qFLT7</i>	Bd3	294.6	Bd21	-	-	-	T2, T3, NP	B, T2, T3, NP
<i>qFLT8</i>	Bd4	90.1	Bd21	-	-	-	NP	-

<sup>a</sup>Chromosome

<sup>b</sup>Allele that reduces flowering time

<sup>c</sup>Environment (see Table S1)

<sup>d</sup>QTL analyses were performed with interval mapping using binary classification (B) and non-parametric analysis (NP), and composite interval mapping using transformed data (T1, T2, and T3).

Among these diverse environments, QTL analyses using binary and non-parametric models (i.e. models that do not assume a normal distribution of the data) were conservative in detecting QTLs controlling flowering time (*qFLT*) (Table 1; Table S2 and Table S3), whereas transformation of flowering time consistently identified QTLs between environments (Table 1 and Table 2; Table S4 and Table S5). Three major QTLs were identified on chromosomes Bd1 and Bd3 that were robustly observed using parametric and non-parametric mapping approaches (Table 1 and Table 2; Figure 6).

**Table 2.** Significant QTLs from composite interval mapping of transformed flowering time phenotypes (T3) in the ABR6 x Bd21 F<sub>4:5</sub> families.

ENV <sup>a</sup>	Locus	Chr <sup>b</sup>	cM	EWT <sup>c</sup>	LOD	AEE <sup>d</sup>	PVE <sup>e</sup>	1-LOD SI <sup>f</sup>
1	<i>qFLT1</i>	Bd1	297.6	3.06	12.96	2.87	36.3%	296.1 - 305.6
1	<i>qFLT6</i>	Bd3	91.2	3.06	4.51	1.64	11.8%	ND
2	<i>qFLT1</i>	Bd1	297.6	3.09	7.59	0.82	20.0%	296.1 - 305.6
2	<i>qFLT4</i>	Bd2	409.0	3.09	3.20	0.47	6.7%	403.2 - 411.0
2	<i>qFLT6</i>	Bd3	93.2	3.09	6.64	0.79	18.2%	72.9 - 97.0
3	<i>qFLT1</i>	Bd1	297.6	3.20	8.61	1.50	31.1%	292.1 - 303.6
3	<i>qFLT6</i>	Bd3	91.2	3.20	5.69	1.20	18.7%	74.9 - 97.0
4	<i>qFLT1</i>	Bd1	297.6	3.19	3.49	1.77	15.9%	292.1 - 305.6
4	<i>qFLT7</i>	Bd3	294.6	3.19	3.79	1.59	14.0%	273.9 - 300.7
5	<i>qFLT1</i>	Bd1	297.6	3.17	8.62	3.43	37.5%	294.1 - 301.6
5	<i>qFLT3</i>	Bd2	338.3	3.17	3.70	-1.75	9.9%	323.7 - 348.0
5	<i>qFLT7</i>	Bd3	294.6	3.17	5.61	2.02	13.6%	275.9 - 302.0

<sup>a</sup>Environment (see Table S1)

<sup>b</sup>Chromosome

<sup>c</sup>Experiment-wide permutation threshold

<sup>d</sup>Additive effect estimate for transformed phenotypes

<sup>e</sup>Percent of phenotypic variance explained

<sup>f</sup>One-LOD support interval (cM); ND denotes QTLs not detected using standard interval mapping.

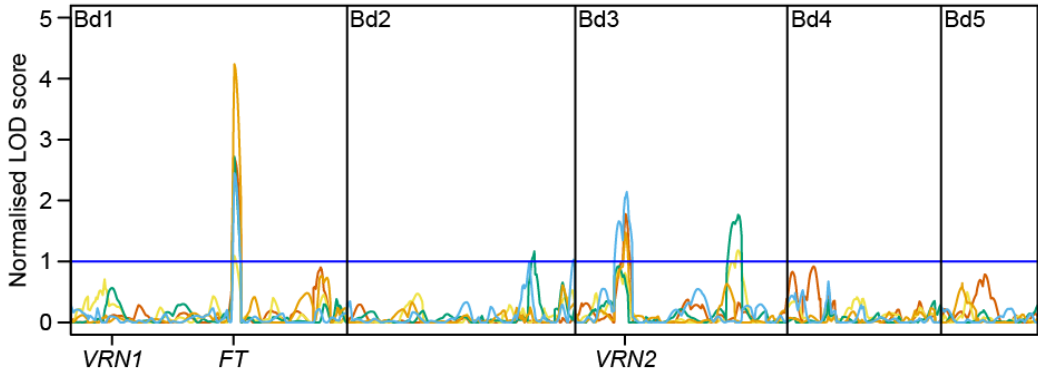


**Figure 6.** Linkage mapping of flowering time in the ABR6 x Bd21 population. Time to flowering for 114 F<sub>4:5</sub> families of the population was transformed into ordered rank values, QTL analysis performed using composite interval mapping under an additive model hypothesis test ( $H_0$ : $H_1$ ), and plotted based on normalised permutation thresholds. The blue horizontal line represents the threshold of statistical significance based on 1,000 permutations. Orange = Environment 1 (April to July, natural light supplemented for 20h, 22°C/20°C, no vernalisation), blue = Environment 2 (April to July, natural light supplemented for 20h, 22°C/20°C, six weeks vernalisation), red = Environment 3 (May to July, natural light and temperatures, no vernalisation), yellow = Environment 4 (September to November, natural light supplemented for 16h, minimum 18°C/11.5°C, no vernalisation), green = Environment 5 (March to May, natural light and temperatures, no vernalisation). See Table S1 for full environmental details. The genetic positions of the previously identified homologs of *VRN1*, *VRN2*, and *FT* are indicated (compare Higgins *et al.* 2010 and Ream *et al.* 2012).

The QTL on Bd1 (*qFLT1*, peak marker Bd1\_47808182) appeared to be the major locus governing flowering time in this population, as it was the major QTL in all five environments, explaining the most phenotypic variation (phenotypic variance explained; PVE) compared to any other QTL (Table 2). PVE values for this locus ranged from 15.9% to 37.5%. Another QTL on Bd3 (*qFLT6*, peak marker Bd3\_8029207) was also detected in all five studies, though its contribution was only significant in three environments. PVE values for the statistically significant QTLs ranged from 11.8% to 18.7%. Bd21 alleles at these two loci promoted early flowering, whereas individuals with ABR6 alleles at both loci had maximal flowering time or did not flower within the timescale of the experiment (Figure 7).

Interestingly, in the two environments where this former locus did not have a significant contribution, two other QTLs were identified. A QTL on Bd3 (*qFLT7*, peak marker Bd3\_44806296) explained 13.6% and 14.0% of the variation observed in these studies and a QTL on Bd2 (*qFLT3*, peak marker Bd2\_53097824) was identified through a combination of non-parametric and parametric analyses of Environments 4 and 5. Additional QTLs on Bd1 (*qFLT2*), Bd2 (*qFLT4*), Bd3 (*qFLT5*), and Bd4 (*qFLT8*) were not significant in more than one of the environments tested (Table 1).

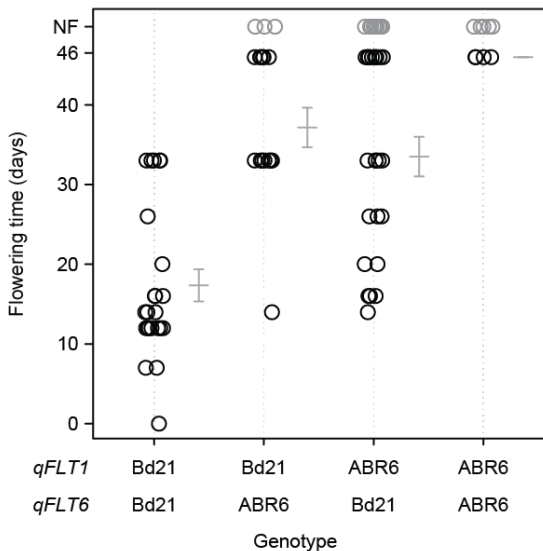


**Figure 7.** Phenotype by genotype plot for the two major loci controlling flowering time in the ABR6 x Bd21 mapping population. Days to flowering in Environment 3 for the ABR6 x Bd21 F<sub>4:5</sub> families homozygous at *qFLT1* and *qFLT6* shows that the Bd21 alleles at these two loci promote early flowering. Error bars represent one standard error; NF = not flowering.

Previous studies identified the *B. distachyon* homologs of flowering regulators from *Arabidopsis*, wheat, barley, and rice (Higgins *et al.* 2010; Ream *et al.* 2012). The one-LOD support intervals of all statistically significant QTLs were combined to identify the maximal one-LOD support interval for each QTL. Several of the previously identified *B. distachyon* homologs of flowering regulators are candidate genes underlying these QTLs (Table 3).

**Table 3.** Previously identified *B. distachyon* homologs of flowering regulators in *Arabidopsis* (*At*), hexaploid and diploid wheat (*Ta* and *Tm*), barley (*Hv*), and rice (*Os*) within the one-LOD support intervals of the statistically significant QTLs under transformation T3.

List of the statistically significant QTLs under transformation 13				
Locus	Chr <sup>a</sup>	1-LOD SI <sup>b</sup>	<i>B. distachyon</i> gene	Homologous genes <sup>c</sup>
<i>qFLT1</i>	Bd1	292.1 - 305.6	Bradi1g45810	<i>AtAGL24, TaVRT2, OsMADS55</i>
			Bradi1g46060	<i>AtABF1</i>
			Bradi1g48340	<i>AtCLF, OsCLF</i>
			Bradi1g48830	<i>AtTSF, HvFT1, OsHd3a/OsFTL2</i>
<i>qFLT3</i>	Bd2	323.7 - 348.0	Bradi2g53060	<i>AtFDP</i>
			Bradi2g54200	<i>AtNF-YB10</i>
			Bradi2g55550	<i>AtbZIP67</i>
<i>qFLT4</i>	Bd2	403.2 - 411.0	Bradi2g60820	<i>AtFY, OsFY</i>
			Bradi2g62070	<i>AtLUX, OsLUX</i>
<i>qFLT6</i>	Bd3	72.9 - 97.0	Bradi3g08890	<i>OsFTL13</i>
			Bradi3g10010	<i>TaVRN2, TmCCT2, OsGhd7</i>
			Bradi3g12900	<i>AthUA2</i>
<i>qFLT7</i>	Bd3	273.9 - 300.7	Bradi3g41300	<i>OsMADS37</i>
			Bradi3g42910	<i>AtSPY, OsSPY</i>
			Bradi3g44860	<i>OsRCN2</i>

<sup>a</sup>Chromosome

<sup>b</sup>Combined maximal one-LOD support interval (cM) from all significant OTLs

<sup>c</sup>Identified in Higgins *et al.* 2010 and Ream *et al.* 2012

Although several homologs fall within the one-LOD support intervals of *qFLT1* on Bd1 (292.1 - 305.6 cM) and *qFLT6* on the short arm of Bd3 (72.9 - 97.0 cM), these loci also harbour the *B. distachyon* homologs of *FT* (Bradi1g48830) and *VRN2* (Bradi3g10010), which have been previously implicated in flowering time regulation in *B. distachyon* through a series of mainly reverse genetic studies (Lv *et al.* 2014; Ream *et al.* 2014; Woods *et al.* 2014; Woods *et al.* 2016).

#### *Natural variation in FT and VRN2*

Analysis of the resequencing and RNAseq data allowed an initial evaluation of candidate genes underlying these QTLs. A *de novo* assembly was created from the ABR6 resequencing reads and the resulting contigs were probed with the Bd21 sequences of *FT* (Bradi1g48830) and *VRN2* (Bradi3g10010), enabling the identification of structural variation between ABR6 and Bd21 (Figure 8; Table S6). Spliced alignment of RNAseq reads permits further characterisation of candidate genes underlying an identified QTL through the confirmation of polymorphisms between two parental genotypes, verification of annotated candidate gene models, qualitative assessment of expression of candidate genes in the sampled tissue, and discovery of potential splice variants.

No polymorphisms were found in the coding sequence of Bradi1g48830, the *B. distachyon* homolog of *FT*. However, two indels (two and four bp, respectively) and a SNP mapped to the 3'-UTR. Additionally, two SNPs and three indels (including a 33 bp indel 590 bps upstream of Bradi1g48830) were found in the promoter region (2 kb upstream). The terminator region (2 kb downstream) contained three SNPs and four indels. Bradi1g48830 was not expressed in ABR6 and barely detectable in Bd21 (only two reads mapped to the gene). Owing to the low expression, it was not possible to confirm the published gene model with our RNAseq data.

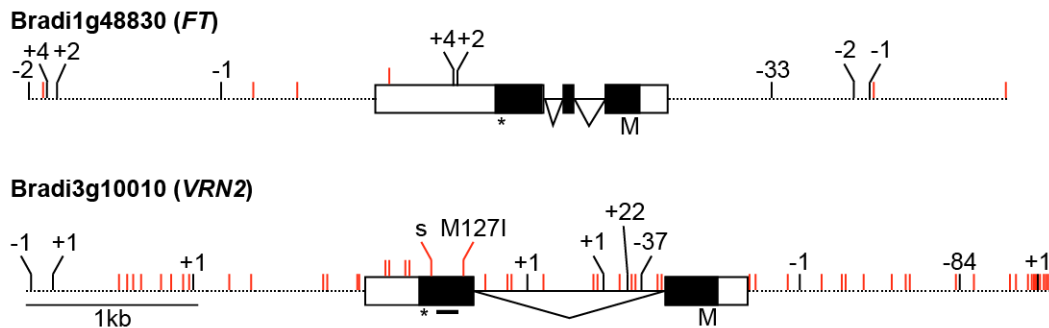


**Figure 8.** Comparison of the flowering regulators *FT* and *VRN2* between the *B. distachyon* accessions Bd21 and ABR6. Contigs of the ABR6 *de novo* assembly were aligned to the Bd21 reference sequence (Version 3) and polymorphisms were identified in the genes of interest and 2 kb promoter and terminator sequence (1.9 kb promoter for *VRN2*). Red ticks represent SNPs and black ticks represent indels. The length of indels (bp) is shown with + for insertion and – for deletion. The amino acid change of the non-synonymous SNP in *VRN2* is indicated. s = synonymous SNP; dashed line = promoter or terminator; white box = 5'-UTR or 3'-UTR; black box = exon; black line = intron; M = methionine/translation start; star = translation stop; black bar under *VRN2* = CCT domain.

Greater sequence variation was observed at Bradi3g10010, the *B. distachyon* homolog of *VRN2*, and its flanking regions. Only 1.9 kb of the promoter region is present on the Bradi3g10010 contig, but this region contains 29 SNPs and three indels (including an 84 bp indel 1.4 kb upstream of Bradi3g10010). The 2 kb terminator region contains 14 SNPs and three 1 bp indels. Additionally, 11 SNPs and four indels (including a 37 bp and a 22 bp indel) were localised in the intron, two SNPs in the coding sequence, and four SNPs in the 3'-UTR. Bradi3g10010 was expressed in leaves from both Bd21 and ABR6 and spliced alignment of RNAseq reads confirmed the published annotation of Bradi3g10010 for both ABR6 and Bd21. Moreover, the six SNPs predicted in the exons were supported by the RNAseq data and these may contribute to the observed effect on flowering time in this mapping population. Two SNPs map to the annotated coding sequence and four SNPs map to the 3'-UTR. One of the two SNPs in the annotated coding sequence is predicted to cause a non-synonymous mutation (Figure 8).

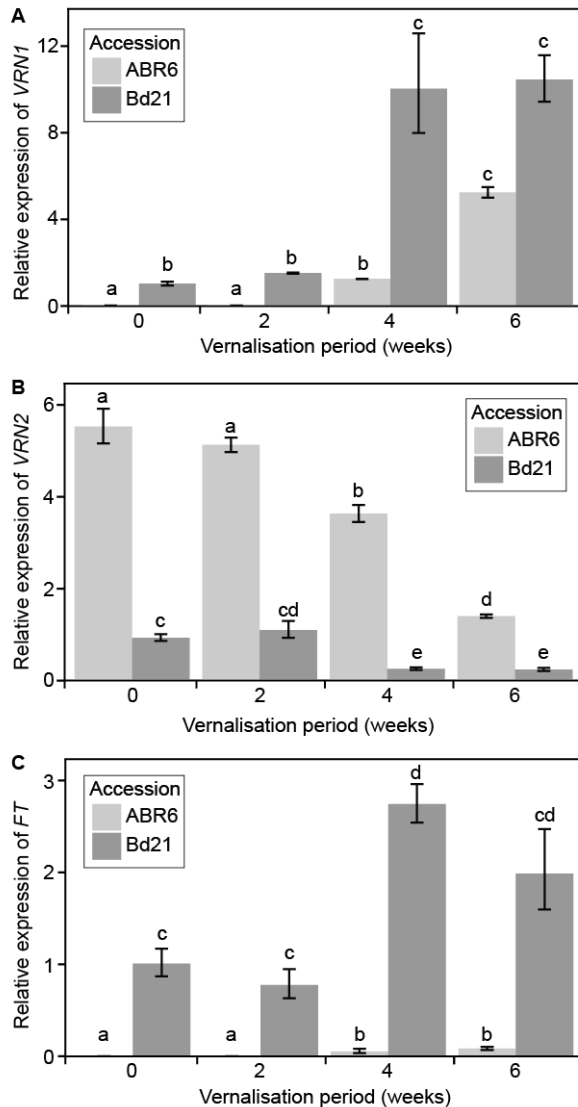


**Figure 9.** *VRN1*, *VRN2*, and *FT* expression in fourth leaf of ABR6 and Bd21 after varying periods of cold treatment. Seeds were imbibed with water and not vernalised or vernalised for two, four, or six weeks, and transferred to a growth chamber with parameters similar to Environment 2. Fully expanded fourth leaves were harvested in the middle of the photoperiod. Relative gene expression of *VRN1* (A), *VRN2* (B), and *FT* (C) was determined using RT-qPCR and analysed using the  $2^{-\Delta\Delta Ct}$  method. All genes were normalised to 1 based on Bd21 expression with no cold treatment (0 weeks) and *UBQ18* was used as internal control. Bars represent the mean of three biological replicates with error bars showing  $\pm 1$  standard error. Different letters represent statistically significant differences based on pairwise *t*-tests using a multiple hypothesis corrected *p*-value threshold of 0.05 with the Benjamini-Hochberg approach.

#### *Expression of VRN1, VRN2, and FT in response to vernalisation*

To understand the transcriptional dynamics of *VRN1*, *VRN2*, and *FT* in response to vernalisation, we assessed steady state levels of mRNA expression in plants at the fourth leaf stage after exposure to two, four, and six weeks of vernalisation at 5°C or to no vernalisation (Figure 9). *VRN1* and *FT* had a similar pattern in steady state levels

of gene expression in response to vernalisation (Figure 9A and 9C). For both genes, very low levels of expression were observed in ABR6, whereas Bd21 had fairly high levels of transcript abundance. After experiencing four weeks of vernalisation, ABR6 had similar levels of *VRN1* transcript as Bd21 without vernalisation treatment. In contrast, *FT* expression had a marginal increase after four and six weeks of vernalisation in ABR6 relative to no vernalisation or two weeks of vernalisation. *FT* expression levels were significantly lower than Bd21 across all periods of vernalisation. Both *VRN1* and *FT* expression increased significantly between Bd21 samples vernalised for two or four weeks. *VRN2* expression in ABR6 was inversely correlated with the length of vernalisation, with similar levels of expression after no vernalisation and two weeks vernalisation and increasingly lower levels of expression after four and six weeks of vernalisation (Figure 9B). Bd21 exhibited a similar reduction in *VRN2* expression, although lower levels of expression were observed without vernalisation compared to ABR6 with six weeks vernalisation. The trends of all three genes highlighted the importance of at least four weeks of vernalisation as the inflection point in transcriptional abundance, which coincides with a significant reduction in days to flowering in ABR6 (Figure 3).

## Discussion

In our advancement of the ABR6 x Bd21 population, we observed substantial variation in flowering time. To define the genetic architecture of flowering time, we developed a comprehensive genetic map and assessed F<sub>4:5</sub> families in multiple environments. We uncovered three major QTLs, with two QTLs coincident with the *B. distachyon* homologs of *VRN2* and *FT*. Interestingly, *VRN1* was not associated with flowering time and was found to have no mutations within the transcribed sequence (Table S6). Further minor effect QTLs were identified, suggesting that additional regulators play a role in controlling flowering time in *B. distachyon*.

### *Segregation distortion in the ABR6 x Bd21 population*

Segregation distortion is a common observation in the development of mapping populations in plants, including grasses such as rice, *Aegilops*, maize, or barley (Xu *et al.* 1997; Faris *et al.* 1998; Lu *et al.* 2002; Muñoz-Amatriaín *et al.* 2011). In the ABR6

x Bd21 population, significant deviation from expected genotype frequencies was observed at two loci on chromosomes Bd1 and Bd4 (Figure 4). Interestingly, heterozygosity was not affected at these loci, but the ABR6 allele was overrepresented. It is likely that these loci are linked to traits that were inadvertently selected during population advancement based on genetic and/or environmental factors. Several genetic mechanisms can contribute to segregation distortion in intraspecific crosses, including hybrid necrosis (Bomblies and Weigel 2007), genes involved in vernalisation requirement and flowering time (such as the *vrn2* locus in the Haruna Nijo x OHU602 doubled-haploid barley population (Muñoz-Amatriaín *et al.* 2011)), or preferential transmission of a specific parental genotype. While segregation distortion at these loci was not associated with the identified flowering time QTLs, canonical resistance genes encoding nucleotide-binding, leucine-rich repeat proteins are present at the Bd4 locus (Bomblies *et al.* 2007; Tan and Wu 2012).

#### *The genetic architecture of flowering time in B. distachyon*

In *Arabidopsis*, natural variation has been used as a complementary forward genetics-based approach for investigating flowering time (Koornneef *et al.* 2004). In our work, we identified two major QTLs controlling flowering time (*qFLT1* and *qFLT6*; Figure 7) in both vernalised and non-vernalised environments that colocalised with the *B. distachyon* homologs of *FT* (Bradi1g48830) and *VRN2* (Bradi3g10010). These observations are consistent with previous reverse genetic studies on the role of *FT* and *VRN2* in controlling flowering time (Lv *et al.* 2014; Ream *et al.* 2014; Woods *et al.* 2014; Woods *et al.* 2016). Two additional QTLs on chromosomes Bd2 (*qFLT3*) and Bd3 (*qFLT7*) were detected in two environments, whereas four minor effect QTLs (*qFLT2*, *qFLT4*, *qFLT5*, and *qFLT8*) were found in individual environments only. Two recent genome-wide association studies (GWAS) used the natural variation found within *B. distachyon* germplasm to identify SNPs associated with flowering time (Tyler *et al.* 2016; Wilson *et al.* 2016). Tyler *et al.* (2016) identified nine significant marker-trait associations, none of which overlap with the QTLs identified in our study. In contrast, Wilson *et al.* (2016) identified a much simpler genetic architecture consisting of three significant marker-trait associations, one of which could be linked to *FT*. These additional QTLs and marker-trait associations identified in our study and the GWAS studies could either correspond to one of the identified

homologs of flowering genes in *B. distachyon* (Table 3; compare Higgins *et al.* 2010) or constitute novel loci as hypothesised by Schwartz *et al.* (2010). With the exception of the proximal QTL on Bd2 (*qFLT3*), all alleles that prolonged time to flowering in our study were contributed by ABR6 (Table 1). Bd21 has previously been classified as a “spring annual” (Schwartz *et al.* 2010) or “extremely rapid flowering” (Ream *et al.* 2014). However, increased vernalisation times still led to a modest reduction in flowering time (Figure 3), which is explained by the detection of a QTL contributed by Bd21.

We hypothesised that structural variation between ABR6 and Bd21 would underlie the observed variation in flowering time. No structural variation in *FT* was observed between ABR6 and Bd21 in the coding sequence, however, several indels map to the promoter region (Figure 8). These polymorphisms may explain expression differences between these two accessions. As expected, no *FT* expression was found in ABR6 seedlings, and only two Bd21 RNAseq reads mapped to this gene. Steady-state expression levels of *FT* in the fourth leaf were significantly lower in ABR6 relative to Bd21 without vernalisation (Figure 9C). After four weeks vernalisation, *FT* expression levels increased in ABR6, although they were significantly lower than Bd21 steady-state levels after any level of vernalisation. It was previously shown that in barley, wheat, and *B. distachyon*, *FT* expression is upregulated after vernalisation (Sasani *et al.* 2009; Chen and Dubcovsky 2012; Ream *et al.* 2014). Our observations indicate that *FT* is expressed in Bd21 and increases less than *VRN1* in response to vernalisation. In contrast, *FT* in ABR6 only increases marginally after four weeks of vernalisation and remains significantly below the levels observed in Bd21 after no vernalisation.

Interestingly, an intact copy of the flowering repressor *VRN2* is also present in Bd21 (Ream *et al.* 2012), which does not have a strong vernalisation response (Vogel *et al.* 2006; Garvin *et al.* 2008). The lack of vernalisation requirement in some *B. distachyon* accessions cannot, therefore, be explained by an absence of *VRN2* (Ream *et al.* 2012). Intriguingly, early-flowering mutants identified in genetic screens have thus far not mapped in the *VRN2* region (Ream *et al.* 2014). Moreover, expression levels for *VRN2* also did not vary among early and late flowering accessions and *VRN2* mRNA levels are likely not rate limiting (Ream *et al.* 2014). An earlier study by Schwartz *et al.* (2010) described potential correlation between different *VRN2* alleles and flowering

time. The authors did not rule out the effects of population structure and proposed that elucidating the role of *VRN2* in *B. distachyon* will require more in-depth genetic studies. A recent comprehensive analysis of population structure in *B. distachyon* collections revealed that flowering time, and not geographic origin, is indeed the major distinguishing factor between genotypically distinct clusters (Tyler *et al.* 2016). Our results confirm *VRN2* as an important flowering regulator in the ABR6 x Bd21 mapping population and highlight structural and expression variation between parental accessions. However, none of the SNPs identified in the coding sequence map to the CCT domain. A point mutation in this domain results in a spring growth habit in cultivated *Triticum monococcum* accessions (Yan *et al.* 2004). It is unclear whether the structural variation surrounding *VRN2* corresponds to the allelic variation observed by Schwartz *et al.* (2010). We observed a negative correlation between *VRN2* transcript accumulation and vernalisation period in ABR6 and Bd21 (Figure 9B). Similar decreases were observed for ABR6 and Bd21, although transcript abundance in Bd21 were significantly lower than ABR6 under any vernalisation period. Ream *et al.* (2014) also observed a slight reduction in *VRN2* expression post-vernalisation in the *B. distachyon* accessions Bd21, Bd21-3, and Bd1-1. However, the authors also note that the decreased post-vernalisation expression is in contrast to increased expression during vernalisation. Woods and Amasino (2016) hypothesise that even though *VRN2* may not be involved in vernalisation control in *B. distachyon*, it may still possess an ancestral role in flowering regulation. This is further supported by the observation that *VRN2* expression is not controlled by *VRN1* in *B. distachyon*, yet *VRN2* was found to be a functional repressor of flowering in this species (Woods *et al.* 2016). Among other findings, the authors base this conclusion on the fact that *VRN2* expression in non-core pooids (i.e. also in *B. distachyon*) also decreases after a control warm treatment (Woods *et al.* 2016). Therefore, our identification of natural variation in *VRN2* among geographically diverse *B. distachyon* accessions further supports *VRN2* as a core flowering regulator in this non-domesticated grass. As our RT-qPCR analysis focused on expression post-vernalisation, it remains unclear how *VRN2* expression levels may have differed during cold treatment. If, as Woods and Amasino (2016) suggest, *VRN2* can have two different functions (i.e. a flowering regulator in non-core pooids and a vernalisation regulator in the core pooids), this may explain the ambiguity obtained when interpreting *VRN2* expression data in *B. distachyon*.

In our study of the natural variation between two morphologically and geographically diverse *B. distachyon* accessions we failed to implicate *VRN1* as a flowering regulator. However, *VRN1* expression during and after cold treatment and the failure of *VRN1* silenced lines to flower suggests a conserved role of *VRN1* as a promoter of flowering (Woods and Amasino 2016; Woods *et al.* 2016). Interestingly, a QTL in the Bd21 x Bd1-1 *B. distachyon* mapping population colocalised with *VRN1* and the light receptor *PHYTOCHROME C (PHYC)* (Woods *et al.* 2017). Between ABR6 and Bd21, sequence variation was found in the promoter and terminator regions of *VRN1* and a strong positive correlation was observed with extended periods of vernalisation (Figure 9A), particularly at four weeks vernalisation, which was a critical inflection point for flowering time in ABR6. Despite this sequence and expression variation, *VRN1* was not found to contribute to flowering time in the ABR6 x Bd21 mapping population. Interestingly, an assessment of allelic variation in 53 *B. distachyon* accessions currently available in Phytozome (Version 11.0.2, <https://phytozome.jgi.doe.gov>) found that none of these accessions possess structural variation in the *VRN1* annotated coding sequence. These findings suggest that *VRN1* is a crucial regulator of flowering in *B. distachyon* and under strong selection pressure.

### *Conclusions*

Thanks to their economic and evolutionary importance, flowering time pathways are of particular interest in the cereals and related grasses. Our report adds to this body of research by using natural variation to map vernalisation dependency in a *B. distachyon* mapping population. Since *B. distachyon* is partly sympatric with the wild relatives of wheat and barley, it seems likely that the species would have been subject to similar selective pressure and therefore is a useful model for understanding pre-domestication or standing variation. We investigated this standing variation by assessing segregation of flowering regulators in a mapping population derived from two geographically diverse accessions of *B. distachyon*. Notably, we found additional support for the roles of *FT* and *VRN2* in controlling flowering in wild temperate grasses. Additionally, allelic variation may explain the ambiguity around the role of the *VRN2* homolog observed in *B. distachyon*. Further fine-mapping will be required to confirm the roles of these genes in *B. distachyon* flowering time. However, we also detected novel components in the form of additional QTLs, which reflects the power of studying

natural variation in mapping populations derived from phenotypically diverse parents. During population advancement, we have observed a variety of additional morphological and pathological characteristics segregating in this population and it will serve as a useful resource for other researchers investigating standing variation in non-domesticated grasses.

## Materials and methods

### *Plant growth for assessing ABR6 and Bd21 vernalisation response*

Six seeds for ABR6 and Bd21 were germinated on paper (in darkness at room temperature) and transferred to an equal mixture of the John Innes Cereal Mix and a peat and sand mix (Vain *et al.* 2008) four days after germination. Vernalisation was initiated 14 days after germination for either two, three, four, five, six, seven, or eight weeks (8 h day length; 1.2 klux light intensity; 5°C). The different sets were staggered to ensure that all sets left vernalisation on the same date. After vernalisation plants were grown in a Sanyo Versatile Environmental Test Chamber (Model MLR-351; 16 h photoperiod; 8.0 klux light intensity; 22°C/20°C day/night temperatures) for 35 days and then transferred to a greenhouse without light and temperature control (late April to mid July 2013; Norwich, UK). Days to flowering was measured from the end of vernalisation until the emergence of the first spike and was averaged across all six biological replicates (only five replicates were available for Bd21 after 7 weeks of vernalisation). Statistical significances were assessed by pairwise comparisons using *t*-tests with pooled standard deviations and Bonferroni correction for multiple comparisons.

### *Resequencing of ABR6*

Seedlings were grown in a Sanyo Versatile Environmental Test Chamber (16h photoperiod; 8.0 klux light intensity; 22°C) in an equal mixture of the John Innes Cereal Mix and a peat and sand mix. Seven-week-old plants were placed in darkness for three days prior to collecting tissue. Genomic DNA was extracted using a standard CTAB protocol and a library of 800 bp inserts was constructed and sequenced with 100 bp paired-end reads and an estimated coverage of 25.8x on an Illumina HiSeq 2500. Library preparation and sequencing was performed at The Genome Analysis Centre (Norwich, UK). The resulting reads were mapped to the Bd21 reference sequence (Version 1) (The International Brachypodium Initiative 2010) with the Galaxy wrapper, which used the BWA (Version 0.5.9) *aln* and *sampe* options (Li and Durbin 2009). Polymorphisms between ABR6 and Bd21 were identified with the *mpileup2snp* and *mpileup2indel* tools of *VarScan* (Version 2.3.6) using default

settings (Koboldt *et al.* 2009). A *de novo* assembly was created from the raw ABR6 reads using default settings of the CLC Assembly Cell (Version 4.2.0) and default parameters. Potential structural variation between ABR6 and Bd21 was investigated by performing a BLAST search with the Bd21 regions of interest against the ABR6 *de novo* assembly and mapping contigs for hits with at least 95% identity and an E-value under  $1e^{-20}$  to the Bd21 reference sequence (Version 3).

#### *Development of the ABR6 x Bd21 F<sub>4</sub> population and genetic map*

The *B. distachyon* accessions ABR6 and Bd21 were crossed and three ABR6 x Bd21 F<sub>1</sub> individuals, confirmed as hybrid by SSR marker analysis (data not shown), were allowed to self-pollinate to generate a founder F<sub>2</sub> population comprised of 155 individuals. After single seed descent, DNA was extracted from leaf tissue of 114 independent F<sub>4</sub> lines using a CTAB gDNA extraction protocol modified for plate-based extraction (Dawson *et al.* 2016). SNPs for genetic map construction were selected based on a previously characterised Bd21 x Bd3-1 F<sub>2</sub> genetic map to ensure an even distribution of markers relative to physical and genetic distances (Huo *et al.* 2011). SNPs without additional sequence variation in a 120 bp window were selected every 10 cM. The Agena Bioscience MassARRAY design suite was used to develop 17 assays that genotyped 449 putative SNPs using the iPLEX Gold assay at the Iowa State University Genomic Technologies Facility. Markers were excluded for being monomorphic (106), dominant (34), or for missing data for the parental controls (33). Heterozygous genotype calls for some markers were difficult to distinguish and classified as missing data. Additional SNPs between ABR6 and Bd21 in six markers developed for the Bd21 x Bd3-1 F<sub>2</sub> genetic map (Barbieri *et al.* 2012) were converted into CAPS markers (Konieczny and Ausubel 1993). The integrity of these 282 markers was evaluated using R/qtl (Version 1.33-7) recombination fraction plots (Broman *et al.* 2003). Two markers were removed for not showing linkage and one marker was moved to its correct position based on linkage. Genetic distances were calculated using the Kosambi function in MapManager QT (Version b20) (Manly *et al.* 2014). Removal of unlinked and redundant markers produced a final ABR6 x Bd21 F<sub>4</sub> genetic map consisting of 252 SNP-based markers. Segregation distortion was assessed using a chi-square test with Bonferroni correction for multiple comparisons (Holm 1979).

### *Plant growth and phenotyping of flowering time in the ABR6 x Bd21 F<sub>4:5</sub> families*

Three to five plants for each of the 114 ABR6 x Bd21 F<sub>4:5</sub> families were grown under five different environmental conditions as detailed in Table S1. For the phenotyping performed in Aberystwyth, individual seeds were sown in 6 cm pots with a mixture of 20% grit sand and 80% Levington F2 peat-based compost. Seeds were grown for 2 weeks in greenhouse conditions (22°C/20°C, natural light supplemented with 20 h lighting) and then either maintained in the greenhouse or transferred to a vernalisation room for six weeks (16 h day length, 5°C). Plants were returned to the greenhouse following vernalisation and grown to maturity. Flowering time was defined as the emergence of the first inflorescence and was measured from the first day that flowering was observed in the entire mapping population. Flowering time was averaged across the individuals of an F<sub>4:5</sub> family. For the phenotyping performed in Norwich, plants were first subjected to growth conditions and pathogen assays as described by Dawson *et al.* 2015. Plants were germinated in a peat-based compost in 1 L pots and grown for six weeks in a controlled environment room (18°C/11°C, 16 h light period). Six weeks post germination, the fourth or fifth leaf of each plant was cut off for pathological assays. The plants were transplanted into 9 cm pots with an equal mixture of the John Innes Cereal Mix and a peat and sand mix (Vain *et al.* 2008) and transferred to the respective growth environments for flowering assessment (Table S1). Flowering time was defined as the emergence of the first inflorescence within an F<sub>4:5</sub> family and was measured from the first day that flowering was observed in the entire mapping population. Families that did not flower 60 days after emergence of the first inflorescence in the mapping population were scored as not flowering.

### *Quantitative trait locus analysis for flowering time*

Flowering phenotypes were assessed for normality using the Shapiro-Wilk test (Royston 1982). In an initial analysis, phenotypic values were converted into a binary classification based on whether families flowered (F) or did not flower (NF). Interval mapping was performed with the *scanone* function in R/qtl under a *binary* model with conditional genotype probabilities computed with default parameters and the Kosambi map function (Xu and Atchley 1996; Broman *et al.* 2006). Simulation of genotypes was performed with a fixed step distance of 2 cM, 128 simulation replicates, and a

genotyping error rate of 0.001. Statistical significance for QTLs was determined by performing 1,000 permutations and controlled at  $\alpha = 0.05$  (Doerge and Churchill 1996). Non-parametric interval mapping was performed with similar parameters in R/qtl under an *np* model (Kruglyak and Lander 1995). For parametric mapping, flowering time data were transformed (T) using the following approaches: (T1) the removal of all  $F_{4:5}$  families that did not flower within the timescale of the experiment, (T2) transforming all non-flowering phenotypic scores to one day above the maximum observed, and (T3) transforming by ranking families according to their flowering time. For the third transformation approach (T3), the earliest flowering family was given a rank score of 1 and subsequent ordered families given incremental scores based on rank (2, 3, 4, etc.). When two or more families had shared flowering time, they were given the same rank and the next ranked family was given an incremental rank score based on the number of preceding shared rank families. Non-flowering families were given the next incremental rank after the last flowering rank. For all three transformations, composite interval mapping was performed under an additive model ( $H_0:H_1$ ) using QTL Cartographer (Version 1.17j) with the selection of five background markers, a walking speed of 2 cM, and a window size of 10 cM (Zeng 1993; Zeng 1994; Basten *et al.* 2004). Statistical significance for QTLs was determined by performing 1,000 permutations with reselection of background markers and controlled at  $\alpha = 0.05$  (Doerge and Churchill 1996; Lauter *et al.* 2008). One-LOD support intervals were estimated based on interval mapping (Lander and Botstein 1989).

#### *RNAseq of ABR6 and Bd21*

Plants were grown in a controlled environment room with 16 h light at 22°C and fourth and fifth leaves were harvested as soon as the fifth leaf was fully expanded (roughly 28 days after germination). RNA was extracted using the TRI Reagent (Sigma-Aldrich®) according to the manufacturer's specifications. TruSeq libraries were generated from total RNA and mean insert sizes were 251 bp and 254 bp for ABR6 and Bd21, respectively. Library preparation and sequencing was performed at The Genome Analysis Centre (Norwich, UK). Sequencing was carried out using 150 bp paired-end reads on an Illumina HiSeq 2500 and ABR6 and Bd21 yielded 38,867,987 and 37,566,711 raw reads, respectively. RNAseq data quality was assessed with FastQC and reads were removed using Trimmomatic (Version 0.32) (Bolger *et al.*

2014) with parameters set at ILLUMINACLIP:TruSeq 3-PE.fa:2:30:10, LEADING:3, TRAILING:3, SLIDINGWINDOW:4:15, and MINLEN:100. These parameters will remove all reads with adaptor sequence, ambiguous bases, or a substantial reduction in read quality. The sequenced reads were mapped to the Bd21 reference genome using the TopHat (Version 2.0.9) spliced alignment pipeline (Trapnell *et al.* 2009).

#### *RT-qPCR analyses*

ABR6 and Bd21 seeds were surface sterilised (70% ethanol for 30 seconds, washed in autoclaved dH<sub>2</sub>O, 1.3% sodium hypochlorite for 4 minutes, washed in autoclaved H<sub>2</sub>O three times), transferred to moistened Whatman filter paper, left at room temperature in darkness overnight, and vernalised for either two, four, or six weeks (in darkness at 5°C). A control set was surface sterilised and transferred to filter paper overnight, but not vernalised. Following vernalisation, plants were transferred to soil and grown in a Sanyo Versatile Environmental Test Chamber in conditions similar to Environment 2 (20h photoperiod; 4.0 klux light intensity; 22°C/20°C). Once fully expanded, fourth leaves were collected in the middle of the photoperiod and flash frozen in liquid nitrogen.

Total RNA was extracted using TRI reagent according to manufacturer's instructions (Sigma-Aldrich®). RNA samples were treated with DNase I (Roche) prior to cDNA synthesis. Quality and quantity of RNA samples were assessed using a NanoDrop spectrophotometer followed by agarose electrophoresis. First-strand cDNA was synthesised according to manufacturer's instructions (Invitrogen). Briefly, 1 µg of total RNA, 1 µL of 0.5 µM poly-T primers, and 1 µL of 10 mM dNTP were incubated at 65°C for 5 min and 4°C for 2 min, with subsequent reverse transcription reactions performed using 2 µL of 10x reverse transcription buffer, 4 µL of 25 mM MgCl<sub>2</sub>, 2 µL of 0.1 M DTT, 1 µL of RNaseOUT (40 U/µL), and 1 µL of SuperScript III reverse transcriptase (200 U/µL) at 50°C for 50 min. Reverse transcription was inactivated by incubating at 85°C for 5 min and residual RNA was removed with the addition of 1 µL Rnase H (2 U/µL) and incubation at 37°C for 20 min.

Quantitative real time PCR was performed in 20 µL reaction volumes using 10 µL of SYBR-Green mix (Sigma-Aldrich), 1 µL of 10 µM forward and reverse primers, 4 µL

water, and 4  $\mu$ L of cDNA diluted 10-fold. The program for PCR amplification involved an initial denaturation at 95°C for 3 min and then 40 cycles of 94°C for 10 sec, 60°C for 15 sec, and 72°C for 15 sec. Fluorescence data was collected at 72°C at the extension step and during the melting curve program on a CFX96 Real-Time system (Bio-Rad).

Relative gene expression was determined using the  $2^{-\Delta\Delta CT}$  method described by Livak and Schmittgen (2001) using *UBIQUITIN-CONJUGATING ENZYME18* for normalisation (Hong *et al.* 2008; Schwartz *et al.* 2010). All primers were previously used by Ream *et al.* (2014) and had PCR efficiency ranging from 95 to 110%. Statistical analysis of gene expression was performed using R (Version 3.2.3). Comparisons between all genotype by treatment combinations were made with pairwise *t*-tests using log transformed relative expression levels, with *p*-values corrected for multiple hypothesis testing based on the Benjamini-Hochberg approach.

#### *Accession numbers for data in public repositories*

Raw resequencing reads of ABR6 have been submitted to the NCBI Short Read Archive under the BioProject ID PRJNA319372 and SRA accession SRX1720894. The ABR6 *de novo* assembly has been deposited at DDBJ/ENA/GenBank under the accession LXJM00000000. The version described in this chapter is version LXJM01000000. Raw RNAseq reads have been submitted to the NCBI Short Read Archive under the BioProject ID PRJNA319373 and SRA accessions SRX1721358 (ABR6) and SRX1721359 (Bd21).

### **3. The genetic architecture of intermediate nonhost resistance to stripe rust (*Puccinia striiformis*) in *B. distachyon***

One sentence summary: A simple genetic architecture underlies intermediate nonhost resistance to wheat and barley stripe rust in *Brachypodium distachyon*.

#### **Introduction**

Since the dawn of agriculture, breeding crop varieties that display durable resistance to pathogens, i.e. long-lasting resistance when deployed over a large area (Johnson 1981), has been a major challenge. The reliance on monocultures in modern agriculture presents a difficult dilemma for plant breeders, because as cultivars with novel resistance are released, plant pathogens experience a strong selective pressure and virulent isolates emerge (McDonald and Linde 2002). Norman Borlaug and others highlighted one form of durable disease resistance that remains untapped: nonhost resistance (Borlaug 2000; Heath 2000; Fan and Doerner 2012; Lee *et al.* 2016). The durability of nonhost resistance stems from the observation that a plant is generally resistant to the vast majority of potential pathogens in the environment and only susceptible to a small number of adapted pathogens (Lipka *et al.* 2008). Such resistance towards non-adapted pathogens is called nonhost resistance (Nürnberg and Lipka 2005; Schulze-Lefert and Panstruga 2011). By definition nonhost resistance is broad spectrum (i.e. effective against all isolates of a non-adapted pathogen) and durable (Hammond-Kosack and Parker 2003; Mysore and Ryu 2004; Fan and Doerner 2012). A major challenge is to identify the genes underlying nonhost resistance and test the feasibility of their use in agriculture.

The molecular basis of plant immunity to pathogenic microbes has primarily been established in host systems, i.e. the interaction of plants with adapted pathogens. This has revealed a layered immune system that detects pathogens at two stages (Jones and Dangl 2006). As a first barrier, pattern recognition receptors (PRRs) recognise conserved pathogen-associated molecular patterns (PAMPs) to initiate PAMP-triggered immunity (PTI). PRRs are immune receptors with potentially broader recognition capability, which are directly involved in limiting pathogen ingress (Zipfel 2008). Examples of PRRs include the membrane-bound receptor kinases FLS2 and

EFR recognising bacterial pathogens (Zipfel *et al.* 2004; Zipfel *et al.* 2006) and CERK1 and LYK5 recognising fungal pathogens (Miya *et al.* 2007; Cao *et al.* 2014). Pathogens can suppress PTI and manipulate the host plant by secreting effector molecules (Toruño *et al.* 2016). In turn, plants have evolved nucleotide binding, leucine-rich repeat (NB-LRR) proteins to either directly or indirectly (e.g. by guarding plant proteins) detect effector molecules (Jones and Dangl 2006). This leads to effector-triggered immunity (ETI), commonly observed as a gene-for-gene interaction between the plant and pathogen (Flor 1971; Jones and Dangl 2006). ETI can be suppressed by other effectors, prompting an evolutionary arms race between the pathogen and host (Jones and Dangl 2006). The vast majority of cloned resistance genes in host-pathogen interactions encode NB-LRRs (Liu *et al.* 2007; Lukasik and Takken 2009).

Following recognition via PRRs or NB-LRRs, plants mount active defence responses against further pathogen ingress. In the case of PRRs, activation often involves the formation of hetero- or homodimeric complexes, such as FLS2 with BAK1 or the self-association of CERK1 (Macho and Zipfel 2014; Couto and Zipfel 2016). In the well-studied example of FLS2, heterodimerisation with BAK1 allows phosphorylation of the FLS2-associated kinase BIK1, which in turn phosphorylates RBOHD, leading to a ROS (reactive oxygen species) burst (Kadota *et al.* 2014; Li *et al.* 2014; Couto and Zipfel 2016). An alternative downstream pathway builds on the activation of MAPK signalling cascades, resulting in the transcriptional activation of PAMP-induced genes (Couto and Zipfel 2016). With regard to fungal infections of plants, chitinases form part of the defence response and expression of chitinases is upregulated after infection (Punja and Zhang 1993; Salzer *et al.* 2000). The activation and function of NB-LRR proteins is discussed in the next chapter. Briefly, following pathogen recognition and NB-LRR activation, downstream signalling cascades lead to localised cell death, called a hypersensitive response. This response is thought to stop infection of biotrophic pathogens (Jones and Dangl 2006).

Several researchers have proposed that the genetic architecture and molecular basis of nonhost resistance are fundamentally different from the gene-for-gene interactions observed in host systems (Heath 1981; Heath 1991; Niks and Marcel 2009). Niks and Marcel (2009) suggest that shared pathways underlie nonhost resistance and basal host resistance, which are independent of NB-LRR encoding resistance genes. This

hypothesis is based on the observation that a complex genetic architecture with multiple isolate-specific QTLs confers resistance to heterologous rust species in several barley mapping populations (Jafary *et al.* 2006; Jafary *et al.* 2008). These findings are complemented by the identification of quantitative, multigenic resistance in barley towards various *Blumeria graminis formae speciales* (Aghnoum and Niks 2010). However, the latter observation is in contrast to previous research, which associated a simple genetic architecture based on gene-for-gene interactions with resistance to segregating populations that were derived from crosses between different *B. graminis formae speciales* (Tosa 1989). Similarly, Lee *et al.* (2014) found that recognition of *Phytophthora infestans* effectors, an oomycete pathogen of potato, by pepper (nonhost to *P. infestans*) lead to a hypersensitive response, the hallmark of NB-LRR mediated resistance. The authors propose that the interaction between multiple effectors and NB-LRRs provides the durable resistance observed in this system. Schulze-Lefert and Panstruga (2011) integrate these hypotheses by suggesting that the dependency on NB-LRR mediated resistance decreases as the phylogenetic distance between host and nonhost plant increases. Accordingly, NB-LRRs might play a role if the plant is phylogenetically close to the adapted host, but other genes such as PRRs condition nonhost resistance if the plant is phylogenetically distant to the adapted host.

Stripe rust (*Puccinia striiformis*) is an agronomically important obligate biotrophic fungal pathogen of wheat, barley, and other domesticated crops, as well as many non-domesticated grasses (Roelfs *et al.* 1992; Hovmøller *et al.* 2011; Beddow *et al.* 2015). Stripe rust isolates adapted to certain host genera are differentiated as *formae speciales*, including *P. striiformis* f. sp. *tritici* with wheat as the main host (wheat stripe rust, *Pst*) and *P. striiformis* f. sp. *hordei* with barley as the main host (barley stripe rust, *Psh*) (Eriksson 1894). However, this classification is complicated by the existence of *formae speciales* with overlapping host ranges. For example, a *P. striiformis* race emerged on triticale in Denmark and Sweden in 2008 and 2009, which also infected spring wheat, barley, and rye (Hovmøller and Justesen 2007; Hovmøller *et al.* 2011). As pathogens are often able to infect or colonise plants other than their adapted host, this gives rise to a range of interactions, which are difficult to assign to a host or nonhost state. Regarding the rusts, we proposed to distinguish between host and nonhost based on the degree of colonisation and life cycle completion by the pathogen (Bettgenhaeuser *et al.* 2014). This classification is based on the diversity

observed at the species level for both plant and rust. Within an intermediate nonhost species, for example, no accessions support life cycle completion by the different rust isolates, but some accessions allow a degree of colonisation.

Straib (1935) investigated the host range of *Pst* and *Psh* isolates on a panel of 227 mainly non-domesticated grass species and observed chlorotic or necrotic flecks as well as pustule formation in some genera. The *Brachypodium distachyon* accession used was completely immune to the isolates studied. Draper *et al.* (2001) identified some *B. distachyon* accessions that produced disease symptoms in the form of “brown flecking” upon *Pst* and *Psh* inoculation. These observations were confirmed by Barbieri *et al.* (2011), who described “large dark flecks” on some *B. distachyon* accessions in response to infection with *Pst* and *Psh* isolates. A comprehensive analysis of *B. distachyon*–*Pst* interactions linked these macroscopic flecks with hyphal colonisation (Ayliffe *et al.* 2013), which led to the application of a robust and quantitative phenotyping assay to a diversity set of *Brachypodium* spp. accessions inoculated with two UK *Pst* isolates (Dawson *et al.* 2015). A strong correlation between macroscopic leaf browning and hyphal colonisation was observed across 210 *Brachypodium* spp. accessions. These studies established *B. distachyon* as an intermediate nonhost of *Pst* and *Psh* and laid the foundation for dissecting the genetic architecture underlying this resistance.

Using three differential *B. distachyon* mapping populations and a quantitative microscopic assay, we found that colonisation resistance to three phylogenetically diverse *Pst* and *Psh* isolates is governed by a simple genetic architecture. Across all populations, resistance is largely provided by two major effect QTLs, with both QTL functional against *Pst*, whereas a single QTL mediates resistance to *Psh*. Lastly, we assessed the genomic regions encompassing these QTL and discovered the presence of several canonical resistance genes.

## Results

### *Leaf browning and hyphal colonisation are strongly correlated in segregating *B. distachyon* mapping populations*

The quantitative nature of phenotypes observed in the transition from host to nonhost interactions has provided an obstacle to studying the genetic basis of intermediate interactions (Niks 1987). In the *B. distachyon*–*Pst* interaction, infection symptoms manifest themselves in the form of leaf browning (Figure 10A). A survey of 210 *Brachypodium* spp. accessions found a strong correlation between macroscopic leaf browning and hyphal growth (percent colonisation, pCOL; Figure 10B) of the *Pst* isolate 08/21 (Dawson *et al.* 2015). While leaf browning and hyphal colonisation are correlated traits in diverse germplasm, it remained unclear whether a shared genetic architecture controls these phenotypes. To this end, leaf browning and pCOL phenotypes in response to the *Pst* isolate 08/21 were assessed in three segregating *B. distachyon* populations.

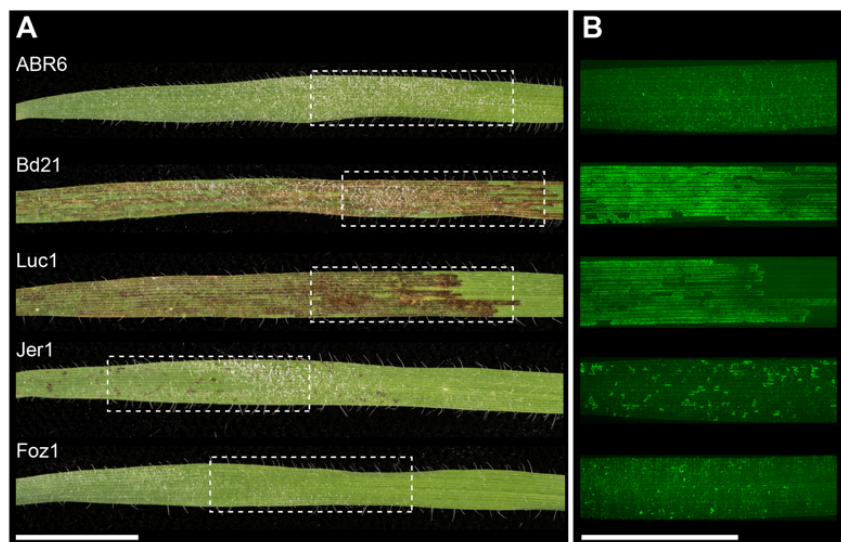


**Figure 10.** *Puccinia striiformis* f. sp. *tritici* (wheat stripe rust) infection symptoms on several *Brachypodium distachyon* accessions. (A) Leaf browning 14 days after inoculation with *Pst* isolate 08/21. (B) Micrograph of the same leaves cleared and stained with a chitin-binding fluorophore (WGA-FITC) to visualise hyphal growth (Dawson *et al.* 2015). Boxed leaf area in (A) corresponds approximately to leaf area in (B). The bar is equal to 10 mm.

The ABR6 x Bd21 F<sub>4</sub> population constitutes a geographically wide cross between a Spanish accession (ABR6) and the Iraqi reference accession (Bd21), which differ substantially at the genomic level (Bettgenhaeuser *et al.* 2017; Gordon and Vogel, personal communication). Two infection replicates were performed for 114 F<sub>4:5</sub> families and phenotyping scores were averaged across replicates. Leaf browning and pCOL phenotypes in the ABR6 x Bd21 F<sub>4</sub> population were not normally distributed and heavily skewed towards resistance (Figure 11 A and B). The segregation pattern for pCOL phenotypes displayed greater detail and also allowed the identification of transgressive segregation. Leaf browning and pCOL showed strong correlation ( $\rho = 0.85$ ; Figure 11C).

*B. distachyon* accessions collected in the western Mediterranean (predominantly Spain) displayed a greater phenotypic diversity upon infection with *Pst* than accessions derived from the eastern Mediterranean (Turkey to Iraq) (Dawson *et al.* 2015). Therefore, to explore the genetic architecture of this resistance in phenotypically diverse germplasm, 188 F<sub>2</sub> individuals from two crosses between the Spanish accessions Luc1 x Jer1 and Foz1 x Luc1 were evaluated for leaf browning 14 days post inoculation (dpi) and for both leaf browning and pCOL 23 dpi. Similar to observations on the ABR6 x Bd21 population, the leaf browning and pCOL phenotypes were not normally distributed.

All three phenotyping results for Foz1 x Luc1 and the Luc1 x Jer1 14 dpi phenotyping result were skewed towards resistance (Figure 12 A – C, E). Interestingly, 23 dpi the Luc1 x Jer1 leaf browning phenotypes were distributed uniformly (Figure 12F) and the pCOL phenotypes were almost normally distributed (Figure 12G). The 23 dpi leaf browning and pCOL phenotypes were correlated with correlation coefficients of 0.86 and 0.76 for Foz1 x Luc1 and Luc1 x Jer1, respectively (Figure 12 D and H). Transgressive segregation towards increased susceptibility was observed in the Foz1 x Luc1 population and towards increased resistance and susceptibility in the Luc1 x Jer1 population

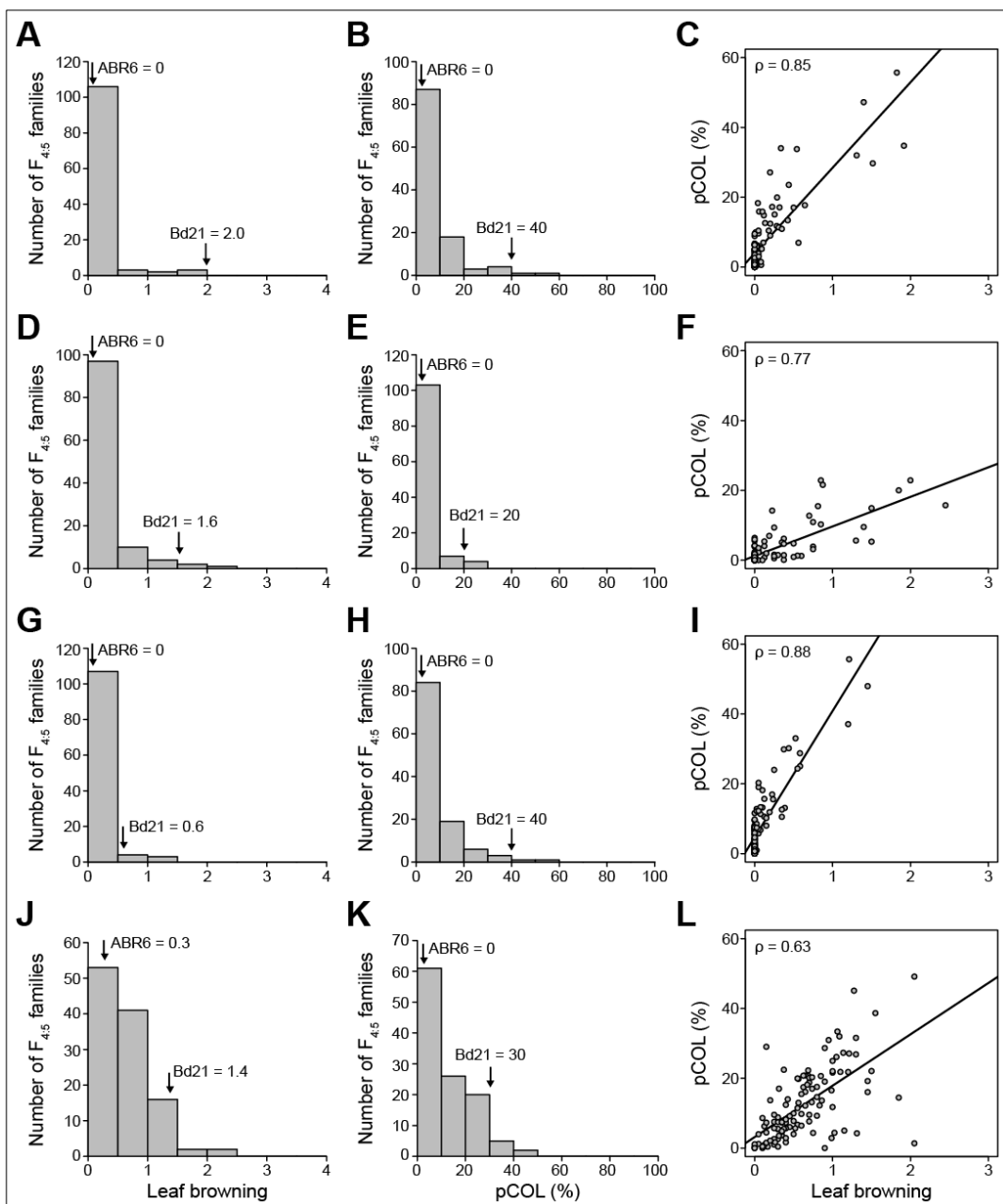


**Figure 11.** Frequency distribution and correlation of leaf browning and pCOL phenotypes in the ABR6 x Bd21 population inoculated with several isolates of *P. striiformis* f. sp. *tritici*. Distribution of leaf browning (A, D, G, and J) and pCOL (B, E, H, and K) and the correlation between these two phenotypes (C, F, I, and L) in the F<sub>4.5</sub> families averaged across the two replicates for *Pst* isolates 08/21 (A – C), 08/501 (D – F), and 11/08 (G – I), and for *Psh* isolate B01/2 (J – L). Arrows indicate parental phenotypes.  $\rho$  = correlation coefficient.

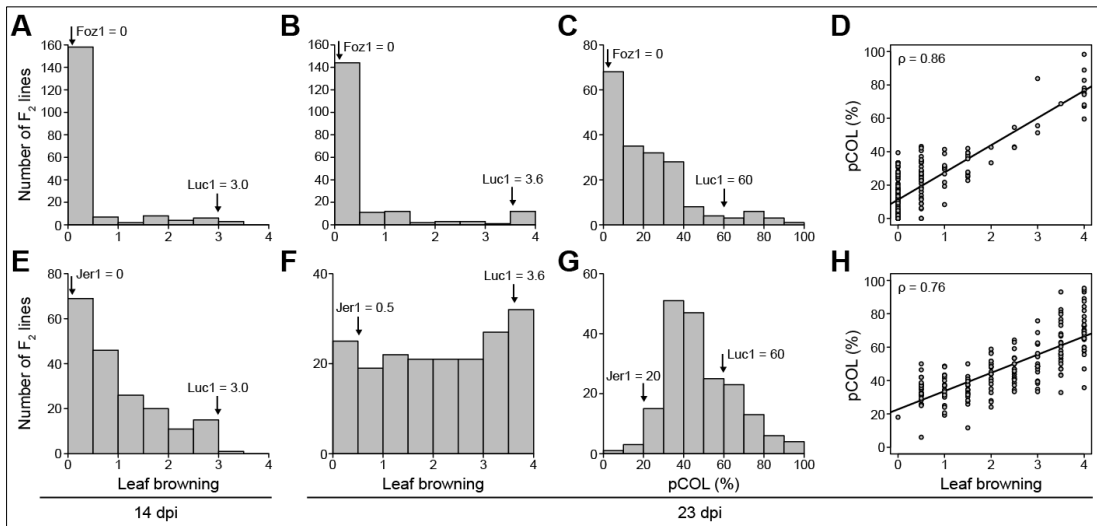


**Figure 12.** Frequency distribution and correlation of leaf browning and pCOL phenotypes in the Foz1 x Luc1 and Luc1 x Jer1 F<sub>2</sub> populations inoculated with *P. striiformis* f. sp. *tritici* isolate 08/21. Leaf browning phenotypes were collected 14 dpi (A and E) and 23 dpi (B and F), and pCOL phenotypes were collected 23 dpi (C and G). Correlation between leaf browning and pCOL phenotypes at 23 dpi is shown (D and H). Arrows indicate parental phenotypes. dpi = days post inoculation;  $\rho$  = correlation coefficient.

The strong correlation of leaf browning and pCOL in segregating populations highlights the robustness of the microscopic assay and likely causal association of fungal development on the physiological status of infected *B. distachyon* plants. In addition, assessment of the segregation towards *Pst* resistance in the three mapping populations suggests that a multigenic architecture underlies this intermediate nonhost resistance in *B. distachyon*.

#### *A simple genetic architecture underlies resistance to Pst isolate 08/21 in three B. distachyon mapping populations*

To explore the genetic architecture of this interaction, SNP-based genetic maps were created for the newly developed Foz1 x Luc1 and Luc1 x Jer1 F<sub>2</sub> populations. Following iterative cycles of marker development, the preliminary Foz1 x Luc1 genetic map contains 90 non-redundant markers and has a cumulative size of 1119 cM (Figure S3) and the finished Luc1 x Jer1 genetic map contains 107 markers and has a cumulative size of 1,446 cM (Figure S4). The quality of the finished Luc1 x Jer1 genetic map was confirmed by assessing the two-way recombination fraction plots for all markers (Figure S5) and by analysing all chromosomes for segregation distortion (data not shown).

**Table 4.** Significant QTLs from composite interval mapping of averaged leaf browning and percent colonisation phenotypes for *P. striiformis* isolates in the ABR6 x Bd21 F<sub>4:5</sub> families.

Isolate <sup>a</sup>	Phenotype <sup>b</sup>	Locus	Chr <sup>c</sup>	cM	EWT <sup>d</sup>	LOD	AEE <sup>e</sup>	PVE <sup>f</sup>
<i>Pst</i> 08/21	Browning	<i>Yrr3</i>	Bd2	328.0	2.71	6.21	-0.16	17.8
<i>Pst</i> 08/21	Browning	<i>Yrr1</i>	Bd4	142.8	2.71	5.60	-0.13	10.9
<i>Pst</i> 08/21	pCOL	<i>Yrr3</i>	Bd2	328.0	2.78	10.95	-0.05	24.0
<i>Pst</i> 08/21	pCOL	<i>Yrr1</i>	Bd4	139.7	2.78	10.27	-0.05	18.3
<i>Pst</i> 08/501	Browning	<i>Yrr3</i>	Bd2	328.0	2.87	10.19	-0.32	24.6
<i>Pst</i> 08/501	Browning	<i>Yrr1</i>	Bd4	144.8	2.87	8.57	-0.24	21.7
<i>Pst</i> 08/501	pCOL	<i>Yrr3</i>	Bd2	328.0	3.00	8.34	-0.02	19.4
<i>Pst</i> 08/501	pCOL	<i>Yrr2</i>	Bd4	92.1	3.00	5.31	-0.02	11.1
<i>Pst</i> 08/501	pCOL	<i>Yrr1</i>	Bd4	139.7	3.00	8.05	-0.02	17.2
<i>Pst</i> 11/08	Browning	<i>Yrr3</i>	Bd2	328.0	2.61	6.02	-0.10	15.6
<i>Pst</i> 11/08	Browning	<i>Yrr1</i>	Bd4	142.8	2.61	6.70	-0.10	15.6
<i>Pst</i> 11/08	pCOL	<i>Yrr3</i>	Bd2	328.0	2.86	11.94	-0.05	23.0
<i>Pst</i> 11/08	pCOL	<i>Yrr2</i>	Bd4	89.2	2.86	3.25	-0.03	4.5
<i>Pst</i> 11/08	pCOL	<i>Yrr1</i>	Bd4	139.7	2.86	9.66	-0.04	14.9
<i>Pst</i> 11/08	pCOL	-	Bd5	74.3	2.86	3.27	-0.02	5.3
<i>Psh</i> B01/2	Browning	-	Bd2	169.8	3.11	3.43	0.17	11.8
<i>Psh</i> B01/2	Browning	<i>Yrr3</i>	Bd2	326.2	3.11	10.32	-0.25	28.3
<i>Psh</i> B01/2	pCOL	<i>Yrr3</i>	Bd2	328.9	3.14	10.50	-0.06	27.3
<i>Psh</i> B01/2	pCOL	-	Bd3	323.0	3.14	3.98	-0.03	8.0

<sup>a</sup>*Puccinia striiformis* isolate (*Pst* = f. sp. *tritici*, *Psh* = f. sp. *hordei*)

<sup>b</sup>Browning = leaf browning; pCOL = percent colonisation

<sup>c</sup>Chromosome

<sup>d</sup>Experiment-wide permutation threshold

<sup>e</sup>Additive effect estimate

<sup>f</sup>Percent of variation explained

Linkage analyses using composite interval mapping were performed on all three mapping populations in order to identify the genetic architecture underlying resistance to the UK reference *Pst* isolate 08/21. For the ABR6 x Bd21 population, linkage analyses were performed with the phenotypic scores from averaged (Table 4; Figure 13) and individual replicates (Figure S6; Table S7). Linkage analyses in the F<sub>2</sub> populations were performed for the 188 F<sub>2</sub> lines studied, which was validated in the Luc1 x Jer1 population with 95 F<sub>2:3</sub> derived families (Table 5). Both leaf browning and pCOL were assessed for all three populations. Significant loci were designated *Yrr* (*Yellow rust resistance*), based on the established naming convention for resistance loci in *B. distachyon* (Cui *et al.* 2012).

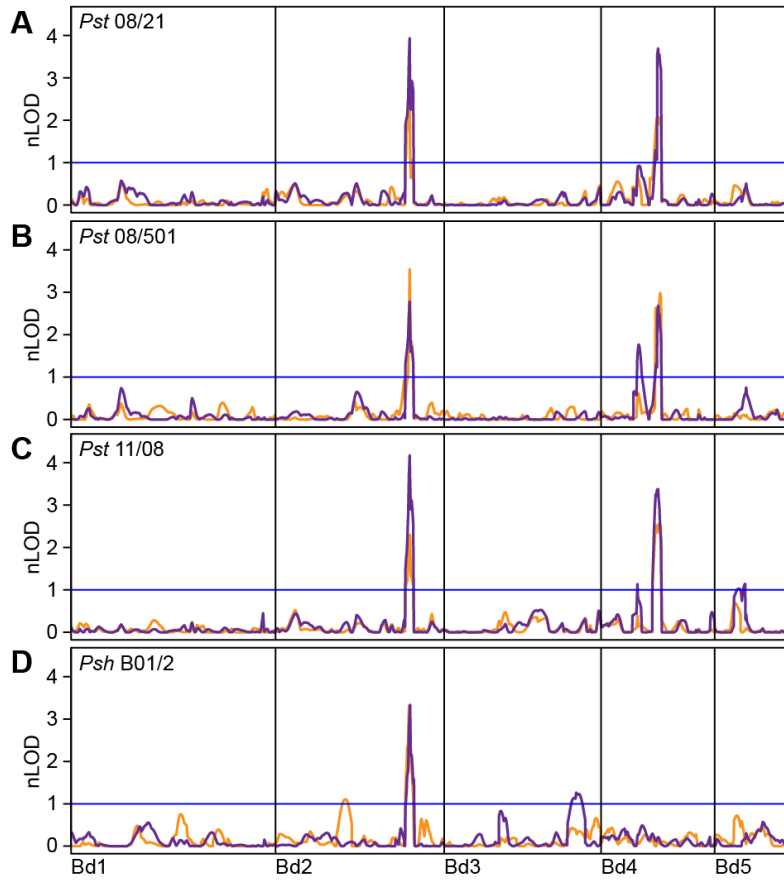


**Figure 13.** Two major effect loci govern *P. striiformis* resistance in the ABR6 x Bd21 population. Composite interval mapping using averaged phenotypes of  $F_{4:5}$  families scored 14 days post inoculation with *P. striiformis* f. sp. *tritici* (*Pst*) isolates 08/21 (A), 08/501 (B), and 11/08 (C), and *P. striiformis* f. sp. *hordei* (*Psh*) isolate B01/2 (D). Leaf browning (orange) and pCOL (purple) were averaged across replicates before performing linkage analysis using an additive model ( $H_0:H_1$ ). Results were plotted based on normalised permutation thresholds (nLOD), using the threshold of statistical significance based on 1,000 permutations (blue horizontal line).  $N = 114 F_{4:5}$  families.

Two major effect QTLs were found to control leaf browning and pCOL for *Pst* isolate 08/21 across all three populations. In the ABR6 x Bd21 population, a QTL at 328.0 cM on chromosome Bd2 (peak marker Bd2\_51527431) controlled 17.8% of the phenotypic variation for leaf browning and 24.0% of the phenotypic variation for pCOL (Figure 13A; Table 4). A second QTL with peak markers near 140 cM on chromosome Bd4 controlled 10.9% of the phenotypic variation for leaf browning and 18.3% of the phenotypic variation for pCOL.

These QTLs on chromosomes Bd2 and Bd4 have been designated *Yrr3* and *Yrr1*, respectively. Phenotype by genotype analysis showed that *Yrr1* and *Yrr3* behave as dominant resistance genes, as each locus independently significantly reduces colonisation by *Pst* isolate 08/21 (Figure 14A).

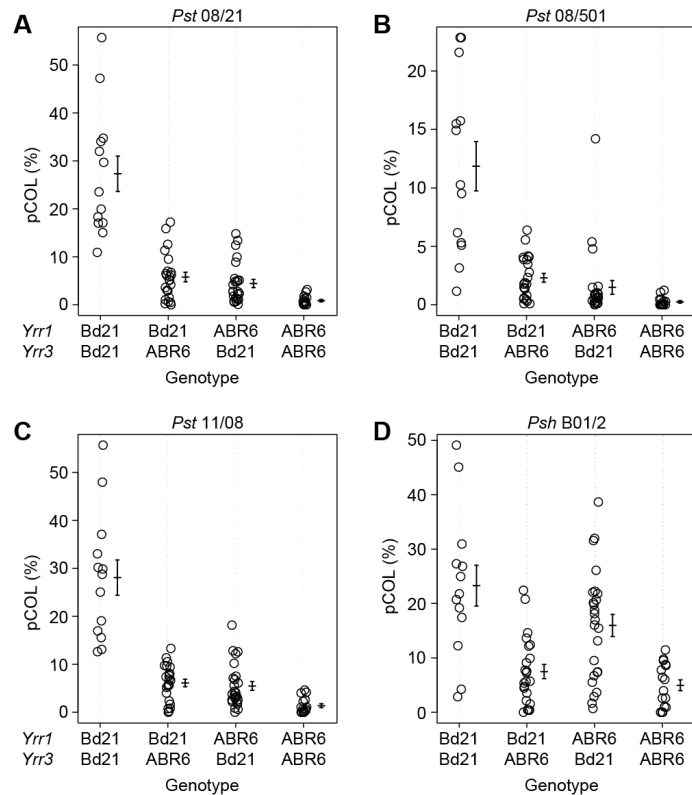


**Figure 14.** Restriction of *P. striiformis* f. sp. *tritici* and *P. striiformis* f. sp. *hordei* colonisation in the ABR6 x Bd21 population by *Yrr1* and *Yrr3*. Phenotype by genotype for the major effect loci *Yrr1* and *Yrr3* for *Pst* isolates 08/21 (A), 08/501 (B), and 11/08 (C), and *Psh* isolate B01/2 (D). pCOL phenotypes for lines homozygous at *Yrr1* and *Yrr3* show that ABR6 alleles at both loci provide resistance to *Pst* isolates, whereas only *Yrr3* contributes to resistance against *Psh* isolate B01/2. Error bars represent one standard error. Number of families for the four homozygous groups from left to right: 13, 23, 25, and 16.

Only one additional minor effect QTL was detected for *Pst* isolate 08/21, which explained 4.5% of the phenotypic variation for pCOL in the first replicate (Figure S6A; Table S7), but not in second replicate or the averaged dataset. All statistically significant QTLs were contributed by the resistant parent ABR6 (Table 4).

Similar to the ABR6 x Bd21 population, the two major effect loci *Yrr1* and *Yrr3* also contribute to resistance in the Foz1 x Luc1 population (Figure 15A). A QTL analysis was performed with the preliminary Foz1 x Luc1 genetic map (Table 5). *Yrr1* explained between 33.3 % and 49.3% of the variation observed for the three phenotypes. However, *Yrr3* was only statistically significant for the pCOL phenotype and explained 26.3% of the variation observed. All detected loci were contributed by Foz1.

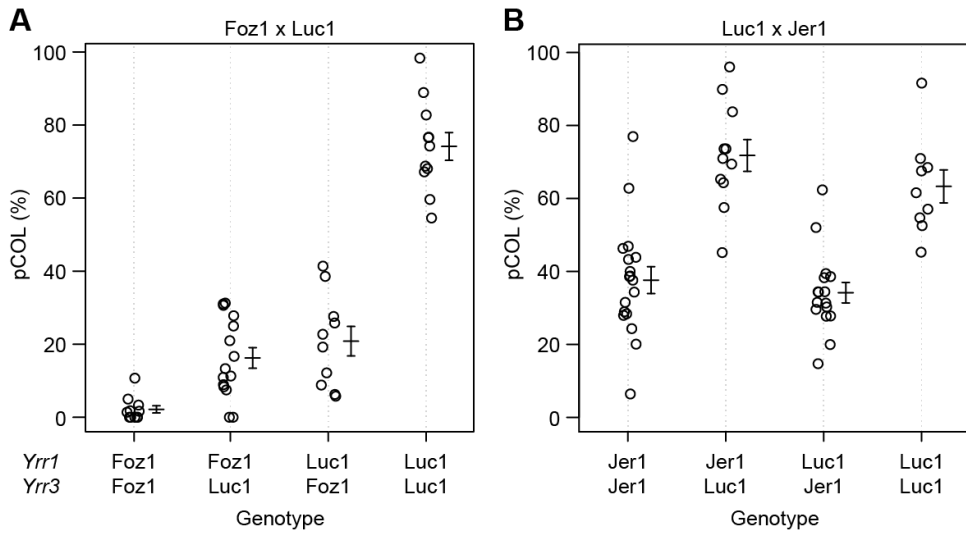


**Figure 15.** Restriction of *P. striiformis* f. sp. *tritici* colonisation in Foz1 x Luc1 and Luc1 x Jer1 F<sub>2</sub> populations by *Yrr1* and *Yrr3*. Phenotype by genotype for the major effect loci *Yrr1* and *Yrr3* in the (A) Foz1 x Luc1 and (B) Luc1 x Jer1 F<sub>2</sub> populations. pCOL phenotypes for lines homozygous at *Yrr1* and *Yrr3* show that Foz1 alleles at both loci provide resistance in the Foz1 x Luc1 population, whereas only *Yrr3* contributes to resistance in the Luc1 x Jer1 population. Error bars represent one standard error. Number of individuals for the four homozygous groups from left to right: 11, 15, 10, and 11 (Foz1 x Luc1), and 18, 11, 16, and 9 (Luc1 x Jer1).

Development of the Foz1 x Luc1 genetic map is still in progress and with the exception of chromosome Bd4 all chromosomes are currently split into several linkage groups (Figure S3). These large gaps in marker coverage (> 30 cM) can have adverse effects on composite interval mapping and the results from the linkage analysis will likely change with completion of the genetic map.

In contrast to the ABR6 x Bd21 and Foz1 x Luc1 populations, only one major effect QTL controlled resistance in the Luc1 x Jer1 population (Figure 15B). *Yrr3* explained between 27.2% and 46.5% of the variation observed for the four phenotypes and time points (Table 5). The physical positions of the peak markers (Bd2\_50755888\_80\_R and Bd2\_51772031\_60\_F) correspond to the physical position observed in the ABR6 x Bd21 population. Five minor effect QTLs on the other chromosomes were not statistically significant with more than one of the phenotypic scores analysed. With the exception of the minor effect QTLs on the long arm of chromosome Bd1 and the short arm of chromosome Bd4, all QTLs were contributed by the resistant parent Jer1.

**Table 5.** Significant QTLs from composite interval mapping of leaf browning and percent colonisation phenotypes for *P. striiformis* f. sp. *tritici* isolate 08/21 in the Foz1 x Luc1 and Luc1 x Jer1 F<sub>2</sub> populations.

Population	Trait <sup>a</sup>	dpi <sup>b</sup>	Locus	Chr <sup>c</sup>	cM	EWT <sup>d</sup>	LOD	AEE <sup>e</sup>	PVE <sup>f</sup>
Foz1xLuc1	Browning	14	<i>Yrr1</i>	Bd4	100.4	15.17	29.43	-0.65	43.9
	Browning	23	<i>Yrr1</i>	Bd4	100.4	14.77	36.11	-0.98	49.3
	pCOL	23	<i>Yrr3</i>	Bd2b	159.0	3.64	18.69	-0.15	26.8
	pCOL	23	<i>Yrr1</i>	Bd4	100.4	3.64	25.63	-0.17	33.3
Luc1xJer1	Browning	14	<i>Yrr3</i>	Bd2	263.3	3.74	28.40	0.95	46.5
	Browning	23	-	Bd1	213.0	3.64	4.00	-0.45	7.3
	Browning	23	<i>Yrr3</i>	Bd2	258.6	3.64	16.05	1.09	27.2
	Browning	23	-	Bd3	236.7	3.64	3.91	0.42	6.0
	pCOL	23	<i>Yrr3</i>	Bd2	263.3	3.51	26.44	0.16	40.4
	pCOL	23	-	Bd3	50.5	3.51	7.53	0.08	10.3
	pCOL	23	<i>Yrr2</i>	Bd4	87.4	3.51	9.40	-0.09	14.5
	Browning <sup>g</sup>	14	<i>Yrr3</i>	Bd2	260.6	3.89	15.10	0.52	41.3
	Browning <sup>g</sup>	14	-	Bd5	96.2	3.89	4.54	0.06	11.1

<sup>a</sup>Browning = leaf browning; pCOL = percent colonisation

<sup>b</sup>Days post inoculation

<sup>c</sup>Chromosome

<sup>d</sup>Experiment-wide permutation threshold

<sup>e</sup>Additive effect estimate

<sup>f</sup>Percent of variation explained

<sup>g</sup>F<sub>2:3</sub> derived families phenotyped

### *Yrr1 and Yrr3 confer resistance to diverse Pst isolates in the ABR6 x Bd21 mapping population*

Only two major effect QTLs were identified in the three mapping populations in response to *Pst* isolate 08/21. To investigate if isolate-specific effects influence genetic architecture underlying *Pst* resistance in *B. distachyon*, the ABR6 x Bd21 population was inoculated with *Pst* isolates 08/501 and 11/08. These isolates are genetically distinct and have differential phenotypic responses on wheat accessions with various *Yr* resistance genes. (Hubbard *et al.* 2015).

As with *Pst* isolate 08/21, the phenotypes of the ABR6 x Bd21 population were heavily skewed towards resistance and showed a high correlation between leaf browning and pCOL (Figure 11 D – I). Linkage analyses with the leaf browning phenotype identified *Yrr1* and *Yrr3* as the two major effect QTLs for both isolates (Figure 13 B and C; Figure 14 B and C; Table 4). *Yrr1* explained 21.7% and 15.6% of the phenotypic variation for *Pst* isolates 08/501 and 11/08, whereas *Yrr3* explained 24.6% and 15.6% of the phenotypic variation for these two isolates. No additional

QTLs were identified in the individual replicates for leaf browning (Figure S6; Table S7).

These two QTLs were also conserved as major effect QTLs controlling pCOL, with *Yrr1* explaining 17.2% and 14.9% and *Yrr3* explaining 19.4% and 23.0% of the phenotypic variation for *Pst* isolates 08/501 and 11/08, respectively (Figure 13 B and C; Table 4). The greater resolution obtained with the pCOL phenotype allowed the identification of two additional minor effect QTLs, which exhibited isolate specificity. A QTL on the short arm of chromosome Bd4 explained 4.5% of the variation for *Pst* isolate 11/08 and 11.1% of the variation for *Pst* isolate 08/501 (Figure 13 B and C; Table 4). As this QTL was statistically significant for more than one *Pst* isolate tested, it was designated *Yrr2*. A QTL on chromosome Bd5 was only statistically significant for *Pst* isolate 11/08 and explained 5.3% of the phenotypic variation (Figure 13C; Table 4). Analysis of the individual replicates mirrored the results obtained from the averaged datasets (Figure S6; Table S7).

*Yrr3 confers intermediate nonhost resistance to both *P. striiformis* f. sp. *tritici* and *P. striiformis* f. sp. *hordei**

Despite studying the genetic architecture of *Pst* resistance towards three diverse *Pst* isolates, no isolate-specificity was observed for *Yrr1* and *Yrr3*. To explore whether these major effect loci are unique to *Pst* resistance or conserved for broader resistance towards other stripe rust *formae speciales*, we inoculated the mapping population with *Psh* isolate B01/2. Similar to *Pst*, phenotypes obtained for *Psh* were not normally distributed and skewed towards resistance for both leaf browning and pCOL (Figure 11 J and K). Transgressive segregation was observed with some F<sub>4:5</sub> families displaying increased susceptibility compared to Bd21. In contrast to the three *Pst* isolates tested, ABR6 displayed some infection symptoms and had a leaf browning score of 0.3, whereas no hyphal colonisation was observed. Leaf browning and pCOL phenotypes were correlated with a correlation coefficient of 0.63 (Figure 11 L).

Despite the phenotypes being skewed towards resistance, this was reduced as compared to the three *Pst* isolates and the distribution of the phenotypes was reminiscent of the expected segregation pattern of a single major effect locus. Linkage analysis confirmed this hypothesis and revealed that *Yrr3* is the only major effect locus

conferring resistance towards *Psh*. This locus explained 28.3% and 27.3% of the phenotypic variation for leaf browning and pCOL (Figure 13D; Figure 14D; Table 4). No statistically significant QTLs were observed on chromosome Bd4 with the averaged data (Figure 13D; Table 4) or individual replicates (Figure S6 G and H; Table S7). Chromosome Bd4 harbours the major effect locus *Yrr1* and the minor effect locus *Yrr2*, which both confer resistance to *Pst* isolates. While *Yrr3* possesses greater recognition capability towards other stripe rust *formae speciales*, *Yrr1* and *Yrr2* appear to specifically recognize *Pst* isolates.

Interestingly, two minor effect QTLs also contributed towards *Psh* resistance (Figure 13D; Table 4). A QTL on chromosome Bd2 (peak marker Bd2\_16663092) was contributed by ABR6 and detected with the leaf browning phenotype, whereas another minor effect QTL on chromosome Bd3 (peak marker Bd3\_49234576) was contributed by Bd21 and detected with the pCOL phenotype. These minor effect QTLs explained 11.8% and 8.0% of the phenotypic variation observed for leaf browning and pCOL, respectively.

#### *Canonical resistance genes are associated with intermediate nonhost resistance to stripe rust in *B. distachyon**

Several classes of protein encoding genes are known to confer immunity to plant pathogens, including NB-LRR, kinase-kinase, and LRR-kinase encoding genes (Hammond-Kosack and Parker 2003; Krattinger and Keller 2016). To date, the majority of cloned resistance genes encode NB-LRR proteins (Liu *et al.* 2007; Lukasik and Takken 2009). While the role of NB-LRRs in pathogen recognition in host systems is evident, it remains unclear to what degree NB-LRRs contribute to resistance towards non-adapted pathogens (Thordal-Christensen 2003). To understand the relationship between NB-LRRs and resistance in the *B. distachyon*–stripe rust system, we performed a candidate gene analysis by identifying the one-LOD and two-LOD support intervals for the major effect loci *Yrr1* and *Yrr3* (Table S8). Next, we assessed the presence of genes encoding proteins with a NB domain. This analysis revealed that support intervals for both *Yrr1* and *Yrr3* contain clusters of NB-LRR encoding genes (Figure 16; Table S9).

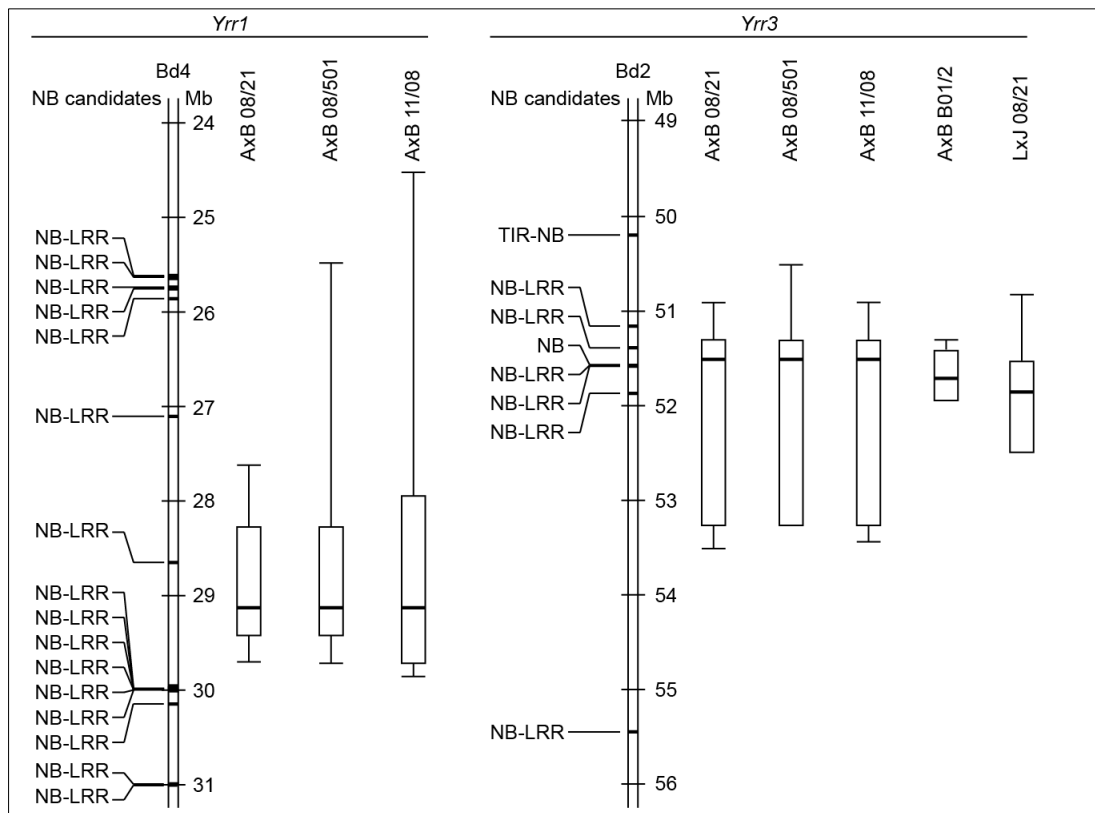


**Figure 16.** Canonical resistance genes associated with *Yrr1* and *Yrr3* loci. Annotated nucleotide binding (NB) domain encoding genes from the Bd21 reference sequence are indicated (Table S9). One-LOD and two-LOD support intervals for pCOL phenotypes were determined with interval mapping in the ABR6 x Bd21 and Luc1 x Jer1 populations. Within boxplots, thick bars denote the peak marker; the box defines the one-LOD support interval, and whiskers delineate the two-LOD support interval. Missing whiskers indicate a shared one-LOD and two-LOD support interval boundary. AxB = ABR6 x Bd21; LxJ = Luc1 x Jer1.

At *Yrr1*, the combined maximum two-LOD support interval of the pCOL phenotypes for the three *Pst* isolates contains seven NB-LRRs. However, only one NB-LRR is present within the one-LOD support intervals and the peak marker falls around 473 kb south of this NB-LRR. At *Yrr3*, the combined maximum two-LOD support interval for the pCOL phenotypes of all four stripe rust isolates contains five NB-LRR encoding genes and one NB domain encoding gene. The *Yrr3* peak markers center around a cluster of two NB-LRRs and the NB domain encoding gene. These associations strongly suggest the involvement of NB-LRR encoding genes in *Yrr3* resistance, whereas their involvement in *Yrr1* mediated resistance remains unclear.

## Discussion

The present study on the genetic architecture of resistance in *B. distachyon* to several diverse stripe rust isolates highlights a simple genetic architecture, underpinned by a few major effect QTLs and additional QTLs of minor effect. Our research constitutes a comprehensive analysis of the genetic architecture underlying intermediate nonhost resistance towards *Pst* and *Psh* in *B. distachyon*, involving several genetic backgrounds of both pathogen and plant. Previous work in rice found little natural variation in resistance to *P. striiformis* (Ayliffe *et al.* 2011), therefore *B. distachyon* is the phylogenetically most distant grass to wheat for which the genetic basis of resistance could be dissected. Crucially, despite looking at a very large phylogenetic distance between the pathogen's adapted host and the plant of study, NB-LRR encoding resistance genes are present within the two major effect loci *Yrr1* and *Yrr3*, implicating their potential role in conferring resistance in this intermediate nonhost system. Further fine-mapping will refine these genetic loci and identify the causal genes underlying resistance.

### *No life cycle completion of stripe rust in B. distachyon*

Extensive diversity exists within barley for the entire range of susceptibility symptoms towards *Pst* infection (Dawson *et al.* 2015). These consist of complete immunity, varying degrees of chlorosis associated with hyphal colonisation, and pustule formation in the absence of chlorosis (as observed in the host interaction between wheat and *Pst*). In the taxonomically distant species *B. distachyon*, no such diversity was found. In a diversity panel of 210 *Brachypodium* spp. accessions, pustule formation was mostly limited to the close allotetraploid relative *B. hybridum* (Bettgenhaeuser and Moscou, unpublished). Our study of three mapping populations incorporated geographically and genotypically diverse parental *B. distachyon* accessions (Gordon and Vogel, personal communication) and diverse stripe rust isolates (Hubbard *et al.* 2015). We did not routinely observe pustule formation in our studies and consequently no phenotypic assay was developed to assess life cycle completion. The parental accessions used for the mapping population never exhibited pustule formation in our experiments. The lack of life cycle completion in the transgressively segregating *B. distachyon* mapping populations could hint at a lack of

variation in the gene or genes controlling pustule formation among the accessions studied. Alternatively, the relatively simple genetic architecture we have identified for colonisation resistance towards *Pst* and *Psh* could be in contrast to a very complex genetic architecture preventing life cycle completion of stripe rust. Ayliffe *et al.* (2013) were able to observe life cycle completion on *B. distachyon* using Australian *Pst* isolates only after altering the temperature regime for plant growth, which can have considerable effects on stripe rust development (Rapilly 1979). In addition, pustules formed three to four weeks post inoculation, which is significantly later than on the host (12 to 14 dpi on wheat (Milus *et al.* 2009)).

#### *A simple genetic architecture underlies resistance to stripe rust in B. distachyon*

True nonhost resistance is defined as all accessions from a plant species being resistant to all isolates of a particular pathogen (Nürnberger and Lipka 2005; Schweizer 2007). For example, rice does not get infected by rust pathogens and is considered a nonhost of rusts (Ayliffe *et al.* 2011; Yang *et al.* 2014). Natural and induced variation has not uncovered susceptible rice accessions and interspecific crosses may therefore be the last genetic approach at dissecting rice nonhost resistance to rusts. Such experiments are generally prevented by the species barrier and limited by our ability to cross plants (Niks and Marcel 2009). Riley and Macer (1966) addressed this problem by introgressing individual rye chromosomes into wheat and inoculating the resulting chromosome addition lines with the wheat and rye *formae speciales* of selected pathogens. Interestingly, resistance to *Pst* was conferred by the long arm of rye chromosome 2 only, whereas resistance to the wheat *formae speciales* of other pathogens was conditioned by genes present on more than one chromosome arm. Furthermore, complete assessment of the genetic architecture of resistance in rye to wheat pathogens was limited to those genes that are functional in a wheat genetic background.

Despite their usefulness, studies involving chromosome addition lines are limited to closely related species. To dissect resistance in phylogenetically more distant species, it is therefore vital to study resistance within species that fall onto the continuum from host to nonhost, i.e. species in which some accessions allow a degree of infection or colonisation, but other accessions are resistant (Niks and Marcel 2009; Gill *et al.*

2015). Previously, *B. distachyon* was identified as an intermediate nonhost to *Pst* (Ayliffe *et al.* 2013; Dawson *et al.* 2015). Even though the majority of *Brachypodium* spp. accessions did not allow colonisation, a subset of the accessions studied showed varying degrees of leaf browning or pCOL. While studying resistance in the *B. distachyon* mapping populations, we found that leaf browning and pCOL for the three *Pst* isolates was often heavily skewed towards resistance, suggesting the involvement of several dominant resistance genes. In contrast, leaf browning and pCOL in response to the *Psh* isolate tested appeared to be controlled by a single dominant resistance gene in the ABR6 x Bd21 population. Transgressive segregation was observed for all four stripe rust isolates, reflecting the activity of additional minor effect QTLs. Linkage analyses confirmed these hypotheses. The two major effect QTLs *Yrr1* and *Yrr3* control colonisation in response to the *Pst* isolates, whereas only *Yrr3* was detected in response to *Psh*. Analysis of the segregation patterns suggested the involvement of dominant resistance genes, which was confirmed by the effects of *Yrr1* and *Yrr3* on *Pst* colonisation in the ABR6 x Bd21 and Foz1 x Luc1 populations (Figure 14 A – C; Figure 15A).

Barbieri *et al.* (2012) identified QTLs governing resistance to the adapted rust *P. brachypodii* in a mapping population derived from the inbred lines Bd3-1 and Bd1-1. Analyses of the F<sub>2</sub> population and F<sub>2:3</sub> families identified three QTLs, two of which govern resistance at the seedling stage and one which governs resistance at the seedling stage and an advanced growth stage. Ayliffe *et al.* (2013) studied the inheritance of resistance to an Australian *Pst* isolate in an F<sub>4</sub> population (BdTR13k x Bd21) and an F<sub>2</sub> population (BdTR10h x Tek-4). Although the authors did not perform any linkage analyses, the described segregation ratios of infection symptoms suggest a simple genetic architecture of two genes and one gene controlling resistance in these populations, respectively. Taken together with our findings, resistance to both adapted and non-adapted rusts seems to be controlled by a simple genetic architecture in *B. distachyon*.

#### *The molecular basis of resistance on the continuum from host to nonhost systems*

The evolutionary arms race between plant and pathogen in host systems leads to single genes often conferring resistance to particular pathogen isolates. Historically, this

allowed Biffen to demonstrate that resistance to stripe rust in wheat follows Mendel's laws (Biffen 1905). Many resistance genes against *Pst* and *Psh* have been mapped in wheat and barley, respectively (see Chen (2005) for a review of *Pst* resistance loci in wheat). These single resistance genes in host systems have often been identified as NB-LRR type genes and act in an isolate-specific manner towards the pathogen (Ayliffe and Lagudah 2004; Liu *et al.* 2007). An open question remains how resistance in intermediate host, intermediate nonhost, and nonhost systems differs from this architecture to provide a more durable form of resistance (Thordal-Christensen 2003).

Remarkably, we observed characteristics typical for host resistance in intermediate nonhost resistance. Namely, these included the identification of major effect genes, isolate specificity for both major and minor effect QTLs, and NB-LRR gene clusters associated with the identified QTLs. *Yrr1* is a major effect QTL controlling leaf browning and pCOL in response to all three *Pst* isolates tested. However, in the ABR6 x Bd21 population this QTL does not control resistance in response to *Psh* isolate B01/2. Additionally, all of the minor effect QTLs detected in the ABR6 x Bd21 population in response to the three *Pst* isolates displayed isolate specificity, although this may be associated with limits of statistical detection. Isolate specificity is a common feature in host-pathogen interactions, due to the gene-for-gene interaction in host systems (Flor 1971). ETI exerts considerable selection pressure on pathogen populations, which leads to adoption of mutations in the effector repertoire to avoid detection by the host plant (Jones and Dangl 2006). The emergence of new isolates with an altered effector repertoire consequently leaves the plant with isolate-specific resistance genes (Jones and Dangl 2006). As resistance towards non-adapted pathogens is commonly thought to be governed by many, minor effect QTLs reminiscent of basal host resistance (Niks and Marcel 2009), we did not expect isolate-specific major effect genes to control the interaction between *B. distachyon* and *Pst* and *Psh* isolates. Our findings highlight how the interactions on the continuum from host to nonhost systems are not only intermediary at the phenotypic level (e.g. pathogen colonisation, without life cycle completion), but also rely on an intermediary molecular basis, building on components frequently associated with host systems only, supported by additional minor effect QTLs.

### *Intermediate nonhost resistance as a source for durable, broad spectrum resistance*

A major goal of plant breeding is the creation of disease resistant crop cultivars, which can then be deployed in agriculture (Ayliffe and Lagudah 2004). Traditionally, this has allowed the introduction of short-lived resistance genes, which can be quickly overcome through mutations in the pathogen and wind dispersal of exotic isolates (Brown and Hovmöller 2002; McDonald and Linde 2002; Wulff *et al.* 2011). Recent technological advances have accelerated our ability to identify resistance genes and transfer them between species (Kawashima *et al.* 2016; Steuernagel *et al.* 2016; Witek *et al.* 2016). However, the transfer of single resistance genes from one species to another will exert similar selection pressures on pathogen populations as traditional plant breeding (Ellis 2006; Wulff and Moscou 2014). Pyramiding of resistance genes or the development of cassettes consisting of multiple resistance genes have been proposed as more durable forms of gene deployment (Joshi and Nayak 2010; Dangl *et al.* 2013; Ellis *et al.* 2014; Wulff and Moscou 2014).

The simple genetic architecture underlying colonisation resistance to *Pst* and *Psh* in *B. distachyon* provides an opportunity to clone the genes governing this resistance. Once identified, it will be of great interest to test these genes in the respective host species wheat and barley. As only a limited number of genes prevent colonisation of *B. distachyon*, this could present an opportunity to create a “natural” resistance gene cassette and recreate intermediate nonhost resistance in the host species. Moreover, the transfer of these resistance genes will allow further characterisation regarding their durability and broad spectrum activity. Examples of cross species transfer of resistance genes, such as *Rxo1* from maize to rice (Zhao *et al.* 2005), have shown that they can possess broader recognition capability in the heterologous plant species.

### *A shared basis for host and nonhost resistance*

While it has been proposed that host and nonhost resistance are inherently different, the simple genetic architecture of resistance in this intermediate nonhost system is reminiscent of a host system. Moreover, the isolate specificity observed for major and minor effect QTLs and the associated NB-LRR encoding candidate genes suggest that the genetic architectures of host and nonhost systems are structurally coupled and share conserved components. Indeed, NB-LRRs have previously been implicated in

conferring resistance to non-adapted pathogens (Zhao *et al.* 2005; Staal *et al.* 2006; Shafiei *et al.* 2007; Borhan *et al.* 2008). Emphasis has been placed on the intrinsic differences between host and nonhost resistance, whereas nonhost resistance may reflect a complete form of resistance, which can draw on a wide range of responses and pathways that might limit pathogen ingress. In the highly specialised interaction between a host plant and an adapted pathogen, most of these will have lost their effectiveness and plant and pathogen are left in an evolutionary arms race cycling through the emergence of isolate-specific resistant accessions and their defeat.

## Materials and methods

### *Plant and fungal material*

The ABR6 x Bd21 F<sub>4</sub> population has been described previously (Bettgenhaeuser *et al.* 2017). Seed for the *B. distachyon* accessions Luc1, Jer1, and Foz1 was obtained from Luis Mur (Aberystwyth University), and F<sub>1</sub> plants were confirmed with CAPS markers (data not shown). To increase F<sub>2</sub> seed yield, F<sub>1</sub> plants were grown in a prolonged vegetative state to increase biomass before vernalisation and flowering (Woods and Amasino 2016). F<sub>2</sub> seed were grown from a single plant for both Luc1 x Jer1 and Foz1 x Luc1 crosses. Tissue for DNA extraction and genetic map construction was collected after phenotyping. *P. striiformis* isolates were collected in the United Kingdom in 2001 (*Psh* B01/2), 2008 (*Pst* 08/21 and 08/501), and 2011 (*Pst* 11/08). Isolates were maintained at the National Institute of Agricultural Botany on susceptible barley and wheat cultivars, respectively, and urediniospores were stored at 6°C after collection.

### *Development of the Luc1 x Jer1 and Foz1 x Luc1 genetic maps*

Resequencing data was obtained from the JGI Genome Portal for the projects 1000598 (Luc1), 404166 (Jer1), and 404167 (Foz1). These sequence data were produced by the US Department of Energy Joint Genome Institute (<http://www.jgi.doe.gov/>) in collaboration with the user community. *De novo* assemblies were created from the raw reads using default settings and parameters of the CLC Assembly Cell (Version 4.2.0). To ensure an equal genetic distribution across the whole genome, marker positions were selected based on the ABR6 x Bd21 genetic map (Bettgenhaeuser *et al.* 2017). A BLAST search was performed with Bd21 sequence based on desired position against the Luc1, Jer1, and Foz1 *de novo* assemblies. The contig sequences for the respective top hits were aligned in Geneious (Version 7.1.8). SNPs without additional sequence variation in a 160 bp window were selected for KASP marker development. To confirm the relative position of the Luc1 x Jer1 and Foz1 x Luc1 markers in the Bd21 reference sequence, a BLAST search was performed with the sequences used for KASP marker development. Markers were named according to the relative SNP position in the Bd21 reference sequence (Version 1). The final Luc1 x Jer1 genetic

map consists of 107 markers and has a size of 1,446 cM. The preliminary Foz1 x Luc1 genetic map consists of 90 markers and has a size of 1119 cM. The quality of the Luc1 x Jer1 genetic map was confirmed by analysing recombination fractions in R/qtl.

#### *Plant growth, inoculation and phenotyping*

For the ABR6 x Bd21 population, 114 F<sub>4:5</sub> families were sown in groups of four in 1 L pots containing peat-based compost. For the Luc1 x Jer1 and Foz1 x Luc1 populations 188 F<sub>2</sub> individuals were sown individually in 24-hole trays containing peat-based compost. Plants were grown at 18°C day and 11°C night in a 16 h photoperiod in a controlled environment room. Seedlings were inoculated four weeks after sowing at the four to five leaf stage. Urediniospores of the different *P. striiformis* isolates were suspended in a 1:16 ratio in talcum powder and applied to the seedlings with compressed air on a spinning platform (Dawson *et al.* 2015). Infected leaves were evaluated according to the previously established macroscopic and microscopic phenotyping assays (Dawson *et al.* 2015). Briefly, for macroscopic phenotyping the observation of leaf browning (Figure 10A) was scored on a nine-point scale from 0 to 4, with increments of 0.5. A score of 0 was given to asymptomatic leaves (i.e. no leaf browning) and a score of 4 was given to leaves fully expressing the leaf browning phenotype (100% of the surface area). By way of example, the respective scores for the leaves shown in Figure 10A are 0 (ABR6), 2.5 (Bd21), 3.0 (Luc1), 0.5 (Jer1), and 0 (Foz1). For microscopic phenotyping, leaves were cleared in a 1.0 M KOH solution, neutralised by washing in 50 mM Tris at pH 7.5, and stained with a chitin-specific fluorophore (20 µg/mL WGA-FITC (L4895- 10MG; Sigma–Aldrich) in 50 mM Tris at pH 7.5), as described in Dawson *et al.* (2015) and adapted from Ayliffe *et al.* (2011; 2013). Fungal growth within the leaves was visualised under blue excitation on a fluorescence microscope with a GFP filter using a 10x objective, which gave a field of view (FOV) of 1.36 mm x 1.02 mm. Percent of leaf colonized (pCOL) was determined by scanning a mounted leaf segment along the longitudinal axis and evaluating disjoint FOVs. Within each FOV scores of 0, 0.5, or 1 were given for hyphal growth less than 15%, between 15 and 50%, or greater than 50% of the FOV area, respectively. The scores for the individual FOVs were averaged to give a final pCOL score ranging from 0 to 100%. In the ABR6 x Bd21 population, leaf browning and pCOL phenotypes were scored 14 dpi (Dawson *et al.* 2015). Phenotypes were

collected for each individual in a family and then averaged. The two *Pst* 08/501 replicates consisted of 20 and five plants per  $F_{4:5}$  family, respectively. The two *Pst* 08/21 replicates consisted of 10 and five plants per  $F_{4:5}$  family, respectively. All replicates of *Pst* 11/08 and *Psh* B01/2 consisted of five plants per  $F_{4:5}$  family. In the *Luc1* x *Jer1* and *Foz1* x *Luc1* populations  $F_2$  plants were phenotyped individually 14 dpi for leaf browning and 23 dpi for leaf browning and pCOL. Additionally, 95 *Luc1* x *Jer1*  $F_{2:3}$  families were phenotyped by growing and inoculating 16  $F_3$  plants in a 1 L pot as described above. Leaf browning phenotypes were collected 14 dpi for each individual in a family and then averaged. Phenotypes were assessed for normality using the Shapiro-Wilk test (Royston 1982) and Pearson rank correlation coefficients ( $\rho$ ) between leaf browning and pCOL phenotypes were determined using the *cor* command in R (v3.2.2).

#### *Quantitative trait locus analyses*

For the *ABR6* x *Bd21* population, composite interval mapping was performed under an additive model ( $H_0:H_1$ ) due to the extensive homozygosity observed at the  $F_4$  stage (~87.5%). For the *Luc1* x *Jer1* and *Foz1* x *Luc1* populations, composite interval mapping was performed using the additive and dominance model  $H_0:H_3$ . QTL Cartographer (Version 1.17j) was used for composite interval mapping with the selection of five background markers, a walking speed of 2 cM, and a window size of 10 cM (Zeng 1993; Zeng 1994; Basten *et al.* 2004). Statistical significance for QTLs was determined by performing 1,000 permutations with reselection of background markers and controlled at  $\alpha = 0.05$  (Doerge and Churchill 1996; Lauter *et al.* 2008). For the *ABR6* x *Bd21* population, QTL analyses were performed with the averaged phenotyping data from the individual replicates, as well as an average across both replicates per isolate tested. For the *Luc1* x *Jer1* and *Foz1* x *Luc1* populations, QTL analyses were performed with the individual phenotyping scores from the  $F_2$  individuals and the averaged phenotyping data from the *Luc1* x *Jer1*  $F_{2:3}$  families. One-LOD and two-LOD support intervals were estimated based on standard interval mapping (Lander and Botstein 1989).

#### *Candidate gene analysis at Yrr1 and Yrr3*

The one-LOD and two-LOD support intervals for the pCOL phenotypes from all three mapping populations were assessed for the presence of canonical resistance genes. The most recent Bd21 reference genome annotation was obtained from Phytozome (Version 11.0.7) and searched for genes annotated as encoding nucleotide binding (NB) domains.

## 4. Isolation, fine-mapping, and characterisation of *Yrr3*, an intermediate nonhost resistance locus to stripe rust in *B. distachyon*

One sentence summary: A CC-NB/NB-LRR cluster confers intermediate nonhost resistance to stripe rust.

### Introduction

Nonhost resistance describes the immunity observed towards non-adapted pathogens and is by definition broad spectrum and durable (Mysore and Ryu 2004; Nürnberg and Lipka 2005; Lipka *et al.* 2008; Schulze-Lefert and Panstruga 2011). Efforts to leverage this durable and broad spectrum resistance against agronomically important pathogens has led to considerable interest in the genetic architecture and molecular basis of nonhost resistance (Hammond-Kosack and Parker 2003; Fan and Doerner 2012; Lee *et al.* 2016). *Brachypodium distachyon* is an intermediate nonhost of stripe rust (*Puccinia striiformis*) (Ayliffe *et al.* 2013; Dawson *et al.* 2015), which is an agronomically important pathogen of wheat (f. sp. *tritici*, *Pst*) and barley (f. sp. *hordei*, *Psh*) (Hovmöller *et al.* 2011; Beddow *et al.* 2015). Some *B. distachyon* accessions allow a degree of colonisation of *Pst*, but not life cycle completion (Dawson *et al.* 2015). We identified a simple genetic architecture, which conferred this colonisation resistance towards both *Pst* and *Psh* isolates (see previous chapter). This simple genetic architecture facilitates efforts to dissect the genes underlying resistance and address open questions regarding the molecular basis of resistance on the transition from host to nonhost systems.

In order to successfully colonise a plant, a pathogen needs to overcome several preformed and inducible barriers (Thordal-Christensen 2003). Germination and differentiation on the plant may depend on certain cues, such as the composition of leaf surface waxes, which can already prevent growth of non-adapted pathogens on the leaf surface (Tsuba *et al.* 2002; Thordal-Christensen 2003). Preformed chemical, structural, or enzymatic barriers can subsequently prevent colonisation of the leaf tissue, such as the antimicrobial avenacins from oat (Papadopoulou *et al.* 1999; Thordal-Christensen 2003). Should the pathogen evade these preformed barriers, the plant may recognise the attempted infection and deploy inducible barriers (Thordal-

Christensen 2003). In *Arabidopsis thaliana* colonisation by non-adapted powdery mildews from barley (*Blumeria graminis* f. sp. *hordei*) and pea (*Erysiphe pisi*) is prevented through the formation of papillae, localised reinforcements of the cell wall which prevent colonisation (Zeyen *et al.* 2002; Lipka *et al.* 2008). Three *PEN* (*PENETRATION*) genes, which encode a plasma membrane-bound SNARE (soluble *N*-ethylmaleimide-sensitive factor attachment protein receptor) domain containing protein, a hydrolase, and an ABC (ATP binding cassette) transporter, regulate the structural rearrangements necessary for the formation of papillae (Collins *et al.* 2003; Lipka *et al.* 2005; Stein *et al.* 2006; Lipka *et al.* 2008). Expression of the *PEN* genes is induced upon perception of flagellin, a bacterial PAMP (pathogen-associated molecular pattern), by the PRR (pattern recognition receptor) FLS2, a receptor-like kinase (Zipfel *et al.* 2004; Lipka *et al.* 2005). Other PAMPs include the bacterial EF-Tu (elongation factor thermo unstable) and fungal chitin, whose recognition by the receptor-like kinases EFR, CERK1, and LYK5 likely results in various induced defence responses (Zipfel *et al.* 2006; Miya *et al.* 2007; Cao *et al.* 2014). Should the pathogen be able to evade or suppress detection at this stage and be successful in obtaining nutrients from the plant, subsequent defence responses by the plant are thought to involve isolate-specific pathogen recognition and not rely on broad spectrum recognition (Thordal-Christensen 2003). Plant interactions with adapted pathogens are typically described as gene-for-gene interactions and rely on the direct or indirect recognition of a pathogen effector by a plant nucleotide binding, leucine-rich repeat (NB-LRR) protein (Flor 1971; Jones and Dangl 2006; Bent and Mackey 2007). Recognition of the pathogen leads to effector triggered immunity (ETI), which consists of the initiation of downstream signalling and localised cell death, also known as a hypersensitive response, the hallmark of NB-LRR mediated resistance (Jones and Dangl 2006).

Whilst NB-LRR mediated resistance plays a major role in host systems, i.e. in the plant-pathogen interactions where the majority of barriers described above are overcome, it remains unclear to what degree NB-LRRs contribute to resistance in plant interactions with non-adapted pathogens. Generally, NB-LRRs are hypothesised to be less prevalent in these latter interactions, while other resistance genes like PRRs are proposed to play a greater role (Schulze-Lefert and Panstruga 2011). However, a number of studies have found direct or indirect evidence that NB-LRR mediated

recognition is important for initiating defence responses towards non-adapted pathogens. Indirect evidence comes from studies which found recognition of effectors and induction of a hypersensitive response in intermediate or nonhost systems, such as the recognition of *Pseudomonas syringae* pv. *tomato* effectors by soybean or *Arabidopsis thaliana* (Kobayashi *et al.* 1989; Sohn *et al.* 2012) and *Phytophthora infestans* effectors by pepper (Lee *et al.* 2014). ETI is therefore thought to be a contributing factor in limiting the pathogen's host range, as was demonstrated for *Pseudomonas syringae* pv. *tomato* infection of *Nicotiana benthamiana* (Wei *et al.* 2007), *Erwinia amylovora* infection of rosaceous host and nonhost species (Asselin *et al.* 2011), *Magnaporthe oryzae* infection of weeping lovegrass (Kang *et al.* 1995; Sweigard *et al.* 1995), and in a more comprehensive study by characterising the response of 59 plant genotypes towards 171 *Pseudomonas* and *Ralstonia* effectors (Wroblewski *et al.* 2009). The identification of NB-LRRs that recognise or provide resistance to non-adapted pathogens provides direct evidence for NB-LRR involvement in intermediate or nonhost resistance. The NB-LRR *RLM1* and NB encoding *RLM3* provide resistance against the non-adapted pathogen *Leptosphaeria maculans* in *A. thaliana* (Staal *et al.* 2006; Staal *et al.* 2008). Similarly, *WRR4* recognises non-adapted *Albugo* isolates in *A. thaliana* (Borhan *et al.* 2008). It is unlikely that these NB-LRRs specifically recognise only non-adapted pathogens, but likely that they recognise effectors similar to or shared with host pathogens, or guard targets, which are attacked by both adapted and non-adapted pathogens. Evidence for this comes from *LOV1* and *Rxo1*, two NB-LRRs from *A. thaliana* and *Zea mays* (maize) (Zhao *et al.* 2004; Lorang *et al.* 2012). The necrotrophic oat pathogen *Cochliobolus victoriae* secretes victorin toxin, which targets a thioredoxin guarded by the *Arabidopsis thaliana* *LOV1*, leading to the initiation of defence responses and susceptibility to the necrotroph (Lorang *et al.* 2012). *Rxo1* was identified as a maize resistance gene against the non-adapted rice (*Oryza sativa*) pathogen *Xanthomonas oryzae* pv. *oryzicola*, but was later found to also provide resistance against the maize pathogen *Burkholderia andropogonis* (Zhao *et al.* 2004; Zhao *et al.* 2005). Yang *et al.* (2013) hypothesise that a "constrained divergence" underlies NB-LRR differentiation and that recognition of non-adapted pathogen could be a common feature of rapidly evolving NB-LRRs. The authors randomly selected rapidly evolving NB-LRRs from maize, sorghum (*Sorghum bicolor*), and *B. distachyon* and showed that some provide race-specific resistance against *M. oryzae* when transferred to rice (Yang *et al.* 2013).

NB-LRRs are part of the signal transduction ATPases with numerous domains (STAND) family (Lukasik and Takken 2009). As such, they are modular proteins and consist of several conserved domains (Lukasik and Takken 2009; Takken and Goverse 2012; Bentham *et al.* 2016; Sukarta *et al.* 2016). The NB domain forms the nucleotide binding pocket, whereas evidence suggests that the highly variable LRR domain is involved in pathogen perception and autoinhibition in the absence of the pathogen (Bentham *et al.* 2016; Sukarta *et al.* 2016). N-terminal adaptor domains (coiled coil (CC) or Toll/interleukin-1 receptor homology (TIR) domains) are thought to mediate signalling via protein-protein interactions in homo- or heterodimeric complexes (Maekawa *et al.* 2011; Hao *et al.* 2013; Williams *et al.* 2014; Bentham *et al.* 2016). Additional domains (generally represented with an “X”) have been described, such as the WRKY domain of *A. thaliana* RRS1 (Le Roux *et al.* 2015; Sarris *et al.* 2015). These are hypothesised to function as integrated decoys and facilitate the detection of pathogen effectors (Cesari *et al.* 2014; Nishimura *et al.* 2015; Sarris *et al.* 2016). Putative resistance proteins do not always possess all of these domains. Annotation of *A. thaliana* genes that encode at least some of these common resistance protein domains (CC, TIR, NB, or LRR) showed that 149 contain an LRR domain, while 58 did not (Meyers *et al.* 2003). This latter group included 21 TIR-NB and four CC-NB proteins (Meyers *et al.* 2003).

In the previous chapter I have described the characterisation of resistance to *Pst* isolate 08/21 in three mapping populations and resistance to two additional *Pst* isolates and a *Psh* isolate in the ABR6 x Bd21 mapping population. In all of these interactions, *Yrr3* was a major effect locus limiting pathogen colonisation of leaf tissue. *Yrr3* acted together with *Yrr1* in the ABR6 x Bd21 and Foz1 x Luc1 populations, but was the only major effect locus in the Luc1 x Jer1 population. Here I describe the isolation, fine-mapping, and characterisation of *Yrr3* in the ABR6 x Bd21 and Luc1 x Jer1 populations. Initially, fine-mapping delineated a 72 kb consensus gain of function interval centred around a cluster of a CC-NB and two NB-LRR genes. A recombination screen narrowed this candidate region down to two SNPs, which cause non-synonymous mutations in or close to conserved motifs in the NB domains of the CC-NB and one of the NB-LRR, respectively. Constructs have been created for the resistant alleles of all three candidate genes and transformation is underway.

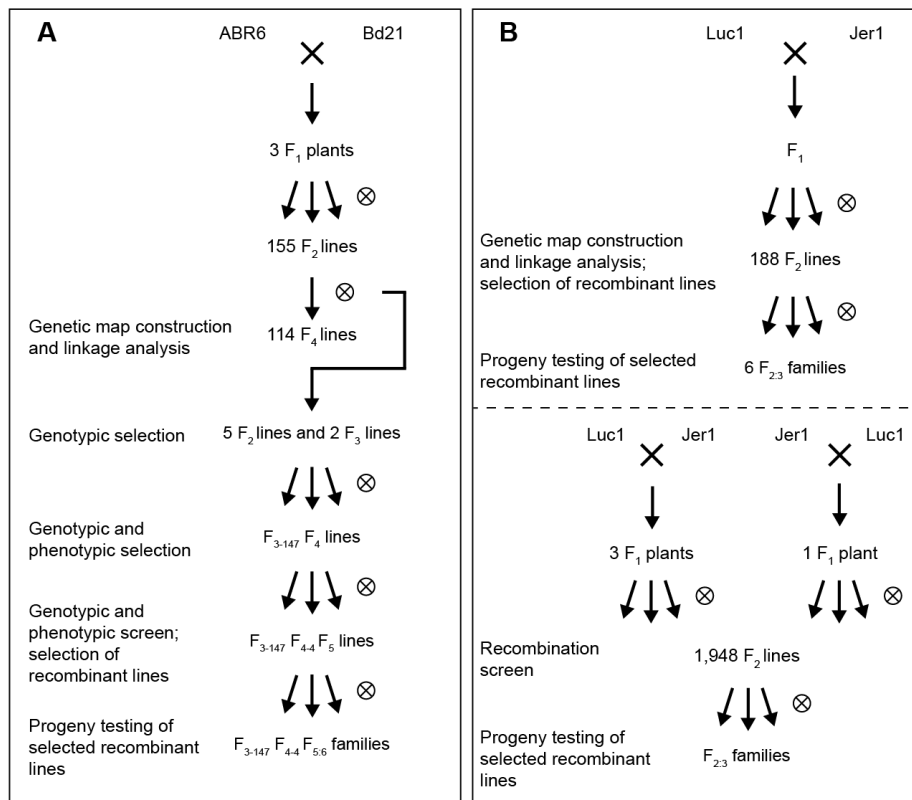


**Figure 17.** Isolation and fine-mapping of *Yrr3* in two independent populations. (A) ABR6 x Bd21 lines heterozygous for the *Yrr3* locus and homozygous for the *Yrr1* locus were identified and cosegregation with resistance was evaluated in the progeny. Analysis of F<sub>5:6</sub> families derived from recombinant F<sub>5</sub> lines were used to delineate the *Yrr3* gain of function interval. (B) Unresolved recombinant Luc1 x Jer1 F<sub>2</sub> lines were selected for progeny testing, which delineated the initial Luc1 x Jer1 gain of function interval (top panel). A recombination screen of Luc1 x Jer1 and Jer1 x Luc1 F<sub>2</sub> lines identified 23 additional recombinant lines, whose progeny were evaluated (bottom panel).

## Results

### Parallel fine-mapping delineates *Yrr3* to a 72 kb gain of function interval

Of the three populations studied in the previous chapter, the ABR6 x Bd21 population represented the widest cross. Two major effect loci, *Yrr1* and *Yrr3*, confer resistance to stripe rust in this population and isolation of the *Yrr3* locus was therefore needed before additional fine-mapping was feasible. QTL analyses with three UK *Pst* isolates and one UK *Psh* isolate indicated Bd2\_51527431 and Bd2\_51728490 as the closest linked markers in the *Yrr3* locus (see previous chapter). However, the maximal two-LOD support interval of the four QTLs spanned across an interval of 26.7 cM, which equates to a region of roughly 3 Mb (Figure 16). In order to isolate *Yrr3* and delineate the region of interest further, we identified lines homozygous for the susceptible genotype (Bd21) at the *Yrr1* locus and heterozygous at the *Yrr3* locus (Figure 17).

**Table 6.** Average phenotypic scores from progeny testing of selected ABR6 x Bd21 F<sub>2</sub> and F<sub>3</sub> lines based on genotype at the *Yrr3* peak marker.

Line	ABR6	Heterozygous	Bd21
F <sub>2-161</sub>	1.3 (2) <sup>a</sup>	1.5 (4)	2.4 (4)
F <sub>2-181</sub>	0.8 (3)	1.1 (7)	2.0 (5)
F <sub>2-195</sub>	-	1.7 (10)	2.2 (6)
F <sub>2-203</sub>	1.8 (2)	1.7 (6)	-
F <sub>2-226</sub>	0 (1)	0.3 (5)	1.0 (1)
F <sub>3-38</sub>	0.4 (4)	0.6 (7)	0.9 (4)
F <sub>3-147</sub>	0.3 (3)	0.9 (11)	2.5 (1)

<sup>a</sup>Numbers in brackets indicate individuals per genotype.

Progeny of five F<sub>2</sub> and two F<sub>3</sub> lines that fulfilled these criteria were phenotyped and genotyped and line F<sub>3-147</sub>, whose progeny showed clear cosegregation between genotypes and phenotypes, was selected for fine-mapping *Yrr3* (Table 6). Of the 15 F<sub>4</sub> plants grown and tested from this line, four plants were resistant (leaf browning scores below 1.0) and heterozygous for the region spanning *Yrr3*, facilitating phenotypic screening in the progeny. Cosegregation between phenotypes and the *Yrr3* marker was evaluated among 46 individuals in F<sub>4:5</sub> families derived from these four lines. Based on this preliminary assessment, cosegregation was evaluated on an extended set of 184 F<sub>5</sub> individuals of family F<sub>3-147</sub> F<sub>4-4</sub> (Figure 18).

The results were validated by phenotyping 16 F<sub>6</sub> progeny for 94 F<sub>3-147</sub> F<sub>4-4</sub> F<sub>5</sub> lines. Three northern (lines 45, 70, and 87) and two southern (lines 3 and 77) recombination events delineated a 131 kb gain and loss of function interval among these 94 lines. Further marker saturation separated the two southern recombination events and delineated a 103 kb gain of function and 109 kb loss of function interval (Figure 20).

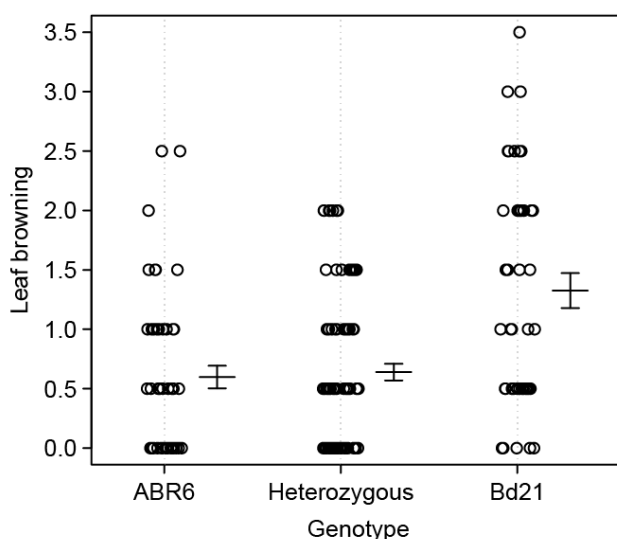


**Figure 18.** *Yrr3* cosegregates with resistance in ABR6 x Bd21 F<sub>5</sub> progeny from line F<sub>3-147</sub> F<sub>4-4</sub>. Phenotype by genotype plot for leaf browning 14 days after inoculation and the *Yrr3* peak marker. Error bars represent one standard error; N = 51 (ABR6), 86 (heterozygous), and 43 (Bd21).

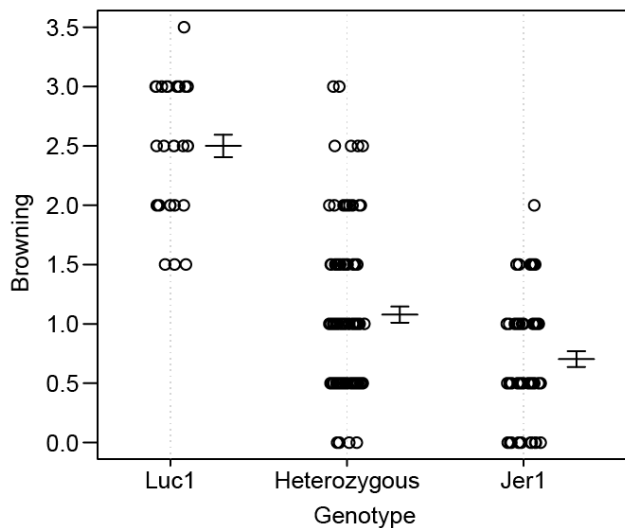


**Figure 19.** *Yrr3* is almost mendelised in the Luc1 x Jer1 population. Cosegregation with resistance in Luc1 x Jer1 F<sub>2</sub> lines reveals only limited overlap between the Luc1 and Jer1 phenotypic pools. Phenotype by genotype plot for leaf browning 14 days after inoculation and the *Yrr3* peak marker. Error bars represent one standard error; N = 33 (Luc1), 96 (heterozygous), and 59 (Jer1).

In parallel to the fine-mapping and candidate region annotation in the ABR6 x Bd21 population, two additional *B. distachyon* populations were developed. Of these, the Luc1 x Jer1 population was found to singularly possess *Yrr3* as major effect locus conferring resistance to *Pst* isolate 08/21. Among the 188 F<sub>2</sub> lines phenotyped and genotyped, *Yrr3* explained up to 46.5% of the phenotypic variation observed for leaf browning (see previous chapter). *Yrr3* was almost mendelised among the F<sub>2</sub> lines, as there was only limited overlap of phenotypes from lines homozygous Luc1 and homozygous Jer1 at *Yrr3* (Figure 19).

Marker saturation across the *Yrr3* locus identified recombination events, which delineated a 225 kb gain of function interval and 315 kb loss of function interval (data not shown). These incorporated the gain and loss of function intervals identified in the ABR6 x Bd21 population. Four additional recombination events within the gain of function interval could not be resolved in the F<sub>2</sub> lines, as the phenotypes could not be unambiguously assigned to the respective cluster. To resolve these recombination events, 32 F<sub>3</sub> progeny of the two delineating recombinants and the four unresolved recombinants were phenotyped and genotyped (Figure 17). Cosegregation between phenotype and genotype among these lines reduced the gain of function interval to 74 kb, whereas no additional loss of function recombination events were observed (Figure 20).

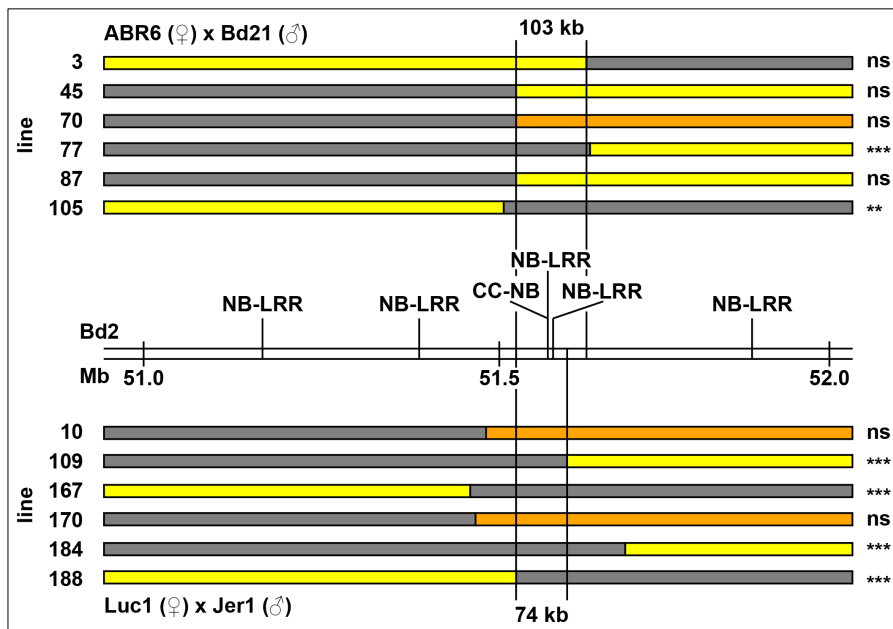


**Figure 20.** Fine-mapping of a 72 kb consensus gain of function interval in two independent populations. Marker regression identified the statistical significance of cosegregation between phenotype and genotype among progeny, which delineated a 103 kb gain of function interval in the ABR6 x Bd21 population (16 progeny tested per line) and a 74 kb gain of function interval in the Luc1 x Jer1 population (32 progeny tested per line). The six most critical recombinant lines from each population are shown and the positions of the NB domain containing genes identified in the previous chapter are indicated. Yellow = homozygous maternal genotype (ABR6 and Luc1), grey = heterozygous, orange = homozygous paternal genotype (Bd21 and Jer1). Statistical significance of cosegregation: \*\*\* =  $p$ -value under 0.001, \*\* =  $p$ -value under 0.01, ns = not significant (see Table S10).

*Yrr3* was independently isolated and fine-mapped to overlapping genomic regions in two unrelated *B. distachyon* populations. The two gain of function intervals identified between ABR6 x Bd21 and Luc1 x Jer1 share a 72 kb consensus region, with the ABR6 x Bd21 gain of function interval delineating the northern border and the Luc1 x Jer1 gain of function interval delineating the southern border (Figure 20).

#### *Yrr3 recombination screen demarcates two SNPs separating an 11.3 kb interval*

As *Yrr3* is the only major effect locus segregating in the Luc1 x Jer1 population, a recombination screen was initiated to identify additional recombinants within the 74 kb gain of function interval delineated among the  $F_{2:3}$  families. Markers delimiting this interval were used to screen 1,948  $F_2$  plants (i.e. 3,896 gametes) derived from three Luc1 x Jer1  $F_1$  plants and one Jer1 x Luc1  $F_1$  plant (Figure 17).

Of these 1,948 F<sub>2</sub> plants, 23 F<sub>2</sub> lines had recombination events within the 74 kb gain of function interval and 32 seedlings were phenotyped and genotyped for each recombinant line. Additional markers were developed from WGS *de novo* contigs across the 74 kb interval in order to locate the recombination events. Statistically significant cosegregation between phenotypes and the heterozygous region of the individual recombinants was narrowed down to two SNPs, which demarcate an 11.3 kb interval. One northern and six southern recombination events delineate the two SNPs (Figure 21). This result was confirmed by calculating the mean browning score of all homozygous recombinant F<sub>3</sub> lines. With the exception of progeny derived from one line (JB\_0332-C3), homozygous recombinant lines with the Luc1 genotype across the interval had significantly higher browning scores than homozygous recombinant lines with the Jer1 genotype at the two SNPs at 14 days post inoculation (Table S11). Enhanced cosegregation was observed when plants were phenotyped again at 21 days post inoculation.

#### *Luc1 and Jer1 are near identical across the CC-NB/NB-LRR cluster*

The two SNPs identified among the recombinant lines fall within a cluster of a CC-NB encoding gene (Bradi2g52430) and two NB-LRR encoding genes (Bradi2g52437 and Bradi2g52450), which was associated with the *Yrr3* peak markers in the QTL analyses (see Figure 16 in previous chapter). In order to investigate the sequence variation between Luc1 and Jer1 across this cluster, the *de novo* assemblies created from the Luc1 and Jer1 resequencing reads were probed with the Bd21 reference sequence of the interval. Two large contigs were identified (70 kb for Jer1 and 77 kb for Luc1), which covered around 48 kb of the original 74 kb gain of function interval from the southern border (Figure 21B) and the complete 11.3 kb interval delineated in the recombination screen. The 48 kb of both contigs within the gain of function interval were near identical and no additional sequence variation to the SNPs already used as markers differentiated the parental accessions across this cluster. One of the SNPs maps to the annotated coding sequence of Bradi2g52430, the CC-NB encoding gene, and the annotated 3' untranslated region (3'-UTR) of Bradi2g52437, the NB-LRR on the opposite strand to Bradi2g52430. The other SNP maps to the annotated coding sequence of Bradi2g52450, the other NB-LRR in the cluster.

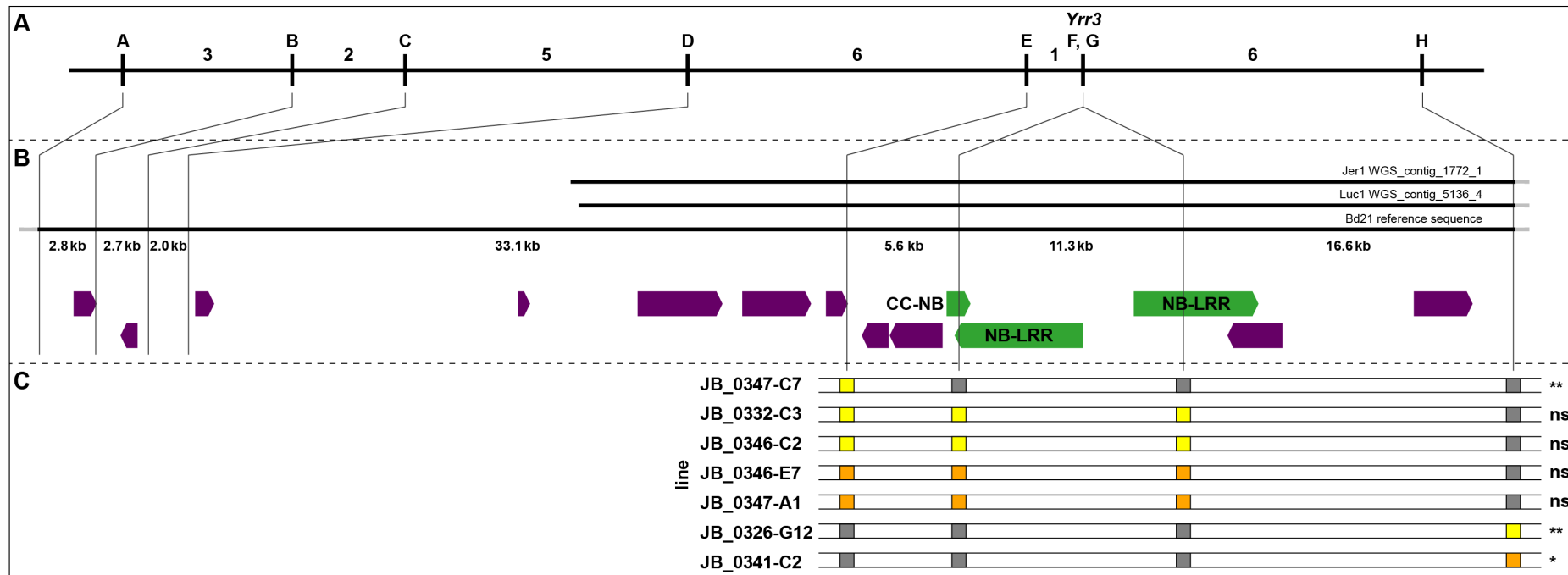


**Figure 21.** Fine-mapping of *Yrr3* within the Luc1 x Jer1 population. A recombination screen identified 23 recombinant lines (A), which fall within the original 74 kb gain of function interval defined within the Luc1 x Jer1 *F*<sub>2</sub> population (B). The seven most critical recombinant lines are shown (C) and cosegregation between marker and phenotype among progeny narrows *Yrr3* down to two SNPs encompassing a 11.3 kb interval. Based on contigs from WGS *de novo* assemblies no additional sequence variation exists between Luc1 and Jer1 within this interval (B). Thin lines = marker/SNP positions. Annotated genes: Green = Bradi2g52430, Bradi2g52437, and Bradi2g52450; purple = other annotated genes within the original 74 kb gain of function interval defined in the Luc1 x Jer1 *F*<sub>2</sub> population. Colour scheme for markers in (C): Yellow = homozygous Luc1, grey = heterozygous, and orange = homozygous Jer1. Statistical significance of cosegregation: \*\* = *p*-value under 0.01, \* = *p*-value under 0.05, and ns = not significant (see Table S10). Markers in (A): A = Bd2\_51764532\_60\_F, B = Bd2\_51767364\_60\_F, C = Bd2\_51770065\_60\_R, D = Bd2\_51772031\_60\_F, E = Bd2\_51805111\_80\_F, F = Bd2\_51810746\_80\_R, G = Bd2\_51822083\_60\_F, and H = Bd2\_51838682\_60\_F.

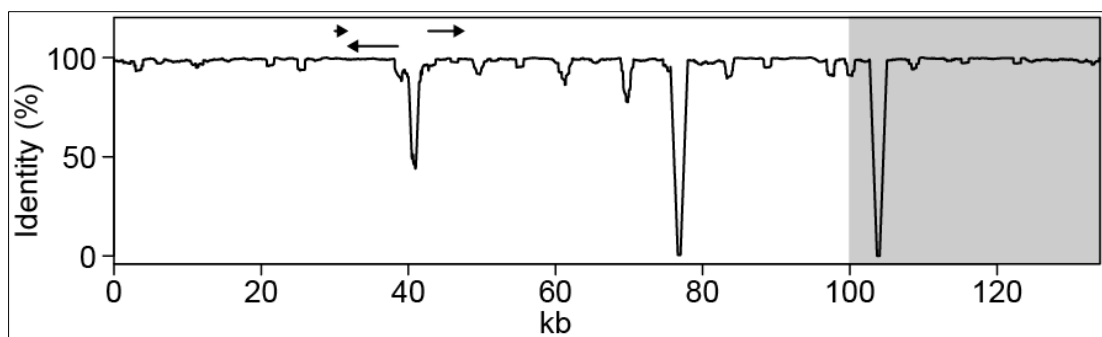


**Figure 22.** Nucleotide identity between ABR6 and Bd21 drops within the CC-NB/NB-LRR cluster. The consensus sequence obtained from two ABR6 BACs was aligned to the Bd21 reference sequence and nucleotide identity was evaluated in 1 kb sliding windows with a step size of 1bp. The positions of Bradi2g52430, Bradi2g52437, and Bradi2g52450 within the alignment are indicated by arrows. The area shaded in grey falls outside of the 103 kb gain of function interval delineated in the ABR6 x Bd21 population.

*ABR6 and Bd21 possess greater structural variation across the CC-NB/NB-LRR cluster*

As ABR6 and Bd21 are genotypically diverged, we wanted to assess the structural variation present between these lines at the *Yrr3* locus. Bradi2g52437 is at the centre of the CC-NB/NB-LRR cluster and primers were designed within this NB-LRR to screen a BAC library generated from ABR6. Two BACs were isolated and sequenced using PacBio-SMRT (single molecule, real-time sequencing). Reads were assembled into single contigs with lengths of 100,210 bp and 117,993 bp, which largely overlapped with a consensus sequence of 134,432 bp.

Pair-wise alignment to the Bd21 reference genome showed that the BACs cover the entire CC-NB/NB-LRR cluster delineated in the recombination screen. Despite being genotypically diverged, ABR6 and Bd21 still shared a high degree of sequence similarity across this region. The two parental lines had 95.6% nucleotide identity over the entire length of the alignment, though this dropped to 76.1% across the shared promoter region of the two head-to-head NB-LRRs. A more in-depth analysis across the length of the alignment using a sliding window of 1 kb and a walking speed of 1 bp revealed that the identity between the two lines drops to 44.0% in the shared promoter region of the CC-NB/NB-LRR cluster (Figure 22).

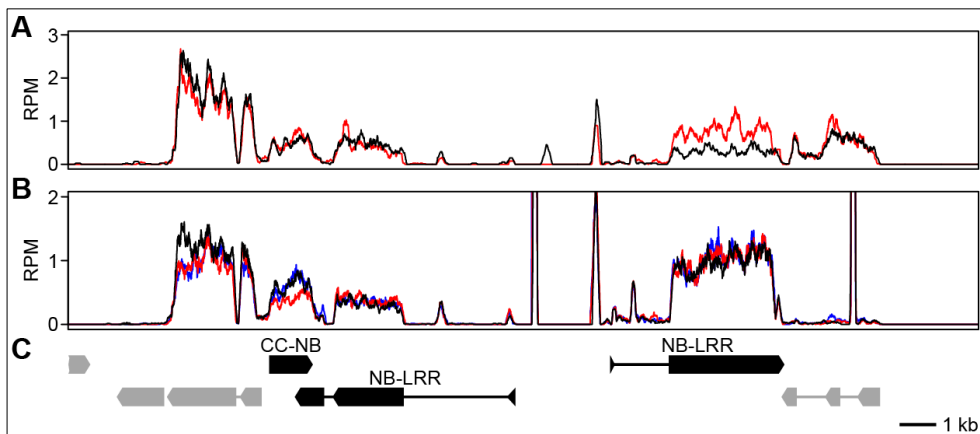


**Figure 23.** All three candidate genes are expressed in both resistant and susceptible accessions. (A) Bowtie alignment of RNAseq reads from ABR6 (red) and Bd21 (black), (B) Bowtie alignment of RNAseq reads from Luc1 (black), Jer1 (red), and Foz1 (blue). Extreme peaks of expression within (B) are due to alignment of unspecific repeat reads from elsewhere in the genome. (C) Annotated genes within interval: Bradi2g52430, Bradi2g52437, and Bradi2g52450 are shown in black, other annotated genes in grey. RPM = reads per million.

*The delineated CC-NB/NB-LRR cluster is highly conserved across monocot species*

The 72 kb consensus interval initially identified between the ABR6 x Bd21 and Luc1 x Jer1 populations incorporates 14 annotated genes, which are largely syntenic with a region on rice chromosome Os1 (The International Brachypodium Initiative 2010). Notably, within this interval the *B. distachyon* genes from Bradi2g52410 to Bradi2g52450 are colinear with the rice genes from Os1g58490 to Os1g58530. Comparison with the syntenic rice region revealed that this CC-NB/NB-LRR cluster is conserved in rice and prompted us to look for conservation among other monocot species with gold-standard sequenced genomes. This analysis demonstrated that the CC-NB/NB-LRR cluster is also conserved in sorghum and maize. In each species, the order and relative orientation of the three top hits is maintained (Table S12).

*All three candidate genes in the cluster are expressed in resistant and susceptible accessions*

In order to characterise the *Yrr3* locus further and determine whether the genes at the CC-NB/NB-LRR cluster are expressed, RNAseq was performed on fourth and fifth leaves from two susceptible lines (Bd21 and Luc1) and three resistant lines (ABR6, Jer1, and Foz1). RNAseq reads were mapped to a 25 kb region encompassing the CC-NB and the NB-LRRs using Bowtie in Geneious, allowing an initial assessment of

gene expression. All three genes are expressed in both the susceptible lines Bd21 and Luc1, as well as the resistant lines ABR6, Jer1, and Foz1 (Figure 23). As the RNAseq data are not quantitative, no conclusions can be made regarding the expression levels in the different accessions.

*Two non-synonymous mutations in conserved NB motifs differentiate Luc1 from the resistant accessions*

As all three candidate genes are expressed in both resistant and susceptible accessions and lack of gene expression is therefore not responsible for susceptibility, we explored the effect of sequence variation between the accessions. As described above, based on resequencing data only two SNPs differentiate these candidate genes between Luc1 and Jer1, whereas ABR6 and Bd21 displayed greater diversity across these candidate genes, especially in the shared promoter region of the NB-LRRs. A *de novo* assembly was generated from the RNAseq reads and probed with the Bd21 reference sequence for the three candidate genes. This allowed identification and comparison of the open reading frames for the candidate genes among the five accessions and at the same time reinforces the polymorphisms observed with the WGS *de novo* assemblies.

The four Spanish accessions Luc1, ABR6, Jer1, and Foz1 were near identical at the nucleotide and amino acid level, while the Iraqi Bd21 was more diverged (Table 7; Figure S7). Notably, the nucleotide and amino acid sequences of the three *Yrr3* containing accessions were identical for all three genes at the CC-NB/NB-LRR cluster (Table 7). As expected, of the two *yrr3* lines Bd21 was the most diverged from the resistant lines. Between the amino acid sequence of the resistant lines and the Bd21 amino acid sequence seven non-synonymous mutations occur in Bradi2g52430, five non-synonymous mutations in Bradi2g52437, and 13 non-synonymous mutations in Bradi2g52450 (Table 7). In contrast, Luc1 is almost identical to the resistant lines, with only one amino acid change occurring in Bradi2g52430 and one amino acid change in Bradi2g52450.

**Table 7.** Nucleic acid and amino acid differences between the three *Yrr3* candidates among the five accessions.

Genes and length		ABR6	Jer1	Foz1	Luc1	Bd21
Bradi2g52430 1,197 bp 398 aa	ABR6	-	0	0	1	9
	Jer1	0	-	0	1	9
	Foz1	0	0	-	1	9
	Luc1	1	1	1	-	10
	Bd21	7	7	7	8	-
Bradi2g52437 1,878 bp 625 aa	ABR6	-	0	0	0	12
	Jer1	0	-	0	0	12
	Foz1	0	0	-	0	12
	Luc1	0	0	0	-	12
	Bd21	5	5	5	5	-
Bradi2g52450 2,838 bp 945 aa	ABR6	-	0	0	1	20
	Jer1	0	-	0	1	20
	Foz1	0	0	-	1	20
	Luc1	1	1	1	-	21
	Bd21	13	13	13	14	-

Predicted open reading frames and amino acid sequences based on RNAseq *de novo* assemblies and RNAseq alignments were compared in Geneious. Numbers above the dashes indicate nucleic acid differences, numbers below the dashes indicate amino acid differences. bp = base pairs; aa = amino acids.

Consequently, various amino acid changes in all three candidate genes could contribute to the observed phenotype in the ABR6 x Bd21 population, whereas only two amino acid changes in Bradi2g52430 and Bradi2g52450 could contribute to the observed phenotype in the Luc1 x Jer1 population. In order to analyse the location and possible impact of the non-synonymous mutations, a MAST (motif alignment and search tool) analysis was performed to annotate conserved motifs commonly found in CC, NB, and LRR domains. This analysis revealed that the amino acid changes between Luc1 and Jer1 map to the Kinase-2 motif of Bradi2g52430 (V257G) and to the MHDV motif of Bradi2g52450 (R345Q), both of which are part of the NB domain (Figure S7). Of the amino acid changes observed between ABR6 and Bd21 two map to the RNBS-A motif of Bradi2g52430, one to the RNBS-D part I motif of Bradi2g52450, and one to an LRR motif of Bradi2g52450 (Figure S7). All other amino acid changes observed between ABR6 and Bd21 map outside of the motifs annotated in our MAST analysis.

### *Complementation of candidate genes*

As the two non-synonymous mutations between Luc1 and Jer1 could not be separated with a recombination event, complementation will be required to confirm the causal mutation. Initial attempts at amplifying the three candidate genes from genomic DNA were hampered by the sequence similarity of NB-LRRs within the genome. As the three candidate genes are identical at the amino acid level among the resistant accessions, we cloned the entire CC-NB/NB-LRR cluster in six overlapping fragments from one of the ABR6 BACs (BAC 4932-1D) spanning the *Yrr3* locus and assembled the three candidate genes using Gibson Assembly (Gibson *et al.* 2009). The final constructs contain the annotated coding region of the candidate genes with around 2 kb of promoter and terminator sequence. Transformation of all three candidate genes into Bd21 and Luc1 is underway, as well as into susceptible wheat and barley lines.

### **Discussion**

While the *Yrr3* locus was found to be in coupling with several NB-LRR encoding genes, it remained unclear whether one or more of these genes contributes to *Yrr3* mediated resistance. We initiated isolation and fine-mapping of *Yrr3* in two independent mapping populations, which delineated a 72 kb consensus gain of function interval centred around a cluster of a CC-NB and two NB-LRR encoding genes. Although ABR6 and Bd21 display greater structural variation across this cluster, a recombination screen within the Luc1 x Jer1 population reduced the causal mutation down to two SNPs, which lead to amino acid changes within the conserved Kinase-2 and MHDV motifs in the NB domains of the CC-NB and one of the NB-LRRs.

### *Non-synonymous mutations are associated with NB motifs that regulate nucleotide binding*

Although no full-length structure of a plant NB-LRR has been solved yet, homology studies based on the structures of the animal nucleotide-binding oligomerisation domain (NOD) containing proteins APAF-1 (Riedl *et al.* 2005), CED-4 (Yan *et al.* 2005), and later NLRC4 (Hu *et al.* 2013) allowed the formulation of some hypotheses regarding the function of conserved motifs within plant NB domains and their amino

acid residues (DeYoung and Innes 2006; McHale *et al.* 2006). The NB domain binds ADP and ATP (Tameling *et al.* 2002; Takken and Goverse 2012). The conserved motifs are thought to regulate binding and hydrolysis of these nucleotides, as well as the necessary conformational changes, and mutation studies targeting conserved residues have helped to clarify these proposed roles (recently reviewed by Bentham *et al.* (2016)). Plant NB domains are further divided into three subdomains (Figure 24B): the NB subdomain, the ARC1 subdomain (a helical domain also known as HD1), and the ARC2 subdomain (a winged-helical domain also known as WHD) (Bentham *et al.* 2016; Sukarta *et al.* 2016). Notably, the NB subdomain contains the P-loop and Kinase-2 motifs, which coordinate nucleotide binding via hydrogen bonds with the  $\beta$ - and  $\gamma$ -phosphates, as well as hydrolysis by positioning a  $Mg^{2+}$  ion in the case of the Kinase-2 motif (Bentham *et al.* 2016; Sukarta *et al.* 2016). Mutation studies have shown that the plant NB-LRRs I-2 and Mi-1 are both able to bind and hydrolyse ATP (Tameling *et al.* 2002), but binding, not hydrolysis was found to be necessary for signalling in plants (DeYoung and Innes 2006; Tameling *et al.* 2006). The GPLP motif of the ARC1 subdomain is thought to be involved in nucleotide-dependent conformational changes (Iyer *et al.* 2004; Bentham *et al.* 2016), while the ARC2 subdomain contains the highly conserved MHDV motif, whose equivalent in APAF-1 binds the  $\beta$ -phosphate of ADP (Riedl *et al.* 2005). The resulting MHDV motif mediated interaction between the ARC2 and NB subdomains likely stabilises the ADP-bound inactive conformation (Bentham *et al.* 2016). The crystal structure of the full-length NOD-like receptor NLRC4 suggests that another helical subdomain (HD2) interacts with the LRR domain via hydrogen bonds (Hu *et al.* 2013). Conformational changes upon ATP binding lead to activation of downstream signalling, possibly by making binding sites available for downstream partners and ATP hydrolysis reverts the NB-LRR back into the inactive state (Takken and Goverse 2012; Bentham *et al.* 2016). Recent findings from the L6 and L7 flax rust NB-LRRs suggest that NB-LRRs constantly switch between on and off states (Bernoux *et al.* 2016). In the absence of the pathogen, the equilibrium is in favour of the off state, but effector binding is thought to stabilise the on state and allow defence signalling to occur (Bernoux *et al.* 2016)

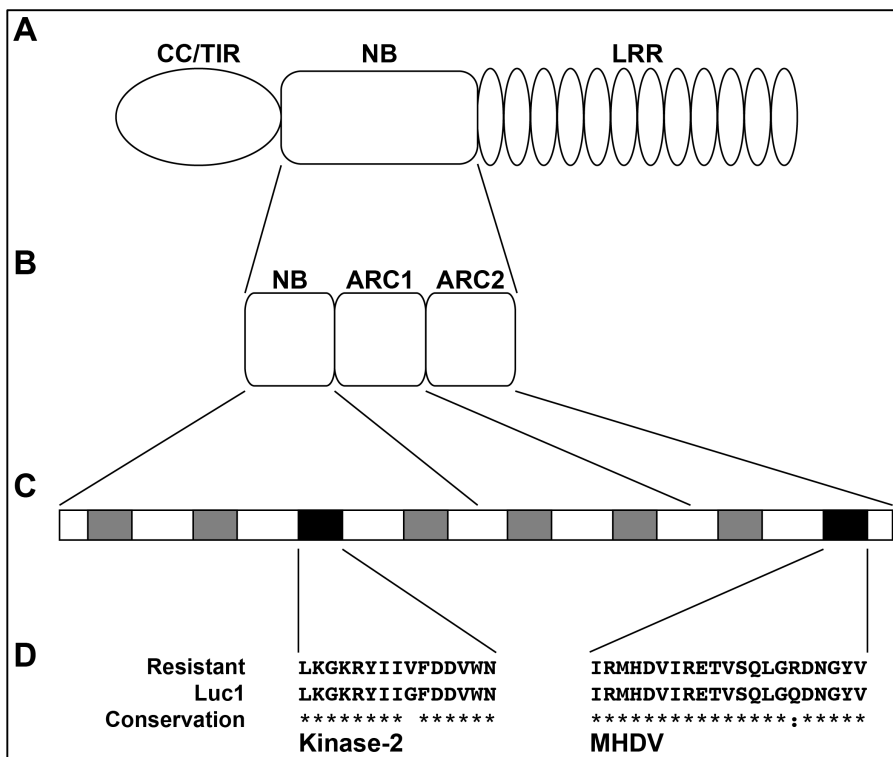


**Figure 24.** Structure of nucleotide-binding (NB) domain containing proteins. (A) NB domain containing proteins often possess an N-terminal adaptor domain (coiled coil (CC) domain or Toll/interleukin-1 receptor homology (TIR) domains) and a C-terminal leucine rich repeat (LRR) domain. (B) The NB domain is further divided into the three subdomains: the NB subdomain, the adaptor shared by APAF-1, R proteins and CED-4 (ARC) 1 subdomain, and the ARC2 subdomain. (C) The NB subdomain contains four conserved motifs (P-loop, RNBS-A, Kinase-2, and RNBS-B), the ARC1 subdomain two motifs (RNBS-C and GPL), and the ARC2 subdomain two motifs (RNBS-D and MHDV), shown as grey or black boxes. The Kinase-2 and MHDV motifs are shown in black. (D) In the CC-NB Bradi2g52430 the V257G amino acid change observed in Luc1 maps to the Kinase-2 motif, whereas in the NB-LRR Bradi2g52450 the R345Q amino acid change observed in Luc1 maps to the MHDV motif. Level of conservation determined by Clustal Omega: “\*” = identical amino acids, “:” = conservation between strongly similar amino acids, space = non-conservative polymorphism. Sizes of individual domains, subdomains, and motifs are not drawn to scale. Subdomain-motif association is based on van Ooijen *et al.* (2008).

The V257G amino acid change in Bradi2g52430 maps to the Kinase-2 motif (Figure 24D; Figure S7), also called the Walker B motif (Walker *et al.* 1982; Traut 1994). This motif is highly conserved and consists of four consecutive hydrophobic amino acids followed by an aspartic acid (Iyer *et al.* 2004), although in plant NB-LRR proteins the hydrophobic amino acids are generally followed by two aspartic acids (van der Biezen and Jones 1998; Tameling *et al.* 2006; van Ooijen *et al.* 2008). Based on the crystal structures of APAF-1, CED-4, and NLRC4 the four conserved hydrophobic amino acids form a  $\beta$ -strand, which positions the aspartic acids (DeYoung and Innes 2006). Mutation studies of the Kinase-2 motif have focused on these two conserved

negatively charged residues (Takken *et al.* 2006). The first conserved aspartic acid of the Kinase-2 motif is the catalytic site and hydrolyses the  $\gamma$ -phosphate group of ATP via a  $Mg^{2+}$  ion (Story and Steitz 1992; Dinesh-Kumar *et al.* 2000; Muneyuki *et al.* 2000; Iyer *et al.* 2004). The V257G substitution observed in Luc1 affects the third hydrophobic residue within the Kinase-2 motif. It has been suggested that the hydrophobic  $\beta$ -strand alleviates non-specific hydrolysis by excluding water from the reaction centre (Fry *et al.* 1986). This function may be impacted by the valine to glycine substitution observed in Luc1. However, Tameling *et al.* (2006) showed that ATP binding, not ATP hydrolysis, is required for defence signalling in the NB-LRR I-2. In this context, the V257G substitution might disrupt the  $\beta$ -strand, which could alter the spatial orientation of the catalytic aspartic acid. Alternatively, the valine side chain might interact with other residues, which could be disrupted in the susceptible line. Such changes might disable ATP binding, locking the CC-NB in an ADP-bound off state, or prevent ATP hydrolysis, which would lock the CC-NB in an ATP-bound state. However, based on our MAST analysis the predicted CC-NB amino acid sequence is lacking the MHDV motif found in the ARC2 subdomain (Figure S7) and it is questionable whether it is able to bind nucleotides at all. The histidine residue within the MHDV motif is highly conserved and orients the bound nucleotide (McHale *et al.* 2006; Lukasik and Takken 2009). On the other hand, mutation studies of paired NB-LRRs have shown that only one of these NB-LRRs requires a functional NB domain (Césari *et al.* 2014; Williams *et al.* 2014; Bentham *et al.* 2016). Depending on interactions with other proteins, Bradi2g52430 may therefore not require the ARC2 subdomain for its role in resistance.

The R345Q amino acid change in Bradi2g52450 maps 10 amino acids downstream of the highly conserved MHDV motif in the ARC2 domain of the NB-LRR (Figure 24D; Figure S7). The ARC2 domain is thought to activate the NB-LRR upon pathogen perception by the LRR, while autoinhibiting signalling in the absence of a pathogen (van Ooijen *et al.* 2008). Based on the homology with APAF-1, this motif likely directly interacts with the  $\beta$ -phosphate of ADP (Riedl *et al.* 2005; Albrecht and Takken 2006). Mutations of the conserved histidine and aspartate residues in the NB-LRRs Rx, I-2, Mi-1, Rpi-blb1, NRC1, and L6 lead to autoactive mutants (Bendahmane *et al.* 2002; de la Fuente van Bentem *et al.* 2005; Howles *et al.* 2005; Gabriëls *et al.* 2007; van Ooijen *et al.* 2008), while mutations elsewhere in the ARC2 domains of RPM1,

RPS2, and L6 produced loss of function alleles (Mindrinos *et al.* 1994; Grant *et al.* 1995; Axtell *et al.* 2001; Tornero *et al.* 2002; Howles *et al.* 2005). While R345Q in Bradi2g52450 may not directly impact the interaction with the  $\beta$ -phosphate of ADP, it could impact the conformational change required for NB-LRR activation, leading to a loss of downstream signalling after stripe rust perception.

#### *The NB-LRR and CC-NB pose different modes of stripe rust recognition at Yrr3*

Recognition of pathogen secreted effectors by NB-LRRs can occur either directly or indirectly (reviewed by Bentham *et al.* (2016) and Sukarta *et al.* (2016)). In a direct interaction model the effector is often recognised by the LRR domain, as has been demonstrated for Pi-ta from rice (Jia *et al.* 2000), L6 and M from flax (Dodds *et al.* 2006; Wang *et al.* 2007a; Catanzariti *et al.* 2010; Ve *et al.* 2013), and RPP1 from *A. thaliana* (Krasileva *et al.* 2010). If direct recognition of an effector underlies resistance to stripe rust in *B. distachyon*, this would likely be coordinated by the full length NB-LRR Bradi2g52450. Following effector binding, the arginine to glutamine amino acid change in Luc1 may prevent the conformational change required for NB-LRR signalling. In such a scenario, an interesting question is what role the pathogen's effector repertoire and effector deployment plays in the interaction between stripe rust and the infected plant. Does the *B. distachyon* NB-LRR interact with an effector that is recognised by NB-LRRs in wheat and barley? Or are different sets of effectors recognised in the host systems?

The function of NB domain encoding genes without an LRR domain, such as Bradi2g52430, is only poorly understood. Research to date has focused on *A. thaliana*, which possesses 58 annotated NB domain containing genes without an LRR domain, of which 21 are TIR-NB proteins and four are CC-NB proteins (Meyers *et al.* 2003). The *A. thaliana* TIR-NB genes are often found paired with a TIR-NB-LRR or in complex clusters consisting of several TIR-NB and TIR-NB-LRR genes (Meyers *et al.* 2002). Similar to Bradi2g52430 and Bradi2g52437, in these pairs or clusters the TIR-NBs are commonly oriented in the opposite direction of the TIR-NB-LRR, which could limit recombination between the paired or clustered TIR-NBs and TIR-NB-LRRs (Meyers *et al.* 2002). Although the role of TIR-NB or CC-NB proteins lacking the LRR domain is not yet well described, at least TIR-NBs have been shown to

contribute to resistance. The TIR-NB *RLM3* is required for efficient callose deposition downstream of *RLM1*, a TIR-NB-LRR recognising *L. maculans* in *A. thaliana* (Staal *et al.* 2006; Staal *et al.* 2008). *rlm3* mutants also displayed enhanced susceptibility to three other necrotrophs (Staal *et al.* 2008). The TIR-NB *TN2* associates with EXO70B1, a subunit of the exocyst complex involved in secretory pathways (Zhao *et al.* 2015). *TN2* expression was upregulated in *exo70B1* mutants and the authors hypothesise that effector targeting of EXO70B1 initiates *TN2* dependent defence pathways (Zhao *et al.* 2015). *TN2* occurs in a cluster with another TIR-NB (*TN1*) and a TIR-NB-LRR. *TN1* mutations cause temperature-dependent auto-immunity (Wang *et al.* 2013; Zbierzak *et al.* 2013), but it remains unclear whether the linked TIR-NB-LRR is involved in *TN1* or *TN2* function (Zhao *et al.* 2015). In a different study, transient overexpression of several *A. thaliana* TIR-NB or TIR-X genes induced chlorosis in *Nicotiana benthamiana* and stable overexpression in *A. thaliana* produced phenotypes associated with basal innate immune responses (Nandety *et al.* 2013). Phenotypes in both systems were dependent on *EDS1* (*ENHANCED DISEASE RESISTANCE 1*), one of the regulators downstream of NB-LRR recognition (Aarts *et al.* 1998; Wiermer *et al.* 2005; Nandety *et al.* 2013). These putative resistance proteins were also found to interact with various effectors and plant NB-LRRs in a yeast two-hybrid screen (Nandety *et al.* 2013). Meyers *et al.* (2002) suggested that TIR-NBs may act as downstream adaptors for TIR-NB-LRR mediated immunity, similar to the MyD88 and Mal TIR proteins for Toll-like receptors (TLR) in mammalian and *Drosophila* innate immunity (Kopp and Medzhitov 1999; Xu *et al.* 2000; Fitzgerald *et al.* 2001; Horng and Medzhitov 2001). Building on this, Staal and Dixieius (2008) comment that these adaptors should be involved in broader resistance than the individual NB-LRR. Indeed, *RLM3* was found to regulate resistance to several necrotrophic pathogens (Staal *et al.* 2008). Complementarily, the two CC-X genes *RPW8.1* and *RPW8.2* confer resistance to all tested powdery mildew isolates (Xiao *et al.* 2001). Furthermore, overexpression increased resistance to other biotrophic pathogens and susceptibility to necrotrophic pathogens (Wang *et al.* 2007b).

In contrast to the direct effector recognition model described above, other NB-LRRs have been shown to detect the pathogen indirectly by guarding an effector target or via a decoy (Dangl and Jones 2001; van der Hoorn and Kamoun 2008; Cesari *et al.* 2014). Zhao *et al.* (2015) proposed a similar role for the TIR-NB *TN2*, showing that it

is activated upon EXO70B loss of function, which suggests that TN2 could monitor the integrity of the secretory pathway against effector targeting and also that an LRR domain is not required for this function. Moreover, Nandety *et al.* (2013) demonstrated that TIR-NB and TIR-X proteins can interact with effectors and NB-LRRs. Therefore, in an indirect interaction model, it is plausible that a conserved *Pst* and *Psh* effector targets a plant protein, which is independently targeted by an adapted pathogen of *B. distachyon* and therefore guarded. Such a scenario is conceivable for both candidate genes at the locus. In the case of the CC-NB, similarly to sensor NB-LRRs and TN2, a functional NB domain or an LRR domain may not be required as resistance could be conferred by a heterodimeric complex. In this complex, the role of the CC-NB could be recognition of the pathogen, while a functional NB-LRR, such as Bradi2g52437 at the locus, may initiate defence signalling. Similar to TIR-NBs and TIR-NB-LRRs in *A. thaliana*, Bradi2g52437 is closely linked to Bradi2g52430. Although our MAST analysis did not detect a CC domain within Bradi2g52437, a cursory InterProScan motif annotation suggested that the NB-LRR contains a CC domain (data not shown) and a full manual annotation of the three candidate genes is needed. However, in this scenario interaction between the two proteins could be mediated by the CC domains and the tightly linked genomic location would ensure co-inheritance.

In this context, it is interesting to note that the CC-NB/NB-LRR cluster identified for *Yrr3* is highly conserved among a variety of grass species. The respective top hits for the CC-NB and NB-LRRs identified in rice, sorghum, and maize retain the order and relative orientation as in *B. distachyon*. This is a remarkable observation, as NB-LRRs are a rapidly diversifying gene family and *B. distachyon* NB-LRRs almost never retained their syntenic order in a comparison with NB-LRRs from rice and sorghum (The International Brachypodium Initiative 2010).

Host-tracking and host jumps are features thought to underlie plant-pathogen interactions over evolutionary time (Stukenbrock and McDonald 2008). These events are often difficult to demonstrate due to the lack of a fossil record (Troch *et al.* 2014), but some examples exist, such as the host jump to rice and subsequent diversification by *M. oryzae* (Couch *et al.* 2005). Cereal rusts could have evolved in temperate climates on their alternate host barberry (*Berberis* spp.), then incorporated grasses in

their life cycle during host jumps, and subsequently diversified with the cereals during domestication. In contrast, rice is a tropical grass and neither has an adapted rust pathogen nor allows colonisation of non-adapted rust pathogens (Ayliffe *et al.* 2011; Yang *et al.* 2014). These factors could mean that the *Yrr3* locus not only predates the diversification of the grasses, but also the evolution of cereal rusts. It could have evolved in an ancient monocot and then been adopted to confer resistance to new pathogens during the diversification of the grasses. Yang *et al.* (2013) hypothesised that NB-LRR divergence is constrained and tested rapidly evolving NB-LRRs for their ability to give resistance to non-adapted pathogens. In contrast, the *Yrr3* locus has diverged little over a great evolutionary time period, yet provides resistance to non-adapted pathogens.

#### *How could NB-LRR mediated resistance be broad spectrum and durable?*

NB-LRR mediated resistance is commonly associated with gene-for-gene interactions and the specific recognition of individual pathogen isolates (Flor 1971; Jones and Dangl 2006). However, *Yrr3* was mapped to a CC-NB/NB-LRR encoding cluster and confers broad spectrum resistance to a *Psh* and three *Pst* isolates. *Yrr1*, the second major effect locus we detected in *B. distachyon* against stripe rust isolates, only conferred resistance to *Pst* isolates and not to *Psh*. Interestingly, *Pst* and *Psh* resistance in barley also does not always colocalise (Dawson and Moscou, personal communication). This suggests that the genetic architecture of stripe rust resistance in both systems builds on recognising unique as well as shared components. *Pst* and *Psh* may possess shared core effectors, which are essential for targeting highly conserved pathways within plants. These would be complemented by effectors specific to *Pst* or *Psh*, which fulfil a unique role within wheat and barley, respectively, or which have been exposed to selection by resistance genes. NB-LRR recognition of a core effector essential for infecting any plant may explain how some NB-LRRs can confer broad spectrum resistance. For example, such a core effector could be involved in early infection processes that are shared among many fungal pathogens, e.g. leaf colonisation.

Durable resistance is generally defined as resistance which is still effective when deployed over a large area (Johnson 1981). Crucially, Johnson (1981) points out that

this definition is independent of the genetic basis or underlying mechanisms of resistance, or whether the resistance is race-specific. Additionally, this definition is based on spatial and not temporal characteristics (Johnson 1981). However, in many cases a resistance that is durable over a large area will also be effective over a longer period of time. Such resistance that is effective over a longer period of time and over a larger area probably does not rely on a single mechanism, but rather on matching and combining different pathways, which all help to prevent pathogen ingress. When addressing the usefulness of various resistance genes in an agricultural context, discussions generally centre around the particular mode of action of a single gene and our knowledge of a type of gene gained from greenhouse studies. However, this line of discussion is misguided, because on a species level more than a single gene will provide resistance against a pathogen. A single NB-LRR or PRR may not pose much of a challenge to a pathogen with a large population size under strong selective pressure, but combined or coupled with other processes that inhibit pathogen ingress, they may form a powerful barrier. In this context it is important to note that *Yrr1* has been fine-mapped to a 75 kb interval (Gilbert and Ayliffe, personal communication). This interval does not contain any NB-LRRs or other classical resistance genes (data not shown). In addition, so far only colonisation resistance seems to involve NB-LRRs, as we have no knowledge about what prevents life cycle completion in the interaction between *B. distachyon* and *P. striiformis*.

The implication of NB-LRRs in nonhost resistance suggests that nonhost and host resistance are not fundamentally different as they rely on the same molecular mechanisms. Cook *et al.* (2015) point out that nonhost resistance cannot be defined by a unique mechanism, but rather is a combination of different aspects of plant-microbe interactions, which may range from general incompatibility to recognition resulting in ETI. This observation connects with the different barriers to pathogen infection discussed by Thordal-Christensen (2003). Whether or not a plant is a host or nonhost of a pathogen does not depend on the molecular process underlying resistance, but on the final output of whether the pathogen can complete its life cycle on the plant or not. In a tropical forest system, it was shown that a fungal pathogen's ability to infect a given plant also decreases with an increasing phylogenetic distance between the host plant and the other plants (Gilbert and Webb 2007). From an evolutionary standpoint, a pathogen will have to overcome many different physiological and

genetic barriers when a plant species is distant from the adapted host. On the other hand, if a plant is phylogenetically close to the host plant, many of the barriers will be similar to the host plant and ineffective against the pathogen. The different barriers presented to a pathogen are exemplified by resistance to barley powdery mildew (*Blumeria graminis* f. sp. *hordei*) in *A. thaliana*. As discussed above, this resistance relies on NB-LRR independent pre-invasion resistance provided by the *PEN* genes and cell death dependent post-invasion resistance (Lipka *et al.* 2005; Lipka *et al.* 2008). Interestingly, the barley NB-LRR *MLA1* confers resistance to barley powdery mildew in *A. thaliana* mutants that allow invasion (Maekawa *et al.* 2012). In contrast, within our system the close phylogenetic relationship between *B. distachyon*, barley, and wheat established that post-invasion colonisation resistance uses NB-LRR mediated and NB-LRR independent pathways to limit pathogen growth and thereby life cycle completion on most accessions.

## Materials and methods

### *Plant growth and inoculation*

For infection assays in this chapter plants were either grown in 1 L pots or in a 24-hole tray containing peat-based compost. Plants were grown at 18°C day and 11°C night in a 16 h photoperiod in a controlled environment room. Seedlings were inoculated with *Pst* isolate 08/21 four weeks after sowing at the four to five leaf stage as described previously (Dawson *et al.* 2015). Leaf browning and pCOL phenotypes were scored 14 dpi (Dawson *et al.* 2015).

### *Luc1 x Jer1 recombination screen*

Seed from three Luc1 x Jer1 F<sub>1</sub> and one Jer1 x Luc1 F<sub>1</sub> were grown in 24-hole trays containing peat-based compost in a greenhouse (natural light supplemented for 16 h, min. 18°C/11.5°C temperature) and DNA was extracted from leaf tissue using a standard CTAB protocol. Genotyping of 1,948 F<sub>2</sub> plants with the delineating markers identified 23 lines with recombination events within the gain of function interval. Recombinant lines were transplanted into 9 cm square pots containing an equal mixture of the John Innes Cereal Mix and a peat and sand mix (Vain *et al.* 2008) and regenotyped to rule out mix-ups during the original genotyping, selection of recombinants, and transplanting.

### *Marker development*

SNP-based KASP markers were developed as described for the Luc1 x Jer1 and Foz1 x Luc1 genetic maps in the previous chapter. Briefly, *de novo* assemblies of the parental lines were probed with the Bd21 reference sequence of the desired marker location and contigs were assembled in Geneious, which allowed the identification of SNPs for marker development.

### *Marker regression analysis*

Determining the statistical significance of cosegregation between phenotype and genotype was used to fine-map *Yrr3* in recombinant lines obtained from the ABR6 x

Bd21 and Luc1 x Jer1 populations, as well as the recombination screen. Progeny of recombinant lines were genotyped with a marker in the heterozygous region of the parental line and statistical significance of genotype-phenotype associations was performed with an ANOVA analysis (“anova” command in R Version 3.2.2). In rare cases individual samples with missing genotyping calls were excluded from the analysis.

#### *BAC library screening and BAC sequencing*

Three-week old ABR6 seedlings were placed in darkness for three days prior to harvesting leaf tissue, which was flash-frozen in liquid nitrogen. BAC library construction and screening was performed by Bio S&T Inc. in Lachine, Quebec, Canada. Following DNA extraction and *Hind*III digestion, fragments were cloned in the pCLD04541 plasmid in DH10B *Escherichia coli* cells, giving a 5x pooled BAC library. Positive clones for the *Yrr3* locus were identified by PCR screening with primers for Bradi2g52437. For each BAC, eight colonies were confirmed by fingerprinting with *Hind*III digestion. All colonies produced the same pattern and one colony was chosen for sequencing. BACs were extracted using the QIAGEN Large Construct Kit according to the manufacturer’s instructions. The quality of the extractions was confirmed by agarose gel electrophoresis, fingerprinting with *Hind*III to check for rearrangements during culture growth, and analysis with TapeStation and DropSense. BACs were sequenced using a PacBio-SMRT (single molecule, real-time sequencing) cell at The Genome Analysis Centre (Norwich, UK).

#### *RNAseq of Luc1, Jer1, and Foz1 and RNA analyses*

RNA extraction and sequencing for Luc1, Jer1, and Foz1, was carried out as described for ABR6 and Bd21 in the first chapter (Bettgenhaeuser *et al.* 2017). Mean insert sizes were 253 bp (Luc1), 248 bp (Jer1), and 251 bp (Foz1) and sequencing yielded 134,975,912 (Luc1), 136,308,576 (Jer1), and 131,443,102 (Foz1) raw reads. RNAseq data quality control was performed as described previously (Bettgenhaeuser *et al.* 2017). Reads from all five accessions were paired in Geneious using default settings and Bowtie alignments to the Bd21 reference sequence of the *Yrr3* locus were performed using the “Map to Reference” command in Geneious with default settings

(low sensitivity and five iterations without trimming). A *de novo* transcriptome assembly was generated with Trinity (v2013-11-10) and probed with the Bd21 reference sequence of the three candidate genes. Open reading frames were identified and translated in Geneious.

#### *Characterisation of Yrr3 candidate genes*

To assess the polymorphisms in the three candidate genes between the five accessions, the nucleotide and amino acid sequences of the three genes were aligned in Geneious using the Multiple Align function with default settings (cost matrix 93% similarity for nucleotide sequences and Blossum62 for amino acid sequences). Additionally, to assess the level of conservation of the amino acid changes, a multiple sequence alignment was performed with Clustal Omega on the EMBL-EBI website (<http://www.ebi.ac.uk/Tools/msa/clustalo/>) using default settings.

Conserved motifs within the amino acid sequences were annotated by performing a MAST analysis. A motif-based approach for the identification of NB-LRR encoding genes was developed for potato (Jupe *et al.* 2012) and we sought to develop a similar motif set for monocots using the diversity of NB-LRRs from rice and *B. distachyon*. Rice is estimated to possess 508 NB-LRRs (Li *et al.* 2010), whereas differing estimates of the number of NB-LRR encoding genes have been reported for *B. distachyon*, including 212 (Li *et al.* 2010) and 175 NB-LRRs (Tan and Wu 2012). We generated MEME motifs through a random proportional sample of NB-LRRs from rice (N = 35) and *B. distachyon* (N = 17). The MEME motifs spanned the CC domain (motifs 4, 11, 13, and 15), NB domain (motifs 1, 2, 3, 5, 6, 7, 8, 10, 12, and 14), and the LRR domain (motifs 19, 9, 20, 16, 17, and 18). All the identified motifs could clearly be associated with those previously defined (Meyers *et al.* 2003). MAST significance thresholds of  $1e^{-27}$  and  $1e^{-20}$  were found to identify all annotated NB-LRRs within *B. distachyon*, with respective precisions of 49.8% and 47.5% based on the NB-LRR annotation of Tan and Wu (2012).

### *Construct development for complementation*

High fidelity PCR with Phusion polymerase was performed to amplify initial fragments (1x polymerase, 0.2 mM dNTPs, 10 ng BAC DNA, 0.5  $\mu$ M primers; 98°C for 30 s, 28 cycles of 98°C for 10 s, 60°C for 30 s, and 72°C for 3 min, final extension with 72°C for 10 min). Gel extraction of fragments was performed with the QIAquick Gel Extraction Kit according to the manufacturer's instructions and fragments were A-tailed by incubation at 72°C for 20 min (4 units GoTaq polymerase, 1x GoTaq buffer, 1.5 mM MgCl<sub>2</sub>, 0.2 mM dATP, 13.6  $\mu$ L extraction product). A-tailed fragments were cloned into the pCR-XL-TOPO vector and transformed into One Shot TOP10 *E. coli* competent cells with the TOPO Cloning kit according to the manufacturer's instructions. Positive clones were identified and confirmed by colony PCR (0.15 units GoTaq, 1x GoTaq buffer, 1.5 mM MgCl<sub>2</sub>, 0.2  $\mu$ M primers, 0.2 mM dNTPs; 95°C for 10 s, 32 cycles of 98°C for 30 s, 58°C for 30 s, 72°C for 1.5 min, final extension with 72°C for 5 min), digestion (plasmid extraction of 10 mL cultures with the NucleoSpin Plasmid Purification kit according to the manufacturer's instructions; digestion of 100 ng plasmid DNA with 10 units *Eco*RI in 1x Roche Buffer H), and Sanger sequencing (~150 ng plasmid DNA, 2.5  $\mu$ M primers).

Primers for Gibson Assembly consisted of 20 bp fusions from both fragments to be assembled and were assessed for GC content (~50%) and secondary structures (Mfold (Zuker 2003);  $\Delta G > -3.0$  kcal/mol at 37°C). High fidelity PCR with Phusion polymerase was performed to add overlaps (1x polymerase, 0.2 mM dNTPs, 10 ng BAC DNA, 0.5  $\mu$ M primers; 98°C for 30 s, 28 cycles of 98°C for 10 s, 60°C for 30 s, and 72°C for 30 s per kb, final extension with 72°C for 10 min). PCR products were digested with *Dpn*I to remove circular DNA (20 units *Dpn*I, 1x CutSmart buffer), fragments were resolved with gel electrophoresis (1% agarose in 1x TAE buffer), and extracted with the Zymoclean Gel DNA Recovery kit according to the manufacturer's instructions. Gibson Assembly reactions were performed as described by Gibson *et al.* (2009) with a Gibson Assembly master mix from New England Biolabs. Assembled constructs were transformed into chemically competent DH5 $\alpha$  *E. coli* cells (10  $\mu$ L assembly in 50  $\mu$ L cells; ice for 30 min, 42°C for 1.5 min, ice for 2 min), recovered in 500  $\mu$ L L media at 37°C for 1 hour, and plated on L media plates with selection for overnight growth at 37°C. Colonies were confirmed by digestion (plasmid extraction

of liquid cultures with QIAGEN Plasmid Purification Kit according to the manufacturer's instructions and digestion of 100 ng plasmid DNA with 10 units *EcoRI* in 1x Roche Buffer H). For positive assemblies, the T-DNA sequence was confirmed by Sanger sequencing (~150 ng plasmid DNA, 2.5  $\mu$ M primers) and the constructs were transformed into 50  $\mu$ L *Agrobacterium tumefaciens* AGL1 cells with pulse electroporation, followed by recovery in 500  $\mu$ L L medium at 28°C for 2 hours, and growth on L media plates with selection for two days.

Final constructs contain the coding region of the annotated candidate genes with around 2 kb of promoter and terminator sequence, depending on the nearest available site for primer design. Bradi2g52430 was cloned into the pWBVec8 vector (Wang *et al.* 1998) and the final construct contains 1,934 bp and 2,119 bp of native promoter and terminator sequence. Bradi2g52437 was cloned into the pBract202 vector (Smedley and Harwood 2015) and the final construct contains 1,636 bp and 2,339 bp of native promoter and terminator sequence. Bradi2g52450 was cloned into the pBract202 vector and the final construct contains 2,067 bp and 1,409 bp of native promoter and terminator sequence. As Bradi2g52430 is on the opposite strand to Bradi2g52437, the final Bradi2g52437 construct also contains Bradi2g52430 with 1,645 bp of the promoter sequence and over 2 kb of the terminator sequence. Sanger sequencing was used to confirm the T-DNA of all constructs, which showed that one SNP had been incorporated into the Bradi2g52437 construct during amplification for Gibson Assembly. This SNP is located in the annotated 5'-UTR of Bradi2g52437 and more than 5 kb downstream of Bradi2g52430. The pBract202 vector requires the helper plasmid pSoup (Smedley and Harwood 2015). All constructs are being transformed into the susceptible *B. distachyon* accessions Bd21 and Luc1, the susceptible barley line SusPtrit x Golden Promise DH-47, and the susceptible wheat line Fielder according to previously published protocols (Vain *et al.* 2008; Yeo *et al.* 2014; Ishida *et al.* 2015).

## 5. General Discussion

*“I would like to share one dream that I hope scientists will achieve in the not-too-distant future. Rice is the only cereal that has immunity to the *Puccinia* spp. of rust. Imagine the benefits if the genes for rust immunity in rice could be transferred into wheat, barley, oats, maize, millet, and sorghum. The world could finally be free of the scourge of the rusts, which have led to so many famines over human history.”*

Norman Borlaug (2000)  
[Nobel Prize Laureate for Peace, 1970]

Over the past millennia human populations have transitioned away from societies of hunter-gatherers towards more complex civilisations with hierarchies, bureaucracies, religions, writing systems, dedicated professions, and many other features of modern life (Diamond 1997). The invention of agriculture together with the domestication of crops and animals forms the basis of this transition, as it allows individual humans to produce more food than they need for themselves, enabling members of society to dedicate their time to purposes other than food production (Diamond 1997). Throughout domestication, humans have drawn on the standing genetic variation present in wild populations or occurring randomly as mutations during domestication events, which improved crops with regard to their life history traits (e.g. generation time and yield), resistance to pathogens, or adaptation to novel growth conditions (Doebley *et al.* 2006). The research subjects I discussed in this thesis concern two agriculturally relevant traits: reproduction and disease resistance. The hope is that by understanding the genetic architecture and molecular basis of these traits in non-domesticated systems the knowledge gained will advance our understanding of these traits in crop species, as well as facilitate their effective deployment in agricultural settings.

Several approaches can be employed to dissect the genetic basis controlling a trait. In the case of the vernalisation dependency and disease resistance described in this thesis, clear phenotypic variation exists among *B. distachyon* accessions and a forward genetic approach was chosen. Accessions with different phenotypes were crossed and the genetic basis was assessed in the resulting segregating populations. This approach

is very powerful, as it only requires the generation of a single cross to identify loci controlling a phenotype and the necessary resources (e.g. markers) are easily developed (Bernardo 2016). However, the major constraint lies in the fact that potential regulators can only be detected, if they are polymorphic between the two parental lines chosen. For example, the known flowering regulator *VRN1* was not detected in Chapter 2, presumably because alleles from both parental accessions are functional. In contrast, association mapping (such as GWAS) takes into account the phenotypic and genotypic variation found in a large collection of accessions and does not suffer from the inadvertent bias of choosing two accessions to create a mapping population. Additionally, it does not require the time-consuming generation of crosses and allows higher-resolution mapping by taking advantage of historical recombination events found in large germplasm collections (Bernardo 2016). However, minor-effect loci or rare variants are less likely to be detected and findings can easily be affected by population structure (Bernardo 2016). Multi-parent advanced generation inter-cross (MAGIC) populations, e.g. for *A. thaliana* and maize (Kover *et al.* 2009; Dell'Acqua *et al.* 2015), form an intermediate approach, but are only practical for species that can be crossed relatively easily (which is not the case for *B. distachyon*).

The effective deployment of the uncovered genes is particularly important for disease resistance, as evolution of the pathogen can easily negate breeding efforts and often makes potential gains in the direction of more resistant crop plants short-lived (Flor 1971; McDonald and Linde 2002; Wulff *et al.* 2011; Dangl *et al.* 2013). In the quote above Norman Borlaug expresses his desire to utilise resistance genes from a nonhost species to provide immunity in important crop species and at various points throughout the thesis I have cited other researchers who expressed similar aspirations. For the rusts in particular, rice has been actively investigated as a source for durable resistance in the agronomically important temperate cereals (Ayliffe *et al.* 2011; Yang *et al.* 2014). However, efforts in this direction have so far been to no avail and suffered from the lack of natural variation within rice. Even though this confirms the plant's place as a true nonhost, it impedes any forward genetic studies on the genetic architecture of this resistance to rusts. During my PhD I have addressed this problem by studying the interaction of *Puccinia striiformis* with *Brachypodium distachyon*. *B. distachyon* falls on the transition between host and true nonhost, as a few accessions allow a degree of colonisation (Ayliffe *et al.* 2013; Dawson *et al.* 2015). Life cycle completion

in the form of pustule formation was generally not observed for the pathogen. This natural variation in degree of colonisation enables a forward map-based cloning approach of the genes underlying colonisation resistance. I identified three main loci and initiated map-based cloning of *Yrr3*, a locus which confers broad-spectrum resistance to all *P. striiformis* isolates tested. The locus was fine-mapped to a cluster of genes comprised of a CC-NB and two NB-LRRs. The two parental lines of one population are only differential for two SNPs, which lead to amino acid substitutions in or close to conserved motifs within the nucleotide-binding domains of the CC-NB and one of the NB-LRR.

These observations suggest that recognition of *P. striiformis* and induction of an active defence response by *B. distachyon* underlie colonisation resistance in this system, rather than a passive barrier to pathogen ingress. The leaf browning phenotype observed in this system may either form part of this active defence response against fungal colonisation or be a by-product of recognition and the mounting of an active defence response. If this is the case, the leaf browning may be correlated to hyphal colonisation, but is causally associated with recognition. In such a scenario, one could imagine that some *B. distachyon* accessions are unable to recognise the fungal invasion, allowing a degree of colonisation in the absence of leaf browning. Indeed, when screening the *Brachypodium* spp. diversity set with *Pst* isolate 08/21, some accessions did not show any leaf browning, but had pCOL scores of up to 33% (Dawson *et al.* 2015). The mounting of an active defence response raises important questions about the interaction between plant and pathogen in this system, especially if compared to the interactions between *P. striiformis formae speciales* and their appropriate hosts wheat and barley, and presents prospects for future research, both of which I will discuss in the following.

#### *What prevents life cycle completion of P. striiformis on B. distachyon?*

The dissection of the genetic architecture of colonisation resistance described in the third chapter revealed a surprisingly simple genetic architecture. None of the parental lines used for the crosses allow life cycle completion. Yet, even though transgressive segregation for increased levels of colonisation was observed, life cycle completion was also absent in the segregating progeny. As pointed out in the third chapter, this

could be due to two factors: (a) either there is no natural diversity for the gene or genes which prevent life cycle completion of *P. striiformis* among the parents of our mapping populations, or (b) a very complex genetic architecture prevents life cycle completion and our population sizes are too small to observe rare segregants.

In order to create a “natural” intermediate nonhost resistance gene cassette and confer this resistance from *B. distachyon* into the crop species wheat and barley, understanding the genetic basis of the prevention of life cycle completion would be crucial. Two approaches could be employed to study the genetic basis in the absence of natural variation. Mutagenesis of accessions that allow colonisation would constitute one way to address this question. EMS mutagenesis, for example of Bd21 or Luc1, might produce mutants that are impaired in the genes preventing pustule formation. However, this approach has two major drawbacks. Firstly, it assumes that a simple genetic architecture underlies this step of the interaction, i.e. that it is sufficient to perturb only one or a few genes to allow the formation of pustules. If a complex genetic architecture forms the basis of this, one would need to use a high mutation load and large number of mutants to uncover any lines that allow life cycle completion. The second drawback is the lack of a high-throughput phenotypic assay, requiring the inoculation and time-consuming careful phenotyping of all the generated mutants. An alternative functional genomics approach could be the transcriptional profiling of accessions that allow colonisation, but not life cycle completion, over the time course of infection. Such an approach could reveal genes that are upregulated as the pathogen colonises the leaf and attempts to complete its life cycle. These would be candidate genes involved in the prevention of life cycle completion. This approach assumes that an active defence response based on transcriptional regulation is initiated and that this regulation is required for resistance. In light of *Yrr3* mediated colonisation resistance likely involving an induced defence response, this is a reasonable assumption. Yet, one should bear in mind that preformed barriers could also play a role in the prevention of life cycle completion.

At the beginning of my PhD, I screened a diversity set of 210 *Brachypodium* spp. accessions for resistance to *P. striiformis* (Dawson *et al.* 2015). Among these 210 accessions we only very rarely observed pustules. However, not all of these accessions belonged to *B. distachyon*. What was originally thought to be *B. distachyon* accessions

with different ploidy levels (Draper *et al.* 2001) is now differentiated into three species (Catalán *et al.* 2012): the diploid *B. distachyon* ( $2N = 10$ ), the diploid *B. stacei* ( $2N = 20$ ), and *B. hybridum* ( $2N = 30$ ), the latter of which has been identified as an allotetraploid hybrid between the two diploids. Not all of the 210 accessions within our diversity set have been differentiated into the three species yet. However, based on different morphological characteristics (e.g. plant height and anther number) and our ability to cross with confirmed *B. hybridum* accessions, the accessions within the diversity set that allow life cycle completion seem to belong primarily to *B. hybridum* (Bettgenhaeuser and Moscou, unpublished).

This is an intriguing observation, as genes that prevent life cycle completion of *P. striiformis* in *B. distachyon* presumably are also present within the *B. hybridum* genome. Hybridisation events that generate a polyploid background have a marked effect on the expression and function of genes, including resistance genes (Wulff and Moscou 2014). The introgression of *P. graminis* resistance genes from the diploid *Triticum monococcum* (einkorn wheat) into tetraploid and hexaploid wheat varieties highlighted a negative correlation between ploidy and disease resistance (Kerber and Dyck 1973). Chlorosis was observed in the tetraploid variety and pustules were observed in the hexaploid variety (Kerber and Dyck 1973). The interaction between non-homeologous as well as homeologous genes can cause this suppression of resistance, as similar observations have been made with other resistance genes (Kerber 1991; McIntosh *et al.* 2011; Hurni *et al.* 2014; Wulff and Moscou 2014). *B. hybridum* accessions probably arose from several independent hybridisation events and a similar effect could underlie pustule formation in some but not all *B. hybridum* accessions, depending on the genetic background of the *B. distachyon* and *B. stacei* accessions involved in the various hybridisation events. In some cases, the genes preventing life cycle completion might be suppressed in the polyploid genome of some *B. hybridum* accessions.

*What role does the effector repertoire play in the interaction between *P. striiformis* and infected plants?*

Two major effect loci condition resistance in the *B. distachyon* mapping populations studied in this thesis. *Yrr1* has been fine-mapped to an interval that does not include

any known resistance gene homologs (Gilbert and Ayliffe, personal communication). In contrast, *Yrr3* was narrowed down to two SNPs within the NB domains of a CC-NB and an NB-LRR. This strongly suggests that either direct or indirect effector recognition underlies *Yrr3* mediated resistance. However, while all of the research presented in this thesis has been conducted on the plant side of the *B. distachyon* – *P. striiformis* interaction, plant-pathogen interactions are of a two-way nature and the pathogen genome will also have an important effect on the outcome of this interaction. In this regard, an interesting question is to what degree the effector repertoire of *P. striiformis* is involved in the interaction with *B. distachyon* and how this differs from the interactions with wheat and barley, the hosts of the *formae speciales* studied. Specifically, are the same or different effectors recognised by resistance genes in the intermediate nonhost and the hosts?

The CC-NB/NB-LRR cluster underlying *Yrr3* was found to be highly conserved in maize, sorghum, and rice. As wheat and barley do not have a gold standard sequenced genome, it was unfortunately not possible to assess the presence of this cluster within the genomes of the host species. However, it will be interesting to investigate whether the CC-NB/NB-LRR cluster also exists in these species. Presumably, all effectors within the *P. striiformis* effector repertoire are actively retained and provide an adaptive advantage. Any effectors that are not important for the infection of the host plant will likely have a cost attached to them and be lost. In such a scenario, the loss of the CC-NB/NB-LRR cluster during speciation or domestication could have constituted an important condition in allowing the adaptation of *P. striiformis* to wheat and barley as main hosts. However, this assumes that the genes in the cluster possess the same recognition capabilities across these species and presence of the CC-NB/NB-LRR cluster in wheat and barley may indicate that this assumption is not true. If different effectors are recognised in the interactions of *P. striiformis* with wheat and barley, it would be surprising if the host species have not evolved to recognise this effector, whose recognition in *B. distachyon* provides durable and broad-spectrum colonisation resistance.

In the long term, identifying the effector recognised by the *Yrr3* locus will provide a powerful tool to characterise *Yrr3* mediated resistance. Effectively, this would allow moving away from *B. distachyon* and characterise the interaction between resistance

gene and effector in a more suitable heterologous model system such as *Nicotiana benthamiana*. Regardless of whether the CC-NB or the NB-LRR conditions resistance at the *Yrr3* locus, this provides a system where a single SNP differentiates the resistant and the susceptible phenotype, which allows the instant identification of crucial amino acids involved in pathogen recognition or induction of defence responses.

*Can the resistance identified be transferred to crop species?*

As advocated by Norman Borlaug and others, the transfer of durable disease resistance across species barriers is often a major motivation for research in the area of plant pathology and nonhost resistance genes have been identified as a desirable target for such a transfer (Borlaug 2000; Hammond-Kosack and Parker 2003; Fan and Doerner 2012; Lee *et al.* 2016). Many examples exist for this transfer (reviewed by Wulff *et al.* (2011)), but there are also limits to the ability of transferring a resistance gene from one species to another (Ayliffe *et al.* 2004). NB-LRR mediated resistance relies on the activation of downstream signalling responses in order to stop infection (Aarts *et al.* 1998; Wiermer *et al.* 2005). Presumably, downstream signalling is also required for CC-NB mediated resistance. Therefore, transferring the resistance observed at the *Yrr3* locus in *B. distachyon* to the agronomically important grass species wheat and barley will require these downstream signalling components to be conserved across these species. Examples of NB-LRR transfer between species have often involved related species (e.g. within the Solanaceae) (Wulff *et al.* 2011), but there exists precedence for the phylogenetically wide transfer of NB-LRR mediated immunity across families. In *Arabidopsis thaliana* the *PEN* genes provide broad-spectrum pre-penetration resistance against barley and pea powdery mildews (Collins *et al.* 2003; Lipka *et al.* 2005; Stein *et al.* 2006; Lipka *et al.* 2008). However, in *pen* mutant *A. thaliana* lines the introduction of *MLA1*, an NB-LRR encoding a barley powdery mildew resistance gene from barley, reconstituted resistance against barley powdery mildew in *A. thaliana* (Maekawa *et al.* 2012). In this case, the downstream components of *MLA1* mediated resistance are conserved between barley and *A. thaliana*.

In the fourth chapter I discussed the various models that could underlie *Yrr3* mediated resistance and also suggested, that resistance at this locus may be conditioned by more

than one gene. For example, the CC-NB could interact with one of the NB-LRR to provide resistance against *P. striiformis*. We are currently transforming the susceptible *B. distachyon* accessions Luc1 and Bd21, as well as susceptible wheat and barley lines. If more than one gene is required for resistance, this may not become apparent during *B. distachyon* transformation, as a functional allele of the interacting partner might exist within the genome. Transformation of the genes into the heterologous systems wheat and barley will aid in elucidating the genes that are necessary and sufficient for *Yrr3* mediated resistance. If the transfer of only Bradi2g52430 or Bradi2g52450 provides resistance in these systems, only one gene likely conditions resistance at the *Yrr3* locus. If the transfer of these genes is not sufficient for providing resistance, a combination of two or all three of the genes present at the locus might be needed. Alternatively, *Yrr3* mediated resistance may also rely on genes at other loci within the *B. distachyon* genome, such as downstream signalling components that are not conserved in wheat and barley.

In conclusion, studying the interaction between *B. distachyon* and *P. striiformis* has provided an ideal system to dissect the genetic architecture and molecular basis of intermediate nonhost resistance. It remains to be seen whether this durable and broad-spectrum resistance can be transferred into wheat and barley and provide the same level of protection.

## 6. Appendices

### Supplemental figures

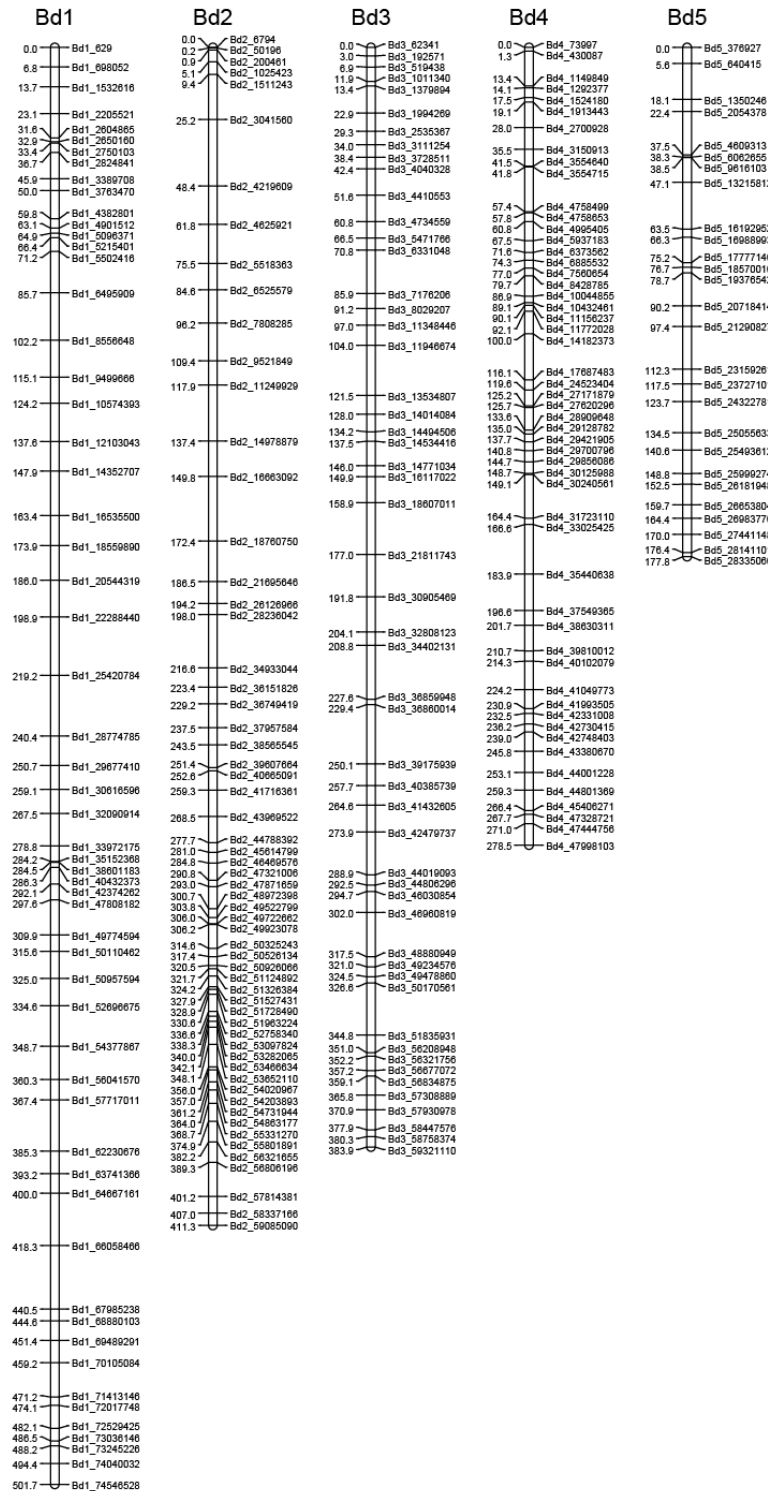


**Figure S1.** Linkage groups of the ABR6 x Bd21 genetic map. Cumulative cM distances and SNP marker names are shown to the left and right of each chromosome, respectively. cM distance at the F4 stage was estimated using the Kosambi function. SNP marker names consist of the corresponding chromosome and physical position in the Bd21 reference genome (Version 3).

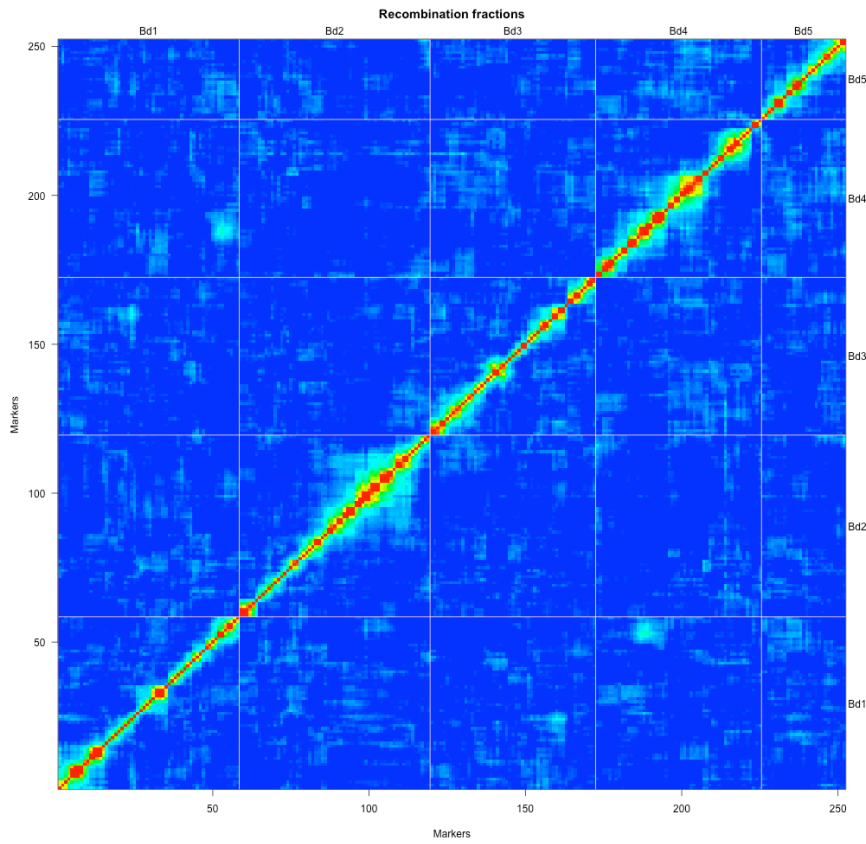


**Figure S2.** Two-way recombination fraction plot for the ABR6 x Bd21 F<sub>4</sub> population.

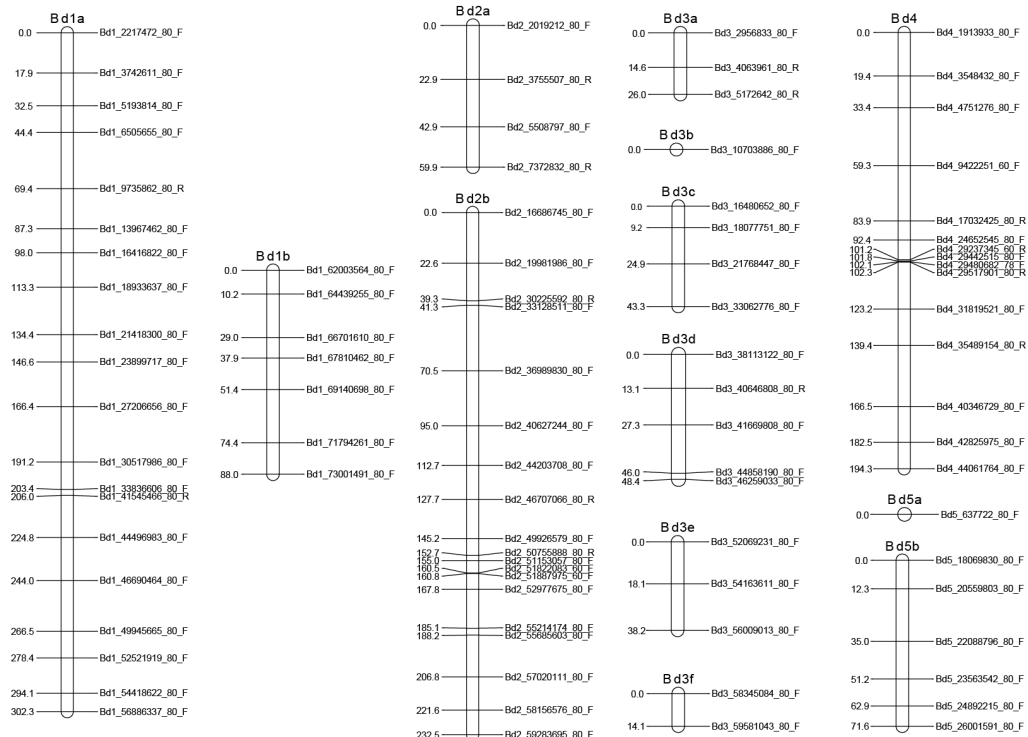


**Figure S3.** Linkage groups of the preliminary Foz1 x Luc1 genetic map. Cumulative cM distances and SNP marker names are shown to the left and right of each chromosome, respectively. cM distance at the F<sub>2</sub> stage was estimated using the Kosambi function. SNP marker names consist of the corresponding chromosome and physical position in the Bd21 reference genome (Version 1).

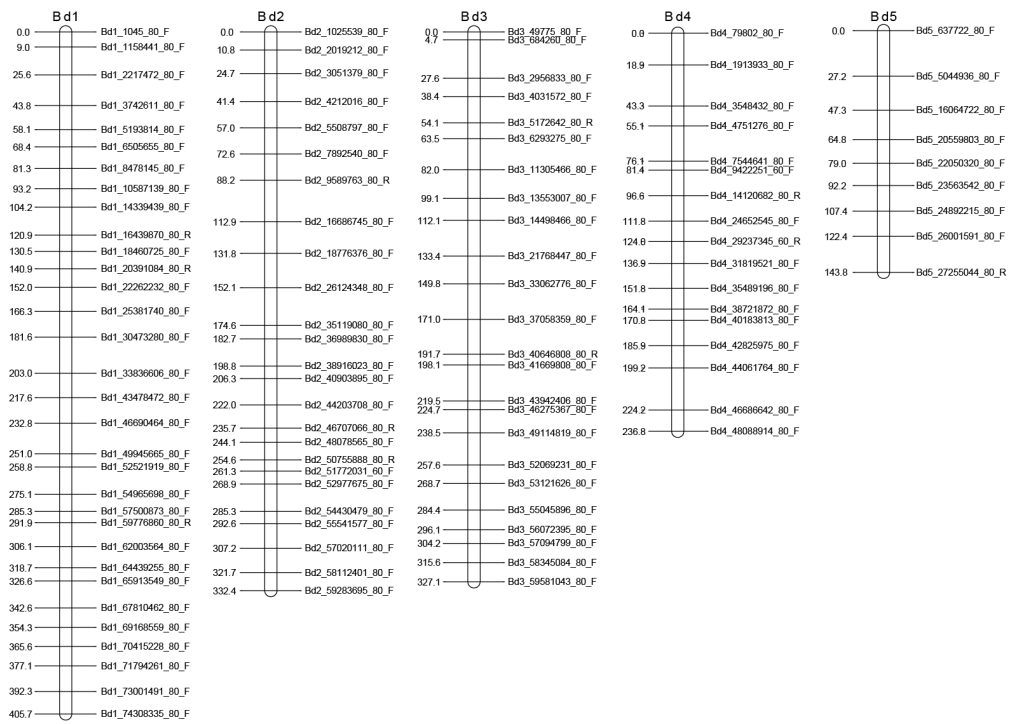


**Figure S4.** Linkage groups of the Luc1 x Jer1 genetic map. Cumulative cM distances and SNP marker names are shown to the left and right of each chromosome, respectively. cM distance at the F<sub>2</sub> stage was estimated using the Kosambi function. SNP marker names consist of the corresponding chromosome and physical position in the Bd21 reference genome (Version 1).

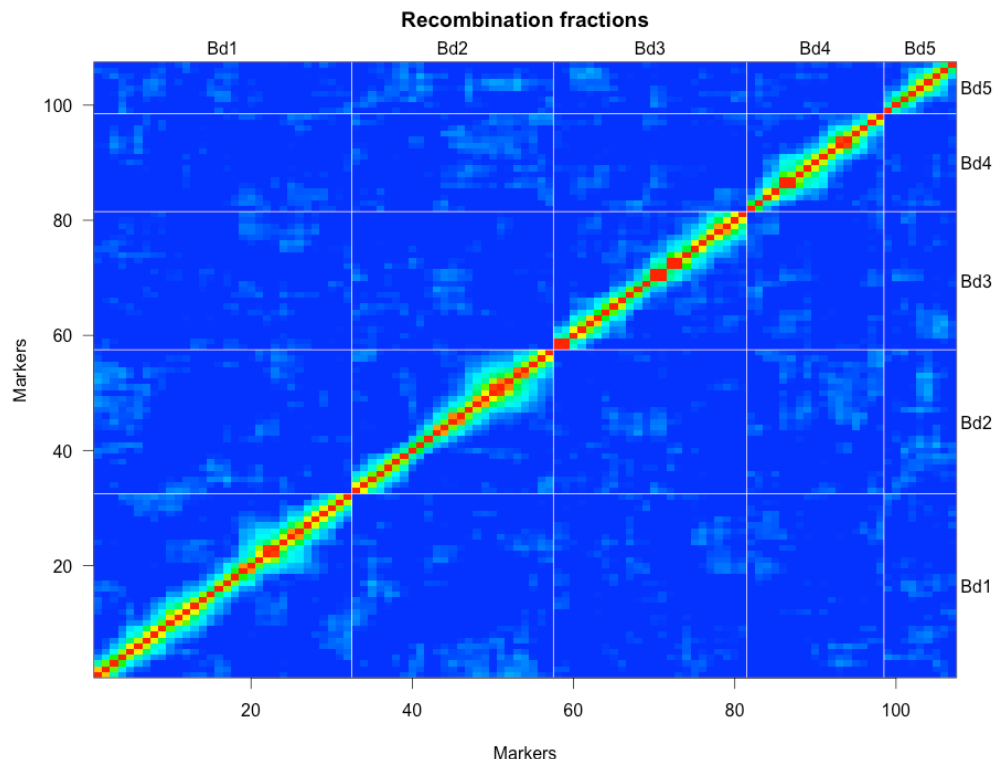


**Figure S5.** Two-way recombination fraction plot for the Luc1 x Jer1 F<sub>2</sub> genetic map.

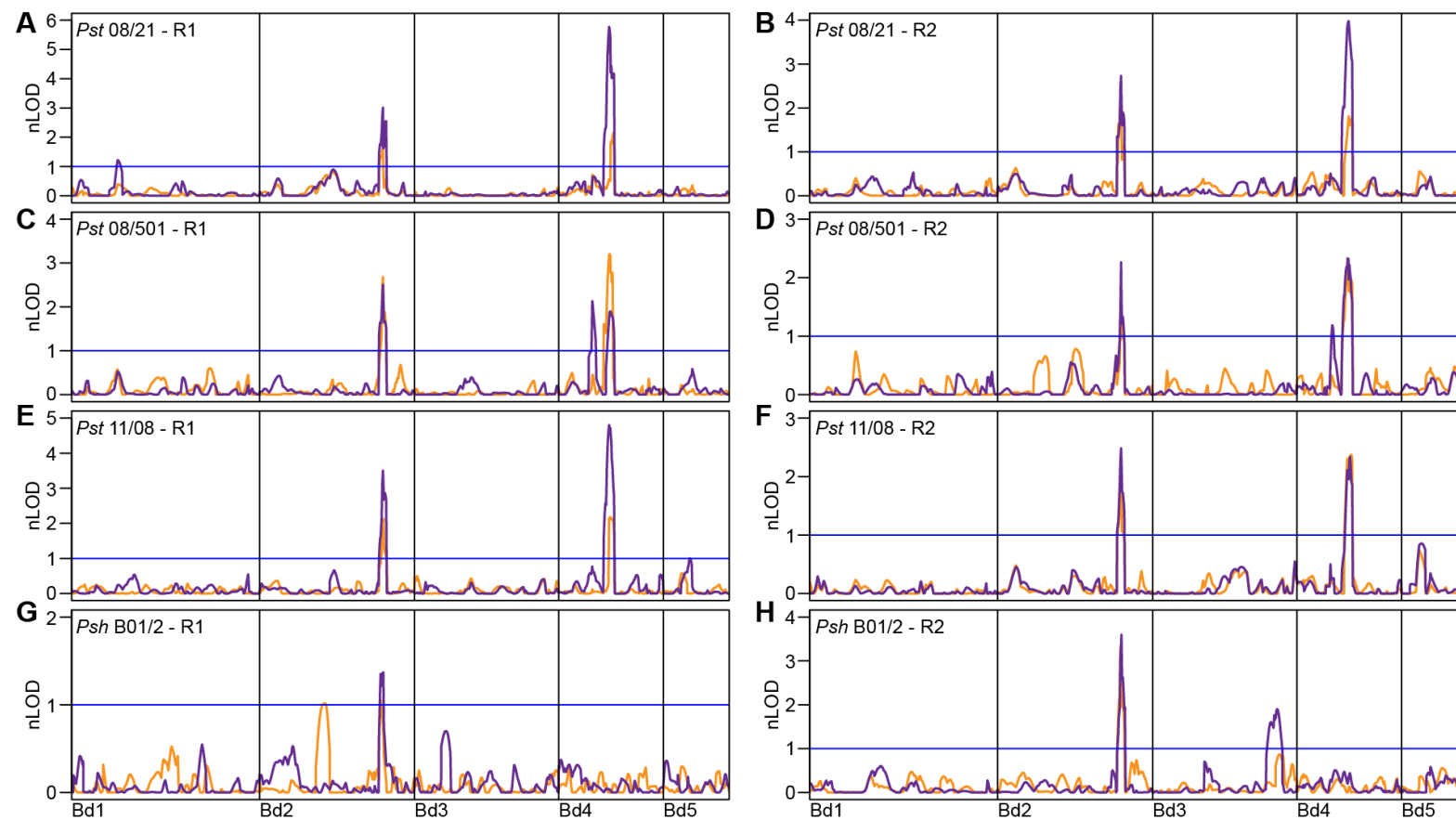


**Figure S6.** Composite interval mapping of leaf browning (orange) and pCOL (purple) in response to the four *P. striiformis* isolates based on individual replicates in the ABR6 x Bd21 F<sub>4:5</sub> families. Phenotypes of F<sub>4:5</sub> families were scored 14 dpi with *P. striiformis* f. sp. *tritici* (*Pst*) isolates 08/21 (A and B), 08/501 (C and D), and 11/08 (E and F), and *P. striiformis* f. sp. *hordei* (*Psh*) isolate B01/2 (G and H). Composite interval mapping was performed under an additive model ( $H_0$ : $H_1$ ). Results were plotted based on normalised permutation thresholds (nLOD), using the threshold of statistical significance based on 1,000 permutations (blue horizontal line). R1 = replicate 1; R2 = replicate 2.

**Figure S7 (next four pages).** Clustal Omega multiple sequence alignment of the amino acid sequences for the three candidate genes obtained from *de novo* transcriptome assemblies of the five accessions studied. Conserved NB-LRR motifs identified by MAST analysis are indicated in bold and underlined, with the motif names below the alignment. Highlighting indicates amino acid substitutions in Luc1 (magenta) and Bd21 (green). The ABR6, Jer1, and Foz1 amino acid sequences are identical. Level of conservation as determined by Clustal Omega: “\*” = identical amino acids, “:” = conservation between strongly similar amino acids, “.” = conservation between weakly similar amino acids, space = non-conservative polymorphism.

**Bradi2g52430 (CC-NB)**

Bradi2g52430_Bd21	MAVVVQFLVRKFVDSLAEAAVELPFSAHFYDMRAELEK <b>A</b> **V**S**TNADELRECLYELNDL
Bradi2g52430_ABR6	MAVVVQFLVRKFVDSLAEAAVELPFSAHFYDMRAELEK <b>A</b> **V**S**TNADELRECLYELNDL
Bradi2g52430_Jer1	MAVVVQFLVRKFVDSLAEAAVELPFSAHFYDMRAELEK <b>A</b> **V**S**TNADELRECLYELNDL
Bradi2g52430_Foz1	MAVVVQFLVRKFVDSLAEAAVELPFSAHFYDMRAELEK <b>A</b> **V**S**TNADELRECLYELNDL
Bradi2g52430_Luc1	MAVVVQFLVRKFVDSLAEAAVELPFSAHFYDMRAELEK <b>A</b> **V**S**TNADELRECLYELNDL
	*****
Bradi2g52430_Bd21	<b>L</b> SQCRIMLTNRPNTRSCFFAPSEAWLSNKVKRVRVAVKRRVLQCVQNNPSEDAAGSQEDN
Bradi2g52430_ABR6	<b>L</b> SQCRIMLTNMPNTRSCFFAPSEAWLSNKVKRVRVAVKRRVLQCVQNNPSEDAAGSQEDN
Bradi2g52430_Jer1	<b>L</b> SQCRIMLTNMPNTRSCFFAPSEAWLSNKVKRVRVAVKRRVLQCVQNNPSEDAAGSQEDN
Bradi2g52430_Foz1	<b>L</b> SQCRIMLTNMPNTRSCFFAPSEAWLSNKVKRVRVAVKRRVLQCVQNNPSEDAAGSQEDN
Bradi2g52430_Luc1	<b>L</b> SQCRIMLTNMPNTRSCFFAPSEAWLSNKVKRVRVAVKRRVLQCVQNNPSEDAAGSQEDN
	*****
Bradi2g52430_Bd21	AATGFSRWTTSWPEQSRMHGFDQQLTELESKAFGDCSPGKLT <b>G</b> V <b>G</b> IV <b>G</b> M <b>G</b> <b>G</b> <b>I</b> <b>G</b> <b>K</b> T <b>A</b> QL
Bradi2g52430_ABR6	AATGFSRWTTSWPEQSRMHGFDQQLTELESKAFGDCSPGKLT <b>G</b> V <b>G</b> IV <b>G</b> M <b>G</b> <b>G</b> <b>I</b> <b>G</b> <b>K</b> T <b>A</b> QL
Bradi2g52430_Jer1	AATGFSRWTTSWPEQSRMHGFDQQLTELESKAFGDCSPGKLT <b>G</b> V <b>G</b> IV <b>G</b> M <b>G</b> <b>G</b> <b>I</b> <b>G</b> <b>K</b> T <b>A</b> QL
Bradi2g52430_Foz1	AATGFSRWTTSWPEQSRMHGFDQQLTELESKAFGDCSPGKLT <b>G</b> V <b>G</b> IV <b>G</b> M <b>G</b> <b>G</b> <b>I</b> <b>G</b> <b>K</b> T <b>A</b> QL
Bradi2g52430_Luc1	AATGFSRWTTSWPEQSRMHGFDQQLTELESKAFGDCSPGKLT <b>G</b> V <b>G</b> IV <b>G</b> M <b>G</b> <b>G</b> <b>I</b> <b>G</b> <b>K</b> T <b>A</b> QL
	*****
Bradi2g52430_Bd21	<b>M</b> FNSPQARGRFFPRIWVCLSRTAC <b>G</b> KD <b>V</b> R <b>E</b> VL <b>Q</b> SILMALGLEEEGILAIDGGGDSLGD
Bradi2g52430_ABR6	<b>M</b> FNSPQARGRFFPRIWVCLSRTAC <b>G</b> KD <b>V</b> R <b>E</b> VL <b>Q</b> SILMALGLEEEGILAIDGGGDSLGD
Bradi2g52430_Jer1	<b>M</b> FNSPQARGRFFPRIWVCLSRTAC <b>G</b> KD <b>V</b> R <b>E</b> VL <b>Q</b> SILMALGLEEEGILAIDGGGDSLGD
Bradi2g52430_Foz1	<b>M</b> FNSPQARGRFFPRIWVCLSRTAC <b>G</b> KD <b>V</b> R <b>E</b> VL <b>Q</b> SILMALGLEEEGILAIDGGGDSLGD
Bradi2g52430_Luc1	<b>M</b> FNSPQARGRFFPRIWVCLSRTAC <b>G</b> KD <b>V</b> R <b>E</b> VL <b>Q</b> SILMALGLEEEGILAIDGGGDSLGD
	*****
	<b>P-loop</b>
Bradi2g52430_Bd21	LELAVHEHL <b>K</b> G <b>K</b> R <b>I</b> <b>I</b> <b>I</b> <b>V</b> FDDVWNIDG <b>W</b> YAD <b>V</b> VG <b>C</b> Q <b>N</b> T <b>V</b> P <b>R</b> GD <b>Q</b> W <b>S</b> D <b>R</b> L <b>A</b> Y <b>G</b> LP <b>K</b> ER <b>G</b> VV
Bradi2g52430_ABR6	LELAVHEHL <b>K</b> G <b>K</b> R <b>I</b> <b>I</b> <b>I</b> <b>V</b> FDDVWNIDG <b>W</b> YAD <b>V</b> VG <b>C</b> Q <b>N</b> T <b>V</b> P <b>R</b> GD <b>Q</b> W <b>S</b> D <b>C</b> L <b>A</b> Y <b>G</b> LP <b>K</b> ER <b>G</b> VV
Bradi2g52430_Jer1	LELAVHEHL <b>K</b> G <b>K</b> R <b>I</b> <b>I</b> <b>I</b> <b>V</b> FDDVWNIDG <b>W</b> YAD <b>V</b> VG <b>C</b> Q <b>N</b> T <b>V</b> P <b>R</b> GD <b>Q</b> W <b>S</b> D <b>C</b> L <b>A</b> Y <b>G</b> LP <b>K</b> ER <b>G</b> VV
Bradi2g52430_Foz1	LELAVHEHL <b>K</b> G <b>K</b> R <b>I</b> <b>I</b> <b>I</b> <b>V</b> FDDVWNIDG <b>W</b> YAD <b>V</b> VG <b>C</b> Q <b>N</b> T <b>V</b> P <b>R</b> GD <b>Q</b> W <b>S</b> D <b>C</b> L <b>A</b> Y <b>G</b> LP <b>K</b> ER <b>G</b> VV
Bradi2g52430_Luc1	LELAVHEHL <b>K</b> G <b>K</b> R <b>I</b> <b>I</b> <b>I</b> <b>V</b> FDDVWNIDG <b>W</b> YAD <b>V</b> VG <b>C</b> Q <b>N</b> T <b>V</b> P <b>R</b> GD <b>Q</b> W <b>S</b> D <b>C</b> L <b>A</b> Y <b>G</b> LP <b>K</b> ER <b>G</b> VV
	*****
	<b>RNBS-A</b>
Bradi2g52430_Bd21	LELAVHEHL <b>K</b> G <b>K</b> R <b>I</b> <b>I</b> <b>I</b> <b>V</b> FDDVWNIDG <b>W</b> YAD <b>V</b> VG <b>C</b> Q <b>N</b> T <b>V</b> P <b>R</b> GD <b>Q</b> W <b>S</b> D <b>R</b> L <b>A</b> Y <b>G</b> LP <b>K</b> ER <b>G</b> VV
Bradi2g52430_ABR6	LELAVHEHL <b>K</b> G <b>K</b> R <b>I</b> <b>I</b> <b>I</b> <b>V</b> FDDVWNIDG <b>W</b> YAD <b>V</b> VG <b>C</b> Q <b>N</b> T <b>V</b> P <b>R</b> GD <b>Q</b> W <b>S</b> D <b>C</b> L <b>A</b> Y <b>G</b> LP <b>K</b> ER <b>G</b> VV
Bradi2g52430_Jer1	LELAVHEHL <b>K</b> G <b>K</b> R <b>I</b> <b>I</b> <b>I</b> <b>V</b> FDDVWNIDG <b>W</b> YAD <b>V</b> VG <b>C</b> Q <b>N</b> T <b>V</b> P <b>R</b> GD <b>Q</b> W <b>S</b> D <b>C</b> L <b>A</b> Y <b>G</b> LP <b>K</b> ER <b>G</b> VV
Bradi2g52430_Foz1	LELAVHEHL <b>K</b> G <b>K</b> R <b>I</b> <b>I</b> <b>I</b> <b>V</b> FDDVWNIDG <b>W</b> YAD <b>V</b> VG <b>C</b> Q <b>N</b> T <b>V</b> P <b>R</b> GD <b>Q</b> W <b>S</b> D <b>C</b> L <b>A</b> Y <b>G</b> LP <b>K</b> ER <b>G</b> VV
Bradi2g52430_Luc1	LELAVHEHL <b>K</b> G <b>K</b> R <b>I</b> <b>I</b> <b>I</b> <b>V</b> FDDVWNIDG <b>W</b> YAD <b>V</b> VG <b>C</b> Q <b>N</b> T <b>V</b> P <b>R</b> GD <b>Q</b> W <b>S</b> D <b>C</b> L <b>A</b> Y <b>G</b> LP <b>K</b> ER <b>G</b> VV
	*****
	<b>Kinase-2</b>
Bradi2g52430_Bd21	<b>V</b> VTSRLEQAAEMMV <b>G</b> K <b>S</b> SI <b>Y</b> R <b>V</b> Q <b>Q</b> L <b>A</b> D <b>R</b> E <b>S</b> W <b>A</b> IF <b>M</b> D <b>A</b> L <b>S</b> K <b>R</b> <b>R</b> <b>S</b> <b>I</b> <b>D</b> <b>L</b> <b>T</b> <b>A</b> <b>V</b> <b>N</b> <b>S</b> <b>M</b> <b>K</b> <b>E</b> <b>I</b> <b>E</b> <b>L</b> <b>E</b>
Bradi2g52430_ABR6	<b>V</b> VTSRLEQAAEMMV <b>G</b> K <b>S</b> SI <b>Y</b> R <b>V</b> Q <b>Q</b> L <b>A</b> D <b>R</b> E <b>S</b> W <b>A</b> IF <b>M</b> D <b>A</b> L <b>S</b> K <b>R</b> <b>R</b> <b>S</b> <b>I</b> <b>D</b> <b>L</b> <b>T</b> <b>A</b> <b>V</b> <b>N</b> <b>S</b> <b>M</b> <b>K</b> <b>E</b> <b>I</b> <b>E</b> <b>L</b> <b>E</b>
Bradi2g52430_Jer1	<b>V</b> VTSRLEQAAEMMV <b>G</b> K <b>S</b> SI <b>Y</b> R <b>V</b> Q <b>Q</b> L <b>A</b> D <b>R</b> E <b>S</b> W <b>A</b> IF <b>M</b> D <b>A</b> L <b>S</b> K <b>R</b> <b>R</b> <b>S</b> <b>I</b> <b>D</b> <b>L</b> <b>T</b> <b>A</b> <b>V</b> <b>N</b> <b>S</b> <b>M</b> <b>K</b> <b>E</b> <b>I</b> <b>E</b> <b>L</b> <b>E</b>
Bradi2g52430_Foz1	<b>V</b> VTSRLEQAAEMMV <b>G</b> K <b>S</b> SI <b>Y</b> R <b>V</b> Q <b>Q</b> L <b>A</b> D <b>R</b> E <b>S</b> W <b>A</b> IF <b>M</b> D <b>A</b> L <b>S</b> K <b>R</b> <b>R</b> <b>S</b> <b>I</b> <b>D</b> <b>L</b> <b>T</b> <b>A</b> <b>V</b> <b>N</b> <b>S</b> <b>M</b> <b>K</b> <b>E</b> <b>I</b> <b>E</b> <b>L</b> <b>E</b>
Bradi2g52430_Luc1	<b>V</b> VTSRLEQAAEMMV <b>G</b> K <b>S</b> SI <b>Y</b> R <b>V</b> Q <b>Q</b> L <b>A</b> D <b>R</b> E <b>S</b> W <b>A</b> IF <b>M</b> D <b>A</b> L <b>S</b> K <b>R</b> <b>R</b> <b>S</b> <b>I</b> <b>D</b> <b>L</b> <b>T</b> <b>A</b> <b>V</b> <b>N</b> <b>S</b> <b>M</b> <b>K</b> <b>E</b> <b>I</b> <b>E</b> <b>L</b> <b>E</b>
	*****
	<b>RNBS-B</b>
Bradi2g52430_Bd21	<b>T</b> CGGLPSTAKAMAD <b>I</b> F <b>V</b> K <b>S</b> LSI <b>Q</b> T <b>P</b> T <b>S</b> <b>S</b> Q <b>E</b> LR <b>F</b> SG <b>N</b> <b>V</b> <b>R</b>
Bradi2g52430_ABR6	<b>T</b> CGGLPSTAKAMAD <b>I</b> F <b>V</b> K <b>S</b> LSI <b>Q</b> T <b>P</b> T <b>S</b> <b>S</b> Q <b>E</b> LR <b>F</b> SG <b>N</b> <b>V</b> <b>R</b>
Bradi2g52430_Jer1	<b>T</b> CGGLPSTAKAMAD <b>I</b> F <b>V</b> K <b>S</b> LSI <b>Q</b> T <b>P</b> T <b>S</b> <b>S</b> Q <b>E</b> LR <b>F</b> SG <b>N</b> <b>V</b> <b>R</b>
Bradi2g52430_Foz1	<b>T</b> CGGLPSTAKAMAD <b>I</b> F <b>V</b> K <b>S</b> LSI <b>Q</b> T <b>P</b> T <b>S</b> <b>S</b> Q <b>E</b> LR <b>F</b> SG <b>N</b> <b>V</b> <b>R</b>
Bradi2g52430_Luc1	<b>T</b> CGGLPSTAKAMAD <b>I</b> F <b>V</b> K <b>S</b> LSI <b>Q</b> T <b>P</b> T <b>S</b> <b>S</b> Q <b>E</b> LR <b>F</b> SG <b>N</b> <b>V</b> <b>R</b>
	*****
	<b>GPL</b>

**Bradi2g52437 (NB-LRR)**

Bradi2g52437\_Bd21  
Bradi2g52437\_Jer1  
Bradi2g52437\_Luc1  
Bradi2g52437\_Foz1  
Bradi2g52437\_ABR6

MSQERTLEEVVSPFLMQLSKARVLSLTDDDSLLDIKLLFENIEREAHDVEDILKSVSR  
MSQERTLEEVVSPFLMQLSKARVLSLTDDDSLLDIKLLFENIEREAHDVEDILKSVSR  
MSQERTLEEVVSPFLMQLSKARVLSLTDDDSLLDIKLLFENIEREAHDVEDILKSVSR  
MSQERTLEEVVSPFLMQLSKARVLSLTDDDSLLDIKLLFENIEREAHDVEDILKSVSR  
MSQERTLEEVVSPFLMQLSKARVLSLTDDDSLLDIKLLFENIEREAHDVEDILKSVSR  
\*\*\*\*\*

Bradi2g52437\_Bd21  
Bradi2g52437\_Jer1  
Bradi2g52437\_Luc1  
Bradi2g52437\_Foz1  
Bradi2g52437\_ABR6

WENEIINDFGAIARHLDIIEEDSQQQFIHSKLOIVNTEMSNLKDRMKFPLHVPLIKPAA  
WENEIINDFGAIARHLDIIEEDSQQQFIHSKLOIVNTEMSNLKDRMKFPLHVPLIKPAA  
WENEIINDFGAIARHLDIIEEDSQQQFIHSKLOIVNTEMSNLKDRMKFPLHVPLIKPAA  
WENEIINDFGAIARHLDIIEEDSQQQFIHSKLOIVNTEMSNLKDRMKFPLHVPLIKPAA  
WENEIINDFGAIARHLDIIEEDSQQQFIHSKLOIVNTEMSNLKDRMKFPLHVPLIKPAA  
\*\*\*\*\*

Bradi2g52437\_Bd21  
Bradi2g52437\_Jer1  
Bradi2g52437\_Luc1  
Bradi2g52437\_Foz1  
Bradi2g52437\_ABR6

PALLSSSLPSKSLSANASEQWKKLEIERKILECSMISNLQLSYYNLDIQLKLCLLCFSIF  
PALLSSSLPSKSLSANASEQWKKLEIERKILECSMISNLQLSYYNLDIQLKLCLLCFSIF  
PALLSSSLPSKSLSANASEQWKKLEIERKILECSMISNLQLSYYNLDIQLKLCLLCFSIF  
PALLSSSLPSKSLSANASEQWKKLEIERKILECSMISNLQLSYYNLDIQLKLCLLCFSIF  
PALLSSSLPSKSLSANASEQWKKLEIERKILECSMISNLQLSYYNLDIQLKLCLLCFSIF  
\*\*\*\*\*

Bradi2g52437\_Bd21  
Bradi2g52437\_Jer1  
Bradi2g52437\_Luc1  
Bradi2g52437\_Foz1  
Bradi2g52437\_ABR6

PENSIISKRAMIHWWIGEGLVEATKSQTAEDIGKDCFERLITVEMIEPVRHKRIGSVNQC  
PENSIISKRAMIHWWIGEGLVEATKSQTAEDIGKDCFERLITVEMIEPVRHKRIGSVNQC  
PENSIISKRAMIHWWIGEGLVEATKSQTAEDIGKDCFERLITVEMIEPVRHKRIGSVNQC  
PENSIISKRAMIHWWIGEGLVEATKSQTAEDIGKDCFERLITVEMIEPVRHKRIGSVNQC  
PENSIISKRAMIHWWIGEGLVEATKSQTAEDIGKDCFERLITVEMIEPVRHKRIGSVNQC  
\*\*\*\*\*

II Motif 6 M

KLHPWIRMLITVARQERFVEFSDSGNATWGFSGTHRACLVGEHIQVTETGPLRNQSNPD  
KLHPWIRMLITVARQERFVEFSDSGNATWGFSGTHRACLVGEHIQVTETGPLRNQSNPD  
KLHPWIRMLITVARQERFVEFSDSGNATWGFSGTHRACLVGEHIQVTETGPLRNQSNPD  
KLHPWIRMLITVARQERFVEFSDSGNATWGFSGTHRACLVGEHIQVTETGPLRNQSNPD  
KLHPWIRMLITVARQERFVEFSDSGNATWGFSGTHRACLVGEHIQVTETGPLRNQSNPD  
\*\*\*\*\*

**HDV**

YLLTIFNVNEQYLQFDKNWFMDLRKIEVLQIGRWHSLYRHHIEVDSTEYLEGLQSSKQLK  
YLLTIFNVNEQYLQFDKNWFMDLRKIEVLQIGRWHSLYRHHIEVDSTEYLEGLQSSKQLK  
YLLTIFNVNEQYLQFDKNWFMDLRKIEVLQIGRWHSLYRHHIEVDSTEYLEGLQSSKQLK  
YLLTIFNVNEQYLQFDKNWFMDLRKIEVLQIGRWHSLYRHHIEVDSTEYLEGLQSSKQLK  
YLLTIFNVNEQYLQFDKNWFMDLRKIEVLQIGRWHSLYRHHIEVDSTEYLEGLQSSKQLK  
\*\*\*\*\*

YLCLRGISRVTELPAVGALTNLRILDLHACHNLERLTESITSLQLLTHLDVSECYLLLEG  
YLCLRGISRVTELPAVGALTNLRILDLHACHNLERLTESITSLQLLTHLDVSECYLLLEG  
YLCLRGISRVTELPAVGALTNLRILDLHACHNLERLTESITSLQLLTHLDVSECYLLLEG  
YLCLRGISRVTELPAVGALTNLRILDLHACHNLERLTESITSLQLLTHLDVSECYLLLEG  
\*\*\*\*\*

LRR LRR

MPRGIGLLAELQVLKGFVIGGSIGNSNCRVAELVLVRLDKLKKLSIYIGSKVLVTEDNEV  
MPRGIGLLAELQVLKGFVIGGSIGNSNCRVAELVLVRLDKLKKLSIYIGSKVLVTEDNEV  
MPRGIGLLAELQVLKGFVIGGSIGNSNCRVAELVLVRLDKLKKLSIYIGSKVLVTEDNEV  
MPRGIGLLAELQVLKGFVIGGSIGNSNCRVAELVLVRLDKLKKLSIYIGSKVLVTEDNEV  
\*\*\*\*\*

LRR L

ENIKALRVLTITWAVLLSKKGAGQDSAATLLTSSLPPHLEKLDLRCFPGVDMPVWL  
ENIKALRVLTITWAVLLSKKGAGQDSAATLLTSSLPPHLEKLDLRCFPGVDMPVWL  
ENIKALRVLTITWAVLLSKKGAGQDSAATLLTSSLPPHLEKLDLRCFPGVDMPVWL  
ENIKALRVLTITWAVLLSKKGAGQDSAATLLTSSLPPHLEKLDLRCFPGVDMPVWL  
ENIKALRVLTITWAVLLSKKGAGQDSAATLLTSSLPPHLEKLDLRCFPGVDMPVWL  
\*\*\*\*\*

RR LRR

LGRILRRLRRLYFTGGMLHTFGESTILRLKFLNDLVLEWTQVREMFPKLTFLEVFQ  
PGRILRRLRRLYFTGGMLHTFGESALWNVEILRLKFLNDLVLEWTQVHEMFPKLTFLEVFQ  
PGRILRRLRRLYFTGGMLHTFGESALWNVEILRLKFLNDLVLEWTQVHEMFPKLTFLEVFQ  
PGRILRRLRRLYFTGGMLHTFGESALWNVEILRLKFLNDLVLEWTQVHEMFPKLTFLEVFQ  
\*\*\*\*\*

LRR LRR

CSRIKSFPCDKDGVWMSCDQETEE  
CSRIKSFPCDKDGVWMSCDQETEE  
CSRIKSFPCDKDGVWMSCDQETEE  
CSRIKSFPCDKDGVWMSCDQETEE  
CSRIKSFPCDKDGVWMSCDQETEE  
\*\*\*\*\*

**Bradi2g52450 (NB-LRR)**

(continued on next page)

Bradi2g52450\_Bd21  
Bradi2g52450\_Foz1  
Bradi2g52450\_ABR6  
Bradi2g52450\_Jer1  
Bradi2g52450\_Luc1

MASYFCFRKPMRPIPSFAIPOYQIPRYQISCDMLCLVLRPEGEVVVIEGIGGSGTKWAA  
MASYFCFRKPMRPIPSFAIPOYQIPRYQISCDMLCLVLRPEGEVVVIEGIGGSGTKWAA  
MASYFCFRKPMRPIPSFAIPOYQIPRYQISCDMLCLVLRPEGEVVVIEGIGGSGTKWAA  
MASYFCFRKPMRPIPSFAIPOYQIPRYQISCDMLCLVLRPEGEVVVIEGIGGSGTKWAA  
MASYFCFRKPMRPIPSFAIPOYQIPRYQISCDMLCLVLRPEGEVVVIEGIGGSGTKWAA  
\*\*\*\*\*

**P-loop**

Bradi2g52450\_Bd21  
Bradi2g52450\_Foz1  
Bradi2g52450\_ABR6  
Bradi2g52450\_Jer1  
Bradi2g52450\_Luc1

KAAFETSKNSNRFEDYIWVSLSRCSLRRCIEKIATCLSIEIGEELLSSRIAVMIKEHLA  
KAAFETSKNSNRFEDYIWVSLSRCSLRRCIEKIATCLSIEIGEELLSSRIAVMIKEHLA  
KAAFETSKNSNRFEDYIWVSLSRCSLRRCIEKIATCLSIEIGEELLSSRIAVMIKEHLA  
KAAFETSKNSNRFEDYIWVSLSRCSLRRCIEKIATCLSIEIGEELLSSRIAVMIKEHLA  
KAAFETSKNSNRFEDYIWVSLSRCSLRRCIEKIATCLSIEIGEELLSSRIAVMIKEHLA  
\*\*\*\*\*

**RNBS-A**

Bradi2g52450\_Bd21  
Bradi2g52450\_Foz1  
Bradi2g52450\_ABR6  
Bradi2g52450\_Jer1  
Bradi2g52450\_Luc1

RRKFLLVLDNAYFVEANILSHLGIPHPREQGFGSKVIVTTRARALSVMEPATVILPQL  
RRKFLLVLDNAYFVEANILSHLGIPHPREQGFGSKVIVTTRARALSVMEPATVILPQL  
RRKFLLVLDNAYFVEANILSHLGIPHPREQGFGSKVIVTTRARALSVMEPATVILPQL  
RRKFLLVLDNAYFVEANILSHLGIPHPREQGFGSKVIVTTRARALSVMEPATVILPQL  
RRKFLLVLDNAYFVEANILSHLGIPHPREQGFGSKVIVTTRARALSVMEPATVILPQL  
\*\*\*\*\*

**Ki**

Bradi2g52450\_Bd21  
Bradi2g52450\_Foz1  
Bradi2g52450\_ABR6  
Bradi2g52450\_Jer1  
Bradi2g52450\_Luc1

TYEASHDLLREKLGDIDLELIDNCFGMPLSIIILLAGALCDAPTHEEFHKLISAAHVAQG  
TYEASHDLLREKLGDIDLELIDNCFGMPLSIIILLAGALCDAPTHEEFHKLISAAHVAQG  
TYEASHDLLREKLGDIDLELIDNCFGMPLSIIILLAGALCDAPTHEEFHKLISAAHVAQG  
TYEASHDLLREKLGDIDLELIDNCFGMPLSIIILLAGALCDAPTHEEFHKLISAAHVAQG  
TYEASHDLLREKLGDIDLELIDNCFGMPLSIIILLAGALCDAPTHEEFHKLISAAHVAQG  
\*\*\*\*\*

**GLPL**

Bradi2g52450\_Bd21  
Bradi2g52450\_Foz1  
Bradi2g52450\_ABR6  
Bradi2g52450\_Jer1  
Bradi2g52450\_Luc1

PKVSVPNTMTRLVNFGYRQLPSDTARHCFLYCLLFPDDEAISVKDLIFFWKLDMSIQEAO  
PKVSVPNTMTRLVNFGYRQLPSATARHCFLYCLLFPDDEAISVKDLIFFWKLDMSIQEAO  
PKVSVPNTMTRLVNFGYRQLPSATARHCFLYCLLFPDDEAISVKDLIFFWKLDMSIQEAO  
PKVSVPNTMTRLVNFGYRQLPSATARHCFLYCLLFPDDEAISVKDLIFFWKLDMSIQEAO  
PKVSVPNTMTRLVNFGYRQLPSATARHCFLYCLLFPDDEAISVKDLIFFWKLDMSIQEAO  
\*\*\*\*\*

**RNBS-B**

Bradi2g52450\_Bd21  
Bradi2g52450\_Foz1  
Bradi2g52450\_ABR6  
Bradi2g52450\_Jer1  
Bradi2g52450\_Luc1

TYEASHDLLREKLGDIDLELIDNCFGMPLSIIILLAGALCDAPTHEEFHKLISAAHVAQG  
TYEASHDLLREKLGDIDLELIDNCFGMPLSIIILLAGALCDAPTHEEFHKLISAAHVAQG  
TYEASHDLLREKLGDIDLELIDNCFGMPLSIIILLAGALCDAPTHEEFHKLISAAHVAQG  
TYEASHDLLREKLGDIDLELIDNCFGMPLSIIILLAGALCDAPTHEEFHKLISAAHVAQG  
TYEASHDLLREKLGDIDLELIDNCFGMPLSIIILLAGALCDAPTHEEFHKLISAAHVAQG  
\*\*\*\*\*

**RNBS-D part I****RNBS-D part II**

Bradi2g52450\_Bd21  
Bradi2g52450\_Foz1  
Bradi2g52450\_ABR6  
Bradi2g52450\_Jer1  
Bradi2g52450\_Luc1

DFHEADCVGKEIIHVVLVKGHLIHFEDNDHIRMHDVIRETSQLGRDNGYVEQPERYFDNE  
DFHEADCVGKEIIHVVLVKGHLIHFEDNDHIRMHDVIRETSQLGRDNGYVEQPERYFDNE  
DFHEADCVGKEIIHVVLVKGHLIHFEDNDHIRMHDVIRETSQLGRDNGYVEQPERYFDNE  
DFHEADCVGKEIIHVVLVKGHLIHFEDNDHIRMHDVIRETSQLGRDNGYVEQPERYFDNE  
DFHEADCVGKEIIHVVLVKGHLIHFEDNDHIRMHDVIRETSQLGRDNGYVEQPERYFDNE  
\*\*\*\*\*

**MHDV**

Bradi2g52450\_Bd21  
Bradi2g52450\_Foz1  
Bradi2g52450\_ABR6  
Bradi2g52450\_Jer1  
Bradi2g52450\_Luc1

VRFEYLAKGGRISLMNTIKEELRFECIAVLGRRISLMNTIKEELVPSPECFSTSTLLR  
VRFEYLAKGGRISLMNTIKEELRFECIAVLGRRISLMNTIKEELVPSPECFSTSTLLR  
VRFEYLAKGGRISLMNTIKEELRFECIAVLGRRISLMNTIKEELVPSPECFSTSTLLR  
VRFEYLAKGGRISLMNTIKEELRFECIAVLGRRISLMNTIKEELVPSPECFSTSTLLR  
VRFEYLAKGGRISLMNTIKEELRFECIAVLGRRISLMNTIKEELVPSPECFSTSTLLR  
\*\*\*\*\*

Bradi2g52450\_Bd21  
Bradi2g52450\_Foz1  
Bradi2g52450\_ABR6  
Bradi2g52450\_Jer1  
Bradi2g52450\_Luc1

GNRHMRТИSEEIFSRLGMLRVLDLSFTGIAILPNSISYLYFYLRLLLLVGCGHLEKIQHIG  
GNRHMRТИSEEFFSRLGMLRVLDLSFTGIAILPNSISYLYFYLRLLLLVGCGHLEKIQHIG  
GNRHMRТИSEEFFSRLGMLRVLDLSFTGIAILPNSISYLYFYLRLLLLVGCGHLEKIQHIG  
GNRHMRТИSEEFFSRLGMLRVLDLSFTGIAILPNSISYLYFYLRLLLLVGCGHLEKIQHIG  
GNRHMRТИSEEFFSRLGMLRVLDLSFTGIAILPNSISYLYFYLRLLLLVGCGHLEKIQHIG  
\*\*\*\*\*

**LR**

Bradi2g52450\_Bd21  
Bradi2g52450\_Foz1  
Bradi2g52450\_ABR6  
Bradi2g52450\_Jer1  
Bradi2g52450\_Luc1

SLEMLEVNASGCGSLKRVECGSFDMRLLKILDLSRTSIEHPLSLAASMELHQLLLQDC  
SLEMLEVNASGCGSLKRVECGSFDMRLLKILDLSRTSIEHPLSLAASMELHQLLLQDC  
SLEMLEVNASGCGSLKRVECGSFDMRLLKILDLSRTSIEHPLSLAASMELHQLLLQDC  
SLEMLEVNASGCGSLKRVECGSFDMRLLKILDLSRTSIEHPLSLAASMELHQLLLQDC  
SLEMLEVNASGCGSLKRVECGSFDMRLLKILDLSRTSIEHPLSLAASMELHQLLLQDC  
\*\*\*\*\*

**R****LRR**

Bradi2g52450\_Bd21  
Bradi2g52450\_Foz1  
Bradi2g52450\_ABR6  
Bradi2g52450\_Jer1  
Bradi2g52450\_Luc1

PYLESEQTTETNAKFCVTNFIKFPYGVSKSGAVRNQLQELASKDLVDWMAMLWLPSGLTFE  
PYLESEQTTETNAKFCVTNFIKFPYGVSKSGAVRNQLQELASKDLVDWMAMLWLPSGLTFE  
PYLESEQTTETNAKFCVTNFIKFPYGVSKSGAVRNQLQELASKDLVDWMAMLWLPSGLTFE  
PYLESEQTTETNAKFCVTNFIKFPYGVSKSGAVRNQLQELASKDLVDWMAMLWLPSGLTFE  
PYLESEQTTETNAKFCVTNFIKFPYGVSKSGAVRNQLQELASKDLVDWMAMLWLPSGLTFE  
\*\*\*\*\*

**LRR**

Bradi2g52450\_Bd21  
Bradi2g52450\_Foz1  
Bradi2g52450\_ABR6  
Bradi2g52450\_Jer1  
Bradi2g52450\_Luc1

LSDRFGTMVSQDVNQNNKTYIHASHPNFVQSLDKDPLWLNLCLRKFHIVMSPLKYDDQTL  
FSDRFGTMVSQDVNQNNKTYIHASHPNFVQSLDKDPLWLNLCLRKFHIVMSPLKYDDQTL  
FSDRFGTMVSQDVNQNNKTYIHASHPNFVQSLDKDPLWLNLCLRKFHIVMSPLKYDDQTL  
FSDRFGTMVSQDVNQNNKTYIHASHPNFVQSLDKDPLWLNLCLRKFHIVMSPLKYDDQTL  
FSDRFGTMVSQDVNQNNKTYIHASHPNFVQSLDKDPLWLNLCLRKFHIVMSPLKYDDQTL  
\*\*\*\*\*

**Bradi2g52450 (NB-LRR)** (continued from previous page)

Bradi2g52450\_Bd21 DNVLGTVRTKFSSVDTHSGDFDRFLEINCVNMPNGIEGILSHAEILISLKGVTATDQVLNL  
 Bradi2g52450\_Foz1 DNVLGTVRTKFSSVDTHSGDFDRFLEINCVNMPNGIEGILSHAEILISLKGVTATDQVLNL  
 Bradi2g52450\_ABR6 DNVLGTVRTKFSSVDTHSGDFDRFLEINCVNMPNGIEGILSHAEILISLKGVTATDQVLNL  
 Bradi2g52450\_Jer1 DNVLGTVRTKFSSVDTHSGDFDRFLEINCVNMPNGIEGILSHAEILISLKGVTATDQVLNL  
 Bradi2g52450\_Luc1 DNVLGTVRTKFSSVDTHSGDFDRFLEINCVNMPNGIEGILSHAEILISLKGVTATDQVLNL  
 \*\*\*\*\*

Bradi2g52450\_Bd21 NTGRLTAARELWIENCHQLENLFLLVEVHGSHELGTLQNIWISNMDNLYFCLEMKDLTS  
 Bradi2g52450\_Foz1 NTGRLTAARELWIENCHQLENLFLLVEVHGSHELGTLQNIWISNMDNLYFCLEMKDLTS  
 Bradi2g52450\_ABR6 NTGRLTAARELWIENCHQLENLFLLVEVHGSHELGTLQNIWISNMDNLYFCLEMKDLTS  
 Bradi2g52450\_Jer1 NTGRLTAARELWIENCHQLENLFLLVEVHGSHELGTLQNIWISNMDNLYFCLEMKDLTS  
 Bradi2g52450\_Luc1 NTGRLTAARELWIENCHQLENLFLLVEVHGSHELGTLQNIWISNMDNLYFCLEMKDLTS  
 \*\*\*\*\*

Bradi2g52450\_Bd21 LRR  
 FSYLKHVLLDCCPKLNFLFPSSLRMPNLCSSLHIRFCDSLERVFDESVVAEYALPGLQSLQ  
 Bradi2g52450\_Foz1 FSYLKHVLLDCCPKLNFLFPSSLRMPNLCSSLHIRFCDSLERVFDESVVAEYALPGLQSLQ  
 Bradi2g52450\_ABR6 FSYLKHVLLDCCPKLNFLFPSSLRMPNLCSSLHIRFCDSLERVFDESVVAEYALPGLQSLQ  
 Bradi2g52450\_Jer1 FSYLKHVLLDCCPKLNFLFPSSLRMPNLCSSLHIRFCDSLERVFDESVVAEYALPGLQSLQ  
 Bradi2g52450\_Luc1 FSYLKHVLLDCCPKLNFLFPSSLRMPNLCSSLHIRFCDSLERVFDESVVAEYALPGLQSLQ  
 \*\*\*\*\*

Bradi2g52450\_Bd21 LWELPELSCICGGVVLPSLKDLKVRGCAKLKKIPIGVTENNPFFTIVIGEMQWWNNLVWDD  
 Bradi2g52450\_Foz1 LWELPELSCICGGVVLPSLKDLKVRGCAKLKKIPIGVTENNPFFTIVIGETQWWNNLVWDD  
 Bradi2g52450\_ABR6 LWELPELSCICGGVVLPSLKDLKVRGCAKLKKIPIGVTENNPFFTIVIGETQWWNNLVWDD  
 Bradi2g52450\_Jer1 LWELPELSCICGGVVLPSLKDLKVRGCAKLKKIPIGVTENNPFFTIVIGETQWWNNLVWDD  
 Bradi2g52450\_Luc1 LWELPELSCICGGVVLPSLKDLKVRGCAKLKKIPIGVTENNPFFTIVIGETQWWNNLVWDD  
 \*\*\*\*\*

Bradi2g52450\_Bd21 EDIKRWMLFRNWGPILVPHFATEG  
 Bradi2g52450\_Foz1 EDIKRWMLFRNWGPILVPHFATEG  
 Bradi2g52450\_ABR6 EDIKRWMLFRNWGPILVPHFATEG  
 Bradi2g52450\_Jer1 EDIKRWMLFRNWGPILVPHFATEG  
 Bradi2g52450\_Luc1 EDIKRWMLFRNWGPILVPHFATEG  
 \*\*\*\*\*

## Supplemental tables

**Table S1.** Summary of the environmental conditions tested.

ENV <sup>a</sup>	N <sup>b</sup>	Time <sup>c</sup>	Location	Light conditions	Temperature (day/night)	Vern. <sup>d</sup>
1	3	April - July 2012	Aberystwyth, UK	natural; supplemented for 20h	22°C/20°C	no
2	3	April - July 2012	Aberystwyth, UK	natural; supplemented for 20h	22°C/20°C	yes
3	5	May - July 2014	Norwich, UK	natural	natural	no
4	5	September - November 2014	Norwich, UK	natural; supplemented for 16h (400w HPS)	minimum 18°C/11.5°C	no
5	5	March - May 2015	Norwich, UK	natural	natural	no

<sup>a</sup>Environment

<sup>b</sup>Number of F<sub>4:5</sub> individuals tested

<sup>c</sup>Time period of experiment

<sup>d</sup>Vernalisation

**Table S2.** Significant QTLs from interval mapping of binary classification of flowering time phenotypes in the ABR6 x Bd21 F<sub>4:5</sub> families.

ENV <sup>a</sup>	Chr <sup>b</sup>	cM	EWT <sup>c</sup>	LOD
1	Bd1	298.0	3.84	13.1
5	Bd3	302.0	3.64	5.08

<sup>a</sup>Environment (see Table S1)

<sup>b</sup>Chromosome

<sup>c</sup>Experiment-wide permutation threshold

**Table S3.** Significant QTLs from interval mapping using a non-parametric model for flowering time phenotypes in the ABR6 x Bd21 F<sub>4:5</sub> families (NP).

ENV <sup>a</sup>	Chr <sup>b</sup>	cM	EWT <sup>c</sup>	LOD
1	Bd1	298.0	3.43	11.60
2	Bd1	298.0	3.42	3.76
3	Bd1	298.0	3.30	4.61
4	Bd2	293.0	3.36	3.64
4	Bd3	294.7	3.36	4.75
4	Bd4	90.1	3.36	4.01
5	Bd1	298.0	3.29	6.22
5	Bd3	295.0	3.29	5.08

<sup>a</sup>Environment (see Table S1)

<sup>b</sup>Chromosome

<sup>c</sup>Experiment-wide permutation threshold

**Table S4.** Significant QTLs from composite interval mapping of transformed flowering time phenotypes in the ABR6 x Bd21 F<sub>4:5</sub> families (T1).

ENV <sup>a</sup>	Chr <sup>b</sup>	cM	EWT <sup>c</sup>	LOD	AEE <sup>d</sup>	PVE <sup>e</sup>
2	Bd1	297.6	3.14	7.50	0.95	19.2%
2	Bd2	409.0	3.14	3.35	0.56	6.6%
2	Bd3	93.2	3.14	5.61	0.82	13.5%
4	Bd3	60.8	3.20	5.12	4.13	16.9%
5	Bd1	297.6	3.35	5.52	8.88	48.0%

<sup>a</sup>Environment (see Table S1)

<sup>b</sup>Chromosome

<sup>c</sup>Experiment-wide permutation threshold

<sup>d</sup>Additive effect estimate for transformed phenotypes

<sup>e</sup>Percent of phenotypic variance explained

**Table S5.** Significant QTLs from composite interval mapping of transformed flowering time phenotypes in the ABR6 x Bd21 F<sub>4:5</sub> families (T2).

ENV <sup>a</sup>	Chr <sup>b</sup>	cM	EWT <sup>c</sup>	LOD	AEE <sup>d</sup>	PVE <sup>e</sup>
1	Bd1	297.6	2.91	9.62	6.08	28.9%
1	Bd1	465.2	2.91	3.28	4.01	9.7%
1	Bd3	91.2	2.91	3.43	3.58	10.0%
3	Bd1	297.6	3.20	7.82	8.54	30.3%
3	Bd3	91.2	3.20	5.47	7.21	20.3%
4	Bd1	297.6	3.24	3.40	5.69	15.5%
4	Bd3	294.6	3.24	3.47	4.97	12.8%
5	Bd1	297.6	3.24	9.08	9.33	40.0%
5	Bd2	338.3	3.24	3.75	-4.62	9.8%
5	Bd3	294.6	3.24	5.15	5.10	12.5%

<sup>a</sup>Environment (see Table S1)

<sup>b</sup>Chromosome

<sup>c</sup>Experiment-wide permutation threshold

<sup>d</sup>Additive effect estimate for transformed phenotypes

<sup>e</sup>Percent of phenotypic variance explained

**Table S6.** Summary of the structural variation between Bd21 and ABR6 for the flowering regulators Bradi1g48830 (*FT*), Bradi3g10010 (*VRN2*), and Bradi1g08340 (*VRN1*).

Gene ID	Name	Position <sup>a</sup>	Polymorphism <sup>b</sup>	Location	Notes
Bradi1g48830	<i>FT</i>	-1986	SNP (A to G)	promoter	
		-1184	SNP (T to G)	promoter	
		-1165	1bp deletion	promoter	
		-1080	2bp deletion	promoter	
		-590	33bp deletion	promoter	
		1242	2bp insertion	3' UTR	
		1257	4bp insertion	3' UTR	
		1616	SNP (A to C)	3' UTR	
		+455	SNP (G to A)	terminator	
		+709	SNP (A to C)	terminator	
		+901	1bp deletion	terminator	
		+1837	1bp insertion	terminator	
		+1905	1bp insertion	terminator	
		+1915	SNP (A to G)	terminator	
		+1995	2bp deletion	terminator	
Bradi3g10010	<i>VRN2</i>	-1949	SNP (A to G)	promoter	
		-1918	SNP (A to T)	promoter	
		-1917	SNP (A to T)	promoter	
		-1916	SNP (A to T)	promoter	
		-1915	SNP (A to C)	promoter	
		-1914	SNP (G to C)	promoter	
		-1912	SNP (A to G)	promoter	
		-1904	SNP (G to C)	promoter	
		-1900	SNP (C to T)	promoter	
		-1896	1bp insertion	promoter	
		-1881	SNP (A to G)	promoter	
		-1864	SNP (C to G)	promoter	
		-1862	SNP (G to T)	promoter	
		-1861	SNP (C to A)	promoter	
		-1851	SNP (T to C)	promoter	
		-1831	SNP (A to G)	promoter	
		-1758	SNP (T to G)	promoter	
		-1718	SNP (G to A)	promoter	
		-1511	SNP (G to T)	promoter	
		-1425	84bp deletion	promoter	
		-1405	SNP (G to C)	promoter	
		-1128	SNP (T to C)	promoter	
		-1123	SNP (A to T)	promoter	
		-1026	SNP (C to G)	promoter	
		-866	SNP (T to C)	promoter	
		-754	SNP (G to C)	promoter	
		-746	SNP (C to G)	promoter	
		-616	SNP (T to C)	promoter	
		-489	1bp deletion	promoter	
		-409	SNP (A to G)	promoter	
		-232	SNP (T to C)	promoter	
		-196	SNP (C to T)	promoter	
		573	SNP (C to G)	intron	
		594	SNP (T to C)	intron	
		692	37bp deletion	intron	
		736	SNP (G to A)	intron	
		745	SNP (C to T)	intron	
		774	22bp insertion	intron	
		825	SNP (C to T)	intron	
		903	1bp insertion	intron	
		952	SNP (C to T)	intron	
		958	SNP (C to T)	intron	

	1263	SNP (A to G)	intron	
	1354	1bp insertion	intron	
	1446	SNP (A to G)	intron	
	1463	SNP (A to G)	intron	
	1616	SNP (C to T)	intron	
	1733	SNP (C to G)	exon2 CDS	non-synonymous (M127I)
	1922	SNP (T to C)	exon2 CDS	synonymous (P190P)
	2051	SNP (T to C)	exon2 3' UTR	
	2064	SNP (A to G)	exon2 3' UTR	
	2166	SNP (A to G)	exon2 3' UTR	
	2183	SNP (T to C)	exon2 3' UTR	
	+62	SNP (G to A)	terminator	
	+63	SNP (A to C)	terminator	
	+239	SNP (T to C)	terminator	
	+251	SNP (G to A)	terminator	
	+683	SNP (T to A)	terminator	
	+807	SNP (A to C)	terminator	
	+1022	1bp insertion	terminator	
	+1030	SNP (G to A)	terminator	
	+1062	SNP (A to C)	terminator	
	+1141	SNP (T to G)	terminator	
	+1199	SNP (C to A)	terminator	
	+1315	SNP (G to C)	terminator	
	+1371	SNP (G to C)	terminator	
	+1398	SNP (T to G)	terminator	
	+1445	SNP (G to A)	terminator	
	+1846	1bp insertion	terminator	
	+1964	1bp deletion	terminator	
Bradi1g08340	<i>VRNI</i>	-1908	1bp insertion	promoter
		-816	SNP (C to G)	promoter
		-368	SNP (G to A)	promoter
		480	SNP (G to C)	intron
		1020	3bp insertion	intron
		1259	SNP (G to T)	intron
		4273	SNP (A to C)	intron
		4574	SNP (C to T)	intron
		5287	SNP (A to G)	intron
		7159	SNP (C to T)	intron
		7757	SNP (C to G)	intron
		8265	SNP (G to T)	intron

<sup>a</sup>Based on Bd21 reference sequence (Version 3)

<sup>b</sup>ABR6 relative to Bd21 reference sequence (Version 3)

**Table S7.** Significant QTLs from composite interval mapping of individual replicates of leaf browning and percent colonisation phenotypes for wheat and barley stripe rust isolates in the ABR6 x Bd21 F<sub>4:5</sub> families.

Isolate <sup>a</sup>	Rep <sup>b</sup>	Trait <sup>c</sup>	Locus	Chr <sup>d</sup>	cM	EWT <sup>e</sup>	LOD	AEE <sup>f</sup>	PVE <sup>g</sup>
<i>Pst</i> 08/21	1	Browning	<i>Yrr3</i>	Bd2	327.95	2.92	4.87	-0.13	13.8
<i>Pst</i> 08/21	1	Browning	<i>Yrr1</i>	Bd4	146.75	2.92	6.35	-0.12	13.1
<i>Pst</i> 08/21	1	pCOL	-	Bd1	124.26	2.86	3.48	-0.03	4.5
<i>Pst</i> 08/21	1	pCOL	<i>Yrr3</i>	Bd2	327.95	2.86	8.62	-0.05	18.2
<i>Pst</i> 08/21	1	pCOL	<i>Yrr1</i>	Bd4	133.63	2.86	16.52	-0.07	32.5
<i>Pst</i> 08/21	2	Browning	<i>Yrr3</i>	Bd2	327.95	2.67	5.86	-0.19	17.9
<i>Pst</i> 08/21	2	Browning	<i>Yrr1</i>	Bd4	137.66	2.67	4.85	-0.16	11.4
<i>Pst</i> 08/21	2	pCOL	<i>Yrr3</i>	Bd2	327.95	2.83	7.74	-0.05	18.8
<i>Pst</i> 08/21	2	pCOL	<i>Yrr1</i>	Bd4	137	2.83	11.28	-0.06	26.5
<i>Pst</i> 08/501	1	Browning	<i>Yrr3</i>	Bd2	327.95	3.03	8.12	-0.33	18.2
<i>Pst</i> 08/501	1	Browning	<i>Yrr1</i>	Bd4	135	3.03	9.71	-0.37	23.5
<i>Pst</i> 08/501	1	pCOL	<i>Yrr3</i>	Bd2	327.95	2.74	6.89	-0.03	17.1
<i>Pst</i> 08/501	1	pCOL	<i>Yrr2</i>	Bd4	89.15	2.74	5.85	-0.03	12.1
<i>Pst</i> 08/501	1	pCOL	<i>Yrr1</i>	Bd4	137	2.74	5.21	-0.02	9.9
<i>Pst</i> 08/501	2	Browning	<i>Yrr3</i>	Bd2	327.95	2.69	4.52	-0.12	13.9
<i>Pst</i> 08/501	2	Browning	<i>Yrr1</i>	Bd4	135	2.69	6.22	-0.13	17.7
<i>Pst</i> 08/501	2	pCOL	<i>Yrr3</i>	Bd2	327.95	3.06	6.94	-0.03	18.0
<i>Pst</i> 08/501	2	pCOL	<i>Yrr2</i>	Bd4	94.12	3.06	3.64	-0.02	11.7
<i>Pst</i> 08/501	2	pCOL	<i>Yrr1</i>	Bd4	135	3.06	7.13	-0.02	15.4
<i>Pst</i> 11/08	1	Browning	<i>Yrr3</i>	Bd2	328.92	2.66	5.65	-0.07	14.4
<i>Pst</i> 11/08	1	Browning	<i>Yrr1</i>	Bd4	137	2.66	5.79	-0.07	13.9
<i>Pst</i> 11/08	1	pCOL	<i>Yrr3</i>	Bd2	327.95	3.15	11.06	-0.05	18.9
<i>Pst</i> 11/08	1	pCOL	<i>Yrr2</i>	Bd4	133.63	3.15	15.15	-0.07	33.8
<i>Pst</i> 11/08	1	pCOL	<i>Yrr1</i>	Bd5	70.33	3.15	3.17	-0.03	6.3
<i>Pst</i> 11/08	2	Browning	<i>Yrr3</i>	Bd2	327.95	2.59	5.07	-0.14	13.1
<i>Pst</i> 11/08	2	Browning	<i>Yrr1</i>	Bd4	144.75	2.59	6.15	-0.14	14.2
<i>Pst</i> 11/08	2	pCOL	<i>Yrr3</i>	Bd2	327.95	2.77	6.88	-0.05	17.3
<i>Pst</i> 11/08	2	pCOL	<i>Yrr1</i>	Bd4	140.78	2.77	6.47	-0.04	12.8
<i>Psh</i> B01/2	1	Browning	-	Bd2	174.41	3.01	3.07	0.17	13.7
<i>Psh</i> B01/2	1	Browning	<i>Yrr3</i>	Bd2	321.74	3.01	3.18	-0.14	9.4
<i>Psh</i> B01/2	1	pCOL	<i>Yrr3</i>	Bd2	328.92	2.99	4.10	-0.04	18.7
<i>Psh</i> B01/2	2	Browning	<i>Yrr3</i>	Bd2	327.95	3.15	10.64	-0.36	28.9
<i>Psh</i> B01/2	2	pCOL	<i>Yrr3</i>	Bd2	328.92	3.15	11.35	-0.10	26.1
<i>Psh</i> B01/2	2	pCOL	-	Bd3	330.64	3.15	5.99	-0.06	12.4

<sup>a</sup>*Puccinia striiformis* isolate (*Pst* = f. sp. *tritici*, *Psh* = f. sp. *hordei*)

<sup>b</sup>Replicate

<sup>c</sup>Browning = leaf browning; pCOL = percent colonisation

<sup>d</sup>Chromosome

<sup>e</sup>Experiment-wide permutation threshold

<sup>f</sup>Additive effect estimate

<sup>g</sup>Percent of variation explained

**Table S8.** Support intervals and peak markers (cM) detected for *Yrr1* and *Yrr3*.

Locus	Population	Isolate <sup>a</sup>	Phenotype <sup>b</sup>	dpi <sup>c</sup>	2-LOD SI <sup>d</sup>	1-LOD SI	Peak	1-LOD SI	2-LOD SI
<i>Yrr1</i>	ABR6xBd21	<i>Pst</i> 08/21	Browning	14	102.0	116.1	135.0	146.8	157.1
			pCOL	14	125.7	129.7	135.0	137.7	140.8
	ABR6xBd21	<i>Pst</i> 08/501	Browning	14	108.0	127.7	135.0	148.7	148.7
			pCOL	14	121.7	129.7	135.0	137.7	140.8
	ABR6xBd21	<i>Pst</i> 11/08	Browning	14	102.0	127.7	135.0	148.7	157.1
			pCOL	14	119.7	127.7	135.0	140.8	144.8
	ABR6xBd21	<i>Pst</i> 08/21	Browning	14	312.2	317.4	328.0	328.9	342.0
			pCOL	14	320.5	324.2	328.0	340.0	344.1
<i>Yrr3</i>	ABR6xBd21	<i>Pst</i> 08/501	Browning	14	324.2	324.2	328.0	330.6	340.0
			pCOL	14	317.4	324.2	328.0	340.0	340.0
	ABR6xBd21	<i>Pst</i> 11/08	Browning	14	314.6	320.5	328.0	330.6	348.1
			pCOL	14	320.5	324.2	328.0	340.0	342.0
	ABR6xBd21	<i>Psh</i> B01/2	Browning	14	321.7	324.2	326.2	328.9	370.7
			pCOL	14	324.2	326.2	328.9	330.6	330.6
	Luc1xJer1	<i>Pst</i> 08/21	Browning	14	256.6	261.3	263.3	265.3	267.3
			Browning	23	254.6	254.6	258.6	265.3	267.3
			pCOL	23	256.6	261.3	263.3	267.3	267.3
			Browning <sup>f</sup>	14	254.6	254.6	258.6	265.3	267.3

<sup>a</sup>*Puccinia striiformis* isolate (*Pst* = f. sp. *tritici*, *Psh* = f. sp. *hordei*)<sup>b</sup>Browning = leaf browning; pCOL = percent colonisation<sup>c</sup>Days post inoculation<sup>d</sup>Support interval (cM)<sup>f</sup>F<sub>2:3</sub> derived families phenotyped

**Table S9.** Canonical resistance genes shown in Figure 15 and their association with the major effect loci *Yrr1* and *Yrr3*.

Locus	Gene ID	Preliminary annotation <sup>a</sup>	2-LOD SI <sup>b</sup>	1-LOD SI
<i>Yrr1</i>	Bradi4g21842	NB-LRR	X	
<i>Yrr1</i>	Bradi4g21890	NB-LRR	X	
<i>Yrr1</i>	Bradi4g21939	NB-LRR	X	
<i>Yrr1</i>	Bradi4g21950	NB-LRR	X	
<i>Yrr1</i>	Bradi4g22017	NB-LRR	X	
<i>Yrr1</i>	Bradi4g22740	NB-LRR	X	
<i>Yrr1</i>	Bradi4g23880	NB-LRR	X	X
<i>Yrr1</i>	Bradi4g24852	NB-LRR		
<i>Yrr1</i>	Bradi4g24857	NB-LRR		
<i>Yrr1</i>	Bradi4g24862	NB-LRR		
<i>Yrr1</i>	Bradi4g24887	NB-LRR		
<i>Yrr1</i>	Bradi4g24914	NB-LRR		
<i>Yrr1</i>	Bradi4g24930	NB-LRR		
<i>Yrr1</i>	Bradi4g25041	NB-LRR		
<i>Yrr1</i>	Bradi4g25780	NB-LRR		
<i>Yrr1</i>	Bradi4g25810	NB-LRR		
<i>Yrr3</i>	Bradi2g50590	TIR-NB		
<i>Yrr3</i>	Bradi2g51807	NB-LRR	X	
<i>Yrr3</i>	Bradi2g52150	NB-LRR	X	X
<i>Yrr3</i>	Bradi2g52430	NB	X	X
<i>Yrr3</i>	Bradi2g52437	NB-LRR	X	X
<i>Yrr3</i>	Bradi2g52450	NB-LRR	X	X
<i>Yrr3</i>	Bradi2g52840	NB-LRR	X	X
<i>Yrr3</i>	Bradi2g57534	NB-LRR		

<sup>a</sup>Phytozome annotation of the Bd21 reference (Version 3)

<sup>b</sup>Presence within support interval of respective locus

**Table S10.** Results of marker regression analyses shown in Figures 19 and 20.

Figure	Population	Line	N <sup>a</sup>	p-value	Symbol <sup>b</sup>
Figure 19	ABR6xBd21	3	16	0.750	ns
		45	16	0.120	ns
		70	16	0.760	ns
		77	16	0.000	***
		87	16	0.360	ns
		105	16	0.001	**
	Luc1xJer1	10	32	0.541	ns
		109	32	0.000	***
		167	32	0.000	***
		170	32	0.774	ns
Figure 20	Luc1xJer1	184	32	0.000	***
		188	32	0.000	***
		JB_0347-C7	32	0.003	**
		JB_0332-C3	32	0.647	ns
		JB_0346-C2	32	0.727	ns
		JB_0346-E7	32	0.786	ns
		JB_0347-A1	32	0.326	ns
		JB_0326-G12	32	0.001	**
		JB_0341-C2	32	0.021	*

<sup>a</sup>Number of progeny tested<sup>b</sup>Statistical significance of cosegregation: \*\*\* = p-value under 0.001, \*\* = p-value under 0.01, \* = p-value under 0.05, ns = not significant (p-value  $\geq$  0.05)

**Table S11.** Average phenotypic scores for homozygous recombinant progeny identified from the 23 recombinant F<sub>2</sub> lines.

Line	Yrr3 genotype	N <sup>a</sup>	14 dpi <sup>b</sup>	STDER <sup>c</sup>	21 dpi	STDER
Luc1	-	15	2.5	0.13	-	-
JB_0329-D1	Luc1	10	1.2	0.21	2.1	0.33
JB_0332-C3	Luc1	5	0.9	0.10	1.5	0.39
JB_0333-A4	Luc1	10	1.6	0.23	-	-
JB_0333-H8	Luc1	8	1.2	0.19	2.5	0.30
JB_0337-F6	Luc1	9	1.9	0.16	-	-
JB_0338-H10	Luc1	10	2.1	0.27	-	-
JB_0340-A6	Luc1	5	1.6	0.33	-	-
JB_0341-C2	Luc1	5	2.5	0.45	2.7	0.27
JB_0346-C2	Luc1	6	1.9	0.08	-	-
JB_0347-A2	Luc1	7	1.9	0.24	-	-
JB_0326-E5	Jer1	9	0.2	0.08	-	-
JB_0326-F9	Jer1	8	0.0	0.00	-	-
JB_0326-G12	Jer1	6	0.3	0.11	0.5	0.00
JB_0333-E2	Jer1	12	0.8	0.21	-	-
JB_0335-H5	Jer1	9	0.1	0.06	-	-
JB_0337-D1	Jer1	6	0.3	0.11	-	-
JB_0339-C12	Jer1	8	0.4	0.13	-	-
JB_0341-C4	Jer1	5	0.1	0.10	-	-
JB_0345-A8	Jer1	7	0.4	0.07	-	-
JB_0346-C1	Jer1	9	0.6	0.18	-	-
JB_0346-E7	Jer1	6	0.2	0.11	-	-
JB_0347-A1	Jer1	5	0.2	0.12	-	-
JB_0347-C7	Jer1	4	0.1	0.13	0.5	0.20
Jer1	-	16	0.4	0.08	-	-

<sup>a</sup>Number of individuals

<sup>b</sup>days post inoculation

<sup>c</sup>standard error

**Table S12.** Gene identifiers for the top hits of the *B. distachyon* (*Bd*) candidate genes in rice (*Os*), sorghum (*Sb*), and maize (*Zm*). Order and orientation of top hits was visualised in Phytozome (<https://phytozome.jgi.doe.gov>).

<i>Bd</i> gene	<i>Os</i> gene	<i>Sb</i> gene	<i>Zm</i> gene
Bradi2g52430	LOC_Os01g58510	Sobic.003G325100	GRMZM2G178704
Bradi2g52437	LOC_Os01g58520	Sobic.003G325200	GRMZM2G103135
Bradi2g52450	LOC_Os01g58530	Sobic.003G325300	GRMZM2G047652

## Unpublished primer sequences from Chapter 3 and Chapter 4

Primers within Bradi2g52437 used to isolate ABR6 BACs:

Forward: Bradi2g52437\_p2\_ABR6\_f AGTGCACCAACGGAAGCA  
 Reverse: Bradi2g52437\_p2\_ABR6\_r AGGAAAATCCTGGAGTGCTCC

Primers used for the initial amplification of the candidate region from BAC 4932-1D.

Fragment	F/R <sup>a</sup>	Primer name	Sequence
37-1	F	Bradi2g52437_BAC_seq_frag1_p3f	CTGCTAGTGAATCAATCCGGT
	R	Bradi2g52437_BAC_seq_frag1_p3r	CAGCATGCTCGTCCACATAG
37-2	F	Bradi2g52437_BAC_seq_frag2_p3f	TCCACCTATGCACGAATTCT
	R	Bradi2g52437_BAC_seq_frag2_p3r	TAACCTTGCACACTTCAGCA
37-3	F	Bradi2g52437_BAC_seq_frag3_p3f	GGATGGAGTGTGGATGAGCT
	R	Bradi2g52437_BAC_seq_frag3_p3r	GAACCTGCGGTAACTCTCGG
50-1	F	Bradi2g52450_BAC_seq_frag1_p3f	TGTGTTCCCTGAGCAATGCA
	R	Bradi2g52450_BAC_seq_frag1_p3r	ACCCCAACTTGTTCAGTC
50-2	F	Bradi2g52450_BAC_seq_frag2_p2f	GCAGCAATCAAGGAGCACAT
	R	Bradi2g52450_BAC_seq_frag2_p2r	GATTGCAGGCCGACAGTATA
50-3	F	Bradi2g52450_BAC_seq_frag3_p3f	CTCCTCTCCACCTCTAGCAC
	R	Bradi2g52450_BAC_seq_frag3_p3r	CTCGACATCCTCCCTCTGCA

<sup>a</sup>forward/reverse

Primers used for confirming cloned fragments by colony PCR.

Fragment	F/R <sup>a</sup>	Primer name	Sequence
37-1	F	M13_forward	GTAAAACGACGCCAGT
	R	Bradi2g52437_p2_ABR6_c9_r	GTTCTGTCCTGCCACGCT
37-2	F	Bradi2g52437_frag2_c5_f	TGTCACACACTCGCCGTG
	R	Bradi2g52437_frag2_c5_r	ATAATGCAGGAGCCGCGG
37-3	F	Bradi2g52437_frag3_c5_f	GTCCGCCTGGTGGAAAGA
	R	Bradi2g52437_frag3_c5_r	CATTGCCTTCCGGATGC
50-1	F	Bradi2g52450_bit3_p2_ABR6_c2_f	CTTGGGAGGTCAAGCCAGC
	R	Bradi2g52450_bit3_p2_ABR6_c2_r	TTGGCCTCCGCAGACAAG
50-2	F	Bradi2g52450_frag2_c5_f	ATCACACAGTGCCTCCGGC
	R	Bradi2g52450_frag2_c5_r	GGGGCCATGGCATCCTAC
50-3	F	Bradi2g52450_bit1_p2_ABR6_c1_f	CGGTCGGAGGGAGTAGCT
	R	Bradi2g52450_bit1_p2_ABR6_c1_r	TAAGCCGCCGACAACTCC

<sup>a</sup>forward/reverse

Primers used for adding overhangs to cloned fragments and vector backbones for Gibson assembly of the final constructs. Top to bottom: Bradi2g52430, Bradi2g52450, and Bradi2g52437 assemblies.

Template <sup>a</sup>	F/R <sup>b</sup>	Primer name	Sequence
37-2	F	pWBVec8L_37-2_p1f	CTAGCTGATAGTGAACCTTAGCGGCTCTGCATTATTGTCA
	R	37-3_37-2_p1f	TGGCTCAGGAGATCAGTGGAAATGAATGAATGGCTG
37-3	F	37-3_37-2_p1r	CAGC CATT CATT CATT CATT CACT GAT CTC TGAG CCA
	R	37-3_pWBVec8R_p2r	GAAACCATTATTGCGCGTCTGTGCCGATGTTCAGCCAA
pWBVec8	F	37-3_pWBVec8R_p2f	TTGGCTGAACATCCGGCACAGAACGCGCAATAATGGTTT
	R	pWBVec8L_37-2_p1r	TGACAAATAATGCAGGAGCCGCTAAGGTCACTATCAGCTAG
50-1	F	pBRACT202L_50-1_p1f	TAAGCTTGATATCGAATTCCACTTGCCGCCGTAACATCTT
	R	50-1_50-2_p1r	GTCGACACGCATTCCGGTGATTTGATAGGTTCTGGAGA
50-2	F	50-1_50-2_p1f	TCTCCAGAAACCTATCAAATCACCGGAATGCGTGTGAC
	R	50-2_50-3_p1r	GATTGCAGGCCGACAGTATATAGATATAATTAAACAA
50-3	F	50-2_50-3_p1f	TTGTA AAA ATTATATATCTATATACTGCGCCTGCAATC
	R	50-3_pBRACT202R_p1r	CGCTCTAGAACTAGTGGATCCAGATCGGCTGCACTGACA
pBract202	F	50-3_pBRACT202R_p1f	TGTCAGTGCAGCCGATCTGGGATCCACTAGTTCTAGAGCG
	R	pBRACT202L_50-1_p1r	AAGATGTTACGGCGCAAGTGGAAATTGATATCAAGCTTA
37-3	F	pBRACT202L_37-3_p2f	TAAGCTTGATATCGAATTCCAGATCGGACGACAGTCTAT
	R	37-2_37-1_p2r	GGATGGAGTGTGGATGAGCTGCGACACCCAGGAAACCGAA
37-2	F	37-2_37-1_p2f	TTCGGTTCCCTGGGTGTCGAGCTCATCCACACTCCATCC
	R	37-3_37-2_p2r	ACTACACGTACGCATGCCATTATACTGTACTTTCAATCT
37-1	F	37-3_37-2_p2f	AGATTGAAAGTACAAGTATAATGGCATGCGTACGTGTAGT
	R	37-1_pBRACT202R_p2r	CGCTCTAGAACTAGTGGATCAGAGTGGAGATTGACCCCTC
pBract202	F	37-1_pBRACT202R_p2f	GAGGGTCAAATCTCCACTCTGATCCACTAGTTCTAGAGCG
	R	pBRACT202L_37-3_p2r	ATAGACGTGTCGTCGATCTGGAATTGATATCAAGCTTA

<sup>a</sup>Cloned fragment or vector backbone

<sup>b</sup>forward/reverse

Primers used for confirming assembled and cloned constructs by colony PCR.

Construct	F/R <sup>a</sup>	Primer name	Sequence
Bradi2g52430/			
Bradi2g52437	F	Bradi2g52437_frag2_c9_p1f	GCGTTGCTTCCCTGGTGTG
	R	Bradi2g52437_frag3_c2_p1r	CGGAGTGGTGGTCGTAC
Bradi2g52450	F	Bradi2g52450_frag1_c5_p1f	TCCACCACTGCGTTCCC
	R	Bradi2g52450_frag2_c2_p1r	GGCTCGCTGGAGATGCTT

<sup>a</sup>forward/reverse

Primers used to confirm developed constructs by Sanger sequencing.

Primer Name	Forward	Reverse
Bradi2g52437_BAC_seq_frag1_c1_p1	TAGGAACGCCGCTTGCCAA	GGGGCGTTGCGAGACATCT
Bradi2g52437_BAC_seq_frag1_c2_p1	GGCAGCGGATCTTGATCCA	TATAGCAACGCCGGCGAG
Bradi2g52437_BAC_seq_frag1_c3_p1	GTGGTAGATCCGGCTCG	AACGCTCCGTCTACACGC
Bradi2g52437_BAC_seq_frag1_c4_p1	GCGTGTAGACGGAGCGTT	GTGGCTGTACACCCCCAC
Bradi2g52437_BAC_seq_frag1_c5_p1	TGCAGAAATCTCTGCCCC	ACGACTCACCTGCGTGG
Bradi2g52437_BAC_seq_frag1_c6_p1	AGATCCGGTTCAAGGCAC	TGACTGGCAGAGGAGTGA
Bradi2g52437_BAC_seq_frag1_c7_p1	TCACTCCTCTGGCCAGTCA	TGGCATGCGTACGTGTAGT
Bradi2g52437_BAC_seq_frag1_c8_p1	TCCACCTATGCACGAAATTCT	GCGCAGGGCAAACACTCTA
Bradi2g52437_BAC_seq_frag2_c1_p1	CCTTGGAACCCAAATTGCC	CCAGCATGCTCGTCCACA
Bradi2g52437_BAC_seq_frag2_c2_p1	ACTACACGTACGCATGCCA	TCGGAGAGAAAAGGCAGCAG
Bradi2g52437_BAC_seq_frag2_c3_p1	TAGAGTTTGGCCCGCGC	TCCCTCCGTCCCCGTAACCA
Bradi2g52437_BAC_seq_frag2_c4_p1	GCAAAGCACGTGACGAA	AGCCACCATGTTCGTCCA
Bradi2g52437_BAC_seq_frag2_c5_p1	TGTCAACACCTCGCGT	ATAATGCAGGAGCCGCGG
Bradi2g52437_BAC_seq_frag2_c6_p1	CCGGCGCTCTGCATTAT	CCACCGACCTAGCTGCAG
Bradi2g52437_BAC_seq_frag2_c7_p1	CACCTTGGATTGCCGT	GTTGGCCCGCTCTTTCT
Bradi2g52437_BAC_seq_frag2_c8_p1	GGGCATGCCAAGGGAAAT	GGTTTCTGGGTGTCGCA
Bradi2g52437_BAC_seq_frag2_c9_p1	GGGTTGCTTCCCTGGTGTG	GTTCTGCTCTGCCACGCT

Bradi2g52437_BAC_seq_frag3_c1_p1	AGAAAGGAGCGGGCCAAC	GTTCTGTCCTGCCACGCT
Bradi2g52437_BAC_seq_frag3_c2_p1	AGCGTGGCAGGACAGAAC	CGGAGTGGTGGTCGTCAC
Bradi2g52437_BAC_seq_frag3_c3_p1	CTCCCTGTCGGCCAACTG	CCACCTCTGGCCTGAGC
Bradi2g52437_BAC_seq_frag3_c4_p1	CCCCGAACGCCCTGGATT	TTACCGTGAATCCCGCA
Bradi2g52437_BAC_seq_frag3_c5_p1	GTCGGCGTTGGTGGAAAGA	CATTGCGCTTCCGGATGC
Bradi2g52437_BAC_seq_frag3_c6_p1	TGGGAAATCCCGTGTCTT	CGTCGTCACCATGCCACT
Bradi2g52437_BAC_seq_frag3_c7_p1	GGACATGGCGCTCAAGT	TGGAACCTTGCAAGCGG
Bradi2g52437_BAC_seq_frag3_c8_p1	GCTGTGTCACGCTGGTCT	GCCCTGCTGATGCTGACA
Bradi2g52450_BAC_seq_frag1_c1_p1	CGGTCGGAGGGAGTAGCT	TAAGCCGCCGACAACCTCC
Bradi2g52450_BAC_seq_frag1_c2_p1	GGAGTGTGCGGCGCTTA	GCAAACCATCAGCGCTGG
Bradi2g52450_BAC_seq_frag1_c3_p1	AGGCAGCTTCGGTTGTTCT	ACGTGAGTCATATGCCACAA
Bradi2g52450_BAC_seq_frag1_c4_p1	GTGTCAGATGAGATCAGGGGT	GCTGCATCTGTGGAGGGG
Bradi2g52450_BAC_seq_frag1_c5_p1	TCCACCACTGCGTTTCCC	TCCGTCGACACGCATTCC
Bradi2g52450_BAC_seq_frag1_c6_p1	TGTGCCAGGTTCTGTGTGA	GCTGCCTCCATGGAGCCTT
Bradi2g52450_BAC_seq_frag2_c1_p1	TCCACCACTGCGTTTCCC	TCCGTCGACACGCATTCC
Bradi2g52450_BAC_seq_frag2_c2_p1	CACCGGAATGCGTGTGA	GGCTCGCTGGAGATGCTT
Bradi2g52450_BAC_seq_frag2_c3_p1	GAGCCACAGCCTGATGCA	TCACCCACAATGACCCGCC
Bradi2g52450_BAC_seq_frag2_c4_p1	TCTTCGCCCAACTTGGC	AACTGCGAGGGCACTGTC
Bradi2g52450_BAC_seq_frag2_c5_p1	ATCACACAGTGTCCGGC	GGGCCATGGCATTCTAC
Bradi2g52450_BAC_seq_frag2_c6_p1	ACTTCGCCCTCTGGACGC	GCCCGAGAGACCGAATCG
Bradi2g52450_BAC_seq_frag2_c7_p1	CGATTGCGTCTCTCGGGC	TTATTGGGTGGGCACGC
Bradi2g52450_BAC_seq_frag3_c1_p1	CGATTGCGTCTCTCGGGC	TTATTGGGTGGGCACGC
Bradi2g52450_BAC_seq_frag3_c2_p1	CTTGGGAGGTCAAGCAGC	TTGGCCTCCGCAAGACAAG
Bradi2g52450_BAC_seq_frag3_c3_p1	CTTGTCTGGGAGGCCAA	AGCTACCCCAGACCCAGG
Bradi2g52450_BAC_seq_frag3_c4_p1	CCGTCTTCCGTGCCCCAG	TTGGCAAGCGCGTTCTTA
Bradi2g52450_BAC_seq_frag3_c5_p1	TAGGAACGCCCTTGCAA	GGGCGTTGCGAGACATCT
Bradi2g52450_BAC_seq_frag3_c6_p1	GGCAGCGGATCTTGTATCCA	TATAGCAACGCCGGCGAG
Bradi2g52450_BAC_seq_frag3_c7_p1	GTGGTAGATCCGGCTCG	AACGCTCCGTCTACACGC
pWBVec8_c1_p1	TGCAAACGCCAGAAC	TGGCGCAAAGATGGGAG
pWBVec8_c2_p1	CTCCCACATTTGCCGCCA	GCCCCAGTATCAGCCCGTC
pWBVec8_c3_p1	AGGTCAAGTGCCTGC	TGGAGAATGGCAGCGCAA
pWBVec8_c4_p1	TGCGCTGCCATTCTCCAA	GCACCGAGGCAAAGGAGT
pWBVec8_c5_p1	AGATGGCGCTCGATGACG	CGCAGAAAGTGGTCCCTGCA
pWBVec8_c6_p1	TTTCCGCCACCTGCTCAG	CCGGCAAACAAACCACCG
pWBVec8_c7_p1	TGAGCGTCAGACCCCGTA	AAAAAGGCCGCGTTGCTG
pWBVec8_c8_p1	CAGCAACGCCGCTTTTT	GTGGCGCTGTTGGTGTG
pWBVec8_c9_p1	TGCCAGGCGGTAAGGTG	AAGCCCATGGAGGCGTT
pWBVec8_c10_p1	GAACGCCCTCATGGGCTT	GCCAGGTCTGATCGACG
pWBVec8_c11_p1	CGGGTGGAAATCCGATCCG	AAACAGGTCAAGCGAGGCC
pWBVec8_c12_p1	GGTCCTGGCAAAGCTCGT	CGAAACCATCGCAAGCCG
pWBVec8_c13_p1	ACTGGAAGGTTTCGCGGG	CCCAACCAGGAAGGGCAG
pWBVec8_c14_p1	TCTGGCATACCGAACCC	CGCATTATGGCGTTGGC
pWBVec8_c15_p1	CAGCGACTTCCGTCAG	CAGGGGTGATGCTGCCAA
pWBVec8_c16_p1	ATAGCGCTGATGTCGGC	CTCGCGAGGGTAGCATG
pWBVec8_c17_p1	CATGCTACCCCTCCGCGAG	TTTGGGACACTGTCGGC
pWBVec8_c18_p1	TCTAGAGGGCCGACGTC	CTTCCGGAATCGGGAGCG
pWBVec8_c19_p1	AACTCACCGCGACGTCTG	GTCCCTGGCCCAAAGCAT
pWBVec8_c20_p1	AGGCCATGGATGCGATCG	CCTTTGCCCTCGACGAG
pWBVec8_c21_p1	ACACAAATGCCCGCAGA	CCGCGGTTTCTGGAGTT
pWBVec8_c22_p1	AACTCCAGAAACCCCGGG	TTTCGTGGAGTCCCGCC
pBract202_p1	GCCTTGATTACGGGGCT	TTTGGGACACTGTCGGC
pBract202_p2	AACTCACCGCGACGTCTG	GTCCCTGGCCCAAAGCAT
pBract202_p3	ACACAAATGCCCGCAGA	GCACGACAGGTTCCCGA
pBract202_p4	CCTCGCTCACTGACTCGC	CGGTGGTTGTTGCCGG
pBract202_p5	GCGATTCGACTCGTCCA	ACGTCTGCTCAAGGCCG
pBract202_p6	ACAGCGGTCAATTGACTGGAG	ACACCGCGCGGATAATTAA
pBract202_p7	GTGTAGGTGCGCTCCAA	TGCCTCGGTGAGTTTCTCC

KASP primers used for genetic map development and genotyping of recombinant lines.

Marker name	Purpose <sup>a</sup>	Forward primer allele 1	Forward primer allele 2	Common reverse primer
Bd1_1045_80_F	LxJ	GAAGGTGGAGTCAACGGATTTTATAATAATGCTTACA	GAAGGTGACCAAGTTATGCTTTATAATAATGCTTACG	ACTGAAGCTGGTGACTTCGAG
Bd1_1158441_80_F	LxJ	GAAGGTGGAGTCAACGGATTGCTGATTCTATCGCACCTTA	GAAGGTGACCAAGTTATGCTGCTGATTCTATCGCACCTG	TGCCCGTGCTTCTGTGTC
Bd1_2217472_80_F	FxL, LxJ	GAAGGTGGAGTCAACGGATTAAACCCACCCACTAGACCTA	GAAGGTGACCAAGTTATGCTAAACCCACCCACTAGACCTT	TGTGGTTTGTCACTAAAGGCT
Bd1_3742611_80_F	FxL, LxJ	GAAGGTGGAGTCAACGGATTCCGCCTCTCGACGGCTACA	GAAGGTGACCAAGTTATGCTCCGCCTCTCGACGGCTACG	GAATCCCGCCCTGGTTC
Bd1_5193814_80_F	FxL, LxJ	GAAGGTGGAGTCAACGGATTACCAAGTATGATTATCGAAG	GAAGGTGACCAAGTTATGCTACCAAGTATGATTATCGAAT	GCTGGGCCTCAGACGTAC
Bd1_6505655_80_F	FxL, LxJ	GAAGGTGGAGTCAACGGATTTCGCACAGTACTTGAGCA	GAAGGTGACCAAGTTATGCTTCCGACAGTACTTGAGCG	TGCTCTCGCAGTGCACATC
Bd1_8478145_80_F	LxJ	GAAGGTGGAGTCAACGGATTCCACTCGAACTCATC	GAAGGTGACCAAGTTATGCTTCCACTCGAACTCATC	ACTCTTGTGAGTCTTGGT
Bd1_9735862_80_R	FxL	GAAGGTGGAGTCAACGGATTGACACTGTAGCGCCACCGTA	GAAGGTGACCAAGTTATGCTGACACTGTAGCGCCACCGTG	CCGAATCGCTCCTCACCC
Bd1_10587139_80_F	LxJ	GAAGGTGGAGTCAACGGATTCTGCACGGTAAGGCCATGC	GAAGGTGACCAAGTTATGCTCTGCACGGTAAGGCCATGT	CGTCTCTTGGCCGTGGTT
Bd1_13967462_80_F	FxL	GAAGGTGGAGTCAACGGATTGATCCTTGCTATTGAGCG	GAAGGTGACCAAGTTATGCTGATCCTTGCTATTGAGCT	GCCTGCTGTGCTTAGTGC
Bd1_14339439_80_F	LxJ	GAAGGTGGAGTCAACGGATTGGCAAGGAGACTTGACTTC	GAAGGTGACCAAGTTATGCTGGCAAGGAGACTTGACTTT	TCAGCAGACAACCGACCG
Bd1_16416822_80_F	FxL	GAAGGTGGAGTCAACGGATTCTTGACTTTAGATCGGGGC	GAAGGTGACCAAGTTATGCTTCTTGACTTTAGATCGGGGT	TCCCACAGCTAACGAGTGT
Bd1_16439870_80_R	LxJ	GAAGGTGGAGTCAACGGATTGAATTATGAAACTGACGGAG	GAAGGTGACCAAGTTATGCTGAATTATGAAACTGACGGAT	CTCGACCACCCGTTGCAA
Bd1_18460725_80_F	LxJ	GAAGGTGGAGTCAACGGATTCCGCCAGCCTGTCAGTGAAC	GAAGGTGACCAAGTTATGCTCCGCCAGCCTGTCAGTGAAT	ACGAGGCAGTTCACTGATCA
Bd1_18933637_80_F	FxL	GAAGGTGGAGTCAACGGATTGCCCTGAAATCCGGCCTA	GAAGGTGACCAAGTTATGCTGCCCTGAAATCCGGCCTC	CGCCGGACTCGTCCAATT
Bd1_20391084_80_R	LxJ	GAAGGTGGAGTCAACGGATTGTAATATTGACACTTAA	GAAGGTGACCAAGTTATGCTGTAATATTGACACTTAA	AGGGGCAAATGTCGCAA
Bd1_21418300_80_F	FxL	GAAGGTGGAGTCAACGGATTAGATTACCAATGAGTTGAGA	GAAGGTGACCAAGTTATGCTAGATTACCAATGAGTTGAGG	GTGGATCACAGCAGGCGA
Bd1_22262232_80_F	LxJ	GAAGGTGGAGTCAACGGATTATTGAAATTCTTCATGC	GAAGGTGACCAAGTTATGCTATTGAAATTCTTCATGT	GCTGATGAAAGCATTAGCCA
Bd1_23899717_80_F	FxL	GAAGGTGGAGTCAACGGATTATGACTTCATGCTGTGA	GAAGGTGACCAAGTTATGCTATATGACTTCATGCTGTGG	ACACGCTTCACCCACACAGT
Bd1_25381740_80_F	LxJ	GAAGGTGGAGTCAACGGATTACAACACTACGAGAACCGAGA	GAAGGTGACCAAGTTATGCTACAACACTACGAGAACCGAGG	ACATTGGGTGCCCCCTCG
Bd1_27206656_80_F	FxL	GAAGGTGGAGTCAACGGATTTCATTGAAAAAGAAAGAC	GAAGGTGACCAAGTTATGCTTCTATTGAAAAAGAAAGAT	TGAGATCGTGCCTCAATGTTG
Bd1_30473280_80_F	LxJ	GAAGGTGGAGTCAACGGATTGTTACGTTTATCTTAACCA	GAAGGTGACCAAGTTATGCTGTTACGTTTATCTTAACG	ATTCCATAGCAACGCGCG
Bd1_30517986_80_F	FxL	GAAGGTGGAGTCAACGGATTACCGAATCTTAATATTCCG	GAAGGTGACCAAGTTATGCTACCGAATCTTAATATTCCG	CTGCCTCGGCCCTCCAAAA
Bd1_33836606_80_F	FxL, LxJ	GAAGGTGGAGTCAACGGATTATGAAAGATTAATCATGC	GAAGGTGACCAAGTTATGCTATGAAAGATTAATCATGG	ACGTATGCCAGTGAGCCA
Bd1_41545466_80_R	FxL	GAAGGTGGAGTCAACGGATTCCGGCGGAGATTACAAGGTAA	GAAGGTGACCAAGTTATGCTCGGGGGAGATTACAAGGTAG	TTACCTGGACGAGCCGA
Bd1_43478472_80_F	LxJ	GAAGGTGGAGTCAACGGATTGAGGTATATCCTCTGCCAC	GAAGGTGACCAAGTTATGCTGAGGTATATCCTCTGCCAT	GGGCAGGACGAAAATCAGC
Bd1_44496983_80_F	FxL	GAAGGTGGAGTCAACGGATTAGGAGATCAAAGCGTGTGC	GAAGGTGACCAAGTTATGCTAGGAGATCAAAGCGTGTGT	TGTCTTACCTTGCCCCACTCTG
Bd1_46690464_80_F	FxL, LxJ	GAAGGTGGAGTCAACGGATTCCTAGCAGATATTCTCTA	GAAGGTGACCAAGTTATGCTCTAGCAGATATTCTCTA	ACTTTGCCAGGAACCGT
Bd1_49945665_80_F	FxL, LxJ	GAAGGTGGAGTCAACGGATTAAAAAAACTCGGGCA	GAAGGTGACCAAGTTATGCTAAAAAAACTCGGGCG	CCACGTTACTCGCAGCGA
Bd1_52521919_80_F	FxL, LxJ	GAAGGTGGAGTCAACGGATTAGGGTAAGGTCTGAGACCA	GAAGGTGACCAAGTTATGCTCAGGGTAAGGTCTGAGACG	TTGCCACATGCCGTCCAT
Bd1_54418622_80_F	FxL	GAAGGTGGAGTCAACGGATTCCGGCTGCCGCCGGCG	GAAGGTGACCAAGTTATGCTGCCGCCGGCG	GCCGAAACGCCGTAAAC
Bd1_54965698_80_F	LxJ	GAAGGTGGAGTCAACGGATTCTCAGACTAAACTTAGTAC	GAAGGTGACCAAGTTATGCTCTCAGACTAAACTTAGTAT	TGCCTCCGACTTAGTACACC
Bd1_56886337_80_F	FxL	GAAGGTGGAGTCAACGGATTATGTCGATGTTACCGAGA	GAAGGTGACCAAGTTATGTCGATGTTACCGAGG	ATGTGCCGATGCCACACA

Bd1_57500873_80_F	LxJ	GAAGGTGGAGTCAACGGATTGAAGGGCCTTTGCCCTTC	GAAGGTGACCAAGTTCATGCTGAAGGGCCTTGCCTTT	GGGTACCCGTGGAAAAACA
Bd1_59776860_80_R	LxJ	GAAGGTGGAGTCAACGGATTTCGTATGGCTCGAACAAAC	GAAGGTGACCAAGTTCATGCTTCATGGCTCGAACAAAT	TGGCGATCCAACGTTGCA
Bd1_62003564_80_F	FxL, LxJ	GAAGGTGGAGTCAACGGATTAGCACCTTGCCAGGGATCA	GAAGGTGACCAAGTTCATGCTAGCACCTTGCCAGGGATCG	TCACGCCTGAGATGTTGCA
Bd1_64439255_80_F	FxL, LxJ	GAAGGTGGAGTCAACGGATTAAACCGGTGCCAAGTTGGG	GAAGGTGACCAAGTTCATGCTAAACCGGTGCCAAGTTGGT	GCAGCAGCCTGAAACAGC
Bd1_65913549_80_F	LxJ	GAAGGTGGAGTCAACGGATTAGCTTGCACCACATTTGCG	GAAGGTGACCAAGTTCATGCTAGCTTGCACCACATTTGCT	TCTGTTCTTCTTGGACGCGA
Bd1_66701610_80_F	FxL	GAAGGTGGAGTCAACGGATTGCGTAGATAAGATGGCGAC	GAAGGTGACCAAGTTCATGCTCGCTAGATAAGATGGCGAT	GTGCACCTGTGGGCTGG
Bd1_67810462_80_F	FxL, LxJ	GAAGGTGGAGTCAACGGATTGTAAGACTACAAGCTCTGG	GAAGGTGACCAAGTTCATGCTGTAAGACTACAAGCTCTGT	CCTGCTCAAGAGGAAATACCG
Bd1_69140698_80_F	FxL	GAAGGTGGAGTCAACGGATTACTCAGAGAGGTCTGGTC	GAAGGTGACCAAGTTCATGCTACTCAGAGAGGTCTGGTC	GCTACGTGTTGCATTCTCG
Bd1_69168559_80_F	LxJ	GAAGGTGGAGTCAACGGATTCAATATCCTCAAACGTGGC	GAAGGTGACCAAGTTCATGCTCAAATATCCTCAAACGTGGT	TGGTTATGCCGTCTAGGC
Bd1_70415228_80_F	LxJ	GAAGGTGGAGTCAACGGATTGGTGGAGATCTTGCACTGCA	GAAGGTGACCAAGTTCATGCTGGTGGAGATCTTGCACTGCT	GGGCTGTCCCCCATGAAG
Bd1_71794261_80_F	FxL, LxJ	GAAGGTGGAGTCAACGGATTAAACGAAAATCATAACGAGG	GAAGGTGACCAAGTTCATGCTAAACGAAAATCATAACGAGT	TCTGTGTGCCACTAGTAGCA
Bd1_73001491_80_F	FxL, LxJ	GAAGGTGGAGTCAACGGATTCCGAGCCAACCCCCAACAC	GAAGGTGACCAAGTTCATGCTCCGAGCCAACCCCCAACAT	AAAATGCGCAGGTTGCC
Bd1_74308335_80_F	LxJ	GAAGGTGGAGTCAACGGATTGCAATTCAAATTAGTCAA	GAAGGTGACCAAGTTCATGCTGCATTCAAATTAGTCAAAG	TGGTACTGACAGTACGTTCCA
Bd2_1025539_80_F	LxJ	GAAGGTGGAGTCAACGGATTACATCTATCTATTAGACC	GAAGGTGACCAAGTTCATGCTTACATCTATCTATTAGACG	TGAAATACTCGCTCCGGCC
Bd2_2019212_80_F	FxL, LxJ	GAAGGTGGAGTCAACGGATTATGCAACTGCAGCAAGAGC	GAAGGTGACCAAGTTCATGCTAATGCAACTGCAGCAAGAGG	TGGGCAGTGAACGTGAGT
Bd2_3051379_80_F	LxJ	GAAGGTGGAGTCAACGGATTATGGCGCAAGGCTATGGAA	GAAGGTGACCAAGTTCATGCTCATGGCGCAAGGCTATGGAG	GCCAATAGCTCGGTGCC
Bd2_3755507_80_R	FxL	GAAGGTGGAGTCAACGGATTTTGTTACCTTTAGATTCAA	GAAGGTGACCAAGTTCATGCTTTGTTACCTTTAGATTCAC	ACAGTATGGTGAGACAAGCTG
Bd2_4212016_80_F	LxJ	GAAGGTGGAGTCAACGGATTGCAATGTATTGCAATGCGA	GAAGGTGACCAAGTTCATGCTTGCATGTATTGCAATGCGG	TGTGCGGGATAACCGGA
Bd2_5508797_80_F	FxL, LxJ	GAAGGTGGAGTCAACGGATTAGCCAATCCATCAGCAATCA	GAAGGTGACCAAGTTCATGCTAGCCAATCCATCAGCAATCC	GGCCAGGGTATTGTGC
Bd2_7372832_80_R	FxL	GAAGGTGGAGTCAACGGATTGACCCAGGCCAGCAAGGTCA	GAAGGTGACCAAGTTCATGCTGACCAGGCCAGCAAGGTTG	ACCTGCGTACAAACATTGGT
Bd2_7892540_80_F	LxJ	GAAGGTGGAGTCAACGGATTACAATTTCACCATTTA	GAAGGTGACCAAGTTCATGCTTACAATTTCACCATTTA	GGAACACAAACAGCCAGGC
Bd2_9589763_80_R	LxJ	GAAGGTGGAGTCAACGGATTGTTGCTCTCTAGCTAGCA	GAAGGTGACCAAGTTCATGCTGTTGCTCTCTAGCTAGCG	ACATCTTCTGCCAATCGAACG
Bd2_16686745_80_F	FxL, LxJ	GAAGGTGGAGTCAACGGATTAGTCGGCGAGCAAGGGCTA	GAAGGTGACCAAGTTCATGCTAGTCGGCGAGCAAGGGCTG	GAGGAGAGCACGAGGCAC
Bd2_18776376_80_F	LxJ	GAAGGTGGAGTCAACGGATTATAATCAACATTCTTAC	GAAGGTGACCAAGTTCATGCTATATAATCAACATTCTTAT	ACACCCCTGGAAGATAAGGT
Bd2_19981986_80_F	FxL	GAAGGTGGAGTCAACGGATTAACGGGATTCAGCCATTAA	GAAGGTGACCAAGTTCATGCTAAAATTGAGAAGGCCATT	ACTCCCCAGTTTGCCACC
Bd2_26124348_80_F	LxJ	GAAGGTGGAGTCAACGGATTCTCTCAAGTTGTTGGGCCAA	GAAGGTGACCAAGTTCATGCTCTCTCAAGTTGTTGGGCCAG	GCACAGTCATGGTTGTCGG
Bd2_30225592_80_R	FxL	GAAGGTGGAGTCAACGGATTACTGTGGGCTGCCAAAGTACA	GAAGGTGACCAAGTTCATGCTACTGTGGGCTGCCAAAGTACC	GCATCTTGCAAGCTATGACAA
Bd2_33128511_80_F	FxL	GAAGGTGGAGTCAACGGATTACGACCGTGAGTGGATTGTC	GAAGGTGACCAAGTTCATGCTACGACCGTGAGTGGATTGTT	GGTGCCTGGCATGCTGCTA
Bd2_35119080_80_F	LxJ	GAAGGTGGAGTCAACGGATTGGAATCCCTCCAATCCCGA	GAAGGTGACCAAGTTCATGCTGGAAATCCCTCCAATCCCGG	TTCTGCCACGCTGTTGCA
Bd2_36989830_80_F	FxL, LxJ	GAAGGTGGAGTCAACGGATTAAATTTGGAGCAACGAC	GAAGGTGACCAAGTTCATGCTAATAATTGGAGCAACGAC	TCGTATGGTTACTCCCTCCA
Bd2_38916023_80_F	LxJ	GAAGGTGGAGTCAACGGATTATGGGCTCAATAAAATTAA	GAAGGTGACCAAGTTCATGCTATGGGCTCAATAAAATTG	TGACGTTGGTTAGGGCTCT
Bd2_40627244_80_F	FxL	GAAGGTGGAGTCAACGGATTGTCGCTCTCAATTACGTTA	GAAGGTGACCAAGTTCATGCTGTGCGTCTCAATTACGTTG	CCGGAGGGGGAGGAAACT
Bd2_40903895_80_F	LxJ	GAAGGTGGAGTCAACGGATTAGTGAAACTGAGGGGGCGA	GAAGGTGACCAAGTTCATGCTAGTGAAACTGAGGGGGCGG	AGCACAATAGGCATCCCGT
Bd2_44203708_80_F	FxL, LxJ	GAAGGTGGAGTCAACGGATTGTGCTGATCAAGAGCTCCG	GAAGGTGACCAAGTTCATGCTGTGCTGATCAAGAGCTCCG	TGATGTACACCACGTGCTGCA
Bd2_46707066_80_R	FxL, LxJ	GAAGGTGGAGTCAACGGATTAGTATTACTCACAATGA	GAAGGTGACCAAGTTCATGCTTAGTATTACTCACAATGCA	ACAACACCAATGCCACCA
Bd2_48078565_80_F	LxJ	GAAGGTGGAGTCAACGGATTACCGCCGCACTCGCACCCA	GAAGGTGACCAAGTTCATGCTACCCGCCGACTCGCACCCG	CCTTGAGCACCAGCACGA

Bd2_49926579_80_F	FxL	GAAGGTGGAGTCAACGGATTGCTGCCATGAACCTTACA	GAAGGTGACCAAGTTCATGCTCGCTGCCATGAACCTTACG	GCGATATGGTCGGTGGCA
Bd2_50755888_80_R	FxL, LxJ	GAAGGTGGAGTCAACGGATTGCTAAAGTGTAAAAGTTG	GAAGGTGACCAAGTTCATGCTGTCAAAGTGTAAAAGTTT	TCCATGCTCCCTCGTTCT
Bd2_51153057_80_F	FxL	GAAGGTGGAGTCAACGGATTGCGTGTAAACAAAATCCA	GAAGGTGACCAAGTTCATGCTCGGTGGTTAAACAAAATCCG	ATGGCTCTACCGCGGA
Bd2_51697434_80_F	LxJ_recs	GAAGGTGGAGTCAACGGATTGCGATCGAGTTGACCAGCGC	GAAGGTGACCAAGTTCATGCTCGCATCGAGTTGACCAGCGT	TGCAATGAACATCCAACCATGT
Bd2_51746686_60_F	AxB_recs	GAAGGTGGAGTCAACGGATTATGAAAACATACAGCCGCC	GAAGGTGACCAAGTTCATGCTATGAAAACATACAGCCGCC	TGCTCTGTTGTCTAGTGGCT
Bd2_51764532_60_F	LxJ_recs	GAAGGTGGAGTCAACGGATTGCGCCGCCGGCCATGCA	GAAGGTGACCAAGTTCATGCTGCCGCCGGCCCATGCT	GGGCGTGTGCTCGGAT
Bd2_51766926_60_F	AxB_recs	GAAGGTGGAGTCAACGGATTACGCTGAAGATGGCGCAACC	GAAGGTGACCAAGTTCATGCTACGCTGAAGATGGCGCAACG	GATCCACGACGGACGAGG
Bd2_51767364_60_F	LxJ_recs	GAAGGTGGAGTCAACGGATTGCGATGCGATTCCGTCGTA	GAAGGTGACCAAGTTCATGCTGCATGCGATTCCGTCGTC	GCCGCGCGTCAAATAAT
Bd2_51770065_60_R	LxJ_recs	GAAGGTGGAGTCAACGGATTAGCTAAACTTATTACGGCAC	GAAGGTGACCAAGTTCATGCTAGCTAAACTTATTACGGCAG	AGGGTTATCGGGGTCT
Bd2_51772031_60_F	LxJ, LxJ_recs	GAAGGTGGAGTCAACGGATTACGGGATGGCGCAGGCAC	GAAGGTGACCAAGTTCATGCTACGGGATGGCGCAGGCAT	CGATCGTCTGGACCTGCG
Bd2_51773941_60_F	AxB_recs	GAAGGTGGAGTCAACGGATTGAGAGAATAGGCTGTATAA	GAAGGTGACCAAGTTCATGCTGAGAGAATAGGCTGTATA	GGCTGGTCGACCGAGAAA
Bd2_51805111_80_F	LxJ_recs	GAAGGTGGAGTCAACGGATTATCAATCGGTGAGATACAG	GAAGGTGACCAAGTTCATGCTATCAATCGGTGAGATACAT	ACCATCGAACAGGCGAACAA
Bd2_51810746_80_R	LxJ_recs	GAAGGTGGAGTCAACGGATTGGGAAGCGATACATCATAGG	GAAGGTGACCAAGTTCATGCTGGGAAGCGATACATCATAGT	TCTCCCTTGGCACGGTA
Bd2_51822083_60_F	FxL, LxJ_recs	GAAGGTGGAGTCAACGGATTACGGTATCACAACTGGACAA	GAAGGTGACCAAGTTCATGCTACGGTATCACAACTGGACG	CAGGCTGTTCCACATAGCCA
Bd2_51838682_60_F	LxJ_recs	GAAGGTGGAGTCAACGGATTCTAGGTTGCGGCCGTGTC	GAAGGTGACCAAGTTCATGCTTCTAGGTTGCGGCCGTGTC	CATTAGCCACCCGGGTTCG
Bd2_51861301_60_R	AxB_recs	GAAGGTGGAGTCAACGGATTATCCAATAGTGTACCAA	GAAGGTGACCAAGTTCATGCTTATCCAATAGTGTACCAT	CCGCTCTGATCCTGCA
Bd2_51869681_60_F	AxB_recs	GAAGGTGGAGTCAACGGATTGTTAGCTAGGCCCTGTA	GAAGGTGACCAAGTTCATGCTTGTAGCTAGGCCCTGTC	TCAGTGACAGGGTATCCGGT
Bd2_51876096_60_F	AxB_recs	GAAGGTGGAGTCAACGGATTGGTTCTTATTCCGTGCCC	GAAGGTGACCAAGTTCATGCTGGGTTCTTATTCCGTGCCC	AGGTGCATGTCACAGGCC
Bd2_51887975_60_F	FxL	GAAGGTGGAGTCAACGGATTATGTTAGGAATTGGAAAAATC	GAAGGTGACCAAGTTCATGCTATGTTAGGAATTGGAAAAATT	CAATCTCTGATGTGCACAGT
Bd2_51923214_60_F	LxJ_recs	GAAGGTGGAGTCAACGGATTCTAGGCCAAAGGCAGCTAAC	GAAGGTGACCAAGTTCATGCTCTAGGCCAAAGGCAGCTAAT	GCCCCATTTGCGACGCCAC
Bd2_52977675_80_F	FxL, LxJ	GAAGGTGGAGTCAACGGATTGCGAGGTTGATAATGAGGC	GAAGGTGACCAAGTTCATGCTTGCGAGGTTGATAATGAGGG	AGCTGTCCTTCTTTGCCA
Bd2_54430479_80_F	LxJ	GAAGGTGGAGTCAACGGATTACCCGTCGAAAAACCCCC	GAAGGTGACCAAGTTCATGCTCACCCGTCGAAAAACCCCC	CCGCGCTCATAGTGTCC
Bd2_55214174_80_F	FxL	GAAGGTGGAGTCAACGGATTAGCACTTTCATAGGGAC	GAAGGTGACCAAGTTCATGCTAGCACTTTCATAGGGAT	AGCTAGCACACACCAAAACA
Bd2_55541577_80_F	LxJ	GAAGGTGGAGTCAACGGATTATCGGCCAGGCCAAAAAC	GAAGGTGACCAAGTTCATGCTCATGCCAGGCCAAAAAT	TCATTTCCAGGGTAGGGT
Bd2_55685603_80_F	FxL	GAAGGTGGAGTCAACGGATTGCTATTGACGAAGAGA	GAAGGTGACCAAGTTCATGCTTGCTATTGACGAAGAGG	CAGGATTGAAGCGTGC
Bd2_57020111_80_F	FxL, LxJ	GAAGGTGGAGTCAACGGATTACATTATAGTATGAAGACC	GAAGGTGACCAAGTTCATGCTAACATTATAGTATGAAGACT	TGTTTGTCTCCACTGCTTCA
Bd2_58112401_80_F	LxJ	GAAGGTGGAGTCAACGGATTGGAACAAGTAAATGTAGAAA	GAAGGTGACCAAGTTCATGCTGGAACAAGTAAATGTAGAAG	TGCAAGGGCAGATGTGGC
Bd2_58156576_80_F	FxL	GAAGGTGGAGTCAACGGATTCCAGATGGACGCCGCCA	GAAGGTGACCAAGTTCATGCTCCACATGGACGCCGCC	GACGCCACATCTCGTACGG
Bd2_59283695_80_F	FxL, LxJ	GAAGGTGGAGTCAACGGATTAACCCCTTACTGTAA	GAAGGTGACCAAGTTCATGCTAAAAACCCCTTACTGTAT	GGAGGACCCCTCGGAATTGG
Bd3_49775_80_F	LxJ	GAAGGTGGAGTCAACGGATTCTATGCTGTAGGCTCA	GAAGGTGACCAAGTTCATGCTTATGCTGTAGGCTTC	AGCGCAAATGACGCACG
Bd3_684260_80_F	LxJ	GAAGGTGGAGTCAACGGATTAGACAATCATATAACCA	GAAGGTGACCAAGTTCATGCTAACAGACAATCATATAACCA	TGTCTCTGGAGGCACTG
Bd3_2956833_80_F	FxL, LxJ	GAAGGTGGAGTCAACGGATTGCTCATCGCTCTCTACC	GAAGGTGACCAAGTTCATGCTTCTCATCGCTCTCTACC	TGCGGTGCAAGCTAGACC
Bd3_4031572_80_F	LxJ	GAAGGTGGAGTCAACGGATTGGGTAGTGAAGAGTGAAC	GAAGGTGACCAAGTTCATGCTTGGTAGTGAAGAGTGAAT	GACAATTAGTGAACGGTGGTCC
Bd3_4063961_80_R	FxL	GAAGGTGGAGTCAACGGATTGGTCATCAAGACGGTACGC	GAAGGTGACCAAGTTCATGCTGGTCATCAAGACGGTACGT	AGGGTGAATCAAGCTAGCTGT
Bd3_5172642_80_R	FxL, LxJ	GAAGGTGGAGTCAACGGATTGAGAATACTAATTCAAGAC	GAAGGTGACCAAGTTCATGCTATGAGAATACTAATTCAAGAC	AGCAGCTCCATTGAGAACCC
Bd3_6293275_80_F	LxJ	GAAGGTGGAGTCAACGGATTCTCAACATAAAAAAAAAA	GAAGGTGACCAAGTTCATGCTTCTCAACATAAAAAAAAAAAT	TGCCTACCGTGTGCATGC

Bd3_10703886_80_F	FxL	GAAGGTGGAGTCAACGGATTATACTTCCTCAAGGGGGACA	GAAGGTGACCAAGTTCATGCTATACTTCCTCAAGGGGGACG	CCACGATGCATCCCGAC
Bd3_11305466_80_F	LxJ	GAAGGTGGAGTCAACGGATTCTCAGATCAAACAAACCG	GAAGGTGACCAAGTTCATGCTTCAGATCAAACAAACCG	AGGAGAGTGAATTGAGGAGT
Bd3_13553007_80_F	LxJ	GAAGGTGGAGTCAACGGATTCTCAGATAGAAAAAGATATT	GAAGGTGACCAAGTTCATGCTCAGATAGAAAAAGATATT	TCTGAGCAGCTCATGGGT
Bd3_14498466_80_F	LxJ	GAAGGTGGAGTCAACGGATTCTCAGATAGAAAAAGATATT	GAAGGTGACCAAGTTCATGCTTCAGATAGAAAAAGATATT	CTTCAGGACAACGCCGGT
Bd3_16480652_80_F	FxL	GAAGGTGGAGTCAACGGATTCTCATGACTTGGCTAACGACA	GAAGGTGACCAAGTTCATGCTTCAGTACTGGCTAACGACA	GATCGCCCCGCTCCATG
Bd3_18077751_80_F	FxL	GAAGGTGGAGTCAACGGATTTCGATTGAGTATCTAAC	GAAGGTGACCAAGTTCATGCTTCGATTGAGTATCTAAC	CTCAGTAAACTTGGCATCCA
Bd3_21768447_80_F	FxL, LxJ	GAAGGTGGAGTCAACGGATTCCGGAGGAGCATACCCCTAA	GAAGGTGACCAAGTTCATGCTGGAGGAGCATACCCCTAA	CCATTCAACCATTCCGAAGC
Bd3_33062776_80_F	FxL, LxJ	GAAGGTGGAGTCAACGGATTCTCATCCAATCGCTCCTTC	GAAGGTGACCAAGTTCATGCTCTCATCCAATCGCTCCTTC	GCCCCAAGCTCTCAAGAGA
Bd3_37058359_80_F	LxJ	GAAGGTGGAGTCAACGGATTAAATCAGATATAACGGA	GAAGGTGACCAAGTTCATGCTTAATCAGATATAACGGA	TTCGGGTTCAGCGTGGAC
Bd3_38113122_80_F	FxL	GAAGGTGGAGTCAACGGATTGATAATACACACTAACCTC	GAAGGTGACCAAGTTCATGCTGATAATACACACTAACCTC	CGAACGGACACTAGAAAAAGC
Bd3_40646808_80_R	FxL, LxJ	GAAGGTGGAGTCAACGGATTCAACATGGTTAACAGTTGC	GAAGGTGACCAAGTTCATGCTCACATGGTTAACAGTTGC	GAGACACCAGCGGACACC
Bd3_41669808_80_F	FxL, LxJ	GAAGGTGGAGTCAACGGATTATAATAAATAGTTAACCTG	GAAGGTGACCAAGTTCATGCTATAATAAATAGTTAACCTG	AGGCCTTGCTTGTAGAGACCA
Bd3_43942406_80_F	LxJ	GAAGGTGGAGTCAACGGATTAGCATTAAAACATCTAGCAA	GAAGGTGACCAAGTTCATGCTAGCATTAAAACATCTAGCAA	GGTGATTGAAGAAGCGAAGGC
Bd3_44858190_80_F	FxL	GAAGGTGGAGTCAACGGATTATTCCAAATCGTTGAAAAA	GAAGGTGACCAAGTTCATGCTATTCCAAATCGTTGAAAAA	ACGGAGGGAGTATCATTGG
Bd3_46259033_80_F	FxL	GAAGGTGGAGTCAACGGATTACCGTCTGCTCACACTACAA	GAAGGTGACCAAGTTCATGCTACCGTCTGCTCACACTACAG	TGAAGATGGTGGCGGAG
Bd3_46275367_80_F	LxJ	GAAGGTGGAGTCAACGGATTGTGTTAGCTGGCCGAGCTC	GAAGGTGACCAAGTTCATGCTGTGTTAGCTGGCCGAGCTC	CGTGACGTGCCCTCCACTT
Bd3_49114819_80_F	LxJ	GAAGGTGGAGTCAACGGATTCAAGCAGGAGGAACGTAA	GAAGGTGACCAAGTTCATGCTCATAGCAGGAGGAACGTAA	GGAACCTGGTGGACGTG
Bd3_52069231_80_F	FxL, LxJ	GAAGGTGGAGTCAACGGATTAAAATGTGTTATCGTCGAC	GAAGGTGACCAAGTTCATGCTAAAATGTGTTATCGTCGAC	CCCCGAGAAAGAAACACGC
Bd3_53121626_80_F	LxJ	GAAGGTGGAGTCAACGGATTGTCATCATAGATCGACTCA	GAAGGTGACCAAGTTCATGCTTCATCATAGATCGACTCA	TTGTGACACAAATTACCCCCA
Bd3_54163611_80_F	FxL	GAAGGTGGAGTCAACGGATTGATTCCCTCTAATCTCCCTC	GAAGGTGACCAAGTTCATGCTGATTCCCTCTAATCTCCCTC	CGAGTCTCCCTCCCGTGA
Bd3_55045896_80_F	LxJ	GAAGGTGGAGTCAACGGATTGGCATGACATGTTGAGAATA	GAAGGTGACCAAGTTCATGCTGGCATGACATGTTGAGAATA	GTGTGAGCCTATGCGGGA
Bd3_56009013_80_F	FxL	GAAGGTGGAGTCAACGGATTGTTGCTCCAATCCTTTCCCG	GAAGGTGACCAAGTTCATGCTTTGCTCCAATCCTTTCCCG	CCCGCATTTGGCCCATG
Bd3_56072395_80_F	LxJ	GAAGGTGGAGTCAACGGATTAAATTGTGATTGCAAAAAAA	GAAGGTGACCAAGTTCATGCTTAATTGTGATTGCAAAAAAA	TTTGGCCTGTGTCATCA
Bd3_57094799_80_F	LxJ	GAAGGTGGAGTCAACGGATTGATGAGGTTGGCGAGCTCC	GAAGGTGACCAAGTTCATGCTGATGAGGTTGGCGAGCTCC	TACCACCCCGATCCAG
Bd3_58345084_80_F	FxL, LxJ	GAAGGTGGAGTCAACGGATTATAATCTCCTAACTCAG	GAAGGTGACCAAGTTCATGCTTATAATCTCCTAACTCAG	TCCTCCACCAGTGCAG
Bd3_59581043_80_F	FxL, LxJ	GAAGGTGGAGTCAACGGATTAGTTAGCAAACATCTACCGC	GAAGGTGACCAAGTTCATGCTAGTTAGCAAACATCTACCGC	TGCAATTGCGTTCATTCAGCA
Bd4_79802_80_F	LxJ	GAAGGTGGAGTCAACGGATTCCCTATATCTTCTGCCA	GAAGGTGACCAAGTTCATGCTCCCTATATCTTCTGCCA	ACACAGGAGCAGCAGTCG
Bd4_1913933_80_F	FxL, LxJ	GAAGGTGGAGTCAACGGATTCTCAGAAAATACTTTAGTAA	GAAGGTGACCAAGTTCATGCTCTCAGAAAATACTTTAGTAA	CAAACCTTTGTCGGAAGCCA
Bd4_3548432_80_F	FxL, LxJ	GAAGGTGGAGTCAACGGATTGGTTGTATCATCTTGTCC	GAAGGTGACCAAGTTCATGCTGGTTGTATCATCTTGTCC	TCATGGCCTGCTCCAACG
Bd4_4751276_80_F	FxL, LxJ	GAAGGTGGAGTCAACGGATTGACGGCGGCCCTCATGCA	GAAGGTGACCAAGTTCATGCTGACGGCGGCCCTCATGCA	TGCAAGTATTGATTGCTTGC
Bd4_7544641_80_F	LxJ	GAAGGTGGAGTCAACGGATTGTAACATTGCAAAACACAA	GAAGGTGACCAAGTTCATGCTGTAACATTGCAAAACACAA	GACCTTGGCATGACCGCT
Bd4_9422251_60_F	FxL, LxJ	GAAGGTGGAGTCAACGGATTCTATCATGAACTAAATAGA	GAAGGTGACCAAGTTCATGCTCATATCATGAACTAAATAGA	TGCAACCAGGAGGCAAGG
Bd4_14120682_80_R	LxJ	GAAGGTGGAGTCAACGGATTCTAGTCTAGAACAGGAGGAC	GAAGGTGACCAAGTTCATGCTCTAGTCTAGAACAGGAGGAC	GGGGAGGATATACCATCGGGA
Bd4_17032425_80_R	FxL	GAAGGTGGAGTCAACGGATTAAATTGCAAGTATAACA	GAAGGTGACCAAGTTCATGCTAAATTGCAAGTATAACA	GTGGAGCATGCTGTGTC
Bd4_24652545_80_F	FxL, LxJ	GAAGGTGGAGTCAACGGATTCAAAAGGTGGATCTGAGGCA	GAAGGTGACCAAGTTCATGCTCAAAGGTGGATCTGAGGCA	AGCATGAAAGCCATGGCCT
Bd4_29237345_60_R	FxL, LxJ	GAAGGTGGAGTCAACGGATTACTTACTCTGGCTCTCGC	GAAGGTGACCAAGTTCATGCTATACTCTGGCTCTCGC	GCGGCGACAAGTCTTTG

Bd4_29442515_80_F	FxL	GAAGGTGGAGTCAACGGATTAGAGCTCACCGTAGTCG	GAAGGTGACCAAGTTCATGCTAGAGCTCACCGTAGTCCT	ATTAGCTCCTCGCGTCG
Bd4_29480682_78_F	FxL	GAAGGTGGAGTCAACGGATTGATAACTTACGGGAAGTGAC	GAAGGTGACCAAGTTCATGCTGATAACTTACGGGAAGTGAG	CCCCCTCCTCGAAAAGCA
Bd4_29517901_80_R	FxL	GAAGGTGGAGTCAACGGATTCAATTATATTGTCAAGAAC	GAAGGTGACCAAGTTCATGCTCAATTATATTGTCAAGAACG	ACGTTTTCCAGATCACGCA
Bd4_31819521_80_F	FxL, LxJ	GAAGGTGGAGTCAACGGATTACCTGGCTCAATCTGGCTTA	GAAGGTGACCAAGTTCATGCTACCTGGCTCAATCTGGCTTC	TGCACGATCCTGTAATGCTC
Bd4_35489154_80_R	FxL	GAAGGTGGAGTCAACGGATTCTCTTCCGGCGGAATTAC	GAAGGTGACCAAGTTCATGCTTCTTCCGGCGGAATTACT	GCAAAGACCGGGGGTTCA
Bd4_35489196_80_F	LxJ	GAAGGTGGAGTCAACGGATTAAGAACTAAATCAGTCACAA	GAAGGTGACCAAGTTCATGCTAAAAGTAAATCAGTCACAG	AGAGCAGCTGCCAGTTCA
Bd4_38721872_80_F	LxJ	GAAGGTGGAGTCAACGGATTCTCCACCCATGAAGATA	GAAGGTGACCAAGTTCATGCTTCTCTCACCCATGAAGATT	TGGGAGAGCCGAGTTCGA
Bd4_40183813_80_F	LxJ	GAAGGTGGAGTCAACGGATTGGTACCTTCCCAGTCA	GAAGGTGACCAAGTTCATGCTGGGTACCTTCCCAGTCA	GTCGCTGCAGAGGGTTGT
Bd4_40346729_80_F	FxL	GAAGGTGGAGTCAACGGATTCTGGTCCACCGGAGATTCC	GAAGGTGACCAAGTTCATGCTCTGGTCCACCGGAGATTCT	GCCCATGTTGTTCAACCGG
Bd4_42825975_80_F	FxL, LxJ	GAAGGTGGAGTCAACGGATTCTTCGATCTGCCGCTTC	GAAGGTGACCAAGTTCATGCTCCTTCGATCTGCCGCTTC	AGACCTGCGACGGGATCT
Bd4_44061764_80_F	FxL, LxJ	GAAGGTGGAGTCAACGGATTGTTAGAGGTGACACACTCC	GAAGGTGACCAAGTTCATGCTGTTAGAGGTGACACACTCT	GCCCTGGTGAGCTCGATG
Bd4_46686642_80_F	LxJ	GAAGGTGGAGTCAACGGATTGATAGGAAACACGGAGCCA	GAAGGTGACCAAGTTCATGCTGATAGGAAACACGGAGCCA	TCTTCCGCCTCCCTCC
Bd4_48088914_80_F	LxJ	GAAGGTGGAGTCAACGGATTAGGATATACGTTAGACA	GAAGGTGACCAAGTTCATGCTAGGATATACGTTAGACA	CGCCGCCAGTTGATTTC
Bd5_637722_80_F	FxL, LxJ	GAAGGTGGAGTCAACGGATTCAAACGGTGAAAACCTAAA	GAAGGTGACCAAGTTCATGCTCAAACGGTGAAAACCTAAG	TGTCTCCAGACAATGTGCGT
Bd5_5044936_80_F	LxJ	GAAGGTGGAGTCAACGGATTGGCCTGATTCAATTCCAAC	GAAGGTGACCAAGTTCATGCTGGCCTGATTCAATTCCAAG	ATGTCCTCCCAGTTGCC
Bd5_16064722_80_F	LxJ	GAAGGTGGAGTCAACGGATTCTCGGGCCCACCCCTGCCA	GAAGGTGACCAAGTTCATGCTCTGGGCCCACCCCTGCCA	AGATGGAAGCGTGCAC
Bd5_18069830_80_F	FxL	GAAGGTGGAGTCAACGGATTCCACCGGGCCCAGGGCACC	GAAGGTGACCAAGTTCATGCTCACCGGGCCCAGGGCACT	AGGCTTGACAGCTGGGG
Bd5_20559803_80_F	FxL, LxJ	GAAGGTGGAGTCAACGGATTGAGACATTAAGTTGTCAC	GAAGGTGACCAAGTTCATGCTTGAGACATTAAGTTGTCAT	TGGTACACTACAGTGAGGGGA
Bd5_22050320_80_F	LxJ	GAAGGTGGAGTCAACGGATTCTGCGCAGTAGGGGAAGCAA	GAAGGTGACCAAGTTCATGCTCGCAGTAGGGGAAGCAG	ATGCCACTAGGTGCACCG
Bd5_22088796_80_F	FxL	GAAGGTGGAGTCAACGGATTGTCGGGCATAAACATGTGG	GAAGGTGACCAAGTTCATGCTGTCCGGCATAAACATGTGT	CCCCAACCACTTCCCTCA
Bd5_23563542_80_F	FxL, LxJ	GAAGGTGGAGTCAACGGATTGTCGGCATTCCGGTCCAGC	GAAGGTGACCAAGTTCATGCTTGCCGATCCGGTCCAGT	TGGCTGGCCTGCATTGTT
Bd5_24892215_80_F	FxL, LxJ	GAAGGTGGAGTCAACGGATTACTACTGGAATCAGAGCACA	GAAGGTGACCAAGTTCATGCTACTACTGGAATCAGAGCACC	TGTTGGTTGCTGCACATGC
Bd5_26001591_80_F	FxL, LxJ	GAAGGTGGAGTCAACGGATTCTTCCAGTAGCCTGCC	GAAGGTGACCAAGTTCATGCTCTTCCAGTAGCCTGCC	GTAAGGGACCTGCCAG
Bd5_27255044_80_R	LxJ	GAAGGTGGAGTCAACGGATTAAAGGATGCCAACCAATGAGG	GAAGGTGACCAAGTTCATGCTAAGGATGCCAACCAATGAGT	GGTCAGACCAGCAGCAGT

<sup>a</sup>FxL = Foz1 x Luc1 genetic map; LxJ = Luc1 x Jer1 genetic map; LxJ\_recs = genotyping of recombinant lines in the Luc1 x Jer1 population; AxB\_recs = genotyping of recombinant lines in the ABR6 x Bd21 population

## Natural Variation in *Brachypodium* Links Vernalization and Flowering Time Loci as Major Flowering Determinants<sup>1[OPEN]</sup>

Jan Bettgenhaeuser, Fiona M.K. Corke, Magdalena Opanowicz<sup>2</sup>, Phon Green, Inmaculada Hernández-Pinzón, John H. Doonan\*, and Matthew J. Moscou\*

The Sainsbury Laboratory, Norwich NR4 7UH, United Kingdom (J.B., P.G., I.H.-P., M.J.M.); Institute of Biological, Environmental, and Rural Sciences, Aberystwyth University, Aberystwyth SY23 3DA, United Kingdom (F.M.K.C., J.H.D.); John Innes Centre, Norwich NR4 7UH, United Kingdom (F.M.K.C., M.O., J.H.D.); and School of Biological Sciences, University of East Anglia, Norwich NR4 7TJ, United Kingdom (M.J.M.)

ORCID IDs: 0000-0002-6901-1774 (J.B.); 0000-0002-1968-0574 (P.G.); 0000-0001-6027-1919 (J.H.D.); 0000-0003-2098-6818 (M.J.M.).

The domestication of plants is underscored by the selection of agriculturally favorable developmental traits, including flowering time, which resulted in the creation of varieties with altered growth habits. Research into the pathways underlying these growth habits in cereals has highlighted the role of three main flowering regulators: *VERNALIZATION1* (*VRN1*), *VRN2*, and *FLOWERING LOCUS T* (*FT*). Previous reverse genetic studies suggested that the roles of *VRN1* and *FT* are conserved in *Brachypodium distachyon* yet identified considerable ambiguity surrounding the role of *VRN2*. To investigate the natural diversity governing flowering time pathways in a nondomesticated grass, the reference *B. distachyon* accession Bd21 was crossed with the vernalization-dependent accession ABR6. Resequencing of ABR6 allowed the creation of a single-nucleotide polymorphism-based genetic map at the F4 stage of the mapping population. Flowering time was evaluated in F4:5 families in five environmental conditions, and three major loci were found to govern flowering time. Interestingly, two of these loci colocalize with the *B. distachyon* homologs of the major flowering pathway genes *VRN2* and *FT*, whereas no linkage was observed at *VRN1*. Characterization of these candidates identified sequence and expression variation between the two parental genotypes, which may explain the contrasting growth habits. However, the identification of additional quantitative trait loci suggests that greater complexity underlies flowering time in this nondomesticated system. Studying the interaction of these regulators in *B. distachyon* provides insights into the evolutionary context of flowering time regulation in the Poaceae as well as elucidates the way humans have utilized the natural variation present in grasses to create modern temperate cereals.

The coordination of flowering time with geographic location and seasonal weather patterns has a profound effect on flowering and reproductive success (Amasino, 2010). The mechanisms underpinning this coordination are of great interest for understanding plant behavior and distribution within natural ecosystems (Wilczek

et al., 2010). Plants that fail to flower at the appropriate time are unlikely to be maximally fertile and, therefore, will be less competitive in the longer term. Likewise, optimal flowering time in crops is important for yield and quality: seed and fruit crops need to flower early enough to allow ripening or to utilize seasonal rains, while delayed flowering may be advantageous for leaf and forage crops (Distelfeld et al., 2009; Jung and Müller, 2009).

Although developmental progression toward flowering can be modulated in several ways, many plants have evolved means to detect seasonal episodes of cold weather and adjust their flowering time accordingly, a process known as vernalization (Ream et al., 2012). Despite the importance of flowering time, the molecular and genetic mechanisms underlying this dependency have been studied in only a few systems, notably the Brassicaceae, Poaceae, and Amaranthaceae (Andrés and Coupland, 2012; Ream et al., 2012). Three major *VERNALIZATION* (*VRN*) genes appear to act in a regulatory loop in temperate grasses. The wheat (*Triticum aestivum*) *VRN1* gene is a MADS box transcription factor that is induced in the cold (Yan et al., 2003; Andrés and Coupland, 2012). This gene is related to the *Arabidopsis* (*Arabidopsis thaliana*) genes *APETALA1* and *FRUITFUL*

<sup>1</sup> This work was supported by the Biotechnology and Biological Sciences Research Council Doctoral Training Programme (grant no. BB/F017294/1) and Institute Strategic Programme (grant no. BB/J004553/1), the Gatsby Charitable Foundation, the Leverhulme Trust (grant no. 10754), the 2Blades Foundation, and the Human Frontiers Science Program (grant no. LT000218/2011).

<sup>2</sup> Present address: Thermo Fisher Scientific, Paisley PA4 9RF, UK.

\* Address correspondence to john.doonan@aber.ac.uk and matthew.moscou@sainsbury-laboratory.ac.uk.

The author responsible for distribution of materials integral to the findings presented in this article in accordance with the policy described in the Instructions for Authors ([www.plantphysiol.org](http://www.plantphysiol.org)) is: Matthew J. Moscou (matthew.moscou@sainsbury-laboratory.ac.uk).

J.B., F.M.K.C., M.O., J.H.D., and M.J.M. conceived the study and participated in its design and coordination; P.G. and I.H.-P. participated in the experiments; J.B., F.M.K.C., J.H.D., and M.J.M. wrote the article; all authors read and approved the final article.

[OPEN] Articles can be viewed without a subscription.

[www.plantphysiol.org/cgi/doi/10.1104/pp.16.00813](http://www.plantphysiol.org/cgi/doi/10.1104/pp.16.00813)

(Yan et al., 2003; Andrés and Coupland, 2012). *VRN2* encodes a small CCT domain protein (Yan et al., 2004) that is repressed by *VRN1* and, in turn, represses *FLOWERING LOCUS T (FT)*, a strong universal promoter of flowering (Kardailsky et al., 1999; Yan et al., 2006; Andrés and Coupland, 2012; Ream et al., 2012). In cereals, active *VRN2* alleles are necessary for a vernalization requirement. Spring barley (*Hordeum vulgare*) and spring wheat varieties, which do not require vernalization to flower, either lack *VRN2* (Dubcovsky et al., 2005; Karsai et al., 2005; von Zitzewitz et al., 2005), have point mutations in the conserved CCT domain (Yan et al., 2004), or possess dominant constitutively active alleles of *VRN1* (repressor of *VRN2*; Yan et al., 2003; Fu et al., 2005) or *FT* (repressed by *VRN2*; Yan et al., 2006).

Investigations of the regulation of flowering in the Poaceae have focused on rice (*Oryza sativa*), wheat, and barley, all domesticated species that have been heavily subjected to human selection over the past 10,000 years. Little information is available on wild species within this family that have not been subjected to human selection. Such a study could provide additional insights into the standing variation present within wild systems and its likely predomestication adaptive significance in the Poaceae (Schwartz et al., 2010). A favorable species for such a study is *Brachypodium distachyon*, a small, wild grass with a sequenced and annotated genome. *B. distachyon* was developed originally as a model system for the agronomically important temperate cereals (Draper et al., 2001; Opanowicz et al., 2008; International Brachypodium Initiative, 2010; Catalán et al., 2014). With the recent availability of geographically dispersed diversity collections, we can ask how wild grasses have adapted to different climatic zones.

Previous studies have begun to explore the molecular basis of vernalization in this system. Higgins et al. (2010) identified homologs of the various flowering pathway genes in *B. distachyon*, and several mainly reverse genetic studies have focused on characterizing these genes further (Schwartz et al., 2010; Lv et al., 2014; Ream et al., 2014; Woods et al., 2014, 2016b). Schwartz et al. (2010) did not find complete correlation between the expression of *VRN1* and flowering and, therefore, hypothesized that *VRN1* could have different activity or roles that are dependent on the genetic background. Yet, Ream et al. (2014) found low *VRN1* and *FT* levels in *B. distachyon* accessions with delayed flowering, suggesting a conserved role of these homologs. Further support for a conserved role of *VRN1* and *FT* comes from the observations that overexpression of these genes leads to extremely early flowering (Lv et al., 2014; Ream et al., 2014) and that RNA interference-based silencing of *FT* and artificial microRNA-based silencing of *VRN1* prevent flowering (Lv et al., 2014; Woods et al., 2016b). The role of *VRN2* in *B. distachyon* is less clear. Higgins et al. (2010) failed to identify a homolog of *VRN2* in *B. distachyon*; however, other studies identified *Bradi3g10010* as the best candidate for the *B. distachyon* *VRN2* homolog (Schwartz et al., 2010; Ream et al., 2012). Recent research supports the functional conservation of

*VRN2* in its role as a flowering repressor but suggests that the regulatory interaction between *VRN1* and *VRN2* evolved after the diversification of the Brachypodieae and the core Pooideae (e.g. wheat and barley; Woods et al., 2016b).

To date, most studies on the regulation of flowering time of *B. distachyon* have used reverse genetic approaches to implicate the role of previously characterized genes from other species (Higgins et al., 2010; Lv et al., 2014; Ream et al., 2014; Woods et al., 2016b), while only a few studies have used the natural variation present among *B. distachyon* accessions to identify flowering loci (Tyler et al., 2016; Wilson et al., 2016). Currently lacking is the characterization of loci that control variation in flowering time in a biparental *B. distachyon* mapping population. The Iraqi reference accession Bd21 does not require vernalization (Vogel et al., 2006; Garvin et al., 2008); in addition, vernalization does not greatly reduce time to flowering in a 16- or 20-h photoperiod (Schwartz et al., 2010; Ream et al., 2014). In contrast, the Spanish accession ABR6 can be induced to flower following a 6-week vernalization period (Draper et al., 2001; Routledge et al., 2004).

In this article, we report on the genetic architecture underlying flowering time in a mapping population developed from ABR6 and Bd21. We observed the segregation of vernalization dependency during population advancement (Fig. 1) and characterized the genetic basis of this dependency in detail at the F4:5 stage in multiple environments. The ability to flower without vernalization was linked to three major loci, two of which colocalize with the *B. distachyon* homologs of *VRN2* and *FT*. Notably, our results further support the role of the *VRN2* locus as a conserved flowering time regulator in *B. distachyon*.



**Figure 1.** Flowering behavior within the ABR6 × Bd21 mapping population. Three months after a 6-week vernalization period, ABR6 (left) is not flowering, whereas Bd21 (center) is flowering, and an individual in the ABR6 × Bd21 mapping population displays an intermediate flowering phenotype (right).

## RESULTS

Development of a *B. distachyon* Mapping Population between Geographically and Phenotypically Distinct Accessions

Initial investigations into the flowering time of ABR6 and Bd21 in response to different vernalization periods showed contrasting effects on the two accessions (Figs. 1 and 2). ABR6 responded strongly to increasing vernalization times with a reduction in flowering by 93 d, ranging from 117 d for a 2-week vernalization period to 24 d for an 8-week vernalization period. This reduction in flowering time for ABR6 was not linear, and the greatest drop of 43 d occurred between 4 and 5 weeks of vernalization (Fig. 2). In contrast, no statistically significant difference was found with respect to the vernalization response of Bd21, although a consistent trend toward a reduced flowering time was observed. A cross was generated from these phenotypically diverse accessions for the creation of a recombinant inbred line population. To develop a single-nucleotide polymorphism (SNP)-based genetic map, ABR6 was resequenced, and reads were aligned to the reference genome. A total of 1.36 million putative SNPs were identified between ABR6 and Bd21, of which 711,052 constituted nonambiguous polymorphisms based on a minimum coverage of 15 $\times$  and a strict threshold for

SNP calling (i.e. 100% of reads with an ABR6 allele, 0% of reads with a Bd21 allele). Following iterative cycles of marker selection, the final genetic map consists of 252 nonredundant markers and has a cumulative size of 1,753 centimorgan (cM; Supplemental Fig. S1). This size is comparable to that of the previously characterized Bd3-1  $\times$  Bd21 mapping population (Huo et al., 2011) and confirms that *B. distachyon* has a high rate of recombination compared with other grass species. The quality of the genetic map was verified by assessing the two-way recombination fractions for all 252 markers (Supplemental Fig. S2). All five chromosomes were scanned for segregation distortion by comparing observed and expected genotype frequencies for each marker. The expected heterozygosity at the F4 stage is 12.5%, and the expected allele frequency for each parental genotype is 43.75%. Although all five chromosomes contained regions of potential segregation distortion (Fig. 3), only two loci on chromosomes Bd1 (peak at 474.1 cM) and Bd4 (peak at 77 cM) deviated significantly from these expected frequencies.

Multiple Quantitative Trait Loci Control Flowering in the ABR6  $\times$  Bd21 Mapping Population

We evaluated the ABR6  $\times$  Bd21 F4:5 population in a number of environments to identify the genetic architecture underlying flowering time (Supplemental Table S1; Supplemental Data S1). Four sets of the population were grown without vernalization, whereas in one additional set, flowering was scored in response to 6 weeks of vernalization. In all experiments, the population was exposed to natural light, although in three experiments, supplemental light was used to ensure a minimum 16- or 20-h growth period. In addition, two experiments did not have any temperature control (i.e. plants were exposed to the natural temperature in the greenhouse), two experiments had the temperature controlled at 22°C/20°C during light/dark cycles, and one experiment had the temperature maintained at a minimum of 18°C/11.5°C during light/dark cycles. Analysis of the nonvernalized environments revealed a bimodal distribution between families that flowered and families that did not flower (Fig. 4). However, considerable residual variation in flowering time existed among the flowering families. For example, in environment 5, flowering occurred over a 42-d period from 63 to 105 d after germination (Fig. 4E). Flowering in the other nonvernalized environments occurred over a similar time period (Fig. 4). Interestingly, transgressive segregation for early- and late-flowering phenotypes was observed in environment 4 (Fig. 4D). Phenotypes in the vernalized environment were heavily skewed toward early flowering (Fig. 4B). Only limited residual variation existed among the vernalized F4:5 families, and all plants flowered within 11 d from the first observation of flowering in the population. The variation in flowering time for all five environments was found to be not normally distributed. Among these diverse

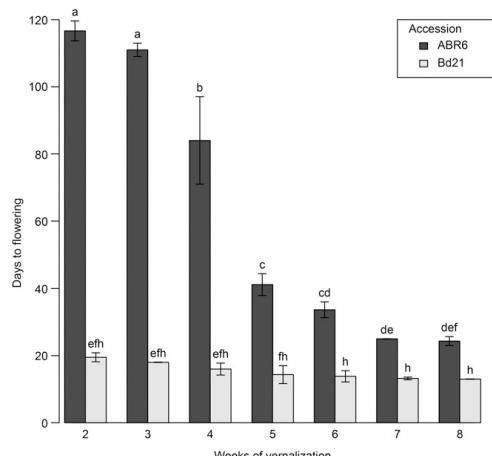


**Figure 2.** Effects of vernalization on flowering time in ABR6 and Bd21. Days to flowering was measured from the end of vernalization for seven different vernalization periods. After vernalization, plants were grown in a growth chamber (16-h photoperiod) for 35 d and then transferred to a greenhouse without light and temperature control (late April to mid July, 2013; Norwich, UK). Mean days to flowering and se are based on six biological replicates. Different letters represent statistically significant differences based on pairwise comparisons using Student's *t* tests with pooled se and Bonferroni correction for multiple comparisons.

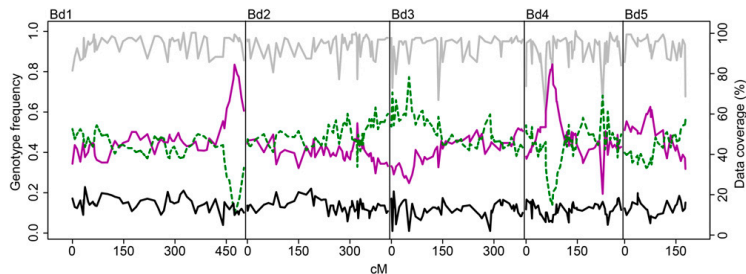


**Figure 3.** Segregation distortion in the ABR6  $\times$  Bd21 F4 population. For each marker of the genetic map, the frequencies of F4 individuals with homozygous ABR6 genotype (solid magenta line), homozygous Bd21 genotype (dashed green line), or heterozygous genotype (solid black line) were calculated (scale on left). Data coverage (percentage of F4 individuals with genotype calls per marker) is represented by the gray line (scale on right).

environments, quantitative trait locus (QTL) analyses using binary and nonparametric models were conservative in detecting QTLs controlling flowering time (*qFLT*; Supplemental Tables S2 and S3), whereas transformation of flowering time consistently identified QTLs between environments (Tables I and II; Supplemental Tables S4 and S5). Three major QTLs were identified on chromosomes Bd1 and Bd3 that were robustly observed using parametric and nonparametric mapping approaches (Tables I and II; Fig. 5). The QTL on Bd1 (*qFLT1*; peak marker Bd1\_47808182) appeared to be the major locus governing flowering time in this population, as it was the major QTL in all five environments, explaining the most phenotypic variation (PVE) compared with any other QTL (Table II). PVE values for this locus ranged from 15.9% to 37.5%. Another QTL on Bd3 (*qFLT6*; peak marker Bd3\_8029207) also was detected in all five studies, although its contribution was significant in only three environments. PVE values for the statistically significant QTLs ranged from 11.8% to 18.7%. Bd21 alleles at these two loci promoted early flowering, whereas individuals with ABR6 alleles at both loci had maximal flowering time or did not flower within the time scale of the experiment (Fig. 6). Interestingly, in the two environments where this former locus did not have a significant contribution, two other QTLs were identified. A QTL on Bd3 (*qFLT7*; peak marker Bd3\_44806296) explained 13.6% and 14% of the variation observed in these studies, and a QTL on Bd2 (*qFLT3*; peak marker Bd2\_53097824) was identified through a combination of nonparametric and parametric analyses of environments 4 and 5. Additional QTLs on Bd1 (*qFLT2*), Bd2 (*qFLT4*), Bd3 (*qFLT5*), and Bd4 (*qFLT8*) were not significant in more than one of the environments tested (Table I).

Previous studies identified the *B. distachyon* homologs of flowering regulators from *Arabidopsis*, wheat, barley, and rice (Higgins et al., 2010; Ream et al., 2012). The 1 – log of the odds (LOD) support intervals of all statistically significant QTLs were combined to identify the maximal 1 – LOD support interval for each QTL. Several of the previously identified *B. distachyon* homologs of flowering regulators are candidate genes underlying these QTLs (Table III). Although several homologs fall within the 1 – LOD support intervals of

*qFLT1* on Bd1 (292.1–305.6 cM) and *qFLT6* on the short arm of Bd3 (72.9–97 cM), these loci also harbor the *B. distachyon* homologs of *FT* (Bradi1g48830) and *VRN2* (Bradi3g10010), which have been implicated previously in flowering time regulation in *B. distachyon* through a series of mainly reverse genetic studies (Lv et al., 2014; Ream et al., 2014; Woods et al., 2014, 2016b).

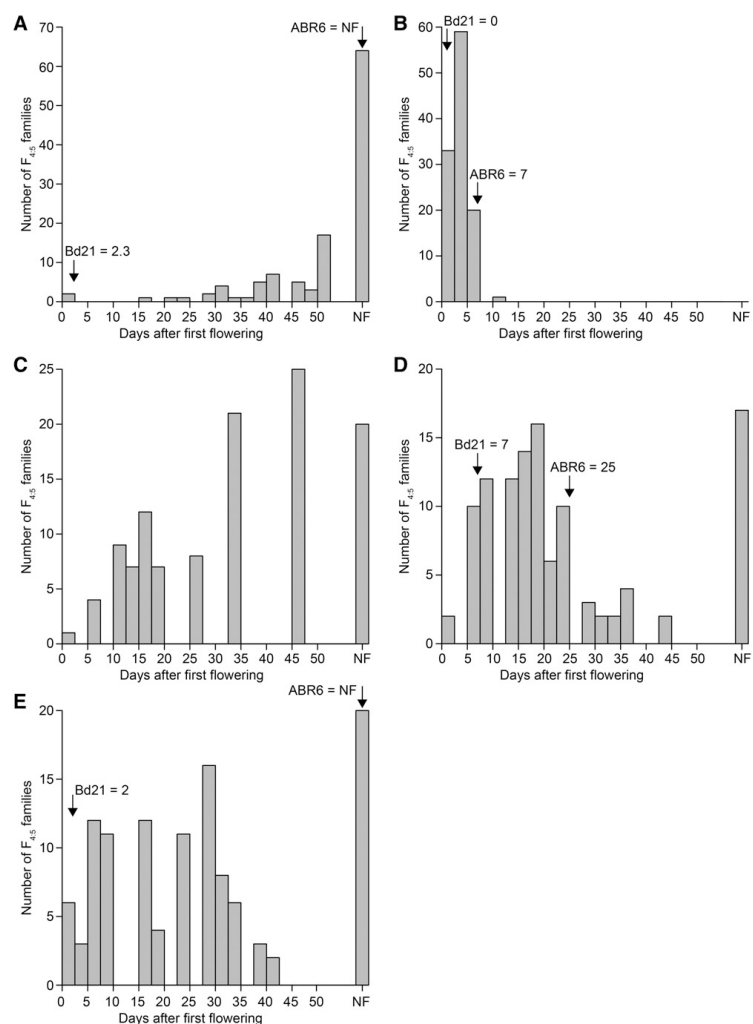
#### Natural Variation in *FT* and *VRN2*

Analysis of the resequencing and RNA sequencing (RNAseq) data allowed an initial evaluation of candidate genes underlying these QTLs. A de novo assembly was created from the ABR6 resequencing reads, and the resulting contigs were probed with the Bd21 sequences of *FT* (Bradi1g48830) and *VRN2* (Bradi3g10010), enabling the identification of structural variation between ABR6 and Bd21 (Fig. 7; Supplemental Table S6). Spliced alignment of RNAseq reads permits the further characterization of candidate genes underlying an identified QTL through the confirmation of polymorphisms between two parental genotypes, verification of annotated candidate gene models, qualitative assessment of the expression of candidate genes in the sampled tissue, and discovery of potential splice variants.

No polymorphisms were found in the coding sequence of Bradi1g48830, the *B. distachyon* homolog of *FT*. However, two indels (2 and 4 bp) and an SNP mapped to the 3' UTR. Additionally, two SNPs and three indels (including a 33-bp indel 590 bp upstream of Bradi1g48830) were found in the promoter region (2 kb upstream). The terminator region (2 kb downstream) contained three SNPs and four indels. Bradi1g48830 was not expressed in ABR6 and was barely detectable in Bd21 (only two reads mapped to the gene). Owing to the low expression, it was not possible to confirm the published gene model with our RNAseq data.

Greater sequence variation was observed at Bradi3g10010, the *B. distachyon* homolog of *VRN2*, and its flanking regions. Only 1.9 kb of the promoter region is present on the Bradi3g10010 contig, but this region contains 29 SNPs and three indels (including an 84-bp indel 1.4 kb upstream of Bradi3g10010). The 2-kb terminator region contains 14 SNPs and three 1-bp indels. Additionally, 11 SNPs and four indels (including a

**Figure 4.** Frequency distribution of flowering time in the ABR6  $\times$  Bd21 population. Flowering time was measured from the first day that flowering was observed in the entire population. A, Environment 1 (April to July; natural light supplemented for 20 h, 22°C/20°C, no vernalization). B, Environment 2 (April to July; natural light supplemented for 20 h, 22°C/20°C, 6 weeks of vernalization). C, Environment 3 (May to July; natural light and temperatures, no vernalization). D, Environment 4 (September to November; natural light supplemented for 16 h, minimum 18°C/11.5°C, no vernalization). E, Environment 5 (March to May; natural light and temperatures, no vernalization). Flowering times for the parental lines are indicated by arrows (no data for environment 3). NF, Not flowering.



37-bp and a 22-bp indel) were localized in the intron, two SNPs in the coding sequence, and four SNPs in the 3' UTR. Bradi3g10010 was expressed in leaves from both Bd21 and ABR6, and spliced alignment of RNAseq reads confirmed the published annotation of Bradi3g10010 for both ABR6 and Bd21. Moreover, the six SNPs predicted in the exons were supported by the RNAseq data, and these may contribute to the observed effect on flowering time in this mapping population. Two SNPs map to the annotated coding sequence and four SNPs map to the 3' UTR. One of the two SNPs in the annotated coding sequence is predicted to cause a nonsynonymous mutation (Fig. 7).

#### Expression of *VRN1*, *VRN2*, and *FT* in Response to Vernalization

To understand the transcriptional dynamics of *VRN1*, *VRN2*, and *FT* in response to vernalization, we assessed steady-state levels of mRNA expression in plants at the fourth leaf stage after exposure to 2, 4, and 6 weeks of vernalization at 5°C or to no vernalization (Fig. 8). *VRN1* and *FT* had a similar pattern in steady-state levels of gene expression in response to vernalization (Fig. 8, A and C). For both genes, very low levels of expression were observed in ABR6, whereas Bd21 had fairly high levels of transcript abundance. After

**Table I.** Significant flowering time QTLs (*qFLT*) in the different environments identified using several binary, nonparametric, and parametric approaches

Dashes, Corresponding QTL was not detected within respective environment.

Locus	Chr <sup>a</sup>	cM	Allele <sup>b</sup>	E1 <sup>c</sup>	E2	E3	E4	E5
<i>qFLT1</i>	Bd1	297.6	Bd21	B, T2, T3, NP <sup>d</sup>	T1, T3, NP	T2, T3, NP	T2, T3	T1, T2, T3, NP
<i>qFLT2</i>	Bd1	465.2	Bd21	T2	—	—	—	—
<i>qFLT3</i>	Bd2	338.3	ABR6	—	—	—	NP	T2, T3
<i>qFLT4</i>	Bd2	409.0	Bd21	—	T1, T3	—	—	—
<i>qFLT5</i>	Bd3	60.8	Bd21	—	—	—	T1	—
<i>qFLT6</i>	Bd3	91.2	Bd21	T2, T3	T1, T3	T2, T3	—	—
<i>qFLT7</i>	Bd3	294.6	Bd21	—	—	—	T2, T3, NP	B, T2, T3, NP
<i>qFLT8</i>	Bd4	90.1	Bd21	—	—	—	NP	—

<sup>a</sup>Chromosome. <sup>b</sup>Allele that reduces flowering time. <sup>c</sup>E1 to E5, Environment (see Supplemental Table S1). <sup>d</sup>QTL analyses were performed with interval mapping using binary classification (B) and nonparametric analysis (NP) and composite interval mapping using transformed data (T1, T2, and T3).

experiencing 4 weeks of vernalization, ABR6 had similar levels of *VRN1* transcript to Bd21 without vernalization treatment. In contrast, *FT* expression had a marginal increase after 4 and 6 weeks of vernalization in ABR6 relative to no vernalization or 2 weeks of vernalization. *FT* expression levels were significantly lower than in Bd21 across all periods of vernalization. Both *VRN1* and *FT* expression increased significantly between Bd21 samples vernalized for 2 or 4 weeks. *VRN2* expression in ABR6 was inversely correlated with the length of vernalization, with similar levels of expression after no vernalization and 2 weeks of vernalization and increasingly lower levels of expression after 4 and 6 weeks of vernalization (Fig. 8B). Bd21 exhibited a similar reduction in *VRN2* expression, although lower levels of expression were observed without vernalization compared with ABR6 with 6 weeks vernalization. The trends of all three genes highlighted the importance of 4 weeks of vernalization as the inflection point in transcriptional abundance, which coincides with a significant reduction in days to flowering in ABR6 (Fig. 2).

## DISCUSSION

In our advancement of the ABR6 × Bd21 population, we observed substantial variation in flowering time. To define the genetic architecture of flowering time, we developed a comprehensive genetic map and assessed F4:5 families in multiple environments. We uncovered three major QTLs, with two QTLs coincident with the *B. distachyon* homologs of *VRN2* and *FT*. Interestingly, *VRN1* was not associated with flowering time and was found to have no mutations within the transcribed sequence (Supplemental Table S6). Further minor-effect QTLs were identified, suggesting that additional regulators play a role in controlling flowering time in *B. distachyon*.

### Segregation Distortion in the ABR6 × Bd21 Population

Segregation distortion is a common observation in the development of mapping populations in plants, including grasses such as rice, *Aegilops tauschii*, maize (*Zea mays*), or barley (Xu et al., 1997; Faris et al., 1998; Lu et al., 2002; Muñoz-Amatriñ et al., 2011). In the

**Table II.** Significant QTLs from composite interval mapping of transformed flowering time phenotypes (T3) in the ABR6 × Bd21 F4:5 families

ENV <sup>a</sup>	Locus	Chr <sup>b</sup>	cM	EWT <sup>c</sup>	LOD	AEE <sup>d</sup>	PVE <sup>e</sup>	1 – LOD SI <sup>f</sup>
1	<i>qFLT1</i>	Bd1	297.6	3.06	12.96	2.87	36.3%	296.1–305.6
1	<i>qFLT6</i>	Bd3	91.2	3.06	4.51	1.64	11.8%	ND
2	<i>qFLT1</i>	Bd1	297.6	3.09	7.59	0.82	20.0%	296.1–305.6
2	<i>qFLT4</i>	Bd2	409.0	3.09	3.20	0.47	6.7%	403.2–411.0
2	<i>qFLT6</i>	Bd3	93.2	3.09	6.64	0.79	18.2%	72.9–97.0
3	<i>qFLT1</i>	Bd1	297.6	3.20	8.61	1.50	31.1%	292.1–303.6
3	<i>qFLT6</i>	Bd3	91.2	3.20	5.69	1.20	18.7%	74.9–97.0
4	<i>qFLT1</i>	Bd1	297.6	3.19	3.49	1.77	15.9%	292.1–305.6
4	<i>qFLT7</i>	Bd3	294.6	3.19	3.79	1.59	14.0%	273.9–300.7
5	<i>qFLT1</i>	Bd1	297.6	3.17	8.62	3.43	37.5%	294.1–301.6
5	<i>qFLT3</i>	Bd2	338.3	3.17	3.70	–1.75	9.9%	323.7–348.0
5	<i>qFLT7</i>	Bd3	294.6	3.17	5.61	2.02	13.6%	275.9–302.0

<sup>a</sup>Environment (see Supplemental Table S1). <sup>b</sup>Chromosome. <sup>c</sup>Experiment-wide permutation threshold. <sup>d</sup>Additive effect estimate for transformed phenotypes. <sup>e</sup>Percentage of phenotypic variance explained. <sup>f</sup>The 1 – LOD support interval (cM). ND denotes QTLs not detected using standard interval mapping.

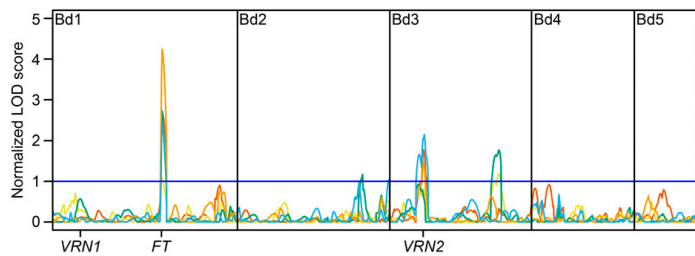


**Figure 5.** Linkage mapping of flowering time in the ABR6 × Bd21 population. Time to flowering for 114 F4:5 families of the population was transformed into ordered rank values, QTL analysis was performed using composite interval mapping under an additive model hypothesis test ( $H_0: H_1$ ), and data were plotted based on normalized permutation thresholds. The blue horizontal line represents the threshold of statistical significance based on 1,000 permutations. Orange line = environment 1 (April to July; natural light supplemented for 20 h, 22°C/20°C, no vernalization), blue line = environment 2 (April to July; natural light supplemented for 20 h, 22°C/20°C, 6 weeks of vernalization), red line = environment 3 (May to July; natural light and temperatures, no vernalization), yellow line = environment 4 (September to November; natural light supplemented for 16 h, minimum 18°C/11.5°C, no vernalization), and green line = environment 5 (March to May; natural light and temperatures, no vernalization). For full environmental details, see Supplemental Table S1. The genetic positions of the previously identified homologs of *VRN1*, *VRN2*, and *FT* are indicated (compare Higgins et al., 2010, and Ream et al., 2012).

ABR6 × Bd21 population, significant deviation from expected genotype frequencies was observed at two loci on chromosomes Bd1 and Bd4 (Fig. 3). Interestingly, heterozygosity was not affected at these loci, but the ABR6 allele was overrepresented. It is likely that these loci are linked to traits that were selected inadvertently during population advancement based on genetic and/or environmental factors. Several genetic mechanisms can contribute to segregation distortion in intraspecific crosses, including hybrid necrosis (Bomblies and Weigel, 2007), genes involved in vernalization requirement and flowering time (such as the *vri2* locus in the Haruna Nijo × OHU602 doubled-haploid barley population; Muñoz-Amatriaín et al., 2011), or preferential transmission of a specific parental genotype. While segregation distortion at these loci was not associated with the identified flowering time QTLs, canonical resistance genes encoding nucleotide-binding, Leu-rich repeat proteins are present at the Bd4 locus (Bomblies et al., 2007; Tan and Wu, 2012).

#### The Genetic Architecture of Flowering Time in *B. distachyon*

In *Arabidopsis*, natural variation has been used as a complementary forward genetics-based approach for investigating flowering time (Koornneef et al., 2004). In our work, we identified two major QTLs controlling flowering time (*qFLT1* and *qFLT6*; Fig. 6) in both vernalized and nonvernalized environments that colocalized with the *B. distachyon* homologs of *FT* (Bradi1g48830) and *VRN2* (Bradi3g10010). These observations are consistent with previous reverse genetic studies on the role of *FT* and *VRN2* in controlling flowering time (Lv et al., 2014; Ream et al., 2014; Woods et al., 2014, 2016b). Two additional QTLs on chromosomes Bd2 (*qFLT3*) and Bd3 (*qFLT7*)

were detected in two environments, whereas four minor-effect QTLs (*qFLT2*, *qFLT4*, *qFLT5*, and *qFLT8*) were found in individual environments only. Two recent genome-wide association studies used the natural variation found within *B. distachyon* germplasm to identify SNPs associated with flowering time (Tyler et al., 2016; Wilson

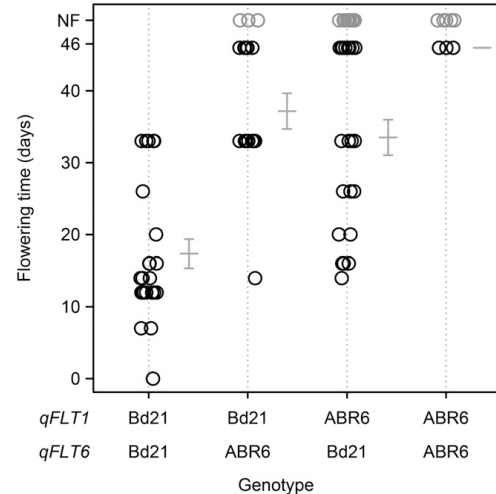


**Figure 6.** Phenotype-by-genotype plot for the two major loci controlling flowering time in the ABR6 × Bd21 mapping population. Days to flowering in environment 3 for the ABR6 × Bd21 F4:5 families homozygous at *qFLT1* and *qFLT6* shows that the Bd21 alleles at these two loci promote early flowering. Error bars represent 1 se; NF, not flowering.

**Table III.** Previously identified *B. distachyon* homologs of flowering regulators in *Arabidopsis* (*At*), hexaploid and diploid wheat (*Ta* and *Tm*), barley (*Hv*), and rice (*Os*) within the 1 – LOD support intervals of the statistically significant QTLs under transformation T3

Locus	Chr <sup>a</sup>	1 – LOD SI <sup>b</sup>	<i>B. distachyon</i> Gene	Homologous Genes <sup>c</sup>
<i>qFLT1</i>	Bd1	292.1–305.6	Bradi1g45810	AtAGL24, <i>TaVRT2</i> , <i>OsMADS55</i>
			Bradi1g46060	AtABF1
			Bradi1g48340	AtCLF, <i>OsCLF</i>
			Bradi1g48830	AtTSF, <i>HvFT1</i> , <i>OsHd3a/OsFTL2</i>
<i>qFLT3</i>	Bd2	323.7–348.0	Bradi2g53060	AtFDP
			Bradi2g54200	AtNF-YB10
			Bradi2g55550	AtbZIP67
<i>qFLT4</i>	Bd2	403.2–411.0	Bradi2g60820	AtFY, <i>OsFY</i>
			Bradi2g62070	AtLUX, <i>OsLUX</i>
<i>qFLT6</i>	Bd3	72.9–97.0	Bradi3g08890	OsFTL13
			Bradi3g10010	<i>TaVRN2</i> , <i>TmCCT2</i> , <i>OsGhd7</i>
<i>qFLT7</i>	Bd3	273.9–300.7	Bradi3g12900	AtHUA2
			Bradi3g41300	OsMADS37
			Bradi3g42910	AtSPY, <i>OsSPY</i>
			Bradi3g44860	OsRCN2

<sup>a</sup>Chromosome. <sup>b</sup>Combined maximal 1 – LOD support interval (cM) from all significant QTLs.

<sup>c</sup>Identified by Higgins et al. (2010) and Ream et al. (2012).

et al., 2016). Tyler et al. (2016) identified nine significant marker-trait associations, none of which overlap with the QTLs identified in our study. In contrast, Wilson et al. (2016) identified a much simpler genetic architecture consisting of three significant marker-trait associations, one of which could be linked to *FT*. These additional QTLs and marker-trait associations identified in our study and the genome-wide association studies could either correspond to one of the identified homologs of flowering genes in *B. distachyon* (Table III; Higgins et al., 2010) or constitute novel loci as hypothesized by Schwartz et al. (2010). With the exception of the proximal QTL on Bd2 (*qFLT3*), all alleles that prolonged time to flowering in our study were contributed by ABR6 (Table I). Bd21 has been classified previously as a spring annual (Schwartz et al., 2010) or extremely rapid flowering (Ream et al., 2014). However, increased vernalization times still led to a modest

reduction in flowering time (Fig. 2), which is explained by the detection of a QTL contributed by Bd21.

We hypothesized that structural variation between ABR6 and Bd21 would underlie the observed variation in flowering time. No structural variation in *FT* was observed between ABR6 and Bd21 in the coding sequence; however, several indels map to the promoter region (Fig. 7). These polymorphisms may explain the expression differences between these two accessions. As expected, no *FT* expression was found in ABR6 seedlings, and only two Bd21 RNAseq reads mapped to this gene. Steady-state expression levels of *FT* in the fourth leaf were significantly lower in ABR6 relative to Bd21 without vernalization (Fig. 8C). After 4 weeks of vernalization, *FT* expression levels increased in ABR6, although they were significantly lower than Bd21 steady-state levels after any level of vernalization. It was shown previously that in barley, wheat, and

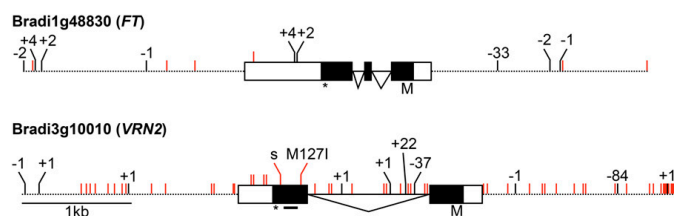


**Figure 7.** Comparison of the flowering regulators *FT* and *VRN2* between the *B. distachyon* accessions Bd21 and ABR6. Contigs of the ABR6 de novo assembly were aligned to the Bd21 reference sequence (version 3), and polymorphisms were identified in the genes of interest and 2-kb promoter and terminator sequences (1.9-kb promoter for *VRN2*). Red ticks represent SNPs, and black ticks represent insertions/deletions (indels). The length of indels (bp) is shown with + for insertion and – for deletion. The amino acid change of the nonsynonymous SNP in *VRN2* is indicated. s = synonymous SNP; dashed line = promoter or terminator; white box = 5' untranslated region (UTR) or 3' UTR; black box = exon; black line = intron; M = Met/translation start; star = translation stop; black bar under *VRN2* = CCT domain.

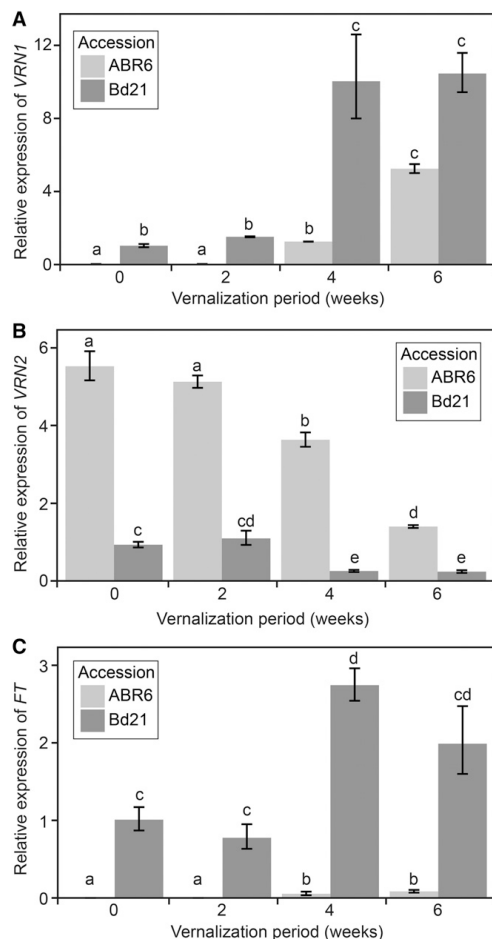


**Figure 8.** *VRN1*, *VRN2*, and *FT* expression in the fourth leaf of ABR6 and Bd21 after varying periods of cold treatment. Seeds were imbibed with water and not vernalized or vernalized for 2, 4, or 6 weeks and transferred to a growth chamber with parameters similar to environment 2. Fully expanded fourth leaves were harvested in the middle of the photoperiod. Relative gene expression of *VRN1* (A), *VRN2* (B), and *FT* (C) was determined using reverse transcription-quantitative PCR and analyzed using the  $2^{-\Delta\Delta Ct}$  method. All genes were normalized to 1 based on Bd21 expression with no cold treatment (0 weeks), and *UBIQUITIN-CONJUGATING ENZYME18* was used as an internal control. Bars represent means of three biological replicates, with error bars showing 1 se. Different letters represent statistically significant differences based on pairwise Student's *t* tests using a multiple hypothesis-corrected *P* value threshold of 0.05 with the Benjamini-Hochberg approach (Benjamini and Hochberg, 1995).

*B. distachyon*, *FT* expression is up-regulated after vernalization (Sasani et al., 2009; Chen and Dubcovsky, 2012; Ream et al., 2014). Our observations indicate that

*FT* is expressed in Bd21 and increases less than *VRN1* in response to vernalization. In contrast, *FT* in ABR6 increases only marginally after 4 weeks of vernalization and remains significantly below the levels observed in Bd21 after no vernalization.

Interestingly, an intact copy of the flowering repressor *VRN2* also is present in Bd21 (Ream et al., 2012), which does not have a strong vernalization response (Vogel et al., 2006; Garvin et al., 2008). The lack of a vernalization requirement in some *B. distachyon* accessions, therefore, cannot be explained by an absence of *VRN2* (Ream et al., 2012). Intriguingly, early-flowering mutants identified in genetic screens thus far have not mapped in the *VRN2* region (Ream et al., 2014). Moreover, expression levels for *VRN2* also did not vary among early- and late-flowering accessions, and *VRN2* mRNA levels are likely not rate limiting (Ream et al., 2014). An earlier study by Schwartz et al. (2010) described a potential correlation between different *VRN2* alleles and flowering time. The authors did not rule out the effects of population structure and proposed that elucidating the role of *VRN2* in *B. distachyon* will require more in-depth genetic studies. A recent comprehensive analysis of population structure in *B. distachyon* collections revealed that flowering time, and not geographic origin, is indeed the major distinguishing factor between genetically distinct clusters (Tyler et al., 2016). Our results confirm *VRN2* as an important flowering regulator in the ABR6  $\times$  Bd21 mapping population and highlight structural and expression variation between parental accessions. However, none of the SNPs identified in the coding sequence map to the CCT domain. A point mutation in this domain results in a spring growth habit in cultivated *Triticum monococcum* accessions (Yan et al., 2004). It is unclear whether the structural variation surrounding *VRN2* corresponds to the allelic variation observed by Schwartz et al. (2010). Woods and Amasino (2016) hypothesize that, even though *VRN2* may not be involved in vernalization control in *B. distachyon*, it may still possess an ancestral role in flowering regulation. This is further supported by the observation that *VRN2* expression is not controlled by *VRN1* in *B. distachyon*, yet *VRN2* was found to be a functional repressor of flowering in this species (Woods et al., 2016b). We observed a negative correlation between *VRN2* transcript accumulation and vernalization period in ABR6 and Bd21 (Fig. 8B). Similar decreases were observed for ABR6 and Bd21, although transcript abundance in Bd21 was significantly lower than in ABR6 under any vernalization period. Therefore, our identification of natural variation in *VRN2* among geographically diverse *B. distachyon* accessions further supports *VRN2* as a core flowering regulator in this nondomesticated grass.

In our study of the natural variation between two morphologically and geographically diverse *B. distachyon* accessions, we failed to implicate *VRN1* as a flowering regulator. However, *VRN1* expression during and after cold treatment and the failure of *VRN1*-silenced lines to flower suggest a conserved role of *VRN1* as a promoter of flowering (Woods and Amasino, 2016; Woods et al.,

2016b). Interestingly, a QTL in the Bd21 × Bd1-1 *B. distachyon* mapping population colocalized with *VRN1* and the light receptor *PHYTOCHROME C* (Woods et al., 2016a). Between ABR6 and Bd21, sequence variation was found in the promoter and terminator regions of *VRN1*, and a strong positive correlation was observed with extended periods of vernalization (Fig. 8A), particularly at 4 weeks of vernalization, which was a critical inflection point for flowering time in ABR6. Despite this sequence and expression variation, *VRN1* was not found to contribute to flowering time in the ABR6 × Bd21 mapping population. Interestingly, an assessment of allelic variation in 53 *B. distachyon* accessions currently available in Phytozome (version 11.0.2; <https://phytozome.jgi.doe.gov>) found that none of these accessions possess structural variation in the *VRN1* annotated coding sequence. These findings suggest that *VRN1* is a crucial regulator of flowering in *B. distachyon* and under strong selection pressure.

## CONCLUSION

Thanks to their economic and evolutionary importance, flowering time pathways are of particular interest in the cereals and related grasses. Our report adds to this body of research by using natural variation to map vernalization dependency in a *B. distachyon* mapping population. Since *B. distachyon* is partly sympatric with the wild relatives of wheat and barley, it seems likely that the species would have been subjected to similar selective pressure and, therefore, is a useful model for understanding predomestication or standing variation. We investigated this standing variation by assessing the segregation of flowering regulators in a mapping population derived from two geographically diverse accessions of *B. distachyon*. Notably, we found additional support for the roles of *FT* and *VRN2* in controlling flowering in wild temperate grasses. Additionally, allelic variation may explain the ambiguity around the role of the *VRN2* homolog observed in *B. distachyon*. Further fine-mapping will be required to confirm the roles of these genes in *B. distachyon* flowering time. However, we also detected novel components in the form of additional QTLs, which reflects the power of studying natural variation in mapping populations derived from phenotypically diverse parents. During population advancement, we observed a variety of additional morphological and pathological characteristics segregating in this population, and it will serve as a useful resource for other researchers investigating standing variation in nondomesticated grasses.

## MATERIALS AND METHODS

### Plant Growth for Assessing ABR6 and Bd21 Vernalization Responses

Six seeds for *Brachypodium distachyon* ABR6 and Bd21 were germinated on paper (in darkness at room temperature) and transferred to an equal mixture of the John Innes Cereal Mix and a peat and sand mix (Vain et al., 2008) 4 d after

germination. Vernalization was initiated 14 d after germination for 2, 3, 4, 5, 6, 7, or 8 weeks (8-h daylength, 1.2 klux light intensity, and 5°C). The different sets were staggered to ensure that all sets left vernalization on the same date. After vernalization, plants were grown in a Sanyo Versatile Environmental Test Chamber (model MLR-351; 16-h photoperiod, 8 klux light intensity, and 22°C/20°C day/night temperatures) for 35 d and then transferred to a greenhouse without light and temperature control (late April to mid July, 2013; Norwich, UK). Days to flowering was measured from the end of vernalization until the emergence of the first spike and was averaged across all six biological replicates (only five replicates were available for Bd21 after 7 weeks of vernalization). Statistical significance was assessed by pairwise comparisons using Student's *t* tests with pooled *sd* and Bonferroni correction for multiple comparisons.

### Resequencing of ABR6

Seeds were grown in a Sanyo Versatile Environmental Test Chamber (16-h photoperiod, 8 klux light intensity, and 22°C) in an equal mixture of the John Innes Cereal Mix and a peat and sand mix. Seven-week-old plants were placed in darkness for 3 d prior to collecting tissue. Genomic DNA was extracted using a standard cetyl-trimethyl-ammonium bromide protocol, and a library of 800-bp inserts was constructed and sequenced with 100-bp paired-end reads and an estimated coverage of 25.8× on an Illumina HiSeq 2500. Library preparation and sequencing were performed at The Genome Analysis Centre. The resulting reads were mapped to the Bd21 reference sequence (version 1; International Brachypodium Initiative, 2010) with the Galaxy wrapper, which used the BWA (version 0.5.9) aligner and sampe options (Li and Durbin, 2009). Polymorphisms between ABR6 and Bd21 were identified with the mpileup2snp and mpileup2indel tools of VarScan (version 2.3.6) using default settings (Koboldt et al., 2009). A de novo assembly was created from the raw ABR6 reads using default settings of the CLC Assembly Cell (version 4.2.0) and default parameters. Potential structural variation between ABR6 and Bd21 was investigated by performing a BLAST search with the Bd21 regions of interest against the ABR6 de novo assembly and mapping contigs for hits with at least 95% identity and an *E* value under  $1e^{-20}$  to the Bd21 reference sequence (version 3).

### Development of the ABR6 × Bd21 F4 Population and Genetic Map

The *B. distachyon* accessions ABR6 and Bd21 were crossed, and three ABR6 × Bd21 F1 individuals, confirmed as hybrid by simple sequence repeat marker analysis (data not shown), were allowed to self-pollinate to generate a founder F2 population composed of 155 individuals. After single-seed descent, DNA was extracted from leaf tissue of 114 independent F4 lines using a cetyl-trimethyl-ammonium bromide genomic DNA extraction protocol modified for plate-based extraction (Dawson et al., 2016). SNPs for genetic map construction were selected based on a previously characterized Bd21 × Bd3-1 F2 genetic map to ensure an even distribution of markers relative to physical and genetic distances (Huo et al., 2011). SNPs without additional sequence variation in a 120-bp window were selected every 10 cM. The Agena Bioscience Mass-ARRAY design suite was used to develop 17 assays that genotyped 449 putative SNPs using the iPLEX Gold assay at the Iowa State University Genomic Technologies Facility (Supplemental Data S2). Markers were excluded for being monomorphic (106), dominant (34), or for missing data for the parental controls (33). Heterozygous genotype calls for some markers were difficult to distinguish and classified as missing data. Additional SNPs between ABR6 and Bd21 in six markers developed for the Bd21 × Bd3-1 F2 genetic map (Barbieri et al., 2012) were converted into cleaved-amplified polymorphic sequence markers (Konieczny and Ausubel, 1993; Supplemental Table S7). The integrity of these 282 markers was evaluated using R/qtl (version 1.33-7) recombination fraction plots (Broman et al., 2003). Two markers were removed for not showing linkage, and one marker was moved to its correct position based on linkage. Genetic distances were calculated using the Kosambi function in MapManager QT (version b20; Manly et al., 2001). Removal of unlinked and redundant markers produced a final ABR6 × Bd21 F4 genetic map consisting of 252 SNP-based markers (Supplemental Data S3). Segregation distortion was assessed using a  $\chi^2$  test with Bonferroni correction for multiple comparisons.

### Plant Growth and Phenotyping of Flowering Time in the ABR6 × Bd21 F4:5 Families

Three to five plants for each of the 114 ABR6 × Bd21 F4:5 families were grown under five different environmental conditions as detailed in Supplemental

Table S1. For the phenotyping performed in Aberystwyth, individual seeds were sown in 6-cm pots with a mixture of 20% grit sand and 80% Levington F2 peat-based compost. Seeds were grown for 2 weeks in greenhouse conditions (22°C/20°C and natural light supplemented with 20 h of lighting) and then either maintained in the greenhouse or transferred to a vernalization room for 6 weeks (16-h daylength at 5°C). Plants were returned to the greenhouse following vernalization and grown to maturity. Flowering time was defined as the emergence of the first inflorescence and was measured from the first day that flowering was observed in the entire mapping population. Flowering time was averaged across the individuals of an F4:5 family. For the phenotyping performed in Norwich, plants were first subjected to growth conditions and pathogen assays as described by Dawson et al. (2015). Plants were germinated in a peat-based compost in 1-L pots and grown for 6 weeks in a controlled environment room (18°C/11°C and a 16-h light period). Six weeks post germination, the fourth or fifth leaf of each plant was cut off for pathological assays. The plants were transplanted into 9-cm pots with an equal mixture of the John Innes Cereal Mix and a peat and sand mix (Vain et al., 2008) and transferred to the respective growth environments for flowering assessment (Supplemental Table S1). Flowering time was defined as the emergence of the first inflorescence within an F4:5 family and was measured from the first day that flowering was observed in the entire mapping population. Families that did not flower 60 d after emergence of the first inflorescence in the mapping population were scored as not flowering.

#### QTL Analysis for Flowering Time

Flowering phenotypes were assessed for normality using the Shapiro-Wilk test (Royston, 1982). In an initial analysis, phenotypic values were converted into a binary classification based on whether families flowered or did not flower. Interval mapping was performed with the scanone function in R/qt under a binary model with conditional genotype probabilities computed with default parameters and the Kosambi map function (Xu and Atchley, 1996; Broman et al., 2006). Simulation of genotypes was performed with a fixed step distance of 2 cM, 128 simulation replicates, and a genotyping error rate of 0.001. Statistical significance for QTLs was determined by performing 1,000 permutations and controlled at  $\alpha = 0.05$  (Doerge and Churchill, 1996). Nonparametric interval mapping was performed with similar parameters in R/qt under an np model (Kruglyak and Lander, 1995). For parametric mapping, flowering time data were transformed using the following approaches: T1, the removal of all F4:5 families that did not flower within the time scale of the experiment; T2, transforming all nonflowering phenotypic scores to 1 d above the maximum observed; and T3, transforming by ranking families according to their flowering time. For the third transformation approach (T3), the earliest flowering family was given a rank score of 1, and subsequent ordered families were given incremental scores based on rank (2, 3, 4, etc.). When two or more families had a shared flowering time, they were given the same rank, and the next ranked family was given an incremental rank score based on the number of preceding shared rank families. Nonflowering families were given the next incremental rank after the last flowering rank. For all three transformations, composite interval mapping was performed under an additive model ( $H_1H_2$ ) using QTL Cartographer (version 1.17) with the selection of five background markers, a walking speed of 2 cM, and a window size of 10 cM (Zeng, 1993, 1994; Basten et al., 2004). Statistical significance for QTLs was determined by performing 1,000 permutations with reselection of background markers and controlled at  $\alpha = 0.05$  (Doerge and Churchill, 1996; Lauter et al., 2008). The 1 – LOD support intervals were estimated based on interval mapping (Lander and Botstein, 1989).

#### RNAseq of ABR6 and Bd21

Plants were grown in a controlled environment room with 16 h of light at 22°C, and fourth and fifth leaves were harvested as soon as the fifth leaf was fully expanded (roughly 28 d after germination). RNA was extracted using TRI Reagent (Sigma-Aldrich) according to the manufacturer's specifications. TruSeq libraries were generated from total RNA, and mean insert sizes were 251 and 254 bp for ABR6 and Bd21, respectively. Library preparation and sequencing were performed at The Genome Analysis Centre. Sequencing was carried out using 150-bp paired-end reads on an Illumina HiSeq 2500, and ABR6 and Bd21 yielded 38,867,987 and 37,566,711 raw reads, respectively. RNAseq data quality was assessed with FastQC, and reads were removed using Trimmomatic (version 0.32; Bolger et al., 2014) with parameters set at ILLUMINACLIP:TruSeq 3-PE:fa:2:30:10, LEADING:3, TRAILING:3, SLIDINGWINDOW:4:15, and MINLEN:100. These parameters will remove all reads with adapter sequence, ambiguous bases, or a substantial reduction in read quality. The sequenced reads were mapped to the

Bd21 reference genome using the TopHat (version 2.0.9) spliced alignment pipeline (Trapnell et al., 2009).

#### Reverse Transcription-Quantitative PCR Analyses

ABR6 and Bd21 seeds were surface sterilized (70% ethanol for 30 s, washed in autoclaved deionized water, 1.3% sodium hypochlorite for 4 min, and washed in autoclaved water three times), transferred to moistened Whatman filter paper, left at room temperature in darkness overnight, and vernalized for 2, 4, or 6 weeks (in darkness at 5°C). A control set was surface sterilized and transferred to filter paper overnight but not vernalized. Following vernalization, plants were transferred to soil and grown in a Sanyo Versatile Environmental Test Chamber in conditions similar to environment 2 (20-h photoperiod, 4 klux light intensity, and 22°C/20°C). Once fully expanded, fourth leaves were collected in the middle of the photoperiod and flash frozen in liquid nitrogen.

Total RNA was extracted using TRI Reagent according to the manufacturer's instructions (Sigma-Aldrich). RNA samples were treated with DNase I (Roche) prior to cDNA synthesis. The quality and quantity of RNA samples were assessed using a NanoDrop spectrophotometer followed by agarose electrophoresis. First-strand cDNA was synthesized according to the manufacturer's instructions (Invitrogen). Briefly, 1 µg of total RNA, 1 µL of 0.5 µM poly-T primers, and 1 µL of 10 mM deoxyribonucleotide triphosphate were incubated at 65°C for 5 min and 4°C for 2 min, with subsequent reverse transcription reactions performed using 2 µL of 10X reverse transcription buffer, 4 µL of 25 mM MgCl<sub>2</sub>, 2 µL of 0.1 M dithiothreitol, 1 µL of RNaseOUT (40 units µL<sup>-1</sup>), and 1 µL of SuperScript III reverse transcriptase (200 units µL<sup>-1</sup>) at 50°C for 50 min. Reverse transcription was inactivated by incubating at 85°C for 5 min, and residual RNA was removed with the addition of 1 µL of RNase H (2 units µL<sup>-1</sup>) and incubation at 37°C for 20 min.

Quantitative real-time PCR was performed in 20-µL reaction volumes using 10 µL of SYBR Green mix (Sigma-Aldrich), 1 µL of 10 µM forward and reverse primers, 4 µL of water, and 4 µL of cDNA diluted 10-fold. The program for PCR amplification involved an initial denaturation at 95°C for 3 min and then 40 cycles of 94°C for 10 s, 60°C for 15 s, and 72°C for 15 s. Fluorescence data were collected at 72°C at the extension step and during the melting curve program on a CFX96 Real-Time system (Bio-Rad).

Relative gene expression was determined using the  $2^{-\Delta\Delta CT}$  method described by Livak and Schmittgen (2001) using *UBIQUITIN-CONJUGATING ENZYME18* (Hong et al., 2008; Schwartz et al., 2010) for normalization. All primers were used previously by Ream et al. (2014) and had PCR efficiency ranging from 95% to 110%. Statistical analysis of gene expression was performed using R (version 3.2.3). Comparisons between all genotype-by-treatment combinations were made with pairwise Student's *t* tests using log-transformed relative expression levels, with *P* values corrected for multiple hypothesis testing based on the Benjamini-Hochberg approach (Benjamini and Hochberg, 1995).

#### Accession Numbers

Raw resequencing reads of ABR6 have been submitted to the National Center for Biotechnology Information Short Read Archive under the BioProject identifier PRJNA319372 and SRA accession number SRX1720894. The ABR6 de novo assembly has been deposited at the DNA Data Bank of Japan/European Nucleotide Archive/GenBank under accession number LXJMO10000000. The version described in this article is version LXJMO10000000. Raw RNAseq reads have been submitted to the National Center for Biotechnology Information Short Read Archive under the BioProject identifier PRJNA319373 and SRA accession numbers SRX1721358 (ABR6) and SRX1721359 (Bd21).

#### Supplemental Data

The following supplemental materials are available.

**Supplemental Figure S1.** Linkage groups of the ABR6 × Bd21 genetic map.

**Supplemental Figure S2.** Two-way recombination fraction plot for the ABR6 × Bd21 F4 population.

**Supplemental Table S1.** Summary of the environmental conditions tested.

**Supplemental Table S2.** Significant QTLs from interval mapping of the binary classification of flowering time phenotypes in the ABR6 × Bd21 F4:5 families.

**Supplemental Table S3.** Significant QTLs from interval mapping using a nonparametric model for flowering time phenotypes in the ABR6 × Bd21 F4:5 families.

**Supplemental Table S4.** Significant QTLs from composite interval mapping of transformed flowering time phenotypes in the ABR6 × Bd21 F4:5 families (T1).

**Supplemental Table S5.** Significant QTLs from composite interval mapping of transformed flowering time phenotypes in the ABR6 × Bd21 F4:5 families (T2).

**Supplemental Table S6.** Summary of the structural variation between Bd21 and ABR6 for the flowering regulators Bradi1g48830 (FT), Bradi3g10010 (VRN2), and Bradi1g08340 (VRN1).

**Supplemental Table S7.** Five cleaved-amplified polymorphic sequence markers included in the ABR6 × Bd21 genetic map design.

**Supplemental Data S1.** Raw, binary, and transformed flowering time data for the ABR6 × Bd21 F4:5 families in the five environments tested.

**Supplemental Data S2.** Sequence information used to develop iPLEX assays for the 247 MassARRAY markers in the ABR6 × Bd21 genetic map design.

**Supplemental Data S3.** ABR6 × Bd21 genetic map.

#### ACKNOWLEDGMENTS

We thank John Vogel for sharing preliminary sequencing data, Burkhard Steuernagel for assistance with the de novo assembly of the ABR6 genome, David Garvin and Luis Mur for providing seed, and Claire Collett, Ray Smith, Tom Thomas, and Aliyah Debbonaire for assistance with population progression. MassARRAY genotyping was performed at the Genomic Technologies Facility at Iowa State University.

Received May 26, 2016; accepted September 18, 2016; published September 20, 2016.

#### LITERATURE CITED

Amasino R (2010) Seasonal and developmental timing of flowering. *Plant J* 61: 1001–1013

Andrés F, Coupland G (2012) The genetic basis of flowering responses to seasonal cues. *Nat Rev Genet* 13: 627–639

Barbieri M, Marcel TC, Niks RE, Francia E, Pasquariello M, Mazzamurro V, Garvin DF, Pecchioni N (2012) QTLs for resistance to the false brome rust *Puccinia brachypodii* in the model grass *Brachypodium distachyon* L. *Genome* 55: 152–163

Basten CJ, Weir BS, Zeng ZB (2004) QTL Cartographer, version 1.17. Department of Statistics, North Carolina State University, Raleigh, NC

Benjamini Y, Hochberg Y (1995) Controlling the false discovery rate: a practical and powerful approach to multiple testing. *J R Stat Soc Series B Stat Methodol* 57: 289–300

Bolger AM, Lohse M, Usadel B (2014) Trimmomatic: a flexible trimmer for Illumina sequence data. *Bioinformatics* 30: 2114–2120

Bombalis K, Leme J, Epple P, Warthmann N, Lanz C, Dangl JL, Weigel D (2007) Autoimmune response as a mechanism for a Dobzhansky–Muller-type incompatibility syndrome in plants. *PLoS Biol* 5: e236

Bombalis K, Weigel D (2007) Hybrid necrosis: autoimmune as a potential gene–flow barrier in plant species. *Nat Rev Genet* 8: 382–393

Broman KW, Sen S, Owens SE, Manichaikul A, Southard-Smith EM, Churchill GA (2006) The X chromosome in quantitative trait locus mapping. *Genetics* 174: 2151–2158

Broman KW, Wu H, Sen S, Churchill GA (2003) R/qtl: QTL mapping in experimental crosses. *Bioinformatics* 19: 889–890

Catalán P, Chalhoub B, Chochio V, Garvin DF, Hasterok R, Manzaneda AJ, Mur LA, Pecchioni N, Rasmussen SK, Vogel JP, et al (2014) Update on the genomics and basic biology of *Brachypodium*: International Brachypodium Initiative (IBI). *Trends Plant Sci* 19: 414–418

Chen A, Dubcovsky J (2012) Wheat TILLING mutants show that the vernalization gene *VRN1* down-regulates the flowering repressor *VRN2* in leaves but is not essential for flowering. *PLoS Genet* 8: e1003134

Dawson AM, Bettgenhaeuser J, Gardiner M, Green P, Hernández-Pinzón I, Hubbard A, Moscou MJ (2015) The development of quick, robust, quantitative phenotypic assays for describing the host–nonhost landscape to stripe rust. *Front Plant Sci* 6: 876

Dawson AM, Ferguson JN, Gardiner M, Green P, Hubbard A, Moscou MJ (2016) Isolation and fine mapping of *Rps6*: an intermediate host resistance gene in barley to wheat stripe rust. *Theor Appl Genet* 129: 831–843

Distelfeld A, Li C, Dubcovsky J (2009) Regulation of flowering in temperate cereals. *Curr Opin Plant Biol* 12: 178–184

Doerge RW, Churchill GA (1996) Permutation tests for multiple loci affecting a quantitative character. *Genetics* 142: 285–294

Draper J, Mur LA, Jenkins G, Ghosh-Biswas GC, Bablak P, Hasterok R, Routledge AP (2001) *Brachypodium distachyon*: a new model system for functional genomics in grasses. *Plant Physiol* 127: 1539–1555

Dubcovsky J, Chen C, Yan L (2005) Molecular characterization of the allelic variation at the *VRN-H2* vernalization locus in barley. *Mol Breed* 15: 395–407

Faris JD, Laddomada B, Gill BS (1998) Molecular mapping of segregation distortion loci in *Aegilops tauschii*. *Genetics* 149: 319–327

Fu D, Szücs P, Yan L, Helguera M, Skinner JS, von Zitzewitz J, Hayes PM, Dubcovsky J (2005) Large deletions within the first intron in *VRN-1* are associated with spring growth habit in barley and wheat. *Mol Genet Genomics* 273: 54–65

Garvin DF, Gu YQ, Hasterok R, Hazen SP, Jenkins G, Mockler TC, Mur LAJ, Vogel JP (2008) Development of genetic and genomic research resources for *Brachypodium distachyon*, a new model system for grass crop research. *Crop Sci* 48: S-69

Higgins JA, Bailey PC, Lauria DA (2010) Comparative genomics of flowering time pathways using *Brachypodium distachyon* as a model for the temperate grasses. *PLoS ONE* 5: e10065

Hong SY, Seo PJ, Yang MS, Xiang F, Park CM (2008) Exploring valid reference genes for gene expression studies in *Brachypodium distachyon* by real-time PCR. *BMC Plant Biol* 8: 112

Huo N, Garvin DF, You FM, McMahon S, Luo MC, Gu YQ, Lazo GR, Vogel JP (2011) Comparison of a high-density genetic linkage map to genome features in the model grass *Brachypodium distachyon*. *Theor Appl Genet* 123: 455–464

International Brachypodium Initiative (2010) Genome sequencing and analysis of the model grass *Brachypodium distachyon*. *Nature* 463: 763–768

Jung C, Müller AE (2009) Flowering time control and applications in plant breeding. *Trends Plant Sci* 14: 563–573

Kardailsky I, Shukla VK, Ahn JH, Dagenais N, Christensen SK, Nguyen JT, Chory J, Harrison MJ, Weigel D (1999) Activation tagging of the floral inducer *FT*. *Science* 286: 1962–1965

Karsai I, Szűcs P, Mészáros K, Filichkina T, Hayes PM, Skinner JS, Láng L, Bedő Z (2005) The *Vrn-H2* locus is a major determinant of flowering time in a facultative × winter growth habit barley (*Hordeum vulgare* L.) mapping population. *Theor Appl Genet* 110: 1458–1466

Koboldt DC, Chen K, Wylie T, Larson DE, McLellan MD, Mardis ER, Weinstock GM, Wilson RK, Ding L (2009) VarScan: variant detection in massively parallel sequencing of individual and pooled samples. *Bioinformatics* 25: 2283–2285

Konieczny A, Ausubel FM (1993) A procedure for mapping *Arabidopsis* mutations using co-dominant ecotype-specific PCR-based markers. *Plant J* 4: 403–410

Koornneef M, Alonso-Blanco C, Vreugdenhil D (2004) Naturally occurring genetic variation in *Arabidopsis thaliana*. *Annu Rev Plant Biol* 55: 141–172

Kruglyak L, Lander ES (1995) A nonparametric approach for mapping quantitative trait loci. *Genetics* 139: 1421–1428

Lander ES, Botstein D (1989) Mapping Mendelian factors underlying quantitative traits using RFLP linkage maps. *Genetics* 121: 185–199

Lauter N, Moscou MJ, Habiger J, Moose SP (2008) Quantitative genetic dissection of shoot architecture traits in maize: towards a functional genomics approach. *Plant Genome* 1: 99

Li H, Durbin R (2009) Fast and accurate short read alignment with Burrows–Wheeler transform. *Bioinformatics* 25: 1754–1760

Livak KJ, Schmittgen TD (2001) Analysis of relative gene expression data using real-time quantitative PCR and the 2-(Delta Delta C(T)) method. *Methods* 25: 402–408

Lu H, Romero-Severson J, Bernardo R (2002) Chromosomal regions associated with segregation distortion in maize. *Theor Appl Genet* 105: 622–628

Lv B, Nitcher R, Han X, Wang S, Ni F, Li K, Pearce S, Wu J, Dubcovsky J, Fu D (2014) Characterization of *FLOWERING LOCUS T1 (FT1)* gene in *Brachypodium* and wheat. *PLoS ONE* 9: e94171

Manly KF, Cudmore RH Jr, Meer JM (2001) Map Manager QT, cross-platform software for genetic mapping. *Mamm Genome* 12: 930–932

Muñoz-Amatriñán M, Moscou MJ, Bhat PR, Svensson JT, Bartoš J, Suchánková P, Šimková H, Endo TR, Fenton RD, Lonardi S, et al (2011) An improved consensus linkage map of barley based on flow-sorted chromosomes and single nucleotide polymorphism markers. *Plant Genome* 4: 238–249

Opanowicz M, Vain P, Draper J, Parker D, Doonan JH (2008) *Brachypodium distachyon*: making hay with a wild grass. *Trends Plant Sci* 13: 172–177

Ream TS, Woods DP, Amasino RM (2012) The molecular basis of vernalization in different plant groups. *Cold Spring Harb Symp Quant Biol* 77: 105–115

Ream TS, Woods DP, Schwartz CJ, Sanabria CP, Mahoy JA, Walters EM, Kaeppler HF, Amasino RM (2014) Interaction of photoperiod and vernalization determines flowering time of *Brachypodium distachyon*. *Plant Physiol* 164: 694–709

Routledge APM, Shelley G, Smith JV, Talbot NJ, Draper J, Mur LAJ (2004) *Magnaporthe grisea* interactions with the model grass *Brachypodium distachyon* closely resemble those with rice (*Oryza sativa*). *Mol Plant Pathol* 5: 253–265

Royston JP (1982) An extension of Shapiro and Wilk's *T* test for normality to large samples. *Appl Stat* 31: 115

Sasani S, Hemming MN, Oliver SN, Greenup A, Tavakkol-Afshari R, Mahfoozi S, Poustini K, Sharifi HR, Dennis ES, Peacock WJ, et al (2009) The influence of vernalization and daylength on expression of flowering-time genes in the shoot apex and leaves of barley (*Hordeum vulgare*). *J Exp Bot* 60: 2169–2178

Schwartz CJ, Doyle MR, Manzaneda AJ, Rey PJ, Mitchell-Olds T, Amasino RM (2010) Natural variation of flowering time and vernalization responsiveness in *Brachypodium distachyon*. *BioEnergy Res* 3: 38–46

Tan S, Wu S (2012) Genome wide analysis of nucleotide-binding site disease resistance genes in *Brachypodium distachyon*. *Comp Funct Genomics* 2012: 418208

Trapnell C, Pachter L, Salzberg SL (2009) TopHat: discovering splice junctions with RNA-Seq. *Bioinformatics* 25: 1105–1111

Tyler L, Lee SJ, Young ND, Delulio GA, Benavente E, Reagon M, Sysopha J, Baldini RM, Troia A, Hazen SP, et al (2016) Population structure in the model grass *Brachypodium distachyon* is highly correlated with flowering differences across broad geographic areas. *Plant Genome* 9: 1–20

Vain P, Worland B, Thole V, McKenzie N, Alves SC, Opanowicz M, Fish LJ, Bevan MW, Snape JW (2008) *Agrobacterium*-mediated transformation of the temperate grass *Brachypodium distachyon* (genotype Bd21) for T-DNA insertional mutagenesis. *Plant Biotechnol J* 6: 236–245

Vogel JP, Garvin DF, Leong OM, Hayden DM (2006) *Agrobacterium*-mediated transformation and inbred line development in the model grass *Brachypodium distachyon*. *Plant Cell Tissue Organ Cult* 84: 199–211

von Zitzewitz J, Szücs P, Dubcovsky J, Yan L, Francia E, Pecchioni N, Casas A, Chen TH, Hayes PM, Skinner JS (2005) Molecular and structural characterization of barley vernalization genes. *Plant Mol Biol* 59: 449–467

Wilczek AM, Burghardt LT, Cobb AR, Cooper MD, Welch SM, Schmitt J (2010) Genetic and physiological bases for phenological responses to current and predicted climates. *Philos Trans R Soc Lond B Biol Sci* 365: 3129–3147

Wilson P, Streich J, Borevitz J (2016) Genomic diversity and climate adaptation in *Brachypodium*. In JP Vogel, ed, *Genetics and Genomics of Brachypodium*. Springer International Publishing, Cham, Switzerland, pp 107–127

Woods D, Amasino R (2016) Dissecting the control of flowering time in grasses using *Brachypodium distachyon*. In JP Vogel, ed, *Genetics and Genomics of Brachypodium*. Springer International Publishing, Cham, Switzerland, pp 259–273

Woods D, Bednarek R, Bouché E, Gordon SP, Vogel J, Garvin DF, Amasino R (2016a) Genetic architecture of flowering-time variation in *Brachypodium distachyon*. *Plant Physiol* 172: 269–279

Woods DP, McKeown MA, Dong Y, Preston JC, Amasino RM (2016b) Evolution of VRN2/Ghd7-like genes in vernalization-mediated repression of grass flowering. *Plant Physiol* 170: 2124–2135

Woods DP, Ream TS, Minevich G, Hobert O, Amasino RM (2014) PHYTOCHROME C is an essential light receptor for photoperiodic flowering in the temperate grass, *Brachypodium distachyon*. *Genetics* 198: 397–408

Xu Y, Atchley WR (1996) Mapping quantitative trait loci for complex binary diseases using line crosses. *Genetics* 143: 1417–1424

Xu Y, Zhu L, Xiao J, Huang N, McCouch SR (1997) Chromosomal regions associated with segregation distortion of molecular markers in F2, backcross, doubled haploid, and recombinant inbred populations in rice (*Oryza sativa* L.). *Mol Gen Genet* 253: 535–545

Yan L, Fu D, Li C, Blechl A, Tranquilli G, Bonafede M, Sanchez A, Valarik M, Yasuda S, Dubcovsky J (2006) The wheat and barley vernalization gene VRN3 is an orthologue of *FT*. *Proc Natl Acad Sci USA* 103: 19581–19586

Yan L, Loukoianov A, Blechl A, Tranquilli G, Ramakrishna W, SanMiguel P, Bennetzen JL, Echenique V, Dubcovsky J (2004) The wheat VRN2 gene is a flowering repressor down-regulated by vernalization. *Science* 303: 1640–1644

Yan L, Loukoianov A, Tranquilli G, Helguera M, Fahima T, Dubcovsky J (2003) Positional cloning of the wheat vernalization gene VRN1. *Proc Natl Acad Sci USA* 100: 6263–6268

Zeng ZB (1993) Theoretical basis for separation of multiple linked gene effects in mapping quantitative trait loci. *Proc Natl Acad Sci USA* 90: 10972–10976

Zeng ZB (1994) Precision mapping of quantitative trait loci. *Genetics* 136: 1457–1468

## 7. Abbreviations

aa	amino acid
ADP	adenosine diphosphate
ARC	adaptor shared by APAF-1, R proteins, and CED-4
ATP	adenosine triphosphate
BAC	bacterial artificial chromosome
bp	base pair
CAPS	cleaved amplified polymorphic sequence
CC	coiled-coil domain
cM	centimorgan
dpi	days post inoculation
ETI	effector-triggered immunity
<i>f. sp.</i>	<i>forma specialis</i>
<i>ff. spp.</i>	<i>formae speciales</i>
GWAS	genome-wide association study
HD	helical domain
indel	insertion/deletion
KAPS	kompetitive allele specific PCR
kb	kilo base
LOD	logarithm of the odds
LRR	leucine-rich repeat
MAGIC	multi-parent advanced generation inter-cross
MAST	motif alignment and search tool
min	minutes
NB	nucleotide-binding domain/subdomain
NOD	nucleotide-binding oligomerisation domain
NLR	NOD-like receptor
PAMP	pathogen-associated molecular pattern
pCOL	percent colonisation
PCR	polymerase chain reaction
PRR	pattern recognition receptor
<i>Psh</i>	<i>Puccinia striiformis</i> f. sp. <i>hordei</i>
<i>Pst</i>	<i>Puccinia striiformis</i> f. sp. <i>tritici</i>
PTI	PAMP-triggered immunity
PVE	percent of variation explained
QTL	quantitative trait locus
s	seconds
SNP	single nucleotide polymorphism
TIR	Toll/interleukin-1 receptor homology domain
UTR	untranslated region
WGS	whole genome sequencing
WHD	winged helical domain
<i>Yrr</i>	<i>Yellow rust resistance</i>

## 8. References

Aarts, N., M. Metz, E. Holub, B. J. Staskawicz, M. J. Daniels *et al.*, 1998 Different requirements for *EDS1* and *NDR1* by disease resistance genes define at least two *R* gene-mediated signaling pathways in *Arabidopsis*. *Proc. Natl. Acad. Sci. USA* 95: 10306-10311.

Aghnoum, R., and R. E. Niks, 2010 Specificity and levels of nonhost resistance to nonadapted *Blumeria graminis* forms in barley. *New Phytol.* 185: 275-284.

Albrecht, M., and F. L. Takken, 2006 Update on the domain architectures of NLRs and R proteins. *Biochem. Biophys. Res. Commun.* 339: 459-462.

Amasino, R., 2010 Seasonal and developmental timing of flowering. *Plant J.* 61: 1001-1013.

Andrés, F., and G. Coupland, 2012 The genetic basis of flowering responses to seasonal cues. *Nat. Rev. Genet.* 13: 627-639.

Asselin, J. E., J. M. Bonasera, J. F. Kim, C. S. Oh and S. V. Beer, 2011 *Eop1* from a *Rubus* strain of *Erwinia amylovora* functions as a host-range limiting factor. *Phytopathology* 101: 935-944.

Axtell, M. J., T. W. McNellis, M. B. Mudgett, C. S. Hsu and B. J. Staskawicz, 2001 Mutational analysis of the *Arabidopsis RPS2* disease resistance gene and the corresponding *Pseudomonas syringae avrRpt2* avirulence gene. *Mol. Plant-Microbe Interact.* 14: 181-188.

Ayliffe, M., R. Devilla, R. Mago, R. White, M. Talbot *et al.*, 2011 Nonhost resistance of rice to rust pathogens. *Mol. Plant-Microbe Interact.* 24: 1143-1155.

Ayliffe, M., D. Singh, R. Park, M. Moscou and T. Pryor, 2013 Infection of *Brachypodium distachyon* with selected grass rust pathogens. *Mol. Plant-Microbe Interact.* 26: 946-957.

Ayliffe, M. A., and E. S. Lagudah, 2004 Molecular genetics of disease resistance in cereals. *Ann. Bot.* 94: 765-773.

Ayliffe, M. A., M. Steinau, R. F. Park, L. Rooke, M. G. Pacheco *et al.*, 2004 Aberrant mRNA processing of the maize *Rp1-D* rust resistance gene in wheat and barley. *Mol. Plant-Microbe Interact.* 17: 853-864.

Barbieri, M., T. C. Marcel and R. E. Niks, 2011 Host status of false brome grass to the leaf rust fungus *Puccinia brachypodii* and the stripe rust fungus *P. striiformis*. *Plant Dis.* 95: 1339-1345.

Barbieri, M., T. C. Marcel, R. E. Niks, E. Francia, M. Pasquariello *et al.*, 2012 QTLs for resistance to the false brome rust *Puccinia brachypodii* in the model grass *Brachypodium distachyon* L. *Genome* 55: 152-163.

Basten, C. J., B. S. Weir and Z.-B. Zeng, 2004 QTL Cartographer, version 1.17. Department of Statistics, North Carolina State University, Raleigh, NC.

Beddow, J. M., P. G. Pardey, Y. Chai, T. M. Hurley, D. J. Kriticos *et al.*, 2015 Research investment implications of shifts in the global geography of wheat stripe rust. *Nature Plants* 1: 15132.

Bendahmane, A., G. Farnham, P. Moffett and D. C. Baulcombe, 2002 Constitutive gain-of-function mutants in a nucleotide binding site-leucine rich repeat protein encoded at the *Rx* locus of potato. *Plant J.* 32: 195-204.

Bent, A. F., and D. Mackey, 2007 Elicitors, effectors, and *R* genes: The new paradigm and a lifetime supply of questions. *Annu. Rev. Phytopathol.* 45: 399-436.

Bentham, A., H. Burdett, P. A. Anderson, S. J. Williams and B. Kobe, 2016 Animal NLRs provide structural insights into plant NLR function. *Ann. Bot.*

Bernardo, R., 2016 Bandwagons I, too, have known. *Theor. Appl. Genet.* 129: 2323-2332.

Bernoux, M., H. Burdett, S. J. Williams, X. Zhang, C. Chen *et al.*, 2016 Comparative analysis of the flax immune receptors L6 and L7 suggests an equilibrium-based switch activation model. *Plant Cell* 28: 146-159.

Bettgenhaeuser, J., F. M. Corke, M. Opanowicz, P. Green, I. Hernández-Pinzón *et al.*, 2017 Natural variation in *Brachypodium* links vernalization and flowering time loci as major flowering determinants. *Plant Physiol.* 173: 256-268.

Bettgenhaeuser, J., B. Gilbert, M. Ayliffe and M. J. Moscou, 2014 Nonhost resistance to rust pathogens - a continuation of continua. *Frontiers in Plant Science* 5: 664.

Biffen, R. H., 1905 Mendel's laws of inheritance and wheat breeding. *The Journal of Agricultural Science* 1: 4.

Blümel, M., N. Dally and C. Jung, 2015 Flowering time regulation in crops - what did we learn from *Arabidopsis*? *Curr. Opin. Biotechnol.* 32: 121-129.

Bolger, A. M., M. Lohse and B. Usadel, 2014 Trimmomatic: a flexible trimmer for Illumina sequence data. *Bioinformatics* 30: 2114-2120.

Bomblies, K., J. Lempe, P. Epple, N. Warthmann, C. Lanz *et al.*, 2007 Autoimmune response as a mechanism for a Dobzhansky-Muller-type incompatibility syndrome in plants. *PLoS Biol.* 5: e236.

Bomblies, K., and D. Weigel, 2007 Hybrid necrosis: autoimmunity as a potential gene-flow barrier in plant species. *Nat. Rev. Genet.* 8: 382-393.

Borhan, M. H., N. Gunn, A. Cooper, S. Gulden, M. Tör *et al.*, 2008 *WRR4* encodes a TIR-NB-LRR protein that confers broad-spectrum white rust resistance in *Arabidopsis thaliana* to four physiological races of *Albugo candida*. *Mol. Plant-Microbe Interact.* 21: 757-768.

Borlaug, N. E., 2000 Ending world hunger. The promise of biotechnology and the threat of antiscience zealotry. *Plant Physiol.* 124: 487-490.

Bouché, F., D. P. Woods and R. M. Amasino, 2017 Winter memory throughout the plant kingdom: different paths to flowering. *Plant Physiol.* 173: 27-35.

Breese, E. L., and K. Mather, 1957 The organisation of polygenic activity within a chromosome in *Drosophila*. *Heredity* 11: 373-395.

Broman, K. W., S. Sen, S. E. Owens, A. Manichaikul, E. M. Southard-Smith *et al.*, 2006 The X chromosome in quantitative trait locus mapping. *Genetics* 174: 2151-2158.

Broman, K. W., H. Wu, S. Sen and G. A. Churchill, 2003 R/qtl: QTL mapping in experimental crosses. *Bioinformatics* 19: 889-890.

Brown, J. K., and M. S. Hovmöller, 2002 Aerial dispersal of pathogens on the global and continental scales and its impact on plant disease. *Science* 297: 537-541.

Cao, Y. R., Y. Liang, K. Tanaka, C. T. Nguyen, R. P. Jedrzejczak *et al.*, 2014 The kinase LYK5 is a major chitin receptor in *Arabidopsis* and forms a chitin-induced complex with related kinase CERK1. *Elife* 3.

Catalán, P., B. Chalhoub, V. Chochois, D. F. Garvin, R. Hasterok *et al.*, 2014 Update on the genomics and basic biology of *Brachypodium*: International *Brachypodium* Initiative (IBI). *Trends Plant Sci.* 19: 414-418.

Catalán, P., J. Müller, R. Hasterok, G. Jenkins, L. A. Mur *et al.*, 2012 Evolution and taxonomic split of the model grass *Brachypodium distachyon*. *Ann. Bot.* 109: 385-405.

Catanzariti, A. M., P. N. Dodds, T. Ve, B. Kobe, J. G. Ellis *et al.*, 2010 The AvrM effector from flax rust has a structured C-terminal domain and interacts directly with the M resistance protein. *Mol. Plant-Microbe Interact.* 23: 49-57.

Cesari, S., M. Bernoux, P. Moncquet, T. Kroj and P. N. Dodds, 2014 A novel conserved mechanism for plant NLR protein pairs: the "integrated decoy" hypothesis. *Frontiers in Plant Science* 5: 606.

Césari, S., H. Kanzaki, T. Fujiwara, M. Bernoux, V. Chalvon *et al.*, 2014 The NB-LRR proteins RGA4 and RGA5 interact functionally and physically to confer disease resistance. *EMBO J.* 33: 1941-1959.

Chen, A., and J. Dubcovsky, 2012 Wheat TILLING mutants show that the vernalization gene *VRN1* down-regulates the flowering repressor *VRN2* in leaves but is not essential for flowering. *PLoS Genet.* 8: e1003134.

Chen, X. M., 2005 Epidemiology and control of stripe rust [*Puccinia striiformis* f. sp *tritici*] on wheat. *Can J Plant Pathol.* 27: 314-337.

Collins, N. C., H. Thordal-Christensen, V. Lipka, S. Bau, E. Kombrink *et al.*, 2003 SNARE-protein-mediated disease resistance at the plant cell wall. *Nature* 425: 973-977.

Cook, D. E., C. H. Mesarich and B. P. Thomma, 2015 Understanding plant immunity as a surveillance system to detect invasion. *Annu. Rev. Phytopathol.* 53: 541-563.

Couch, B. C., I. Fudal, M. H. Lebrun, D. Tharreau, B. Valent *et al.*, 2005 Origins of host-specific populations of the blast pathogen *Magnaporthe oryzae* in crop domestication with subsequent expansion of pandemic clones on rice and weeds of rice. *Genetics* 170: 613-630.

Couto, D., and C. Zipfel, 2016 Regulation of pattern recognition receptor signalling in plants. *Nat. Rev. Immunol.* 16: 537-552.

Cui, Y., M. Y. Lee, N. Huo, J. Bragg, L. Yan *et al.*, 2012 Fine mapping of the *Bsr1* barley stripe mosaic virus resistance gene in the model grass *Brachypodium distachyon*. *PLoS One* 7: e38333.

Dangl, J. L., D. M. Horvath and B. J. Staskawicz, 2013 Pivoting the plant immune system from dissection to deployment. *Science* 341: 746-751.

Dangl, J. L., and J. D. Jones, 2001 Plant pathogens and integrated defence responses to infection. *Nature* 411: 826-833.

Darwin, C., 1868 *The variation of animals and plants under domestication*. John Murray, London.

Dawson, A. M., J. Bettgenhaeuser, M. Gardiner, P. Green, I. Hernández-Pinzón *et al.*, 2015 The development of quick, robust, quantitative phenotypic assays for describing the host-nonhost landscape to stripe rust. *Frontiers in Plant Science* 6.

Dawson, A. M., J. N. Ferguson, M. Gardiner, P. Green, A. Hubbard *et al.*, 2016 Isolation and fine mapping of *Rps6*: an intermediate host resistance gene in barley to wheat stripe rust. *Theor. Appl. Genet.* 129: 831-843.

de la Fuente van Bentem, S., J. H. Vossen, K. J. de Vries, S. van Wees, W. I. Tameling *et al.*, 2005 Heat shock protein 90 and its co-chaperone protein phosphatase 5 interact with distinct regions of the tomato I-2 disease resistance protein. *Plant J.* 43: 284-298.

Dell'Acqua, M., D. M. Gatti, G. Pea, F. Cattonaro, F. Coppens *et al.*, 2015 Genetic properties of the MAGIC maize population: a new platform for high definition QTL mapping in *Zea mays*. *Genome Biology* 16: 167.

DeYoung, B. J., and R. W. Innes, 2006 Plant NBS-LRR proteins in pathogen sensing and host defense. *Nat. Immunol.* 7: 1243-1249.

Diamond, J., 1997 *Guns, germs and steel: A short history of everybody for the last 13,000 years*. W. W. Norton.

Dinesh-Kumar, S. P., W. H. Tham and B. J. Baker, 2000 Structure-function analysis of the tobacco mosaic virus resistance gene *N*. *Proc. Natl. Acad. Sci. USA* 97: 14789-14794.

Distelfeld, A., C. Li and J. Dubcovsky, 2009 Regulation of flowering in temperate cereals. *Curr Opin Plant Biol* 12: 178-184.

Dodds, P. N., G. J. Lawrence, A. M. Catanzariti, T. Teh, C. I. Wang *et al.*, 2006 Direct protein interaction underlies gene-for-gene specificity and coevolution of the flax resistance genes and flax rust avirulence genes. *Proc. Natl. Acad. Sci. USA* 103: 8888-8893.

Doebley, J. F., B. S. Gaut and B. D. Smith, 2006 The molecular genetics of crop domestication. *Cell* 127: 1309-1321.

Doerge, R. W., and G. A. Churchill, 1996 Permutation tests for multiple loci affecting a quantitative character. *Genetics* 142: 285-294.

Draper, J., L. A. Mur, G. Jenkins, G. C. Ghosh-Biswas, P. Bablak *et al.*, 2001 *Brachypodium distachyon*. A new model system for functional genomics in grasses. *Plant Physiol* 127: 1539-1555.

Drinkwater, N. R., and M. N. Gould, 2012 The long path from QTL to gene. *PLoS Genet.* 8: e1002975.

Dubcovsky, J., C. Chen and L. Yan, 2005 Molecular characterization of the allelic variation at the *VRN-H2* vernalization locus in barley. *Mol. Breed.* 15: 395-407.

Ellis, J., 2006 Insights into nonhost disease resistance: can they assist disease control in agriculture? *Plant Cell* 18: 523-528.

Ellis, J. G., E. S. Lagudah, W. Spielmeyer and P. N. Dodds, 2014 The past, present and future of breeding rust resistant wheat. *Frontiers in Plant Science* 5: 641.

Eriksson, J., 1894 Ueber die Specialisirung des Parasitismus bei den Getreiderostpilzen. *Berichte der Deutschen Botanischen Gesellschaft*.

Fan, J., and P. Doerner, 2012 Genetic and molecular basis of nonhost disease resistance: complex, yes; silver bullet, no. *Curr. Opin. Plant Biol.* 15: 400-406.

Faris, J. D., B. Laddomada and B. S. Gill, 1998 Molecular mapping of segregation distortion loci in *Aegilops tauschii*. *Genetics* 149: 319-327.

Fitzgerald, K. A., E. M. Palsson-McDermott, A. G. Bowie, C. A. Jefferies, A. S. Mansell *et al.*, 2001 Mal (MyD88-adapter-like) is required for Toll-like receptor-4 signal transduction. *Nature* 413: 78-83.

Flint, J., W. Valdar, S. Shifman and R. Mott, 2005 Strategies for mapping and cloning quantitative trait genes in rodents. *Nat. Rev. Genet.* 6: 271-286.

Flor, H. H., 1971 Current status of the gene-for-gene concept. *Annu. Rev. Phytopathol.* 9: 275-296.

Fry, D. C., S. A. Kuby and A. S. Mildvan, 1986 ATP-binding site of adenylate kinase: mechanistic implications of its homology with ras-encoded p21, F1-ATPase, and other nucleotide-binding proteins. *Proc. Natl. Acad. Sci. USA* 83: 907-911.

Fu, D., P. Szücs, L. Yan, M. Helguera, J. S. Skinner *et al.*, 2005 Large deletions within the first intron in *VRN-1* are associated with spring growth habit in barley and wheat. *Mol. Genet. Genomics* 273: 54-65.

Gabriëls, S. H., J. H. Vossen, S. K. Ekengren, G. van Ooijen, A. M. Abd-El-Haliem *et al.*, 2007 An NB-LRR protein required for HR signalling mediated by both extra- and intracellular resistance proteins. *Plant J.* 50: 14-28.

Galton, F., 1869 *Hereditary genius: An inquiry into its laws and consequences*. Macmillan and Co., London.

Garvin, D. F., Y.-Q. Gu, R. Hasterok, S. P. Hazen, G. Jenkins *et al.*, 2008 Development of genetic and genomic research resources for *Brachypodium distachyon*, a new model system for grass crop research. *Crop Sci.* 48: S-69.

Geldermann, H., 1975 Investigations on inheritance of quantitative characters in animals by gene markers I. *Methods. Theor. Appl. Genet.* 46: 319-330.

Gibson, D. G., L. Young, R. Y. Chuang, J. C. Venter, C. A. Hutchison, 3rd *et al.*, 2009 Enzymatic assembly of DNA molecules up to several hundred kilobases. *Nat Methods* 6: 343-345.

Gilbert, G. S., and C. O. Webb, 2007 Phylogenetic signal in plant pathogen-host range. *Proc. Natl. Acad. Sci. USA* 104: 4979-4983.

Gill, U. S., S. Lee and K. S. Mysore, 2015 Host versus nonhost resistance: distinct wars with similar arsenals. *Phytopathology* 105: 580-587.

Grant, M. R., L. Godiard, E. Straube, T. Ashfield, J. Lewald *et al.*, 1995 Structure of the *Arabidopsis RPM1* gene enabling dual specificity disease resistance. *Science* 269: 843-846.

Hackett, C. A., 2002 Statistical methods for QTL mapping in cereals. *Plant Mol. Biol.* 48: 585-599.

Hammond-Kosack, K. E., and J. E. Parker, 2003 Deciphering plant-pathogen communication: fresh perspectives for molecular resistance breeding. *Curr. Opin. Biotechnol.* 14: 177-193.

Hao, W., S. M. Collier, P. Moffett and J. Chai, 2013 Structural basis for the interaction between the potato virus X resistance protein (Rx) and its cofactor Ran GTPase-activating protein 2 (RanGAP2). *J. Biol. Chem.* 288: 35868-35876.

Harvey, W., 1651 *Exercitationes de generatione animalium*. Typis Du-Gardianis; Impensis O. Pulleyn, Londini.

Heath, M. C., 1981 A generalized concept of host-parasite specificity. *Phytopathology* 71: 1121-1123.

Heath, M. C., 1991 The role of gene-for-gene interactions in the determination of host species specificity. *Phytopathology* 81: 127-130.

Heath, M. C., 2000 Nonhost resistance and nonspecific plant defenses. *Curr. Opin. Plant Biol.* 3: 315-319.

Higgins, J. A., P. C. Bailey and D. A. Laurie, 2010 Comparative genomics of flowering time pathways using *Brachypodium distachyon* as a model for the temperate grasses. *PLoS One* 5: e10065.

Holm, S., 1979 A simple sequentially rejective multiple test procedure. *Scand. J. Statist.* 6: 65-70.

Hong, S. Y., P. J. Seo, M. S. Yang, F. Xiang and C. M. Park, 2008 Exploring valid reference genes for gene expression studies in *Brachypodium distachyon* by real-time PCR. *BMC Plant Biol* 8: 112.

Horng, T., and R. Medzhitov, 2001 *Drosophila* MyD88 is an adapter in the Toll signaling pathway. *Proc. Natl. Acad. Sci. USA* 98: 12654-12658.

Hovmøller, M. S., and A. F. Justesen, 2007 Appearance of atypical *Puccinia striiformis* f. sp. *tritici* phenotypes in north-western Europe. *Aust. J. Agric. Res.* 58: 518.

Hovmøller, M. S., C. K. Sørensen, S. Walter and A. F. Justesen, 2011 Diversity of *Puccinia striiformis* on cereals and grasses. *Annu. Rev. Phytopathol.* 49: 197-217.

Howles, P., G. Lawrence, J. Finnegan, H. McFadden, M. Ayliffe *et al.*, 2005 Autoactive alleles of the flax *L6* rust resistance gene induce non-race-specific rust resistance associated with the hypersensitive response. *Mol. Plant-Microbe Interact.* 18: 570-582.

Hu, Z., C. Yan, P. Liu, Z. Huang, R. Ma *et al.*, 2013 Crystal structure of NLRC4 reveals its autoinhibition mechanism. *Science* 341: 172-175.

Hubbard, A., C. M. Lewis, K. Yoshida, R. H. Ramirez-Gonzalez, C. de Vallavieille-Pope *et al.*, 2015 Field pathogenomics reveals the emergence of a diverse wheat yellow rust population. *Genome Biology* 16: 23.

Huo, N., D. F. Garvin, F. M. You, S. McMahon, M. C. Luo *et al.*, 2011 Comparison of a high-density genetic linkage map to genome features in the model grass *Brachypodium distachyon*. *Theor. Appl. Genet.* 123: 455-464.

Hurni, S., S. Brunner, D. Stirnweis, G. Herren, D. Peditto *et al.*, 2014 The powdery mildew resistance gene *Pm8* derived from rye is suppressed by its wheat ortholog *Pm3*. *Plant J.* 79: 904-913.

Ishida, Y., M. Tsunashima, Y. Hiei and T. Komari, 2015 Wheat (*Triticum aestivum* L.) transformation using immature embryos in *Agrobacterium Protocols*, edited by K. Wang. Springer Science+Business Media, New York.

Iyer, L. M., D. D. Leipe, E. V. Koonin and L. Aravind, 2004 Evolutionary history and higher order classification of AAA+ ATPases. *Journal of Structural Biology* 146: 11-31.

Jafary, H., G. Albertazzi, T. C. Marcel and R. E. Niks, 2008 High diversity of genes for nonhost resistance of barley to heterologous rust fungi. *Genetics* 178: 2327-2339.

Jafary, H., L. J. Szabo and R. E. Niks, 2006 Innate nonhost immunity in barley to different heterologous rust fungi is controlled by sets of resistance genes with different and overlapping specificities. *Mol. Plant-Microbe Interact.* 19: 1270-1279.

Jansen, R. C., 1993 Interval mapping of multiple quantitative trait loci. *Genetics* 135: 205-211.

Jansen, R. C., and P. Stam, 1994 High-resolution of quantitative traits into multiple loci via interval mapping. *Genetics* 136: 1447-1455.

Jia, Y., S. A. McAdams, G. T. Bryan, H. P. Hershey and B. Valent, 2000 Direct interaction of resistance gene and avirulence gene products confers rice blast resistance. *EMBO J.* 19: 4004-4014.

Johnson, R., 1981 Durable resistance: Definition of, genetic control, and attainment in plant breeding. *Phytopathology* 71: 567-568.

Jones, J. D., and J. L. Dangl, 2006 The plant immune system. *Nature* 444: 323-329.

Joshi, R. K., and S. Nayak, 2010 Gene pyramiding - a broad spectrum technique for developing durable stress resistance in crops. *Biotechnology and Molecular Biology Review* 5: 51-60.

Jung, C., and A. E. Müller, 2009 Flowering time control and applications in plant breeding. *Trends Plant Sci.* 14: 563-573.

Jung, J. H., M. Domijan, C. Klose, S. Biswas, D. Ezer *et al.*, 2016 Phytochromes function as thermosensors in *Arabidopsis*. *Science* 354: 886-889.

Jupe, F., L. Pritchard, G. J. Etherington, K. MacKenzie, P. J. A. Cock *et al.*, 2012 Identification and localisation of the NB-LRR gene family within the potato genome. *BMC Genomics* 13.

Kadota, Y., J. Sklenar, P. Derbyshire, L. Stransfeld, S. Asai *et al.*, 2014 Direct regulation of the NADPH oxidase RBOHD by the PRR-associated kinase BIK1 during plant immunity. *Mol. Cell* 54: 43-55.

Kang, S., J. A. Sweigard and B. Valent, 1995 The *PWL* host specificity gene family in the blast fungus *Magnaporthe grisea*. *Mol. Plant-Microbe Interact.* 8: 939-948.

Kardailsky, I., V. K. Shukla, J. H. Ahn, N. Dagenais, S. K. Christensen *et al.*, 1999 Activation tagging of the floral inducer *FT*. *Science* 286: 1962-1965.

Karsai, I., P. Szücs, K. Mészáros, T. Filichkina, P. M. Hayes *et al.*, 2005 The *Vrn-H2* locus is a major determinant of flowering time in a facultative x winter growth habit barley (*Hordeum vulgare* L.) mapping population. *Theor. Appl. Genet.* 110: 1458-1466.

Kawashima, C. G., G. A. Guimarães, S. R. Nogueira, D. MacLean, D. R. Cook *et al.*, 2016 A pigeonpea gene confers resistance to Asian soybean rust in soybean. *Nat. Biotechnol.* 34: 661-665.

Kearsey, M. J., and A. G. L. Farquhar, 1998 QTL analysis in plants; where are we now? *Heredity* 80: 137-142.

Kerber, E. R., 1991 Stem-rust resistance in 'Canthatch' hexaploid wheat induced by a nonsuppressor mutation on chromosome 7DL. *Genome* 34: 935-939.

Kerber, E. R., and P. L. Dyck, 1973 Inheritance of stem rust resistance transferred from diploid wheat (*Triticum monococcum*) to tetraploid and hexaploid wheat and chromosome location of the gene involved. *Canadian Journal of Genetics and Cytology* 15: 397-409.

Klug, W. S., and M. R. Cummings, 1991 *Concepts of genetics*. Macmillan Publishing Company, New York.

Kobayashi, D. Y., S. J. Tamaki and N. T. Keen, 1989 Cloned avirulence genes from the tomato pathogen *Pseudomonas syringae* pv. *tomato* confer cultivar specificity on soybean. *Proc. Natl. Acad. Sci. USA* 86: 157-161.

Koboldt, D. C., K. Chen, T. Wylie, D. E. Larson, M. D. McLellan *et al.*, 2009 VarScan: variant detection in massively parallel sequencing of individual and pooled samples. *Bioinformatics* 25: 2283-2285.

Kölreuter, J. G., 1761 *Vorläufige Nachricht von einigen, das Geschlecht der Pflanzen betreffenden Versuchen und Beobachtungen*. In der Gleditschischen Handlung, Leipzig.

Konieczny, A., and F. M. Ausubel, 1993 A procedure for mapping *Arabidopsis* mutations using co-dominant ecotype-specific PCR-based markers. *The Plant Journal* 4: 403-410.

Koornneef, M., C. Alonso-Blanco and D. Vreugdenhil, 2004 Naturally occurring genetic variation in *Arabidopsis thaliana*. *Annu Rev Plant Biol* 55: 141-172.

Kopp, E. B., and R. Medzhitov, 1999 The Toll-receptor family and control of innate immunity. *Curr. Opin. Immunol.* 11: 13-18.

Kover, P. X., W. Valdar, J. Trakalo, N. Scarcelli, I. M. Ehrenreich *et al.*, 2009 A Multiparent Advanced Generation Inter-Cross to fine-map quantitative traits in *Arabidopsis thaliana*. *PLoS Genet.* 5: e1000551.

Krasileva, K. V., D. Dahlbeck and B. J. Staskawicz, 2010 Activation of an *Arabidopsis* resistance protein is specified by the in planta association of its leucine-rich repeat domain with the cognate oomycete effector. *Plant Cell* 22: 2444-2458.

Krattinger, S. G., and B. Keller, 2016 Molecular genetics and evolution of disease resistance in cereals. *New Phytol.* 212: 320-332.

Kruglyak, L., and E. S. Lander, 1995 A nonparametric approach for mapping quantitative trait loci. *Genetics* 139: 1421-1428.

Lander, E. S., and D. Botstein, 1989 Mapping mendelian factors underlying quantitative traits using RFLP linkage maps. *Genetics* 121: 185-199.

Lauter, N., M. J. Moscou, J. Habiger and S. P. Moose, 2008 Quantitative genetic dissection of shoot architecture traits in maize: towards a functional genomics approach. *The Plant Genome* 1: 99.

Le Roux, C., G. Huet, A. Jauneau, L. Camborde, D. Trémousaygue *et al.*, 2015 A receptor pair with an integrated decoy converts pathogen disabling of transcription factors to immunity. *Cell* 161: 1074-1088.

Lee, H. A., S. Y. Kim, S. K. Oh, S. I. Yeom, S. B. Kim *et al.*, 2014 Multiple recognition of RXLR effectors is associated with nonhost resistance of pepper against *Phytophthora infestans*. *New Phytol.* 203: 926-938.

Lee, S., V. M. Whitaker and S. F. Hutton, 2016 Mini review: Potential applications of non-host resistance for crop improvement. *Frontiers in Plant Science* 7: 997.

Legris, M., C. Klose, E. S. Burgie, C. C. Rojas, M. Neme *et al.*, 2016a Phytochrome B integrates light and temperature signals in *Arabidopsis*. *Science* 354: 897-900.

Legris, M., C. Nieto, R. Sellaro, S. Prat and J. J. Casal, 2016b Perception and signalling of light and temperature cues in plants. *Plant J.*

Li, H., and R. Durbin, 2009 Fast and accurate short read alignment with Burrows-Wheeler transform. *Bioinformatics* 25: 1754-1760.

Li, J., J. Ding, W. Zhang, Y. Zhang, P. Tang *et al.*, 2010 Unique evolutionary pattern of numbers of gramineous NBS-LRR genes. *Mol. Genet. Genomics* 283: 427-438.

Li, L., M. Li, L. Yu, Z. Zhou, X. Liang *et al.*, 2014 The FLS2-associated kinase BIK1 directly phosphorylates the NADPH oxidase RbohD to control plant immunity. *Cell Host Microbe* 15: 329-338.

Linnaeus, C., 1735 *Systema naturae*. Haak, Lugduni Batavorum.

Linnaeus, C., and D. Rudberg, 1744 *Peloria*, Upsaliae.

Lipka, U., R. Fuchs and V. Lipka, 2008 *Arabidopsis* non-host resistance to powdery mildews. *Curr. Opin. Plant Biol.* 11: 404-411.

Lipka, V., J. Dittgen, P. Bednarek, R. Bhat, M. Wiermer *et al.*, 2005 Pre- and postinvasion defenses both contribute to nonhost resistance in *Arabidopsis*. *Science* 310: 1180-1183.

Liu, J., X. Liu, L. Dai and G. Wang, 2007 Recent progress in elucidating the structure, function and evolution of disease resistance genes in plants. *Journal of Genetics and Genomics* 34: 765-776.

Livak, K. J., and T. D. Schmittgen, 2001 Analysis of relative gene expression data using real-time quantitative PCR and the 2(-Delta Delta C(T)) method. *Methods* 25: 402-408.

Lorang, J., T. Kidarsa, C. S. Bradford, B. Gilbert, M. Curtis *et al.*, 2012 Tricking the guard: Exploiting plant defense for disease susceptibility. *Science* 338: 659-662.

Lu, H., J. Romero-Severson and R. Bernardo, 2002 Chromosomal regions associated with segregation distortion in maize. *Theor Appl Genet* 105: 622-628.

Lukasik, E., and F. L. Takken, 2009 STANDING strong, resistance proteins instigators of plant defence. *Curr. Opin. Plant Biol.* 12: 427-436.

Lv, B., R. Nitcher, X. Han, S. Wang, F. Ni *et al.*, 2014 Characterization of *FLOWERING LOCUS T1 (FT1)* gene in *Brachypodium* and wheat. *PLoS One* 9: e94171.

Lynch, M., and B. Walsh, 1998 *Genetics and analysis of quantitative traits*. Sinauer Associates, Sunderland, MA, USA.

Macho, A. P., and C. Zipfel, 2014 Plant PRRs and the activation of innate immune signaling. *Mol. Cell* 54: 263-272.

Maekawa, T., B. Kracher, S. Vernaldi, E. Ver Loren van Themaat and P. Schulze-Lefert, 2012 Conservation of NLR-triggered immunity across plant lineages. *Proc. Natl. Acad. Sci. USA* 109: 20119-20123.

Maekawa, T., T. A. Kufer and P. Schulze-Lefert, 2011 NLR functions in plant and animal immune systems: so far and yet so close. *Nat. Immunol.* 12: 817-826.

Manly, K. F., R. H. Cudmore and J. M. Meer, 2014 Map Manager QTX, cross-platform software for genetic mapping. *Mamm. Genome* 12: 930-932.

Mather, K., and J. L. Jinks, 1971 *Biometrical genetics. The study of continuous variation*. Chapman & Hall Ltd., London.

McDonald, B. A., and C. Linde, 2002 The population genetics of plant pathogens and breeding strategies for durable resistance. *Euphytica* 124: 163-180.

McHale, L., X. Tan, P. Koehl and R. W. Michelmore, 2006 Plant NBS-LRR proteins: adaptable guards. *Genome Biology* 7: 212.

McIntosh, R. A., P. Zhang, C. Cowger, R. Parks, E. S. Lagudah *et al.*, 2011 Rye-derived powdery mildew resistance gene *Pm8* in wheat is suppressed by the *Pm3* locus. *Theor. Appl. Genet.* 123: 359-367.

Mendel, G., 1866 Versuche über Pflanzenhybriden. *Verhandlungen des naturforschenden Vereines in Brünn*, Bd. IV für das Jahr 1865: 3 - 47.

Meyers, B. C., A. Kozik, A. Griego, H. Kuang and R. W. Michelmore, 2003 Genome-wide analysis of NBS-LRR-encoding genes in *Arabidopsis*. *Plant Cell* 15: 809-834.

Meyers, B. C., M. Morgante and R. W. Michelmore, 2002 TIR-X and TIR-NBS proteins: two new families related to disease resistance TIR-NBS-LRR proteins encoded in *Arabidopsis* and other plant genomes. *Plant J.* 32: 77-92.

Milus, E. A., K. Kristensen and M. S. Hovmøller, 2009 Evidence for increased aggressiveness in a recent widespread strain of *Puccinia striiformis* f. sp. *tritici* causing stripe rust of wheat. *Phytopathology* 99: 89-94.

Mindrinos, M., F. Katagiri, G.-L. Yu and F. M. Ausubel, 1994 The *A. thaliana* disease resistance gene *RPS2* encodes a protein containing a nucleotide-binding site and leucine-rich repeats. *Cell* 78: 1089-1099.

Miya, A., P. Albert, T. Shinya, Y. Desaki, K. Ichimura *et al.*, 2007 CERK1, a LysM receptor kinase, is essential for chitin elicitor signaling in *Arabidopsis*. *Proc. Natl. Acad. Sci. USA* 104: 19613-19618.

Morgante, M., and F. Salamini, 2003 From plant genomics to breeding practice. *Curr. Opin. Biotechnol.* 14: 214-219.

Muneyuki, E., H. Noji, T. Amano, T. Masaike and M. Yoshida, 2000 F0F1-ATP synthase: general structural features of 'ATP-engine' and a problem on free energy transduction. *Biochimica et Biophysica Acta (BBA) - Bioenergetics* 1458: 467-481.

Muñoz-Amatriaín, M., M. J. Moscou, P. R. Bhat, J. T. Svensson, J. Bartoš *et al.*, 2011 An improved consensus linkage map of barley based on flow-sorted chromosomes and single nucleotide polymorphism markers. *Plant Genome* 4: 238-249.

Mysore, K. S., and C. M. Ryu, 2004 Nonhost resistance: how much do we know? *Trends Plant Sci.* 9: 97-104.

Nandety, R. S., J. L. Caplan, K. Cavanaugh, B. Perroud, T. Wroblewski *et al.*, 2013 The role of TIR-NBS and TIR-X proteins in plant basal defense responses. *Plant Physiol.* 162: 1459-1472.

Niks, R. E., 1987 Nonhost plant species as donors for resistance to pathogens with narrow host range I. Determination of nonhost status. *Euphytica* 36: 841-852.

Niks, R. E., and T. C. Marcel, 2009 Nonhost and basal resistance: how to explain specificity? *New Phytol.* 182: 817-828.

Nilsson-Ehle, N. H., 1909 *Kreuzungsuntersuchungen an Hafer und Weizen*. Lunds Univiversitets Årsskrift, Lund.

Nishimura, M. T., F. Monteiro and J. L. Dangl, 2015 Treasure your exceptions: Unusual domains in immune receptors reveal host virulence targets. *Cell* 161: 957-960.

Nürnberg, T., and V. Lipka, 2005 Non-host resistance in plants: new insights into an old phenomenon. *Mol. Plant Pathol.* 6: 335-345.

Opanowicz, M., P. Vain, J. Draper, D. Parker and J. H. Doonan, 2008 *Brachypodium distachyon*: making hay with a wild grass. *Trends Plant Sci* 13: 172-177.

Papadopoulou, K., R. E. Melton, M. Leggett, M. J. Daniels and A. E. Osbourn, 1999 Compromised disease resistance in saponin-deficient plants. *Proc. Natl. Acad. Sci. USA* 96: 12923-12928.

Paran, I., and D. Zamir, 2003 Quantitative traits in plants: beyond the QTL. *Trends Genet.* 19: 303-306.

Penfield, S., 2008 Temperature perception and signal transduction in plants. *New Phytol.* 179: 615-628.

Pflieger, S., V. Lefebvre and M. Causse, 2001 The candidate gene approach in plant genetics: a review. *Mol. Breed.* 7: 275-291.

Price, A. H., 2006 Believe it or not, QTLs are accurate! *Trends Plant Sci.* 11: 213-216.

Punja, Z. K., and Y.-Y. Zhang, 1993 Plant chitinases and their roles in resistance to fungal diseases. *J. Nematol.* 25: 526-540.

Rapilly, F., 1979 Yellow rust epidemiology. *Annu. Rev. Phytopathol.* 17: 59-73.

Rasmusson, J., 1935 Studies on the inheritance of quantitative characters in *Pisum*. *Hereditas* 20: 161-180.

Ream, T. S., D. P. Woods and R. M. Amasino, 2012 The molecular basis of vernalization in different plant groups. *Cold Spring Harbor Symp. Quant. Biol.* 77: 105-115.

Ream, T. S., D. P. Woods, C. J. Schwartz, C. P. Sanabria, J. A. Mahoy *et al.*, 2014 Interaction of photoperiod and vernalization determines flowering time of *Brachypodium distachyon*. *Plant Physiol* 164: 694-709.

Reeve, E. C. R., 2001 *Encyclopedia of genetics*.

Remington, D. L., M. C. Ungerer and M. D. Purugganan, 2001 Map-based cloning of quantitative trait loci: progress and prospects. *Genetics Research* 78: 213-218.

Riedl, S. J., W. Li, Y. Chao, R. Schwarzenbacher and Y. Shi, 2005 Structure of the apoptotic protease-activating factor 1 bound to ADP. *Nature* 434: 926-933.

Riley, R., and R. C. F. Macer, 1966 The chromosomal distribution of the genetic resistance of rye to wheat pathogens. *Canadian Journal of Genetics and Cytology* 8: 640-653.

Roelfs, A. P., R. P. Singh and E. E. Saari, 1992 *Rust diseases of wheat: Concepts and methods of disease management*. CIMMYT, Mexico, D.F.

Routledge, A. P. M., G. Shelley, J. V. Smith, N. J. Talbot, J. Draper *et al.*, 2004 *Magnaporthe grisea* interactions with the model grass *Brachypodium distachyon* closely resemble those with rice (*Oryza sativa*). *Mol. Plant Pathol.* 5: 253-265.

Royston, J. P., 1982 An Extension of Shapiro and Wilk's W Test for Normality to Large Samples. *Applied Statistics* 31: 115.

Salvi, S., and R. Tuberosa, 2005 To clone or not to clone plant QTLs: present and future challenges. *Trends Plant Sci.* 10: 297-304.

Salzer, P., A. Bonanomi, K. Beyer, R. Vögeli-Lange, R. A. Aeschbacher *et al.*, 2000 Differential expression of eight chitinase genes in *Medicago truncatula* roots during mycorrhiza formation, nodulation, and pathogen infection. *Mol Plant Microbe Interact* 13: 763-777.

Sarris, P. F., V. Cevik, G. Dagdas, J. D. Jones and K. V. Krasileva, 2016 Comparative analysis of plant immune receptor architectures uncovers host proteins likely targeted by pathogens. *BMC Biol.* 14: 8.

Sarris, P. F., Z. Duxbury, S. U. Huh, Y. Ma, C. Segonzac *et al.*, 2015 A plant immune receptor detects pathogen effectors that target WRKY transcription factors. *Cell* 161: 1089-1100.

Sasani, S., M. N. Hemming, S. N. Oliver, A. Greenup, R. Tavakkol-Afshari *et al.*, 2009 The influence of vernalization and daylength on expression of flowering-time genes in the shoot apex and leaves of barley (*Hordeum vulgare*). *J Exp Bot* 60: 2169-2178.

Sax, K., 1923 The association of size differences with seed-coat pattern and pigmentation in *Phaseolus vulgaris*. *Genetics* 8: 552-560.

Schulze-Lefert, P., and R. Panstruga, 2011 A molecular evolutionary concept connecting nonhost resistance, pathogen host range, and pathogen speciation. *Trends Plant Sci.* 16: 117-125.

Schwartz, C. J., M. R. Doyle, A. J. Manzaneda, P. J. Rey, T. Mitchell-Olds *et al.*, 2010 Natural variation of flowering time and vernalization responsiveness in *Brachypodium distachyon*. *BioEnergy Research* 3: 38-46.

Schweizer, P., 2007 Nonhost resistance of plants to powdery mildew — new opportunities to unravel the mystery. *Physiol. Mol. Plant Pathol.* 70: 3-7.

Shafiei, R., C. Hang, J. G. Kang and G. J. Loake, 2007 Identification of loci controlling non-host disease resistance in *Arabidopsis* against the leaf rust pathogen *Puccinia triticina*. *Mol. Plant Pathol.* 8: 773-784.

Shull, G. H., 1908 The composition of a field of maize. *J. Hered.* os-4: 296-301.

Smedley, M. A., and W. A. Harwood, 2015 Gateway-compatible plant transformation vectors in *Agrobacterium Protocols*, edited by K. Wang. Springer Science+Business Media, New York.

Sohn, K. H., S. B. Saucet, C. R. Clarke, B. A. Vinatzer, H. E. O'Brien *et al.*, 2012 HopAS1 recognition significantly contributes to *Arabidopsis* nonhost resistance to *Pseudomonas syringae* pathogens. *New Phytol.* 193: 58-66.

Staal, J., and C. Dixelius, 2008 RLM3, a potential adaptor between specific TIR-NB-LRR receptors and DZC proteins. *Communicative & Integrative Biology* 1: 59-61.

Staal, J., M. Kaliff, S. Bohman and C. Dixelius, 2006 Transgressive segregation reveals two *Arabidopsis* TIR-NB-LRR resistance genes effective against *Leptosphaeria maculans*, causal agent of blackleg disease. *Plant J.* 46: 218-230.

Staal, J., M. Kaliff, E. Dewaele, M. Persson and C. Dixelius, 2008 *RLM3*, a TIR domain encoding gene involved in broad-range immunity of *Arabidopsis* to necrotrophic fungal pathogens. *Plant J.* 55: 188-200.

Stein, M., J. Dittgen, C. Sánchez-Rodríguez, B. H. Hou, A. Molina *et al.*, 2006 *Arabidopsis PEN3/PDR8*, an ATP binding cassette transporter, contributes to nonhost resistance to inappropriate pathogens that enter by direct penetration. *Plant Cell* 18: 731-746.

Steuernagel, B., S. K. Periyannan, I. Hernández-Pinzón, K. Witek, M. N. Rouse *et al.*, 2016 Rapid cloning of disease-resistance genes in plants using mutagenesis and sequence capture. *Nat. Biotechnol.* 34: 652-655.

Story, R. M., and T. A. Steitz, 1992 Structure of the recA protein-ADP complex. *Nature* 355: 374-376.

Straib, W., 1935 Infektionsversuche mit biologischen Rassen des Gelbrostes auf Gräsern. *Arbeiten der Biologischen Reichsanstalt Gliesmarode*.

Stukenbrock, E. H., and B. A. McDonald, 2008 The origins of plant pathogens in agro-ecosystems. *Annu. Rev. Phytopathol.* 46: 75-100.

Sukarta, O. C., E. J. Slootweg and A. Goverse, 2016 Structure-informed insights for NLR functioning in plant immunity. *Semin. Cell Dev. Biol.* 56: 134-149.

Sweigard, J. A., A. M. Carroll, S. Kang, L. Farrall, F. G. Chumley *et al.*, 1995 Identification, cloning, and characterization of *PWL2*, a gene for host species specificity in the rice blast fungus. *Plant Cell* 7: 1221-1233.

Takken, F. L., M. Albrecht and W. I. Tameling, 2006 Resistance proteins: molecular switches of plant defence. *Curr. Opin. Plant Biol.* 9: 383-390.

Takken, F. L., and A. Goverse, 2012 How to build a pathogen detector: structural basis of NB-LRR function. *Curr. Opin. Plant Biol.* 15: 375-384.

Tameling, W. I., S. D. Elzinga, P. S. Darmin, J. H. Vossen, F. L. Takken *et al.*, 2002 The tomato *R* gene products I-2 and Mi-1 are functional ATP binding proteins with ATPase activity. *Plant Cell* 14: 2929-2939.

Tameling, W. I., J. H. Vossen, M. Albrecht, T. Lengauer, J. A. Berden *et al.*, 2006 Mutations in the NB-ARC domain of I-2 that impair ATP hydrolysis cause autoactivation. *Plant Physiol.* 140: 1233-1245.

Tan, S., and S. Wu, 2012 Genome wide analysis of nucleotide-binding site disease resistance genes in *Brachypodium distachyon*. *Comp Funct Genomics* 2012: 418208.

Tanksley, S. D., 1993 Mapping polygenes. *Annu. Rev. Genet.* 27: 205-233.

The International Brachypodium Initiative, 2010 Genome sequencing and analysis of the model grass *Brachypodium distachyon*. *Nature* 463: 763-768.

Thoday, J. M., 1961 Location of polygenes. *Nature* 191: 368-370.

Thordal-Christensen, H., 2003 Fresh insights into processes of nonhost resistance. *Curr. Opin. Plant Biol.* 6: 351-357.

Tornero, P., R. A. Chao, W. N. Luthin, S. A. Goff and J. L. Dangl, 2002 Large-scale structure-function analysis of the *Arabidopsis RPM1* disease resistance protein. *Plant Cell* 14: 435-450.

Toruño, T. Y., I. Stergiopoulos and G. Coaker, 2016 Plant-pathogen effectors: Cellular probes interfering with plant defenses in spatial and temporal manners. *Annu. Rev. Phytopathol.* 54: 419-441.

Tosa, Y., 1989 Evidence on wheat for gene-for-gene relationship between formae speciales of *Erysiphe graminis* and genera of gramineous plants. *Genome* 32: 918-924.

Trapnell, C., L. Pachter and S. L. Salzberg, 2009 TopHat: discovering splice junctions with RNA-Seq. *Bioinformatics* 25: 1105-1111.

Traut, T. W., 1994 The functions and consensus motifs of nine types of peptide segments that form different types of nucleotide-binding sites. *Eur. J. Biochem.* 222: 9-19.

Troch, V., K. Audenaert, R. A. Wyand, G. Haesaert, M. Höfte *et al.*, 2014 *Formae speciales* of cereal powdery mildew: close or distant relatives? *Mol. Plant Pathol.* 15: 304-314.

Tsuba, M., C. Katagiri, Y. Takeuchi, Y. Takada and N. Yamaoka, 2002 Chemical factors of the leaf surface involved in the morphogenesis of *Blumeria graminis*. *Physiol. Mol. Plant Pathol.* 60: 51-57.

Tyler, L., S. J. Lee, N. D. Young, G. A. DeJulio, E. Benavente *et al.*, 2016 Population structure in the model grass *Brachypodium distachyon* is highly correlated with flowering differences across broad geographic areas. *The Plant Genome* 9: 1-20.

Vain, P., B. Worland, V. Thole, N. McKenzie, S. C. Alves *et al.*, 2008 *Agrobacterium*-mediated transformation of the temperate grass *Brachypodium distachyon* (genotype Bd21) for T-DNA insertional mutagenesis. *Plant Biotechnol J* 6: 236-245.

van der Biezen, E. A., and J. D. G. Jones, 1998 The NB-ARC domain: a novel signalling motif shared by plant resistance gene products and regulators of cell death in animals. *Curr. Biol.* 8: R226-R228.

van der Hoorn, R. A., and S. Kamoun, 2008 From guard to decoy: a new model for perception of plant pathogen effectors. *Plant Cell* 20: 2009-2017.

van Ooijen, G., G. Mayr, M. M. Kasiem, M. Albrecht, B. J. Cornelissen *et al.*, 2008 Structure-function analysis of the NB-ARC domain of plant disease resistance proteins. *J. Exp. Biol.* 59: 1383-1397.

Ve, T., S. J. Williams, A. M. Catanzariti, M. Rafiqi, M. Rahman *et al.*, 2013 Structures of the flax-rust effector AvrM reveal insights into the molecular basis of plant-cell entry and effector-triggered immunity. *Proc. Natl. Acad. Sci. USA* 110: 17594-17599.

Vogel, J. P., D. F. Garvin, O. M. Leong and D. M. Hayden, 2006 *Agrobacterium*-mediated transformation and inbred line development in the model grass *Brachypodium distachyon*. *Plant Cell Tiss. Org. Cult.* 84: 199-211.

von Zitzewitz, J., P. Szücs, J. Dubcovsky, L. Yan, E. Francia *et al.*, 2005 Molecular and structural characterization of barley vernalization genes. *Plant Mol Biol* 59: 449-467.

Walker, J. E., M. Saraste, M. J. Runswick and N. J. Gay, 1982 Distantly related sequences in the alpha- and beta-subunits of ATP synthase, myosin, kinases and other ATP-requiring enzymes and a common nucleotide binding fold. *EMBO J.* 1: 945-951.

Wang, C. I., G. Gunčar, J. K. Forwood, T. Teh, A. M. Catanzariti *et al.*, 2007a Crystal structures of flax rust avirulence proteins AvrL567-A and -D reveal details of the structural basis for flax disease resistance specificity. *Plant Cell* 19: 2898-2912.

Wang, M., Z. Li, P. R. Matthews, N. M. Upadhyaya and P. M. Waterhouse, 1998 Improved vectors for *Agrobacterium tumefaciens*-mediated transformation of monocot plants. *Acta Horticulturae*: 401-408.

Wang, W., A. Devoto, J. G. Turner and S. Xiao, 2007b Expression of the membrane-associated resistance protein RPW8 enhances basal defense against biotrophic pathogens. *Mol. Plant-Microbe Interact.* 20: 966-976.

Wang, Y., Y. Zhang, Z. Wang, X. Zhang and S. Yang, 2013 A missense mutation in CHS1, a TIR-NB protein, induces chilling sensitivity in *Arabidopsis*. *Plant J.* 75: 553-565.

Wei, C. F., B. H. Kvitko, R. Shimizu, E. Crabbill, J. R. Alfano *et al.*, 2007 A *Pseudomonas syringae* pv. *tomato* DC3000 mutant lacking the type III effector HopQ1-1 is able to cause disease in the model plant *Nicotiana benthamiana*. *Plant J.* 51: 32-46.

Wiermer, M., B. J. Feys and J. E. Parker, 2005 Plant immunity: the EDS1 regulatory node. *Curr. Opin. Plant Biol.* 8: 383-389.

Wilczek, A. M., L. T. Burghardt, A. R. Cobb, M. D. Cooper, S. M. Welch *et al.*, 2010 Genetic and physiological bases for phenological responses to current and predicted climates. *Philos. Trans. R. Soc. Lond., Ser. B: Biol. Sci.* 365: 3129-3147.

Williams, S. J., K. H. Sohn, L. Wan, M. Bernoux, P. F. Sarris *et al.*, 2014 Structural basis for assembly and function of a heterodimeric plant immune receptor. *Science* 344: 299-303.

Wilson, P., J. Streich and J. Borevitz, 2016 Genomic diversity and climate adaptation in *Brachypodium*, pp. 107-127 in *Genetics and Genomics of Brachypodium*, edited by J. P. Vogel. Springer International Publishing.

Witek, K., F. Jupe, A. I. Witek, D. Baker, M. D. Clark *et al.*, 2016 Accelerated cloning of a potato late blight-resistance gene using RenSeq and SMRT sequencing. *Nat. Biotechnol.* 34: 656-660.

Woods, D., and R. Amasino, 2016 Dissecting the control of flowering time in grasses using *Brachypodium distachyon*, pp. 259-273 in *Genetics and Genomics of Brachypodium*, edited by J. P. Vogel. Springer International Publishing.

Woods, D., M. McKeown, Y. Dong, J. C. Preston and R. M. Amasino, 2016 Evolution of *VRN2/GhD7*-like genes in vernalization-mediated repression of grass flowering. *Plant Physiol.* 170: 2124-2135.

Woods, D. P., R. Bednarek, F. Bouché, S. P. Gordon, J. P. Vogel *et al.*, 2017 Genetic architecture of flowering-time variation in *Brachypodium distachyon*. *Plant Physiol.* 173: 269-279.

Woods, D. P., T. S. Ream, G. Minevich, O. Hobert and R. M. Amasino, 2014 PHYTOCHROME C is an essential light receptor for photoperiodic flowering in the temperate grass, *Brachypodium distachyon*. *Genetics* 198: 397-408.

Wright, S., 1968 *Evolution and the genetics of populations: Genetic and biometric foundations*. The University of Chicago Press, Chicago.

Wroblewski, T., K. S. Caldwell, U. Piskurewicz, K. A. Cavanaugh, H. Xu *et al.*, 2009 Comparative large-scale analysis of interactions between several crop species and the effector repertoires from multiple pathovars of *Pseudomonas* and *Ralstonia*. *Plant Physiol.* 150: 1733-1749.

Wulff, B. B., D. M. Horvath and E. R. Ward, 2011 Improving immunity in crops: new tactics in an old game. *Curr. Opin. Plant Biol.* 14: 468-476.

Wulff, B. B., and M. J. Moscou, 2014 Strategies for transferring resistance into wheat: from wide crosses to GM cassettes. *Frontiers in Plant Science* 5: 692.

Xiao, S., S. Ellwood, O. Calis, E. Patrick, T. Li *et al.*, 2001 Broad-spectrum mildew resistance in *Arabidopsis thaliana* mediated by RPW8. *Science* 291: 118-120.

Xu, S. Z., and W. R. Atchley, 1996 Mapping quantitative trait loci for complex binary diseases using line crosses. *Genetics* 143: 1417-1424.

Xu, Y., X. Tao, B. Shen, T. Horng, R. Medzhitov *et al.*, 2000 Structural basis for signal transduction by the Toll/interleukin-1 receptor domains. *Nature* 408: 111-115.

Xu, Y., L. Zhu, J. Xiao, N. Huang and S. R. McCouch, 1997 Chromosomal regions associated with segregation distortion of molecular markers in F2, backcross, doubled haploid, and recombinant inbred populations in rice (*Oryza sativa* L.). *Mol. Gen. Genet.* 253: 535-545.

Yan, L., D. Fu, C. Li, A. Blechl, G. Tranquilli *et al.*, 2006 The wheat and barley vernalization gene *VRN3* is an orthologue of *FT*. *Proc. Natl. Acad. Sci. USA* 103: 19581-19586.

Yan, L., A. Loukoianov, A. Blechl, G. Tranquilli, W. Ramakrishna *et al.*, 2004 The wheat *VRN2* gene is a flowering repressor down-regulated by vernalization. *Science* 303: 1640-1644.

Yan, L., A. Loukoianov, G. Tranquilli, M. Helguera, T. Fahima *et al.*, 2003 Positional cloning of the wheat vernalization gene *VRN1*. *Proc. Natl. Acad. Sci. USA* 100: 6263-6268.

Yan, N., J. Chai, E. S. Lee, L. Gu, Q. Liu *et al.*, 2005 Structure of the CED-4-CED-9 complex provides insights into programmed cell death in *Caenorhabditis elegans*. *Nature* 437: 831-837.

Yang, S., J. Li, X. Zhang, Q. Zhang, J. Huang *et al.*, 2013 Rapidly evolving *R* genes in diverse grass species confer resistance to rice blast disease. *Proc. Natl. Acad. Sci. USA* 110: 18572-18577.

Yang, Y., J. Zhao, H. Xing, J. Wang, K. Zhou *et al.*, 2014 Different non-host resistance responses of two rice subspecies, *japonica* and *indica*, to *Puccinia striiformis* f. sp. *tritici*. *Plant Cell Rep.* 33: 423-433.

Yeo, F. K., G. Hensel, T. Vozábová, A. Martin-Sanz, T. C. Marcel *et al.*, 2014 Golden SusPtrit: a genetically well transformable barley line for studies on the resistance to rust fungi. *Theor. Appl. Genet.* 127: 325-337.

Yule, G. U., 1902 Mendel's laws and their probable relations to intra-racial heredity. *New Phytol.* 1: 222-238.

Zbierzak, A. M., S. Porfirova, T. Griebel, M. Melzer, J. E. Parker *et al.*, 2013 A TIR-NBS protein encoded by *Arabidopsis Chilling Sensitive 1 (CHS1)* limits chloroplast damage and cell death at low temperature. *Plant J.* 75: 539-552.

Zeng, Z.-B., 1993 Theoretical basis for separation of multiple linked gene effects in mapping quantitative trait loci. *Proc. Natl. Acad. Sci. USA* 90: 10972-10976.

Zeng, Z.-B., 1994 Precision mapping of quantitative trait loci. *Genetics* 136: 1457-1468.

Zeyen, R. J., T. L. W. Carver and M. F. Lyngkjaer, 2002 Epidermal cell papillae, pp. 107-125 in *The powdery mildews: A comprehensive treatise*, edited by R. R. Belanger and W. R. Bushnell. APS Press, St. Paul, Minnesota.

Zhao, B., E. Y. Ardales, A. Raymundo, J. Bai, H. N. Trick *et al.*, 2004 The *avrRxo1* gene from the rice pathogen *Xanthomonas oryzae* pv. *oryzicola* confers a nonhost defense reaction on maize with resistance gene *Rxo1*. *Mol. Plant-Microbe Interact.* 17: 771-779.

Zhao, B., X. Lin, J. Poland, H. Trick, J. Leach *et al.*, 2005 A maize resistance gene functions against bacterial streak disease in rice. *Proc. Natl. Acad. Sci. USA* 102: 15383-15388.

Zhao, T., L. Rui, J. Li, M. T. Nishimura, J. P. Vogel *et al.*, 2015 A truncated NLR protein, TIR-NBS2, is required for activated defense responses in the *exo70B1* mutant. *PLoS Genet.* 11: e1004945.

Zipfel, C., 2008 Pattern-recognition receptors in plant innate immunity. *Curr. Opin. Immunol.* 20: 10-16.

Zipfel, C., G. Kunze, D. Chinchilla, A. Caniard, J. D. Jones *et al.*, 2006 Perception of the bacterial PAMP EF-Tu by the receptor EFR restricts *Agrobacterium*-mediated transformation. *Cell* 125: 749-760.

Zipfel, C., S. Robatzek, L. Navarro, E. J. Oakeley, J. D. Jones *et al.*, 2004 Bacterial disease resistance in *Arabidopsis* through flagellin perception. *Nature* 428: 764-767.

Zirkle, C., 1951 Gregor Mendel & his precursors. *Isis* 42: 97-104.

Zuker, M., 2003 Mfold web server for nucleic acid folding and hybridization prediction. *Nucleic Acids Res.* 31: 3406-3415.